

University of Southampton Research Repository ePrints Soton

Copyright © and Moral Rights for this thesis are retained by the author and/or other copyright owners. A copy can be downloaded for personal non-commercial research or study, without prior permission or charge. This thesis cannot be reproduced or quoted extensively from without first obtaining permission in writing from the copyright holder/s. The content must not be changed in any way or sold commercially in any format or medium without the formal permission of the copyright holders.

When referring to this work, full bibliographic details including the author, title, awarding institution and date of the thesis must be given e.g.

AUTHOR (year of submission) "Full thesis title", University of Southampton, name of the University School or Department, PhD Thesis, pagination

UNIVERSITY OF SOUTHAMPTON
FACULTY OF MEDICINE HEALTH AND LIFE SCIENCES
School of Biological Sciences

The effects of elevated carbon dioxide concentration on leaf growth and development
in *Populus*

In one volume

Laura Elizabeth Graham

Thesis for the degree of Doctor of Philosophy

June 2008

CORRECTIONS SHEET

UNIVERSITY OF SOUTHAMPTON
ABSTRACT
FACULTY OF MEDICINE HEALTH AND LIFE SCIENCES
SCHOOL OF BIOLOGICAL SCIENCES

Doctor of Philosophy

The effects of elevated carbon dioxide concentration on leaf growth and development
in *Populus*

Laura Elizabeth Graham

The composition of the Earth's atmosphere is changing. Such changes can largely be attributed either directly or indirectly to anthropogenic activities. However, the effects that these changes will have on terrestrial vegetation in the future, represents an area of great uncertainty. The results that have been published in the literature have generally concluded that elevated atmospheric carbon dioxide concentration ([eCO₂]) causes increased above- and below-ground biomass compared to ambient conditions.

Members of the *Populus* genus have risen to the forefront of plant research into the effects of [eCO₂]. Members of the genus are extremely fast-growing, making them suitable candidates for use as biomass energy crops. The *Populus trichocarpa* sequence was released in 2006, hence unveiling a huge genetic resource to the plant science community.

Although a large amount of studies to date have been dedicated to the effects of [eCO₂] on plant growth, few have focussed on the underlying genetic basis of the changes. However, thanks to the genetic resources that are now freely available, this has now been addressed. In the series of experiments presented in this thesis a combination of morphological measurements, gene expression and protein studies were used to assess the effects of [eCO₂] on *Populus* leaves.

The results of the studies presented here have shown that there were some differences in various aspects of plant growth as a result of [eCO₂], although the magnitude of the response was lower than has been reported previously in the literature. However, there were rather few changes in transcript expression (as assessed by microarrays) due to [eCO₂]. This conclusion was reproducible across different microarray platforms. This result was further confirmed by a proteomics experiment, which showed that there were no proteins whose abundance differed significantly between ambient and elevated [CO₂].

It is possible that [eCO₂] causes an additive effect on gene expression and hence the sensitivity of the techniques was such that these differences could not be identified. However, it may be possible that the plants demonstrate a plastic response to [eCO₂] and that the techniques used to assess the response were inappropriate in this case. In such an instance, more targeted studies on particular biosynthetic pathways of interest (such as cell wall biosynthesis) may be more appropriate for any future trials.

CONTENTS

Title page	i
Corrections sheet	ii
Abstract	iii
Contents	iv
List of Figures	x
List of Tables	xvii
List of abbreviations	xviii
Declaration	xx
Acknowledgements	xxi

CHAPTER 1

General introduction	1
1.0 Overview	1
1.1 Leaf development	2
1.1.1 Leaf formation and growth	2
1.1.1.1 The shoot apical meristem	3
1.1.1.2 Meristem maintenance	4
1.1.1.3 <i>KNOX</i> genes	5
1.1.1.4 Establishing polarity	6
1.1.1.5 Leaf patterning	8
1.1.2 The cellular basis of development	9
1.1.2.1 The cell cycle	9
CDKs	10
Cyclins	11
CDK inhibitor proteins	11
CDK activating kinases	12
RBR and E2F	14
1.1.2.2 Cellular expansion	15
The cell wall	15
XETs/ XTHs	16
Expansins	18
Putative cell wall modifiers	19
The acid growth theory	20
1.1.2.3 Epidermal cell fate	21
Stomatal development	21
Trichome formation	22
1.2 CO ₂ enrichment	23
1.2.1 An enriched atmosphere	23
1.2.2 Plant growth in [eCO ₂]	24
1.2.3 Experimental systems	27
1.2.3.1 Free Air CO ₂ Enrichment experiments	27
1.3 Plant models	28
1.3.1 <i>Populus</i> as a model species	29
1.4 Transcriptomics	31
1.4.1 Microarrays	31
1.4.1.1 History	31
1.4.1.2 Principles	31
1.4.1.3 Substrates	32

1.4.2	cDNA microarrays	33
1.4.2.1	Experimental procedures	33
1.4.2.2	Limitations associated with the use of cDNA microarrays	35
1.4.3	Oligonucleotide microarrays	36
1.4.3.1	Photolithography	36
1.4.3.2	Experimental procedures	38
1.4.4	Experimental design	40
1.4.4.1	Data analysis	41
1.4.5	Real time RT-PCR	43
1.4.5.1	Principles	43
1.4.5.2	DNA binding agents	44
1.5	Proteomics	45
1.5.1	Principles and techniques	45
1.5.2	Peptide identification and analysis	48
1.5.3	Applications	51
1.6	Aims and hypotheses	52

CHAPTER 2

Materials and Methods		54
2.0	Overview	54
2.1	Phenotypic analysis	54
2.1.1	Leaf growth	54
2.1.2	Leaf anatomy	55
2.1.3	Specific Leaf Area	55
2.1.4	Cellular impressions	56
2.1.5	Tree height	56
2.2	RNA	56
2.2.1	Leaf samples	56
2.2.2	RNA extraction	56
2.2.2.1	RNA quantification	57
2.3	Microarrays	58
2.3.1	POP2 microarrays	58
2.3.1.1	cDNA synthesis	58
2.3.1.2	Probe labelling	59
2.3.1.3	Hybridisation	59
2.3.1.4	Scanning	60
2.3.1.5	Image analysis	60
2.3.1.6	Data analysis	60
2.3.2	PICME microarrays	61
2.3.2.1	cDNA synthesis	61
2.3.2.2	Probe labelling	62
2.3.2.3	Hybridisation	62
2.3.2.4	Scanning and image analysis	63
2.3.2.5	Data analysis	63
2.4	qPCR	64
2.4.1	cDNA synthesis	64
2.4.2	Primer design	64
2.4.3	qPCR reactions	64
2.4.4	Programme parameters	65
2.4.5	Data analysis	65

CHAPTER 3

Leaf development in two contrasting <i>Populus</i> species	66
3.0 Overview	66
3.1 Introduction	67
3.2 Materials and Methods	69
3.3 Results	70
3.3.1 Leaf growth analysis	70
3.3.2 Leaf shape index analysis	73
3.3.3 Cell growth analysis	75
3.4 Discussion	77
3.4.1 Leaf growth in <i>P. deltoides</i> and <i>P. trichocarpa</i>	77
3.4.2 Cellular basis of growth in <i>P. deltoides</i> and <i>P. trichocarpa</i>	79
3.5 Conclusion	80

CHAPTER 4

Phenotypic analyses of <i>P. deltoides</i> and <i>P. trichocarpa</i> grown in [eCO ₂] using a FACE experimental system	81
4.0 Overview	81
4.1 Introduction	82
4.2 Materials and Methods	84
4.2.1 The BangorFACE experimental field site	84
4.2.2 Measurements	85
4.2.3 Endogenous XET activity	86
4.3 Results	87
4.3.1 Above-ground growth	87
4.3.2 Cellular analyses	91
4.3.3 Leaf anatomy	93
4.3.4 XET co-localisation	95
4.4 Discussion	97
4.4.1 Leaf growth in [eCO ₂]	97
4.4.2 Leaf epidermal cell characteristics following exposure to FACE	98
4.4.3 XET's and [eCO ₂]	99
4.4.4 The CO ₂ response	101
4.5 Conclusion	102

CHAPTER 5

The transcriptome of <i>Populus</i> following exposure to [eCO ₂] using a FACE experimental system	103
5.0 Overview	103
5.1 Introduction	104
5.2 Materials and Methods	106
5.2.1 The EUROFACE experimental system	106
5.2.2 Leaf samples and RNA extractions	107
5.2.3 POP2 microarrays	108
5.2.3.1 Experimental design	108
5.2.4 qPCR	109
5.2.4.1 Primer design	109
5.2.5 PICME microarrays	111
5.2.5.1 Experimental design	111
5.3 Results	112
5.3.1 POP2 microarray	112
5.3.1.1 Gene Ontologies	114

	5.3.1.2 Pathway analysis	119
	5.3.2 qPCR	121
	5.3.3 PICME microarrays	125
5.4	Discussion	128
	5.4.1 [eCO ₂] and cell wall modifications	128
	5.4.2 Cellulose biosynthesis and the cell wall	129
	5.4.3 Acclimatory response	130
	5.4.4 Genomic regions of interest	131
	5.4.5 Small changes in gene expression	131
	5.4.6 Future directions	133
5.5	Conclusion	134

CHAPTER 6

Phenotypic analyses of selected *Populus* genotypes exposed to [eCO₂] using Closed Topped Chambers

6.0	Overview	135
6.1	Introduction	136
6.2	Materials and Methods	138
	6.2.1 Genotype selection	138
	6.2.2 Experimental design	140
	6.2.3 Phenotyping	142
	6.2.3.1 <i>P. deltoides</i> , <i>P. trichocarpa</i> and the F ₁ genotypes	142
	6.2.3.2 F ₂ yield extreme genotypes	142
	6.2.3.3 All genotypes	143
6.3	Results	145
	6.3.1 Spatial analysis of <i>P. deltoides</i> and <i>P. trichocarpa</i>	145
	6.3.1.1 Leaf growth analyses	145
	6.3.1.2 Leaf shape index	147
	6.3.1.3 Cell growth analyses	148
	6.3.1.4 Leaf anatomy	156
	6.3.2 Temporal analysis of <i>P. deltoides</i> and <i>P. trichocarpa</i>	159
	6.3.2.1 Leaf growth analyses	159
	6.3.3 Temporal analyses of F ₁ and F ₂ genotypes	162
	6.3.4 Temporal growth in all genotypes	166
6.4	Discussion	177
	6.4.1 Leaf growth of <i>P. deltoides</i> and <i>P. trichocarpa</i> in [eCO ₂]	177
	6.4.2 Cellular characteristics of <i>P. deltoides</i> and <i>P. trichocarpa</i> in [eCO ₂]	177
	6.4.3 Leaf anatomy of <i>P. deltoides</i> and <i>P. trichocarpa</i>	178
	6.4.4 Stomatal characteristics	179
	6.4.5 Nutrition	180
	6.4.6 CO ₂ receptors	181
	6.4.7 Yield extreme genotypes	182
	6.4.8 Source-sink regulation	183
6.5	Conclusion	184

CHAPTER 7

The *Populus* transcriptome: a comparative analysis of meristematic tissues and young leaves using two different microarray platforms 185

7.0	Overview	185
7.1	Introduction	186
7.2	Materials and Methods	188
7.2.1	POP2 cDNA microarray	188
7.2.2	Affymetrix microarray	189
7.3	Results	190
7.3.1	cDNA microarrays	190
7.3.1.1	Venn diagrams	192
7.3.1.2	Gene Ontologies	194
7.3.1.3	Pathway analysis	197
7.3.1.4	Leaf growth candidate genes	201
7.3.1.5	Cell Cycle candidate genes	204
7.3.2	Affymetrix microarrays	207
7.4	Discussion	209
7.4.1	Leaf development and patterning in [eCO ₂]	209
7.4.2	The cell cycle	212
7.4.3	Hormone signalling	213
7.4.4	Photosynthesis	216
7.4.5	Affymetrix microarrays and platform comparisons	217
7.4.6	Statistical analysis of microarray data	218
7.4.7	The CO ₂ response	219
7.5	Conclusion	220

CHAPTER 8

The proteome of *Populus* grown in [eCO₂] 221

8.0	Overview	221
8.1	Introduction	222
8.2	Materials and Methods	225
8.2.1	Protein extraction	225
8.2.2	Protein quantification	226
8.2.3	1-DE gels	226
8.2.4	2-DE gels	227
8.2.5	Image analysis	228
8.2.6	Statistical analysis	229
8.2.7	In-gel digestion	229
8.2.8	Protein identification	230
8.3	Results	231
8.3.1	Identifying CO ₂ responsive proteins	232
8.3.2	Species-specific protein expression	234
8.4	Discussion	245
8.4.1	Proteomics and [eCO ₂]	245
8.4.2	Interspecific differences in protein profiles	246
8.4.3	Leaf ontogeny	247
8.4.4	Proteomics and population biology	247
8.5	Conclusion	248

CHAPTER 9	
General discussion	249
9.1 Thesis overview	249
9.2 Morphological changes in [eCO ₂]	250
9.3 Microarrays and [eCO ₂]	251
9.3.1 An additive effect?	251
9.3.2 Magnitude of the response and experimental design	251
9.3.3 Phenotypic plasticity	252
9.3.4 Technical limitations associated with microarrays and [eCO ₂] studies	253
9.4 Proteomics and [eCO ₂]	254
9.5 Future directions	254
9.5.1 Leaves, stems and roots	254
9.5.2 Yield extreme genotypes	255
9.6 Closing statement	255
 PUBLICATIONS	 256
 REFERENCES	 257
 APPENDICES	 286

Note: All appendices are available on the CD accompanying this thesis

LIST OF FIGURES

Figure	Legend	Page
1.1.1.	A model for the three principle axes of leaf development.	2
1.1.2.	The structure of the shoot apical meristem.	3
1.1.3.	The stages of leaf development and formation.	4
1.1.4.	An emerging model of gene expression during early leaf development.	8
1.1.5.	A generalised checkpoint in the eukaryotic cell cycle.	13
1.1.6.	A model for cell wall extension mediated by expansins.	19
1.1.7.	Possible mechanisms for cell wall extension.	20
1.3.1.	The five sections of the <i>Populus</i> genus and possible hybrid combinations.	30
1.4.1.	The experimental procedures involved in conducting a cDNA microarray experiment.	34
1.4.2.	The construction of an oligonucleotide microarray chip using photolithography.	37
1.4.3.	The experimental procedures involved in conducting an oligonucleotide microarray experiment.	39
1.5.1.	Diagrammatic representation of the separation of proteins using 2-DE gels.	47
1.5.2.	A generalised view of the processes associated with the production of protonated ions by electrospray ionisation (ESI) for analysis by mass spectrometry in proteomics.	49
1.5.3.	A generalised view of an ion trap mass analyser for use in proteomics.	50
2.1.1.	A model used to indicate the location of leaf length and width measurements.	54
2.1.2.	A model used to indicate the area in which material was sampled for leaf anatomy analysis.	55
3.1.1.	The natural distribution of <i>P. deltoides</i> and <i>P. trichocarpa</i> .	68

3.3.1.	The average leaf area of <i>P. deltoides</i> during leaf development, grown in ambient [CO ₂].	71
3.3.2.	The average leaf area of <i>P. trichocarpa</i> during leaf development, grown in ambient [CO ₂].	71
3.3.3.	The average absolute growth rate of <i>P. deltoides</i> and <i>P. trichocarpa</i> leaves during development, grown in ambient [CO ₂].	72
3.3.4.	The average relative growth rate of <i>P. deltoides</i> and <i>P. trichocarpa</i> leaves during development, grown in ambient [CO ₂].	73
3.3.5.	The average leaf length to width ratio of <i>P. deltoides</i> during leaf development, grown in ambient [CO ₂].	74
3.3.6.	The average leaf length to width ratio of <i>P. trichocarpa</i> during leaf development, grown in ambient [CO ₂].	75
3.3.7.	The average cell area of <i>P. deltoides</i> and <i>P. trichocarpa</i> during leaf development, grown in ambient [CO ₂].	76
3.3.8.	The average cell number of <i>P. deltoides</i> and <i>P. trichocarpa</i> during leaf development, grown in ambient [CO ₂].	77
4.2.1.	The design of the BangorFACE experimental field site, used to deliver [eCO ₂] to individuals grown within the ring structures.	84
4.2.2.	A diagram of one of the FACE rings at the BangorFACE site used to expose the plants within the ring to [eCO ₂].	85
4.3.1.	The average height of <i>P. deltoides</i> and <i>P. trichocarpa</i> exposed to [aCO ₂] or [eCO ₂] using FACE.	87
4.3.2.	The average number of leaves of <i>P. deltoides</i> and <i>P. trichocarpa</i> exposed to [aCO ₂] or [eCO ₂] using FACE.	88
4.3.3.	The average leaf area of <i>P. deltoides</i> exposed to either [aCO ₂] or [eCO ₂] using FACE.	89
4.3.4.	The average leaf area of <i>P. trichocarpa</i> exposed to either [aCO ₂] or [eCO ₂] using FACE.	89
4.3.5.	The specific leaf area of <i>P. deltoides</i> exposed to either [aCO ₂] or [eCO ₂] using FACE.	90
4.3.6.	The specific leaf area of <i>P. trichocarpa</i> exposed to either [aCO ₂] or [eCO ₂] using FACE.	90
4.3.7.	Average leaf cell area of <i>P. deltoides</i> exposed to either [aCO ₂] or [eCO ₂] using FACE.	91

4.3.8.	Average leaf cell area in <i>P. trichocarpa</i> exposed to either [aCO ₂] or [eCO ₂] using FACE.	91
4.3.9.	The average number of cells per leaf in <i>P. deltoides</i> exposed to [aCO ₂] or [eCO ₂] using FACE.	92
4.3.10.	The average number of cells per leaf in <i>P. trichocarpa</i> exposed to [aCO ₂] or [eCO ₂] using FACE.	93
4.3.11.	Leaf cross sections of <i>P. deltoides</i> and <i>P. trichocarpa</i> exposed to [aCO ₂] or [eCO ₂] using FACE.	94
4.3.12.	Examples of images captured on the Confocal Laser Scanning Microscope in order to quantify XET activity in <i>P. deltoides</i> and <i>P. trichocarpa</i> exposed to [aCO ₂] or [eCO ₂] using FACE.	95
4.3.13.	Quantification of XET co-localisation in <i>P. deltoides</i> and <i>P. trichocarpa</i> exposed to either [aCO ₂] or [eCO ₂] using FACE.	96
4.4.1.	A diagrammatic representation of the XET co-localisation assay.	100
5.2.1.	A plan of the EUROFACE site in Italy.	107
5.2.2.	The design of the POP2 cDNA microarray experiment, which was used compare both treatment ([aCO ₂] or [eCO ₂]) and developmental age of <i>P. euramericana</i> grown at the EUROFACE site.	108
5.2.3.	The experimental design for the PICME cDNA microarrays for the transcript analysis of semi-mature leaves of <i>P. euramericana</i> exposed to [aCO ₂] or [eCO ₂] at the EUROFACE site.	111
5.3.1.	The expression ratios (young leaves:semi-mature leaves) of the four POP2 cDNA microarrays from <i>P. euramericana</i> leaf samples from [aCO ₂] and [eCO ₂] grown at EUROFACE.	112
5.3.2.	The expression ratios ([eCO ₂]: [aCO ₂]) of the four POP2 cDNA microarrays for the young and semi-mature leaves of <i>P. euramericana</i> grown at EUROFACE.	113
5.3.3.	A Venn diagram constructed using GeneSpring, illustrating the transcripts that were two-fold (or more) down-regulated in young leaves in ambient and elevated [CO ₂], as assessed by the POP2 cDNA microarrays.	115
5.3.4.	A Venn diagram constructed using GeneSpring, illustrating the transcripts that were two-fold (or more) up-regulated in young leaves in ambient and elevated [CO ₂] growth conditions, as assessed by the POP2 cDNA microarrays.	116

5.3.5.	A Venn diagram constructed using GeneSpring, illustrating the transcripts that were two-fold (or more) down-regulated in [eCO ₂] in young and semi-mature leaves of <i>P. euramericana</i> , as assessed by the POP2 cDNA microarrays.	117
5.3.6.	A Venn diagram constructed using GeneSpring, illustrating the transcripts that were two-fold (or more) up-regulated in [eCO ₂] in young and semi-mature leaves of <i>P. euramericana</i> , as assessed by the POP2 cDNA microarrays.	118
5.3.7.	The cell wall precursor pathway obtained from Mapman using the expression data from the POP2 cDNA microarrays.	120
5.3.8.	The expression ratios (elevated CO ₂ : ambient CO ₂) from the POP2 cDNA microarrays for four transcripts identified for confirmation using qPCR.	121
5.3.9.	The average expression ratio (elevated CO ₂ : ambient CO ₂) for the young (age 3) and semi-mature (age 6) leaves of <i>P. euramericana</i> for the <i>RUBISCO SSU</i> transcript.	122
5.3.10.	The average expression ratio ([eCO ₂]:[aCO ₂]), from the POP2 cDNA microarrays and qPCR for four of the selected candidate genes in young leaves of <i>P. x euramericana</i> .	123
5.3.11.	The POP2 cDNA microarray and qPCR results for the average fold change in <i>RUBISCO SSU</i> expression levels in <i>P. x euramericana</i> in response to [eCO ₂].	124
5.3.12.	The average fold change in expression in response to [eCO ₂] in <i>P. x euramericana</i> as assessed by the PICME cDNA microarray.	125
6.1.1.	The derivation of Family 331 from <i>P. deltoides</i> and <i>P. trichocarpa</i> .	137
6.2.1.	Frequency histograms of leaf area, specific leaf area, leaf shape index (width: length) and sylleptic density in Family 331 grown in ambient [CO ₂].	138
6.2.2.	The general design plan for the closed topped chamber CO ₂ experiment.	141
6.2.3.	A timeline representing sampling dates during the course of the closed topped chamber experiment.	144
6.3.1.	The average leaf area of <i>P. deltoides</i> and <i>P. trichocarpa</i> grown in the closed topped chambers and exposed to either ambient or elevated [CO ₂].	146

6.3.2.	The average leaf length to width ratios of <i>P. deltoides</i> and <i>P. trichocarpa</i> grown in the closed topped chambers in either ambient or elevated [CO ₂].	148
6.3.3.	The average adaxial cell area of <i>P. deltoides</i> and <i>P. trichocarpa</i> grown in the closed topped chambers in either ambient or elevated [CO ₂].	149
6.3.4.	The average adaxial cell number of <i>P. deltoides</i> and <i>P. trichocarpa</i> grown in the closed topped chambers in either ambient or elevated [CO ₂].	150
6.3.5.	The average abaxial cell area of <i>P. deltoides</i> and <i>P. trichocarpa</i> grown in the closed topped chamber in either ambient or elevated [CO ₂].	151
6.3.6.	The average abaxial cell number of <i>P. deltoides</i> and <i>P. trichocarpa</i> grown in the closed topped chamber in either ambient or elevated [CO ₂].	152
6.3.7.	The transverse cross sections of young leaves of <i>P. deltoides</i> , <i>P. trichocarpa</i> , and the two F ₁ genotypes '242' and '246' grown in the closed topped chambers in either ambient or elevated [CO ₂].	157
6.3.8.	The transverse cross sections of mature leaves of <i>P. deltoides</i> , <i>P. trichocarpa</i> , and the two F ₁ genotypes '242' and '246' grown in the closed topped chambers in either ambient or elevated [CO ₂].	158
6.3.9.	The average percentage change in leaf area of <i>P. deltoides</i> and <i>P. trichocarpa</i> as a result of growth in [eCO ₂] (in the closed topped chambers).	159
6.3.10.	The average percentage change in leaf length of <i>P. deltoides</i> and <i>P. trichocarpa</i> as a result of growth in [eCO ₂] (in the closed topped chambers).	160
6.3.11.	The average percentage change in leaf width of <i>P. deltoides</i> and <i>P. trichocarpa</i> as a result of growth in [eCO ₂] (in the closed topped chambers).	161
6.3.12.	The average leaf area of the two F ₁ genotypes grown in either ambient or elevated [CO ₂] in the closed topped chambers.	162
6.3.13.	The average leaf shape index (length: width) of the two F ₁ genotypes in either ambient or elevated [CO ₂] in the closed topped chambers.	163
6.3.14.	The average leaf area for the high- and low-biomass extreme genotypes grown in ambient or elevated [CO ₂] in the closed topped chambers.	165

6.3.15.	The average height of <i>P. deltoides</i> and <i>P. trichocarpa</i> following exposure to either ambient or elevated [CO ₂] in the closed topped chambers.	167
6.3.16.	The average heights of the two F ₁ genotypes following exposure to either ambient or elevated [CO ₂] in the closed topped chambers.	168
6.3.17.	The average heights of the two groups of biomass extremes following exposure to either ambient or elevated [CO ₂] in the closed topped chambers.	169
6.3.18.	The average biomass of the two groups of F ₂ extreme genotypes grown in either ambient or elevated [CO ₂] in the closed topped chambers.	170
6.3.19.	The average stem diameter of the two groups of biomass extremes grown in either ambient or elevated [CO ₂] in the closed topped chambers.	171
6.3.20.	The average abaxial and adaxial cell areas of the high biomass genotypes grown in either ambient or elevated [CO ₂] in the closed topped chambers.	172
6.3.21.	The average abaxial and adaxial cell areas of the low biomass genotypes grown in either ambient or elevated [CO ₂] in the closed topped chambers.	173
6.3.22.	The average specific leaf area for <i>P. deltoides</i> and <i>P. trichocarpa</i> grown in either ambient or elevated [CO ₂] in the closed topped chambers.	174
6.3.23.	The average specific leaf area of the two F ₁ genotypes grown in either ambient or elevated [CO ₂] in the closed topped chambers.	175
6.3.24.	The average specific leaf area of the biomass extreme genotypes grown in either ambient or elevated [CO ₂] in the closed topped chambers.	176
7.2.1.	The design of the POP2 cDNA microarrays experiment for the plants grown in the closed topped chambers.	189
7.3.1.	The results from the successful hybridisations on the POP2 cDNA microarrays which were conducted on the meristematic tissue and leaf age two of <i>P. deltoides</i> and <i>P. trichocarpa</i> grown in [aCO ₂] or [eCO ₂] in the closed topped chambers.	191
7.3.2.	Venn diagrams illustrating the species comparisons made from the POP2 cDNA microarray data.	193
7.3.3.	Venn diagrams illustrating the age comparisons made from the POP2 cDNA microarray data.	193

7.3.4.	The Gene Ontology information for the differentially expressed transcripts from the POP2 cDNA microarrays in the meristematic tissue and leaf age two of <i>P. deltoides</i> .	195
7.3.5.	The Gene Ontology information for the differentially expressed transcripts from the POP2 cDNA microarrays in the meristematic tissue and leaf age two of <i>P. trichocarpa</i> .	196
7.3.6.	The Calvin Cycle metabolic pathway from Aracyc, containing data from the POP2 cDNA microarrays from the meristematic tissue of <i>P. deltoides</i> .	198
7.3.7.	The Calvin cycle of the meristematic tissue of <i>P. deltoides</i> using microarray data from the POP2 cDNA microarrays.	199
7.3.8.	The average expression values for the gene models representing transcripts involved in the Calvin Cycle in the meristematic tissue of <i>P. deltoides</i> .	200
7.3.9.	The average expression levels of ESTs representing abaxial (<i>YABBY</i> and <i>KANADI</i>) and adaxial (<i>ARGONAUTE</i>) patterning genes.	202
7.3.10.	The Affymetrix data for the youngest unfurled leaves of <i>P. deltoides</i> and <i>P. trichocarpa</i> which were grown in ambient or elevated [CO ₂] in the closed topped chambers.	208
7.4.1.	The major gibberellic acid biosynthetic pathways in higher plants.	215
8.3.1.	2-DE gels from ambient and elevated [CO ₂] from the leaves of <i>P. deltoides</i> .	232
8.3.2.	2-DE gels from ambient and elevated [CO ₂] from the leaves of <i>P. trichocarpa</i> .	233
8.3.3.	A comparison of a 2-DE gel from <i>P. deltoides</i> and <i>P. trichocarpa</i> .	234
8.3.4.	An illustration of manual spot detection of the 2-DE gels.	235
8.3.5.	The Gene Ontology information for the protein spots identified in <i>P. deltoides</i> .	243
8.3.6.	The Gene Ontology information for the protein spots identified in <i>P. trichocarpa</i> .	244

LIST OF TABLES

Table	Legend	Page
5.2.1.	A table representing the <i>P. euramericana</i> leaf samples on each of the eight POP2 cDNA microarrays, according to the design of the experiment shown in Figure 5.2.2.	109
5.3.1.	The results from the PICME cDNA microarrays showing the ESTs that were two-fold (or more) up- or down-regulated in response to [eCO ₂].	126
5.3.2.	The ESTs on the PICME and POP2 cDNA microarrays that were two fold (or more) up- or down-regulated in [eCO ₂] in semi-mature leaves of <i>P. x euramericana</i> .	127
6.3.1.	The average leaf area of <i>P. deltoides</i> and <i>P. trichocarpa</i> grown in the closed topped chambers and exposed to either ambient or elevated [CO ₂].	145
6.3.2.	The average percentage change in leaf length to width ratio in <i>P. deltoides</i> and <i>P. trichocarpa</i> as a result of growth in [eCO ₂] in the closed topped chambers.	147
6.3.3.	The average stomatal density in the abaxial and adaxial surfaces of <i>P. deltoides</i> and <i>P. trichocarpa</i> grown in the closed topped chambers in either ambient or elevated [CO ₂].	154
6.3.4.	The average trichome density in the abaxial and adaxial surfaces of <i>P. trichocarpa</i> grown in the closed topped chambers in either ambient or elevated [CO ₂].	155
7.3.1.	The average expression values for each gene model representing either <i>YABBY</i> or <i>ARGONAUTE</i> for <i>P. deltoides</i> and <i>P. trichocarpa</i> (both age two leaves and the SAM (meristematic tissue)).	203
7.3.2.	The average expression data for transcripts related to the cell cycle in both the meristematic tissue and leaf age two of <i>P. deltoides</i> and <i>P. trichocarpa</i> .	205
8.3.1.	The full annotation for the protein spots identified by MS/MS.	236

LIST OF ABBREVIATIONS

Abbreviation	Definition
1-DE	One dimensional gel electrophoresis
2-DE	Two dimensional gel electrophoresis
ABA	Absciscic acid
[aCO ₂]	Ambient carbon dioxide concentration
AGR	Actual growth rate
ANOVA	Analysis of variance
APS	Amonium persulphate
BLAST	Basic local alignment search tool
BSA	Bovine serum albumin
CAK	Cyclin-dependent activating kinase
CE	Controlled environment
CDK	Cyclin dependent kinase
CHAPS	3-[3-chloamidopropyl dimethylammonio]-1-propane sulphonate
CID	Collision induced dissociation
CKI	CDK inhibitor
CPI	Composite pixel intensity
Ct	Cycle threshold
CTAB	Hexadecyltrimethylammoniumbromide
CTC	Closed topped chamber
CYC	Cyclin
CZ	Central zone
DAP	Days after planting
DEPC	Diethylpyrocarbonate
DP	Dimerization partner
DFE	Days following exposure
dsDNA	Double stranded DNA
DTT	Dithiothreitol
[eCO ₂]	Elevated carbon dioxide concentration
ESI	Electrospray ionisation
EST	Expressed sequence tag
EDTA	Ethylenediamine tetraacetic acid
FACE	Free air CO ₂ enrichment
FC	Fusicoccin
FDR	False discovery rate
GA	Gibberellin/Gibberellic acid
GMC	Guard mother cell
GO	Gene ontology
GPP	Gross primary production
HEPES	Hydroxyethylpiperazineethane sulfonic acid
HPLC	High pressure liquid chromatography
ICAT	Isotope coded affinity tags
IEF	Isoelectric focussing
IPCC	Intergovernmental Panel on Climate Change
IPG	Immobilised pH gradient
iTRAQ	Isobaric tags for relative and absolute quantification

KRP	Kip related protein
LAI	Leaf area index
LOWESS	Locally weighted linear regression
LSU	Large subunit (RUBISCO)
MALDI	Matrix assisted laser desorption ionisation
MOPS	Morpholinopropane sulfonic acid
MS	Mass spectrometry
MS/MS	Tandem mass spectrometry
N	Nitrogen
NASC	Nottingham Arabidopsis stock centre
NBP	Net biome production
NC	Neighbour cell
NEP	Net ecosystem production
NPP	Net primary production
NOAA	National oceanic and atmospheric administration
·OH	Hydroxyl radicals
OTC	Open top chamber
ppm	Parts per million
PQL	Protein quantitative loci
PVP	Polyvinylpyrrolidone
PZ	Peripheral zone
qPCR	Quantitative (real time reverse-transcription) polymerase chain reaction
QTL	Quantitative trait loci
Rb	Retinoblastoma protein
RBR	Retinoblastoma related protein
RGR	Relative Growth Rate
RIL	Recombinant inbred line
RT-PCR	Real time polymerase chain reaction
RUE	Radiation use efficiency
RZ	Rib zone
SAM	Shoot apical meristem
SAPE	Streptavidin phycoerythrin
SDS	Sodium dodecyl sulphate
SLA	Specific leaf area
SSU	Small subunit (RUBISCO)
SUSY	Sucrose synthase
TEMED	Tetramethylethylenediamine
TIGR	The Institute for Genome Research
TNC	Total non-structural carbohydrates
UDP-	Uridine 5'-diphosphate
UPSC	Umeå Plant Science Centre
WB	Wash buffer
WT	Wild type
XET	Xyloglucan endotransglycosylase
XTH	Xyloglucan endotransglycosylase/hydrolase
XGO-SRs	Xyloglucan oligosaccharide sulphorhodamine conjugates

DECLARATION

I, Laura Elizabeth Graham, declare that the thesis entitled 'The effects of elevated carbon dioxide concentration on leaf growth and development in *Populus*' and the work presented in it are my own. I confirm that:

- This work was done wholly or mainly while in candidature for a research degree at this University;
- Where any part of this thesis has previously been submitted for a degree or any other qualification at this University or any other institution, this has been clearly stated;
- Where I have quoted from the work of others, the source is always given. With the exception of such quotations, this thesis is entirely my own work;
- I have acknowledged all main sources of help;
- Where the thesis is based on work done by myself jointly with others, I have made clear exactly what was done by others and what I have contributed myself;
- Parts of this work have been published as;

Taylor G, Street NR, Tricker PJ, Sjödin A, Graham LE, Sköglstrom O, Calfapietra C, Scarascia-Mugnozza G, Jansson S. 2005. The transcriptome of *Populus* in elevated CO₂. *New Phytologist*. **167**; 143-154.

Signed:

Date:

ACKNOWLEDGEMENTS

Firstly, I would like to thank my supervisor, Professor Gail Taylor, for her supervision and guidance during this project. I would particularly like to thank her for the opportunity of being involved in numerous European projects. I would also like to acknowledge the Popgenics project, which provided the majority of the financial support.

I would like to thank Alex Helmsey and Melanie Knibbs for assisting in the data collection and analysis of the results presented in Chapters 3 and 4 respectively.

I would like to thank Carol Wagstaff, Matt Cuttle and Anton Page, for their assistance with the microscopy work and Stephen Fry for supplying the XGO-SR's (Chapter 4).

I would like to thank all members of the laboratory for their help with various tasks over the years, in particular those involved in setting up the Closed Topped Chamber experiment and their help collecting data during this time- Nathaniel Street, Mathew Tallis, Caroline Dixon, Mike Cotton, Penny Tricker, Gaia Biggi, Suzie Milner, Maud Viger, Rebecca Rowe, Maricela Rodriguez-Acosta, Nicole Harris, Harriet Trewin, Charlotte Freer-Smith and Aaron Barry.

I would like to thank Andreas Sjödin and Oskar Sköglstrom for their help with the POP2 microarray experiments and subsequent data analysis. I am indebted to Delphine Vincent for her continual help with all aspects of the proteomics work and for conducting the Blast2GO analysis, and to Aurélien Barre for conducting the statistical analysis on the proteome data.

I would like to thank Mathew Tallis, Penny Tricker and Carol Wagstaff for their support and discussions relating to my studies. I would particularly like to thank Nathaniel Street for his continual help and assistance during data collection, his help with analysing the microarray data and for the inspiring discussions.

Thanks to Stefan Jansson and Christophe Plomion for allowing me the opportunity to work in their research laboratories and gain valuable experience.

Finally, I would like to thank my family and friends for all of their support, encouragement and patience over the past four years.

CHAPTER 1

General Introduction

1.0 Overview

The sessile nature of plants decrees that they must be highly adaptable in order to survive the conditions defined by their environment. The leaves constitute adaptable appendages of the plant and are crucial for function of the organism since they ultimately determine productivity. Leaves represent the interface connecting the plant with its surrounding environment and providing the plant with carbohydrate via photosynthesis following the capture of light energy in the form of photons. However, leaves have other functions besides their photosynthetic capabilities, and modified forms function as protection (scales), defence (thorns), and in the capture of insects (pitchers) in some species (Fleming, 2003). Furthermore, the sepal, petal, stamen and carpel are all considered to be modified leaves (Tsukaya, 2002).

Ultimately, leaves are responsible for maintaining and sustaining terrestrial life. However, exactly how they form, grow and develop is surprisingly still not fully understood. For example, the size and shape of photosynthetic leaves facilitate their function. The most productive and efficient leaf will be one that has the maximal possible surface area to absorb light energy for photosynthesis. However, they must also be thin in order to maximise the exchange of CO₂, O₂ and H₂O (Tsukaya, 2005). But what are the determinants of leaf size and shape? How will plants cope with our changing climatic conditions and altering resource availability? Have we, as scientists, progressed to such a stage where we can address such issues with confidence? The use of model species (particularly *Arabidopsis*) and developing genomic technologies are beginning to unravel some clues regarding plant growth and development under current (ambient) and future predicted climatic scenarios, but there are still many questions left unanswered.

In this chapter I have reviewed what is currently known about leaf growth and development. I have also discussed some of the knowledge regarding plant growth in future predicted concentrations of carbon dioxide ([CO₂]). Finally, I have described the genomic techniques currently available to plant biologists in order to assess growth differences between plants grown under current and predicted future [CO₂].

1.1 Leaf development

1.1.1 Leaf formation and growth

Leaf development is a complex process involving a series of highly coordinated events, occurring along three spatial axes; the dorsi-ventral (adaxial-abaxial), proximo-distal (apical-basal) and medio-lateral (margin-margin) (Figure 1.1.1).

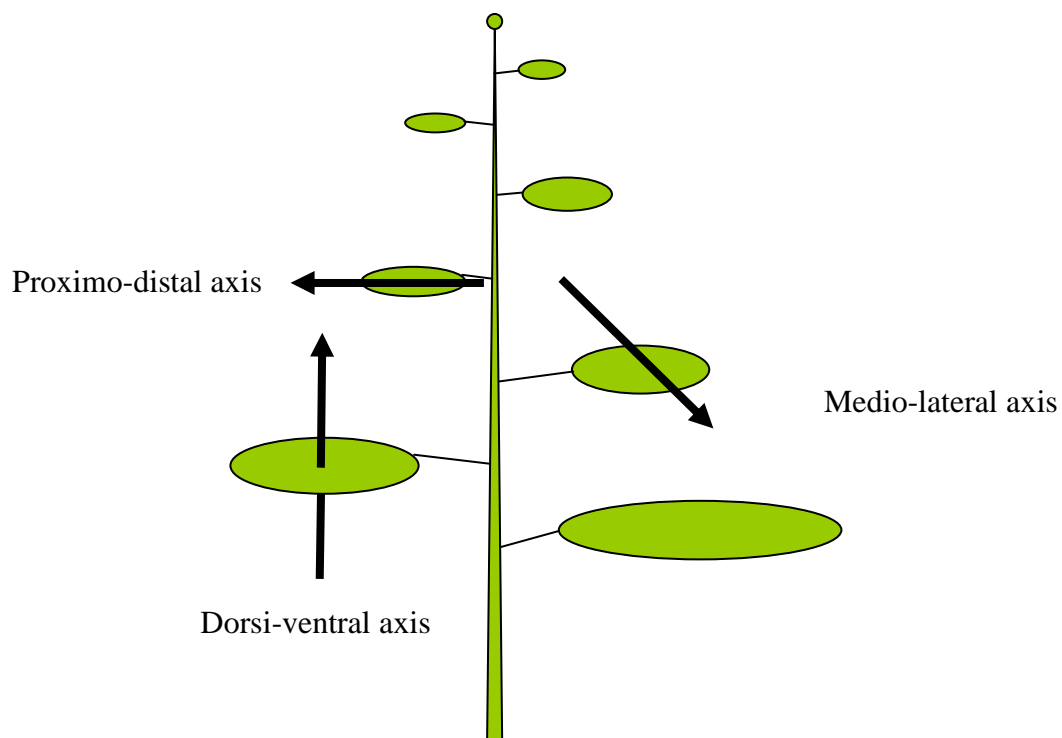


Figure 1.1.1. A model for the three principle axes of leaf development. During leaf formation, development occurs along the proximo-distal (base to apex), medio-lateral (margin to margin) and dorsi-ventral (adaxial to abaxial surface) axes.

1.1.1.1. The Shoot Apical Meristem (SAM)

The formation of fully functional leaves involves many different developmental pathways acting in a coordinated manner, both spatially and temporally. Such processes include the positioning and initiation of leaf primordia, specification of leaf identity, establishment of dorsiventrality, control of cell division and expansion and pattern formation (Micol and Hake, 2003).

Developing leaves are produced on the flanks of shoot apical meristems (SAMs). The SAM is a layered structure consisting of tunica (the surface layer) and corpus (the underlying cell layers). Tunica cells divide anti-clinally and migrate away from the stem cell population and towards the developing primordia (Ingram, 2004).

The cells within the SAM of an angiosperm may be divided into 3 distinct cell layers; L1 and L2 (tunica) and L3 (corpus) (Figure 1.1.2). The cells in the L1 layer become the epidermis, whilst cells in the L2 layer of the primordia become photosynthetic mesophyll cells, and those in the L3 become vascular elements and bundle sheath cells (Taiz and Zeiger, 2002).

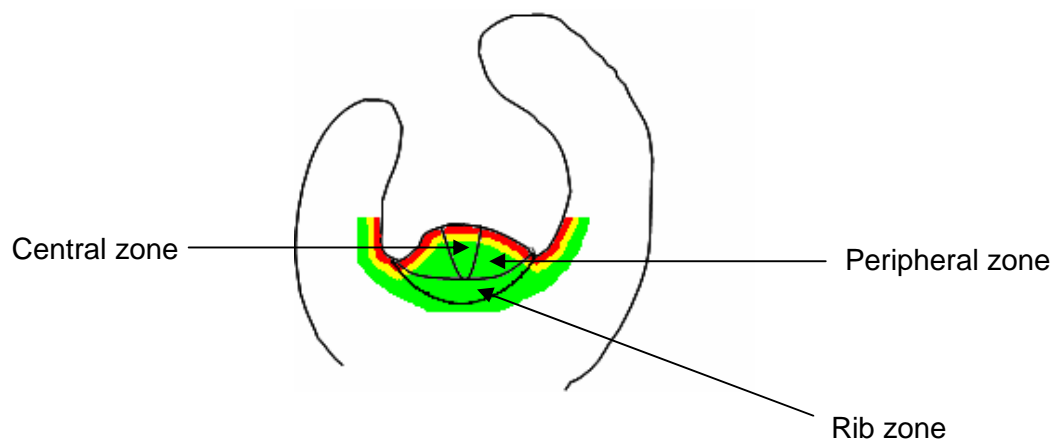


Figure 1.1.2. The structure of the SAM indicating the three cell layers, L1 (red), L2 (yellow) and L3 (green). The three zones of the SAM are indicated. The central zone is involved in meristem maintenance, the peripheral zone is involved in the formation of leaf primordia and the rib zone gives rise to stem tissues.

The SAM is further sub-divided into three separate zones (Figure 1.1.2). The peripheral zone is the area in which the first set of cell divisions occurs, leading to the formation of the leaf primordia. The cells in the central zone are highly vacuolated and flanked by cells from the peripheral zone. They provide a continuous source of stem cells (Hudson and Goodrich, 1997; Traas and Vernoux, 2002). Cells in the rib zone, below the central zone, give rise to the internal tissues of the stem (Taiz and Zeiger, 2002).

Leaves originate from groups of initial cells in the SAM (P0) (Figure 1.1.3). These cells divide rapidly, relative to neighbouring cells, and form the leaf primordia. Auxin flux specifies the site of leaf initiation (Reinhardt *et al*, 2000). The changes in distribution mean auxin levels become concentrated in regions distant from the preceding leaf initiation site (reviewed in Fleming, 2005) thus determining phyllotaxy.

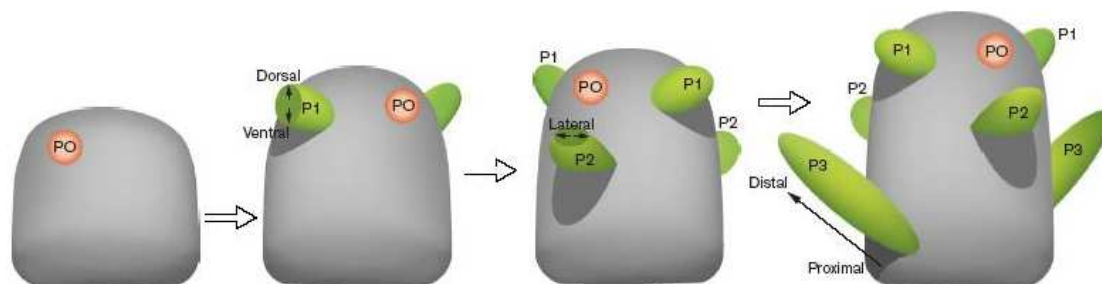


Figure 1.1.3. Plant leaves develop from groups of initial cells within the peripheral zone of the SAM. (P0 is the earliest stage of leaf initiation). The axes of leaf development are indicated on this diagram. Diagram from Hudson (1999).

1.1.1.2. Meristem maintenance

In order to continue to function correctly, the SAM needs to compensate for the cells that have been committed to forming the leaf primordia (Micol and Hake, 2003; Fletcher *et al*, 1999). The *CLAVATA* (*CLV*) signalling pathway is not directly involved in the development of lateral organs but instead represses meristem growth (Hudson and Goodrich, 1997). Along with genes including *WUSCHEL* (*WUS*), the

CLAVATA genes are involved in a feedback system, which maintains the population of stem cells within the SAM.

There are three *CLAVATA* genes, *CLV1*, *CLV2* and *CLV3*, which act to repress the number of cells in the *CLV3* domain (Fletcher *et al*, 1999) (i.e. in the L1 and L2 layers of the central zone in the SAM (see Figure 1.1.2)). The *WUS* gene is expressed in a region deep in the meristem that overlaps with the *CLV1* expression domain (Ingram, 2004). Mutants lacking the *WUS* gene are unable to maintain a functional meristem (Traas and Vernoux, 2002), whereas mutant plants with reduced expression of *CLV* genes possess enlarged meristems due to an accumulation of stem cells (Hudson and Goodrich, 1997; Ingram, 2004). The *CLV* signalling from the stem cell population in the meristem negatively regulates the expression of *WUS* (Schoof *et al*, 2000; Brand *et al*, 2000). The *WUS* gene is required either directly or indirectly, to maintain the expression of *CLV3* and stem cell fate (Ingram, 2004) through a mechanism involving the repression. The fate of the SAM is therefore due to the complex interactions that occur between various genes and their products in the SAM.

1.1.1.3. *KNOX* genes

The regulation of the so-called *KNOX* genes (*KNOTTED-LIKE HOMEODOMAIN*), defined by their homology to *KNOTTED1* in maize (Jackson *et al*, 1994), is crucial for leaf initiation. *KNOX* genes function to maintain meristematic activity and it is known that they activate cytokinin biosynthesis and repress gibberellin biosynthesis to fulfil this purpose (Jasinski *et al*, 2005; Sakamoto *et al*, 2001). The initiation of leaf formation requires the repression of these genes. In particular, ectopic expression of *KNOX* genes has been shown to disrupt normal leaf development (e.g. Byrne *et al*, 2001; Chuck *et al*, 1996).

The *KNOX* gene *SHOOTMERISTEMLESS* (*STM*) acts to repress the expression of *ASYMMETRIC LEAVES1* (*ASI*), thus maintaining the cells in the SAM in an undifferentiated state (Byrne *et al*, 2000). Furthermore, *STM* is also required to maintain *WUS* expression in the meristem, promoting meristematic activity (Mayer *et al*, 1998). *ASI* is homologous to *ROUGH SHEATH2* (*RS2*) in maize (Schneeberger *et al*, 1998; Timmermans *et al*, 1999) and *PHANTASTICA* (*PHAN*) in *Antirrhinum* (Tsiantis *et al*, 1999) (and constitute the ARP family of MYB transcription factors).

These genes are also expressed in lateral organ primordia and act as negative regulators of two different *KNOX* genes (*KNAT1* and *KNAT2*). *AS1* and *AS2* are required to restrict the expression of *KNAT1* and *KNAT2* in the leaves, but not the initial leaf primordia (Ori *et al*, 2000). *AS1* and *AS2* have also been shown to maintain the repression of other *KNOX* genes including *BREVIPEDICELLUS (BP)* (Lin *et al*, 2003) in a pathway regulated by auxin (Hay *et al*, 2006). Furthermore, it is now known that *AS1* and *AS2* bind to each other to suppress *KNAT1* and, in a pathway involving *ERECTA*, promote adaxial cell identity (Xu *et al*, 2003).

1.1.1.4. Establishing leaf polarity

Cell and tissue differentiation occurs whilst the leaf grows. A cell is known to differentiate according to its position within the developing primordia (Brownlee, 2002), which therefore suggests that this is a highly regulated process requiring a large amount of intra- and inter-cell layer communication (Ingram, 2004). The formation of a flat leaf lamina requires spatial and temporal coordination of differential growth throughout the leaf and abnormal morphogenesis occurs when this process is disrupted (Nath *et al*, 2003).

The formation of a polarised leaf is due to signals derived from the meristem (Sussex, 1954; Sussex, 1955). Upon promotion of primordia initiation from the anlagen (i.e. the group of cells capable of forming the primordia), signalling between the two juxtaposed cell layers promotes growth (Waites and Hudson, 1995).

Members of the *YABBY (YAB)* family are transcription factors which are known to affect abaxial cell patterning (Kim and Cho 2006; Kerstetter *et al*, 2001; Sawa *et al*, 1999; Siegfried *et al*, 1999; Golz and Hudson, 1999). *YABBY* genes are expressed initially throughout the incipient primordium but become localised to the abaxial side of each organ (Byrne *et al*, 2001; Fleming, 2005). *YABBY* family members include *CRABS CLAW (CRC)*, *FILAMENTOUS FLOWER/YABBY1 (FIL)*, *YABBY2 (YAB2)*, *YABBY3 (YAB3)*, *INNER NO OUTER/YABBY4 (INO)* and *YABBY5 (YAB5)* (Bowman, 2000). Each member of the family has distinct expression domains. For example, *CRC* is expressed in carpels and nectaries (Bowman and Smyth, 1999), *FIL*, *YAB2* and *YAB3* are all expressed in lateral organs produced by meristematic tissues

(Siegfried *et al*, 1999; Sawa *et al*, 1999) and *INO* is expressed in ovules (Villanueva *et al*, 1999).

A current working model for acquiring leaf polarity involves the class III homeodomain/leucine zipper (HD-ZIP) genes *PHABULOSA* (*PHB*) and *PHAVOLUTA* (*PHV*) (McConnell *et al*, 2001), the *KANADI* (*KAN*) gene family (encoding Golden2/*Arabidopsis* response-regulator/Psr1 (GARP) transcription factors) (Eshed *et al*, 2001; Kerstetter *et al*, 2001) and *YABBY* transcription factors. It has been proposed that *PHB/PHV* is activated by meristem derived signals, causing a repression in the expression of *YABBY* and *KANADI* in cells in the anlagen, closest to the meristem. The adaxial layer (palisade mesophyll) forms from the cells adjacent to the meristem, whilst the reduced *PHB/PHV* signal in the cells distally positioned from the meristem will cause the formation the abaxial (spongy mesophyll) tissue (Bowman *et al*, 2002). The loss of *PHB/PHV* was previously thought to be due to the action of a small, diffusible sterol based factor (McConnell *et al*, 2001), but it has recently been suggested that miRNAs may be involved (Kidner and Martienssen, 2004; Fleming 2005). A summary of these pathways is presented in Figure 1.1.4.

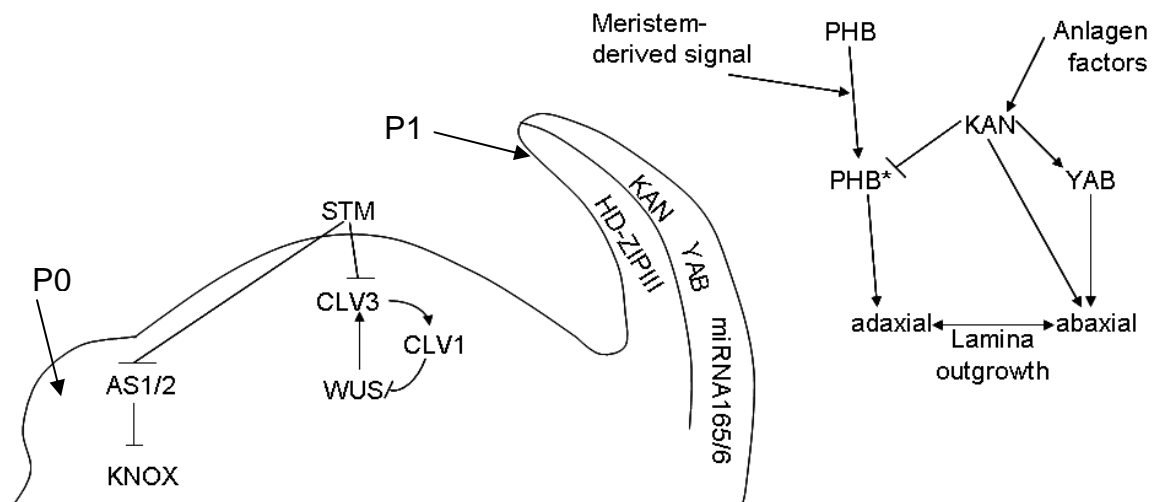


Figure 1.1.4. An emerging model of early leaf development. *STM* acts to repress the expression of *CLV* genes, thus enhancing the expression of *WUS* and therefore maintaining cells in an undifferentiated state. *STM* also represses *AS1/2* expression, which further represses the expression of *KNOX* genes. The pathway on the right of the diagram represents a model for adaxial/ abaxial cell fate. *PHB* (a member of the HD-ZIP III transcription factors) is required for adaxial cell development (note *PHB** represents the activated *PHB* complex). *KAN*, which negatively regulates *PHB**, and *YAB* promote abaxial cell formation. The restriction of HD ZIP III expression to the adaxial side of the leaf is also thought to depend on the activity of miRNAs. Diagram adapted from Bowman *et al*, 2002 and Canales *et al*, 2005. P0 represents the earliest stage in leaf development, whilst P1 represents the forming leaf.

1.1.1.5. Leaf patterning

There are a panoply of patterning genes that affect subsequent growth and development following leaf initiation, as summarised below. Full descriptions are provided in reviews such as Kim and Cho (2006) and Tsukaya (2002b).

Experiments on *ANGUSTIFOLIA* (*AN*) have shown that this gene has a role in regulating leaf width (Tsuge *et al*, 1996) in *Arabidopsis*, which is caused by an abnormal arrangement of cortical microtubules thus altering cell shape (Kim *et al*, 2002). Mutational analyses have shown that alterations in the expression of *ROTUNDIFOLIA3* (*ROT3*) (Kim *et al*, 1999) and *ROT4* (Narita *et al*, 2004) gene cause defects in the leaf length direction. Furthermore, the *CURLY LEAF* (*CLF*) gene in *Arabidopsis* is thought to affect the division and elongation of cells during leaf development (Kim *et al*, 1998).

1.1.2. The cellular basis of development

1.1.2.1. The cell cycle

Any alterations in growth and development are due to changes in either the number or the size of the cells comprising the organ of interest. Therefore, both cell production and cell expansion are critically important in determining organ development and size, and must be considered further here.

There are two main theories that attempt to define the relationship between plant growth and the cell cycle. In the Cell Theory, cells are considered to be the ‘building blocks’ of the organism and growth therefore depends on the rate at which the cells are produced and the size they reach. Conversely, the Organismal Theory states that cell division is a consequence rather than a cause of growth (Beemster *et al*, 2006). In this scenario, cells are considered as ‘compartments in organismal space’ (Beemster *et al*, 2003). Neither theory alone adequately explains the link between the cell cycle and plant growth because they are so intricately linked (Beemster *et al*, 2003). An alternative theory to those detailed above is the *Neo* Cell Theory (Tsukaya, 2002c; Tsukaya, 2003). This theory integrates the role of cell-cell communication in determining organ size and shape.

There are fundamental similarities governing the regulatory processes of the cell cycle in eukaryotes (Lodish *et al*, 2000), but spatial and temporal differences are apparent between different organisms (Hemerly *et al*, 1993). There are four main stages to the cycle; post-mitotic interphase (G1), DNA synthesis (S), post-synthetic interphase (G2) and mitosis (M). Mitosis and endoreduplication represent two different modes of the cell cycle. Endoreduplication involves repetitive chromosomal reduplication with no intervening mitosis or cytokinesis, which thus leads to an increase in ploidy levels. Endoreduplication is also known to affect cell size (Mowforth and Grime, 1989).

During the development of dicotyledonous leaves, cells at the tip of the leaf cease division before those at the base (Nath *et al*, 2003). Increasing cell cycle activity in the basal areas of expanding leaves has been shown to occur in *Arabidopsis* (Donnelly *et al*, 1999).

Growth in elevated concentrations of CO₂ ([eCO₂]) has been shown to influence the duration of the cell cycle. In *Dactylis glomerata*, cell cycle duration was shortened by [eCO₂] and this was attributed to a shortening of the G1 phase (Kinsman *et al*, 1997). An increase in the proportion of cycling cells in the SAM has also been reported in *D. glomerata* (Kinsman *et al*, 1997). In *Populus*, it has been suggested that [eCO₂] affects the G1 and G2/M transition checkpoints (Ferris *et al*, 2001).

Cyclin dependent kinases (CDKs)

In order to function correctly and efficiently, the cell cycle needs to be regulated in a highly coordinated manner. The cyclin dependent kinase (CDK) family are involved in controlling progression through the cell cycle. The CDKs act to regulate the cell cycle by phosphorylating key substrates such as the retinoblastoma protein (De Veylder *et al*, 2001; Morgan, 1997). The activity of CDKs is controlled by transcriptional regulation, protein degradation and interactions with regulatory proteins, of which the largest class are the cyclins (Torres-Acosta *et al*, 2004).

In plants, the CDKs are divided into seven classes (CDKA-CDKG) (Vandepoele *et al*, 2002; Menges *et al*, 2005; Umeda *et al*, 2005; Francis 2007). There are two classes of CDK that permit progression through the cell cycle; A and B. The A-type CDK's are involved in controlling the G1-S and G2-M phase transition (Joubes *et al*, 2000; Inzé and De Veylder, 2006) and protein levels are known to be constant during the progression of the cell cycle (Mironov *et al*, 1999). The B-type CDKs are unique to plants therefore implying that they are involved in plant specific aspects of the cell cycle (Boudolf *et al*, 2004). The PSTAIRE cyclin binding motif is found in all CDKs except CDKB classes. The CDKBs contain either the PPTALRE (in B1 group) or the PPTTLRE (in the B2 group) motif. The activity of the B-type CDKs such as *CDKB1;1* show periodic activity levels, with its peak activity at G2-M phase of the cycle (Joubes *et al*, 2000; Boudolf *et al*, 2004; de Jager *et al*, 2005). The function of CDKC and CDKE are yet to be elucidated, whilst CDKD and CDKF are classified as CDK-activating kinases (Umeda *et al*, 2005).

Cyclins

There are seven classes of cyclins; A, B, C, D, H, T and P (Francis, 2007). The most recently discovered was cyclin P, which has brought the total number of annotated cyclins in the *Arabidopsis* genome to 41 (Torres-Acosta *et al*, 2004). The most well characterised members of the group belong to the A, B and D classes.

The transcript levels of some cyclins and CDKs fluctuate during the progression of the cell cycle (Shaul *et al*, 1996; Mironov *et al*, 1999). The D-type cyclins are most active during the G1/S phase transition as well as the G2/M transition (de Jager *et al*, 2005). However, the abundance of some D-type cyclins is not tightly regulated during the cell cycle (Gaudin *et al*, 2000; Kono *et al*, 2003). For example, transcript levels of *CYCD1* do not change throughout the progression of the cell cycle, but *CYCD2* and *CYCD3* increase at the G1/S phase (Mironov *et al*, 1999). Transgenic tobacco over expressing the *CYCD2*, have a shortened G1 phase, thus increasing cell production with an associated increase in growth rate (Cockcroft *et al*, 2000). However, the transcript levels of cyclins D3a and D3b in *Antirrhinum majus* remain constant throughout the cell cycle (Gaudin *et al*, 2000). It is thought that the D3a and D3b cyclins may not be directly involved in the progression of the cell cycle, but act indirectly by regulating pathways upstream of the cell cycle (Murray, 1997).

Sucrose is a regulator of growth and division (Doonan, 2000) and has a key role in the control of the cell cycle. Levels of A-type cyclins, D-type cyclins and CDKA;1 are influenced by sucrose levels (Richard *et al*, 2002; Rhio-Khamlichi *et al*, 2000; Gaudin *et al*, 2000). Auxin also regulates the transcript levels of cyclins (Ferreira *et al*, 1994). Furthermore, auxin, in combination with cytokinin and sucrose, increase the transcript levels of *CDKB1;1* and *CYCB1;1* in cell cultures of *Arabidopsis* (Richard *et al*, 2002). In the presence of growth factors including sucrose, auxin, cytokinin and brassinosteroids, D-type cyclins associate with A-type CDKs. The resulting (inactivated) complex initiates the G1-S phase transition (Inzé and De Veylder, 2006).

The CDK Inhibitor Proteins

The CDK inhibitor proteins (CKIs) also have the ability to regulate CDK activity, by binding to the cyclin/CDK complex. The ICK1 protein in *Arabidopsis* was the first CKI to be identified in plants (Wang *et al*, 1997). The over-expression of *ICK1*

inhibits cell division and growth (Wang *et al*, 2000), but this effect can be reversed by the expression of D-type cyclins which bind to the CDK inhibitors (Zhou *et al*, 2003).

The Kip/Cip family is one of two groups of CKI proteins that have been identified in mammals. In *Arabidopsis*, seven CKI-like genes known as KRPs (Kip-related proteins) have been identified (De Veylder *et al*, 2001b). The KRPs are active during G1/S phase transition in the cell cycle (de Jager *et al*, 2005). Absciscic acid (ABA) induces the expression of CDK inhibitors and could interrupt the cell cycle by pausing cell division and growth (Doonan, 2000).

CDK Activating Kinases (CAKs)

The activation of CDKs requires the phosphorylation of a tyrosine residue by CDK activating kinases (CAKs). In the *Arabidopsis* genome, there are four CAKs (Shimotohno *et al*, 2004) divided into two classes; CDKD and CDKF (Inzé and De Veylder 2006). Cyclin H is a regulatory subunit of CAK and has been isolated in *Arabidopsis* (*AtcycH1*) (Shimotohno *et al*, 2004), *Populus* (*PscycH1*), and *Oryza sativa* (*OscycH1*) (Yamaguchi *et al*, 2000). The expression of *PscycH1* and *OscycH1* is abundant where cell division activity is high (Yamaguchi *et al*, 2000). However, one of the CAKs that have been isolated in *Arabidopsis*, AtCAK1, has demonstrated cyclin-H independent activity. The AtCAK1 has further been shown to modulate the activities of AtCAK2 and AtCAK4. However, AtCAK2 and AtCAK4 do associate with *AtcycH1* (Shimotohno *et al*, 2000).

The *cdc25* phosphatases are positive regulators of CDKs in yeast and mammals. A small tyrosine phosphatase has also been isolated in *Arabidopsis* (*Arath;cdc25*), which was the first *cdc25*-related protein to be identified in *Arabidopsis* (Landrieu *et al*, 2004), it is active during G2/M phase transition of the cell cycle (de Jager *et al*, 2005). *Arath;cdc25* acts by stimulating the kinase activity of CDKs (Landrieu *et al*, 2004), thus activating them (Figure 1.1.5). However, it has been suggested that B-type CDKs could act as a substitute for *cdc25* phosphatase in order to promote the G2-M phase transition (Boudolf *et al*, 2006)

The Wee1 protein kinases inhibit CDKs. A Wee1 kinase has been isolated in *Zea mays* (*ZmWee1*). This Wee1 kinase was able to inhibit CDK's in maize, and was also

found to be abundant in tissues where a high degree of cell division was occurring (Sun *et al*, 1999). A Wee1 homologue has also been identified in *Arabidopsis* (*AtWee1*), which is active during the G2/M phase transition of the cell cycle (Sorrell *et al*, 2002; de Jager *et al*, 2005). Furthermore *AtWee1* has an identical expression pattern to *AtCDKB1;1*, which is a marker for tissues undergoing cell division. The Wee1 kinases target threonine 14 and tyrosine 15 residues on the CDK. These processes are summarised in Figure 1.1.5.

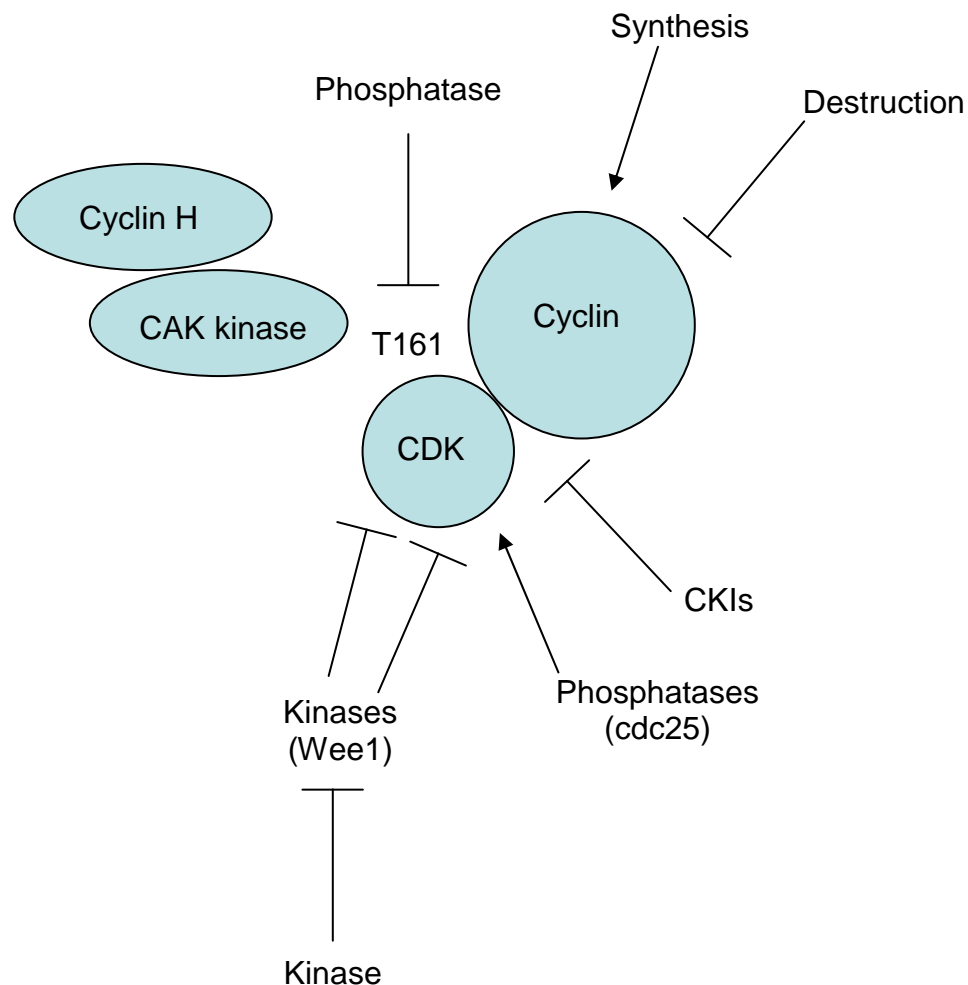


Figure 1.1.5. A generalised checkpoint in the eukaryotic cell cycle. CDKs are activated when bound to the appropriate cyclin. Phosphorylation of a threonine residue by a CAK leads to a binding of the CDK with the cyclin. CDC25 has been isolated in *Arabidopsis* and maize and is a positive regulator of CDKs. The Wee1 kinase acts to inhibit CDKs. The activity of CDKs are also repressed by the action of CKIs (diagram adapted from Francis and Sorrell, 2001).

Retinoblastoma-Related Protein (RBR) and E2F

The retinoblastoma protein (Rb) acts as a suppressor of cell proliferation. The Rb protein is necessary for binding transcription factors (e.g. E2F) that are required for progression through the cell cycle (Doonan, 2000). When dephosphorylated, Rb blocks the entry to G1, thus blocking the cell cycle. When phosphorylated however, Rb dissociates from E2F and its dimerization partner, thereby allowing the activation of the various target genes needed for S phase entry (Lipinski and Jacks, 1999).

Components of the retinoblastoma pathway have been identified in plant systems. For example, D-type cyclins, which contain the LXCXE amino acid motif, known to mediate Rb-binding in humans (Soni *et al*, 1995; Gutierrez, 1998) have been identified. An Rb-related (RBR) protein has been isolated in maize, which contains the functional pocket region of the Rb protein family (Grafi *et al*, 1996).

The interactions that occur between RBR and members of the E2F family of transcription factors permit the progression of the cell cycle. There are six E2F proteins encoded by the *Arabidopsis* genome (designated E2FA-F) (Mariconti *et al*, 2002). E2FA-C form heterodimers with one of two dimerization partners (DPa or DPb). Using E2Fb as a worked example, when bound to DPa and RBR, the complex is inactivated. However, when RBR is phosphorylated (following the phosphorylation of CDKA by a CDKD/cyclin D complex, leading to the binding of CycD3;1 and subsequent activation of CDKA (Francis, 2007)), the E2Fb/DPa complex is released, which promotes transcription necessary for the transition from G1-to-S and G2-to-M phases of the cell cycle (Magyar *et al*, 2005). The over-expression of AtE2Fb in transgenic *Arabidopsis* plants causes modifications to the morphology of the plants, such as reduction in root length and hypocotyl length and a reduction in the cell size of the cotyledons (Sozzani *et al*, 2006). This therefore provides evidence that AtE2Fb is a positive regulator of cell proliferation (Sozzani *et al*, 2006). Furthermore, E2Fb is a target for auxin, and this interaction determines whether cells enter the endocycle, continue in the cell cycle or exit (Magyar *et al*, 2005).

The E2Fa-DPa transcription factor in *Arabidopsis* has been shown to regulate plant cell division. De Veylder *et al*, (2002) showed that E2Fa-DPa in *Arabidopsis* was involved in cell proliferation, differentiation and endoreduplication, and may be an

important rate-limiting factor affecting a cell's ability to divide. Increasing E2Fa-DPa levels was shown to up-regulate the expression levels of S-phase specific genes. This resulted in ectopic cell division correlated with a delay in cell differentiation (De Veylder *et al*, 2002). The transcription of *CDKB1;1*, which promotes the transition to G2-M, is controlled by the E2F pathway (Boudolf *et al*, 2004).

1.1.2.2. Cellular expansion

The cell wall

Plant development and growth involves a highly complex series of events, organised and controlled in a coordinated manner. Growth may be broken down into two categories; cytoplasmic associated growth and vacuole associated growth. During cytoplasmic growth, cells enlarge due to increased cytoplasmic mass and thus require high metabolic activity (Matsubara *et al*, 2006). Increased cell volume by cytoplasmic growth leads to either cell proliferation or endoreduplication (i.e. no intervening mitosis or cytokinesis) (Sugimoto-Shirasu and Roberts, 2003). Vacuole associated growth accounts for the rapid leaf extension in plants (Matsubara *et al*, 2006). This type of growth involves uptake of solutes and water into the vacuole, hence leading to a change in turgor pressure. The structure of the cell must alter in order for it to increase in size, in accordance with an increase in hydrostatic pressure from the osmotic changes in the vacuole. The cell wall is responsible for imposing constraints on cell expansion and thus alterations to its structure are ultimately required for plant growth. The cell wall must be able to withhold the osmotic pressure created within the cell whilst also allowing the cell to expand but not to lose its integrity.

The cell wall is a dynamic structure that modifies its structure throughout the growth and development of the plant (Chivasa *et al*, 2002). The cell wall is composed of two phases; the matrix phase, and the microfibrillar phase. The matrix phase consists of polysaccharides including pectins (e.g. rhamnogalacturonans, galacturonans and galactose and arabinose polymers) and hemicelluloses (e.g. xylans, glucomannans, mannans and xyloglucans), proteins, glycoproteins and phenolic compounds such as lignin. Hemicelluloses are a major constituent of the plant cell wall. The most abundant hemicellulose in the cell walls of dicotyledonous plants is xyloglucan, which form hydrogen bonds with microfibrils.

The microfibrillar phase is comprised of fibrous cellulose microfibrils embedded in the matrix. Sucrose synthase is responsible for the production of uridine 5'-diphosphate (UDP)-glucose following the degradation of sucrose. The UDP-glucose units provide the substrate for cellulose polymerization (Salnikov *et al*, 2001). The processes involved in the biosynthesis of cellulose have been reviewed previously (e.g. Richmond, 2000; Somerville, 2006). Each cellulose microfibril is 3nm in diameter and cross-linked by polysaccharides such as xyloglucan (Somerville *et al*, 2004). Cellulose is comprised of approximately 36 β -1,4-glucan chains (Somerville *et al*, 2004). The cellulose synthase complex (CSC) is responsible for cellulose microfibril biosynthesis. The CSC consists of hexameric rosettes each of which is 25-30nm in diameter (Kimura *et al*, 1999) and each of the six rosette subunits contains five or six CESA proteins (Somerville *et al*, 2004). The distribution of CESA rosettes is partially determined by cortical microtubules (Paradez *et al*, 2006). Ten *CESA* genes have been identified in *Arabidopsis*, and in rice (reported in Tanaka *et al*, 2003), maize has at least 12 (Appenzeller *et al*, 2004), whilst Poplar has at least 18 (Djerbi *et al*, 2005).

Vacuolar associated cell growth relies upon an imbalance between the turgor pressure (hydrostatic pressure) and the tensile force produced by the cell wall. The disparity between the two factors results in the inward flux of water and thereby allows a new physical equilibrium to be reached (Fleming, 2002). The relationship between cell wall expansion and turgor pressure was developed by Lockhart (1965). Influx of water down an osmotic gradient into a plant cell pushes the plasma membrane against the cell wall. The resulting positive internal pressure within the cell increases turgidity, thus providing a force for cell expansion (Brett and Waldron, 1996). An increase in the solute level in the vacuole (due to enhanced photosynthesis in [eCO₂]) could result in a change in turgor and hence wall loosening and growth (Ferris and Taylor, 1994).

XET/XTH

An increase in cell size requires a change in the osmotic potential in the vacuole, along with a change in the main structural components of the cell wall, which restricts cellular growth. Altering the extensibility of the plant cell wall allows turgor pressure

to drive cell expansion (Cosgrove, 1993). A number of proteins have been proposed that are involved in altering the architecture of the cell wall in order to permit cellular growth.

The most widely recognised groups of cell wall modifying proteins are the xyloglucan endotransglycosylases (XETs). This group of enzymes is thought to allow the separation of microfibrils by catalysing the transglycosylation of xyloglucan tethers, the major hemicellulose in cell walls (Fry *et al*, 1992). The xyloglucans cross link adjacent cellulose microfibrils and, once ‘cut’ by the XETs, they facilitate the formation of a new bond with another xyloglucan chain, thus maintaining the integrity of the cell wall (see Figure 1.1.6). However, the role of XETs in plant cell growth has been subject to some controversy (McQueen-Mason *et al*, 1993).

There have been many reports where increased XET activity is correlated with increased cell expansion, and hence, growth (Burstin 2000; Uozo 2000). In *Festuca pratensis*, *FpXET1* has been shown to be a marker for tissue elongation and leaf growth (Reidy *et al*, 2001). Along with their putative role in cell expansion, XETs have also been implicated in the formation of the secondary cell wall (which follows the cessation of cell expansion) (Bourquin *et al*, 2002) as well as disrupting the wall connections between adjacent leaf cells during airspace formation of spongy mesophyll (reported in Campbell and Braam, 1999). However, there have also been reports of the presence of XET in areas where cell expansion has terminated (e.g. Pritchard *et al*, 1993) which may be attributed to increased auxin concentration ([auxin]) (Catalá *et al*, 2000). It has been suggested that in some cases XET may play an alternative role, such as in wall degradation (reported in Bourquin *et al*, 2002).

The nomenclature of the enzymes that catalyze xyloglucan endohydrolysis and/or endotransglycosylation in the literature is somewhat confusing. In the review by Rose *et al* (2002), they suggest using the term XTH (xyloglucan endotransglycosylase/hydrolase) as an all-encompassing term that covers enzymes such as XETs and EXGTs (endoxyloglucan transferases) which essentially belong to the same class of genes.

Expansins

Expansins represent a second group of cell wall loosening proteins, which induce stress relaxation and extension in plant cell walls (Cho and Cosgrove, 2000). These proteins have a unique ability to induce wall extension without a hydrolytic breakdown of the major structural components of the cell wall (Cho and Cosgrove, 2000). It is this property of expansins that allows the cell wall to extend in a controlled and regulated manner without causing lasting changes in the structure (Cosgrove, 2000) (see Figures 1.1.6 and 1.1.7).

There are two classes of expansins; α and β . In *Arabidopsis*, there are 26 α -expansin genes (denoted *EXPA1-EXPA26*) (Cosgrove, 2004) and six β -expansin genes (*EXPB1-EXPB5*). *Populus trichocarpa* has at least 36 expansin genes (Sampedro *et al*, 2006). The expansin that is expressed depends upon tissue type. The α -expansins have been proposed to control cell wall enlargement and may also play a role in cell wall disassembly and cell separation, whilst the β -expansins are involved in the penetration of pollen through maternal tissues into the ovule (Cosgrove, 2000).

The expansin proteins are thought to act by weakening the non-covalent bonding that exists between wall polysaccharides. This allows a 'polymer creep' to occur, since it aids the release and re-binding of the glycans to the cellulose microfibril (see Figure 1.1.6). It is thought that expansin movement is restricted to lateral movement along the microfibril (Cosgrove, 2000).

Along with the effects on the cell wall, expansins also affect plant phyllotaxy. Experiments have been conducted whereby expansin induced leaves were shown to influence subsequent phyllotaxis in *Nicotiana tabacum* (Pien *et al*, 2001). Similar results have been reported in tomato where, after an application of localised expansin, phyllotaxy was disrupted and an ectopic outgrowth was produced (Fleming *et al*, 1997; Fleming *et al*, 1999).

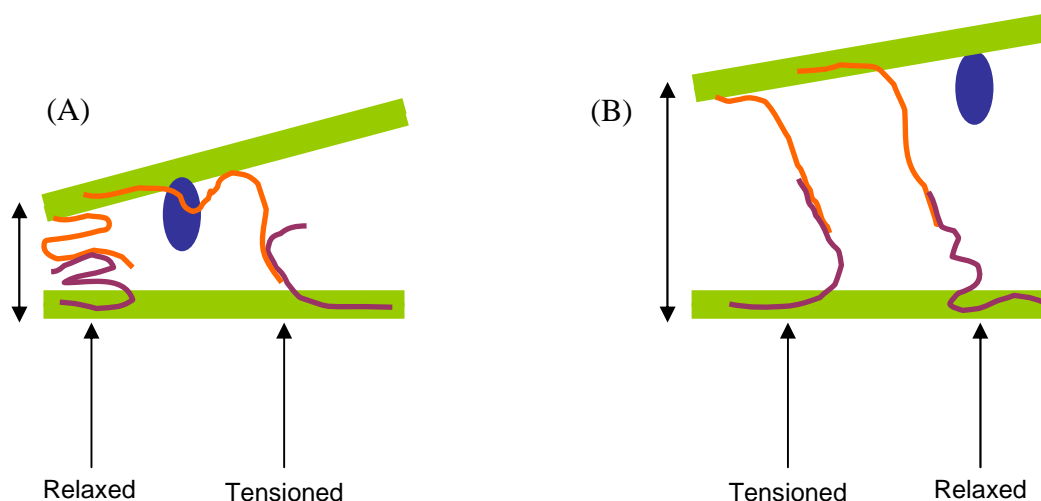


Figure 1.1.6. Cellulose microfibrils within the cell wall are linked by glycans. It has been proposed that the expansin proteins (blue) disrupt bonding of the glycans (orange and purple) to the surface of the microfibril (green) (A), or to each other. This can result in a displacement of the microfibrils (B). Diagram adapted from Cosgrove, (2000).

Putative cell wall modifiers

The involvement of yieldins in cell wall structural modifications is less well known. They affect the extension of cell walls by altering the yield threshold of epidermal and cortical cell walls (Okamoto-Nakazato *et al*, 2001). It is thought that yieldins lower the energy required to split the bonds between microfibrils (see Figure 1.1.7) (Hager, 2003).

Similarly to yieldins, hydroxyl radicals ($\cdot\text{OH}$) represent a less well-documented group of cell wall modifiers. The $\cdot\text{OH}$ are short lived and site specific (Fry *et al*, 1997) and are known to be involved in wall loosening in maize coleoptiles (Schopfer *et al*, 2002). The $\cdot\text{OH}$ radicals cause wall loosening and short-term extension growth similarly to auxin. Incidentally, auxin can also induce the production of $\cdot\text{OH}$. The use of $\cdot\text{OH}$ scavengers, such as benzoate, suppresses the auxin-induced growth of maize coleoptiles (Schopfer *et al*, 2002). It has been suggested that they are important during physiological processes such as germination, growth and fruit ripening (Fry, 1998).

Potassium ions (K^+) have been proposed as having a role in growth since applications of K^+ channel inhibitors such as tetraethylammonium chloride have been shown to reduce the growth rate, whilst growth is restored after the inhibitors are removed

(Tode and Lüthen, 2001). A model of cell wall growth incorporating the possible cell wall modifiers outlined here is shown in Figure 1.1.7.

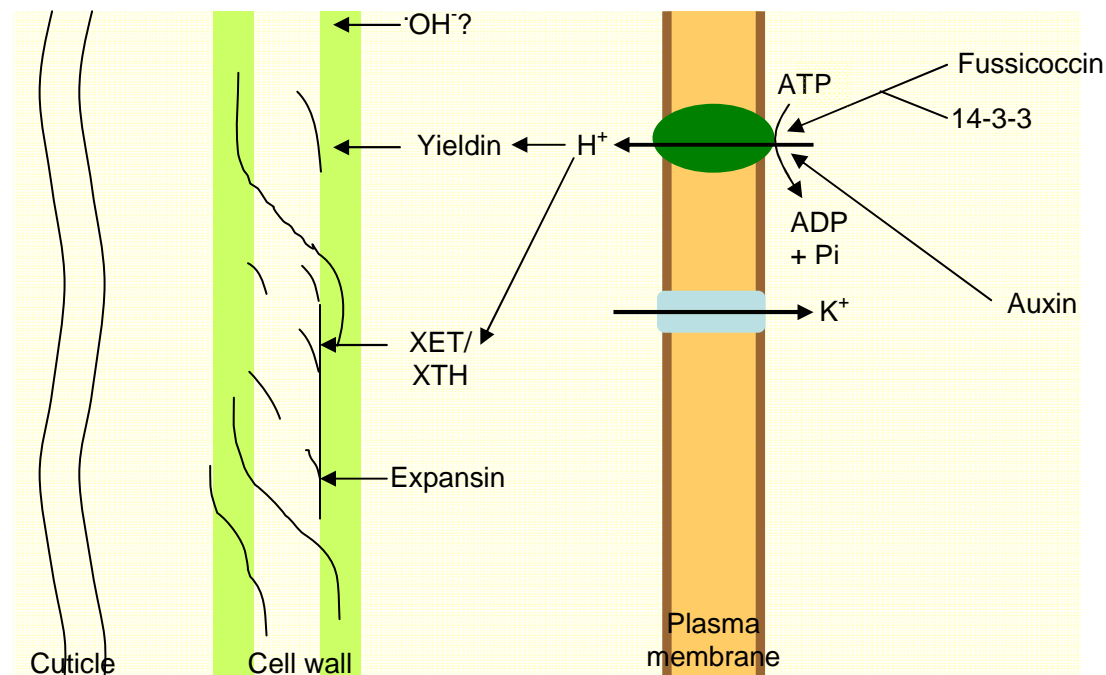


Figure 1.1.7. The proposed mechanism of cell wall expansion. The XETs, expansins and yieldins have all been postulated to play a role in cell wall extension. The XGH/Ts (xyloglucan hydrolase/endotransferase) have also been suggested to hydrolyse xyloglucans. Diagram adapted from Hager 2003.

The acid growth theory

The acid growth theory for auxin induced cell elongation is widely accepted as a mechanism for promoting cellular growth (Rayle and Cleland, 1992), although there are some exceptions (e.g. Kutschera and Schopfer, 1985; Keller and Van Volkenburgh, 1998). An alternative mechanism proposes that auxin stimulates gene expression of some glucanases that catalyse the hydrolysis of cell wall polysaccharides (Tanimoto and Masuda, 1968), although this hypothesis has received little attention.

The acid growth theory stems from several observations, which have shown that cell extension increases if the surrounding milieu is acidic. According to the acid growth theory, protons act as an intermediate between auxin and cell wall loosening. Auxin is produced at the shoot apex and transported basipetally to the tissues below the shoot

apex. The reversible binding of auxin can activate the H^+ ATPase on the plasma membrane, causing a decrease in pH due to the import of protons and extrusion of potassium ions. Whilst auxin is thought to activate the plasma membrane H^+ ATPase in a regulated feedback system, the fungal toxin fusicoccin (FC) activates it irreversibly (Hager, 2003).

The increased activity of putative cell wall loosening factors under acidic conditions has lent further support to the theory of acid growth. High levels of XET activity correlate with acidic conditions and yieldins have also been shown to be activated by a low pH (Okamoto-Nakazato *et al*, 2000).

1.1.2.3. Epidermal cell fate

Stomatal development

Stomata regulate gas exchange (of water vapour and CO_2) between the plant and its environment. It is this role which makes stomata important in the context of carbon assimilation and water use efficiency, and they are therefore important in determining the overall productivity of the plant in its environment. The amount of carbon that passes through stomata has been estimated at 300×10^{15} g per year (Bergmann, 2005).

In *Arabidopsis*, the initial stage in stomatal initiation is the asymmetric division of a protodermal cell. This produces one large cell (which is destined to become a pavement cell) and a small cell known as a meristemoid. The meristemoid behaves similarly to a stem cell and may undergo 1-3 asymmetric divisions, thus producing further meristemoids as well as epidermal cells known as neighbour cells (NCs). After this set of asymmetric divisions, guard mother cells (GMCs) are produced, which divide symmetrically to produce a stoma. The NCs may also undergo asymmetric divisions, which give rise to a daughter cell and a smaller cell, termed the satellite meristemoid. Stomatal patterning involves the appropriate orientation of asymmetric divisions in the NCs, which should result in the satellite meristemoid being finally positioned away from any pre-existing stoma or stomatal precursors (thus maintaining the one cell distance). In *Arabidopsis* cotyledons, stomatal precursor cell formation stops earlier in the adaxial than the abaxial epidermis, and of the stomata that do form,

75% are derived from satellite meristemoids in the abaxial surface, compared with 35% in the adaxial surface (Geisler *et al*, 2000; Geisler and Sack, 2002).

In *Arabidopsis*, a number of genes have been identified as being involved in stomatal development in *Arabidopsis*, including *TOO MANY MOUTHS (TMM)*, *STOMATAL DENSITY AND DISTRIBUTION1 (SDD1)*, *FOUR LIPS (FLP)* and *FAMA*. Mutations in either *TMM* or *SDD1* result in an increase in stomatal density (SD) and a degree of stomatal clustering and thus breaching the one cell distance rule (Berger and Altmann, 2000; Bergmann *et al*, 2004). The *TMM* gene is involved in determining the correct orientation for the plane of the asymmetric divisions that pattern the stomata (Nadeau and Sack, 2003). In developing leaves, expression of *TMM* is highest in the youngest cells of a stomatal lineage (Nadeau and Sack, 2002). The *TMM* gene is known to be a receptor-like protein localised on the plasma membrane, although its signalling partner has yet to be identified (Bergmann, 2005).

Stomata have the ability to respond to changes in the local and global environment (Hetherington and Woodward, 2003). Such responses can occur within minutes of an environmental change, or over a timescale of many thousands of years. This therefore means that stomatal density and distribution data can be used to predict atmospheric CO₂ concentrations from millions of years ago (Royer, 2001). The mechanism for this response has recently been elucidated in *Arabidopsis*. Mature leaves of *Arabidopsis* grown in [eCO₂] signal to young leaves, which then develop with reduced stomatal density (Lake *et al*, 2001). In *Arabidopsis*, the HIC (high carbon dioxide) gene has been identified, which encodes an enzyme involved in fatty acid synthesis and acts as a negative regulator of stomatal development (Gray *et al*, 2000).

Trichome formation

In contrast with stomatal development, the formation of trichomes (epidermal hairs) does not involve a set of stereotypical cell divisions. The formation of trichomes is thought to be due to competitive interactions between neighbouring cells (Schnittger *et al*, 1999).

Trichome initiation occurs in the basal regions of young leaves (Hülkamp *et al*, 1994; Larkin *et al*, 1996). There are a number of genes that have been identified as

having a role in the initiation and formation of trichomes. The *TRANSPARENT TESTA GLABRA1* (*TTG1*) (Koorneef, 1981) and *GLABRA1* (*GL1*) (Koorneef *et al*, 1982) loci are known to govern trichome development. *TTG1* interacts with basic helix loop helix (bHLH) proteins, which in turn interact with a third set of proteins which include *GL1*. The bHLH proteins include *GL3* (Payne *et al*, 2000), *ENHANCER OF GLABRA3* (*EGL1*) (Zhang *et al*, 2003) and *TRANSPARENT TESTA8* (*TT8*) (Nesi *et al*, 2000). Whilst *GL1* and *TTG1* (which interacts with ‘*R*’ (Lloyd *et al*, 1992; Galway *et al*, 1994)) are activators of trichome initiation, *TRIPTYCHON* (*TRY*) acts as an inhibitor (Schnittger *et al*, 1999).

Trichomes are examples of endoreduplicating cells, with a distinctive structure depending on their location. For example, leaf trichomes have a characteristic branched structure, whilst those located on stems are generally unbranched. The *SIAMESE* (*SIM*) gene encodes a mitosis repressor and hence is involved in the process of endoreduplication in *Arabidopsis* (Walker *et al*, 2000).

CO₂ enrichment

1.2.1 An enriched atmosphere

The increase in the concentration of greenhouse gases such as CO₂ is altering the composition of the Earth’s atmosphere. The increase in [CO₂] in recent years can largely be attributed to anthropogenic activities such as burning of fossil fuels and land use changes such as large-scale deforestation events, which occur on a global scale.

The levels of CO₂ began to increase following the onset of the industrial revolution in the 19th Century, at which time levels were estimated to be around 280ppm (Prentice *et al*, 2001). Data collected from the National Oceanic and Atmospheric Administration (NOAA) Mauna Loa observatory has estimated that [CO₂] was 376ppm in 2003 (Bhattacharya, 2004), and peaked in May 2004 when levels were 380.63ppm (<http://cdrg.ucsd.edu/maunaloa.html>).

Whilst some of the CO₂ produced is absorbed by terrestrial ecosystems and oceans, the remainder accumulates in the atmosphere (approximately 3.2 gigatons per year

(Schimel, 1995)). Carbon uptake increases with decreasing latitude (Valentini *et al*, 2000) and European forests are currently acting as a terrestrial carbon sink (Janssens *et al*, 2003). The quantification of carbon sequestration potential of a forest requires information regarding gross primary productivity (GPP), net primary productivity (NPP) and net ecosystem productivity (NEP). Carbon is lost sequentially along this pathway. The NEP has been used to assess the extent to which ecosystems remove carbon from the atmosphere (Grace *et al*, 2004). Studies on *P. alba*, *P. nigra* and *P. x euramericana* at the EUROFACE site in Italy have shown that GPP is stimulated under Free Air CO₂ Enrichment (FACE) conditions (Wittig *et al*, 2005). This stimulation declined over three years of study, but this was attributed to the transition from an open to a closed canopy, rather than photosynthesis acclimation (Wittig *et al*, 2005). Information regarding GPP, NPP and NEP is required in order to determine a value for the net biome production (NBP), which represents the amount of carbon that remains after respiratory and non-respiratory (e.g. fire and forest clearance) factors have been taken into account. Approximately two thirds of terrestrial carbon is stored below ground. This store contributes a large proportion to the NBP, since it is protected from above-ground disturbances that result in a loss of stored terrestrial carbon (e.g. fires) (IGBP Terrestrial Carbon Working Group, 1998). NBP is the parameter to consider for long-term carbon storage potential (IGBP Terrestrial Carbon Working Group, 1998).

1.2.2 Plant growth in [eCO₂]

Numerous studies have been conducted in a variety of plant species in order to elucidate the responses to [eCO₂] and to predict how they will grow under future climatic scenarios. The observation that plant growth is stimulated in [eCO₂] is almost unanimous in all published work, although the degree of response is dependent upon the species studied. For example, a study on native chalk grassland herbs has shown that responses to CO₂ differed between each of the four species in terms of specific leaf area (SLA), leaf area, biomass and number of leaves (Ferris and Taylor 1993). Similarly, above-ground responses to [eCO₂] and [eO₃] differ in magnitude between different aspen clones (Karnosky *et al*, 2003). Furthermore, the response to [eCO₂] in dioecious species (*P. tremuloides*) has been shown to be dependent upon gender (Wang and Curtis, 2001).

At the whole-plant level, leaf area (Tricker *et al.*, 2004), leaf shape (Taylor *et al.*, 2003), petiole length (Rae *et al.*, 2006), leaf area index (Wittig *et al.*, 2005; Liberloo *et al.*, 2004), plant height and branching (Pritchard *et al.*, 1999) are all stimulated under [eCO₂]. The stimulation in leaf growth has been attributed to a number of key processes. Firstly, photosynthesis increases in [eCO₂] (Bernacchi *et al.*, 2003) which hence leads to increased production of carbohydrates. An increase in assimilate transport and carbohydrate availability at the SAM causes an increase in cell division (reported in Pritchard *et al.*, 1999). Secondly, stimulated root growth (Lukac *et al.*, 2003; Calfapietra *et al.*, 2003) and increased water use efficiency (Drake *et al.*, 1997) in plants grown in [eCO₂] may result in an increase in cell expansion due to changes in cell turgor. Furthermore, cell growth is facilitated by alterations in the structure of the cell wall. Elevated CO₂ affects the structure of the cell wall by altering the polysaccharides (Ferris *et al.*, 2001). Cell wall plasticity (i.e. the irreversible extension of the cell wall) increases in [eCO₂], along with the activity of the putative cell wall loosening factor, XET (Ferris *et al.*, 2001, Taylor *et al.*, 2003).

Plant growth in [eCO₂] causes increased rates of photosynthesis, increased light-use efficiency, improved water-use efficiency, decreased stomatal conductance (and stomatal aperture) and decreased transpiration (Drake *et al.*, 1997). It is known that seasonal leaf carbon gain is due to the capacity for photosynthesis and the timing and rate of development (Curtis *et al.*, 1995). The fixation of carbon via the Calvin cycle depends upon the protein Rubisco (Ribulose-1,5-bisphosphate carboxylase/oxygenase). This enzyme is involved in carboxylation reactions (in photosynthesis) and oxygenation reactions in photorespiration. Both CO₂ (for photosynthesis) and O₂ (for photorespiration) compete for the active site of Rubisco. An increase in [CO₂] is associated with an increase in carboxylation rate of Rubisco, at the expense of oxygenation of RuBP, thus causing a decrease in photorespiration and hence increased water-use efficiency. This increase in carbon fixation requires no additional light, water or nutrients (Drake *et al.*, 1997). In the current climate, Rubisco is not saturated with CO₂ and therefore it will still respond to increasing levels with more carboxylation reactions (Drake *et al.*, 1997).

The increase in growth and productivity as a result of exposure to [eCO₂] leads to further increase in productivity through positive feedback, (i.e. increased leaf area

initially resulting in increased photosynthetic activity, leading to further plant growth) (Long *et al*, 2004). However, plants do not respond to [eCO₂] indefinitely. An increase in photosynthesis levels in plants grown under high [CO₂] causes an increase the carbohydrate pool in source leaves (Curtis *et al*, 1995). The plant's capacity to utilise this additional carbohydrate determines further responses to CO₂ enrichment (reviewed in Rogers and Ainsworth, 2006). Commonly, the increase in photosynthesis and concomitant increase in soluble sugars is indicative of a source-sink imbalance (Stitt, 1991) and results in a repression of further photosynthetic activity. This photosynthetic acclimation to [eCO₂] is due to a repression of the genes involved in photosynthesis and the mobilization of stored reserves, along with the induction of genes required for carbon metabolism or storage (Pego *et al*, 2000). This carbon metabolite mediated repression of gene expression is common to all higher plants (Pego *et al*, 2000).

Associated with prolonged [eCO₂] exposure is a reduction in Rubisco SSU (small subunit) levels. Using 'switching experiments' (i.e. grow the plants in [aCO₂] and transfer to [eCO₂] and *vice versa*) it has been possible to investigate sink-limited and source-limited photosynthesis (Gesch *et al*, 1998). Such experiments have shown that transcript levels of Rubisco SSU are reduced following switching from [aCO₂] to [eCO₂] (relative to the [aCO₂] control) and increased when switched from [eCO₂] to [aCO₂] (relative to the [eCO₂] control) (Gesch *et al*, 1998). The reduction in photosynthesis in plants acclimated to [eCO₂] may be due to redistribution of nitrogen from Rubisco and other Calvin cycle enzymes to newly developing leaves, although this idea has received little support from FACE experiments (Ainsworth and Long, 2005).

The repression of photosynthetic activity during prolonged growth in [eCO₂] is due to sugar-mediated signal transduction events (Smeekens, 2000). The action of cell invertases causes the hydrolysis of sucrose into hexose sugars (glucose and fructose). High invertase activity induces the 'cycling' of sucrose and hexose sugars (Goldschmidt and Huber, 1992). The hexose sugars evoke a series of signal transduction events leading to the down-regulation of photosynthesis (Long *et al*, 2004). Hexokinase is an enzyme that phosphorylates hexose to hexose phosphate and acts as a 'hexose flux sensor'. Hexokinase mediates the repression of Rubisco SSU

transcription (Moore *et al*, 1998; Moore *et al*, 1997; Jang and Sheen, 1994) at night (Cheng *et al*, 1998). Prolonged night time hexose metabolism ultimately reduces the levels of Rubisco protein by sugar-mediated repression of genes involved in photosynthesis (Cheng *et al*, 1998).

1.2.3 Experimental systems

The development of appropriate experimental systems is important in providing information regarding response to [eCO₂] at the ecosystem level. Such experimental systems have allowed the study of the effects of [eCO₂] on various aspects of plant physiology, including leaf development.

1.2.3.1. Free Air CO₂ Enrichment experiments

The Free Air CO₂ Enrichment (FACE) system is designed to release pure CO₂ to the surrounding environment at high velocity through a series of small pipes (Miglietta *et al*, 2001). The use of FACE experimental systems allows crops, forest plantations and natural vegetation to be exposed to elevated carbon dioxide levels (Miglietta *et al*, 2001). The Web-FACE design provides an alternative to the traditional octagonal infrastructure associated with FACE experiments. This type of system uses a series of tubes interwoven amongst the forest canopy to deliver CO₂ to the plants (Pepin and Körner, 2002). However, the octagonal ring design of conventional FACE systems remains the most popular choice.

One of the main advantages of the FACE system is that it allows large areas of undisturbed canopy to be studied (over more than one growing season), whilst avoiding edge effects and other unnatural disturbances in the growing environment (Rogers *et al*, 2004). Furthermore, rooting volume is not restricted, a factor which is known to influence the response of plants to [eCO₂] (Thomas and Strain, 1991).

Numerous studies monitoring plant growth under future predicted climatic scenarios using FACE systems have been conducted to date (e.g. see Li *et al*, 2007 for review) in a diversity of species. Such species include cotton, wheat and sorghum (in the Arizona FACE system (<http://www.uswcl.ars.ag.gov/epd/co2/co2face.htm>)); white clover and perennial ryegrass (Switzerland) and rice (Japan (http://ws234.niaes.affrc.go.jp/riceface/Introduction_to_RiceFACE/English/sld001.ht

m)). The infrastructure of the FACE system may also be altered in order to study the effects of [eCO₂] on trees. Such experiments include EUROFACE (*Populus euramericana*, *P. alba* and *P. nigra* (<http://www.unitus.it/euroface/>)); ASPENFACE (*Populus tremuloides* (<http://aspenface.mtu.edu/>)); and BangorFACE (*Betula pendula*, *Alnus glutinosa*, *Fagus sylvatica* (<http://www.bangorface.org.uk/>)).

There are some problems associated with the use of FACE technology. For example, a large infrastructure is required in order to supply the canopy with the appropriate amount of CO₂ (Miglietta *et al*, 2001). Furthermore, there are associated problems with short-term fluctuations in [CO₂] due to natural turbulence, as well as the cost of setting up and running such a large-scale experiment. However the system does have the advantage over other experimental systems (such as Open Topped Chambers (OTCs), Controlled Environments (CEs), solar domes) in that it enables researchers to investigate responses at the ecosystem level.

The type of experimental system used in [eCO₂] studies is known to influence plant responses (Van Oijen *et al*, 1999). There have been a number of studies reporting the effects of [eCO₂] on leaf growth mechanisms in FACE systems (Ferris *et al*, 2001; Taylor *et al*, 2003; Tricker *et al*, 2004) and in open top chambers and controlled environments (Taylor *et al*, 2001) which have highlighted the importance of careful data interpretation, taking into consideration the type of experimental system used. Taylor *et al*, (2001) have shown that the absolute rates of leaf extension in *Populus* were affected by the growth conditions, i.e. FACE, OTC or CE.

1.3 Plant models

Arabidopsis is the most commonly recognised model plant species. Its ease of propagation, widespread availability and potential for genetic manipulation, has facilitated progression and understanding of complex processes in plant molecular biology. Furthermore, it was the first plant to have its entire genome sequenced (AGI, 2000). However, the practicality of using such a plant is limited, especially when considering experimentation within a broad, ecological context. For example, *Arabidopsis* may not be used for investigations into wood formation or seasonality of growth (Jansson and Douglas, 2007). In order to study the effects of a wider range of

biological processes than can be assessed by *Arabidopsis* alone, the *Populus* genus has emerged as an alternative model species.

1.3.1 *Populus* as a model species

Populus is the model tree genera and includes deciduous trees such as aspens, poplars and cottonwoods (Bradshaw *et al*, 2000). There are approximately 40 species in the *Populus* genus all of which are widely distributed throughout the Northern hemisphere in a range of diverse habitats (Sterky *et al*, 2004). *Populus*, which, along with *Arabidopsis*, also belongs to the angiosperm Eurosida I clade (Jansson and Douglas, 2007), is an economically important genus, responsible for pulp and paper, veneer, engineered wood products, lumber and energy production (Rae *et al*, 2007).

Populus is extensively favoured as a model tree due to its rapid growth rate and wide natural distribution, which, similarly to *Arabidopsis*, provides a huge potential source of variation. Such properties of *Populus* ensure direct applications of poplar research in disciplines such as ecology, conservation, breeding and biotechnology (Strauss and Martin, 2004). The natural variation in *Populus* is manifested in various aspects of tree morphology, anatomy, physiology, phenology and response to biotic and abiotic stress (Bradshaw *et al*, 2000).

The *Populus* genus can be split into 5 sections (Figure 1.3.1). *Populus trichocarpa* and *P. deltoides*, which are the main subjects of this report, belong to sections Tacamahaca and Aigeros respectively. *Populus* hybrids are common in natural environments, but some incompatibility exists within and between sections (Figure 1.3.1).

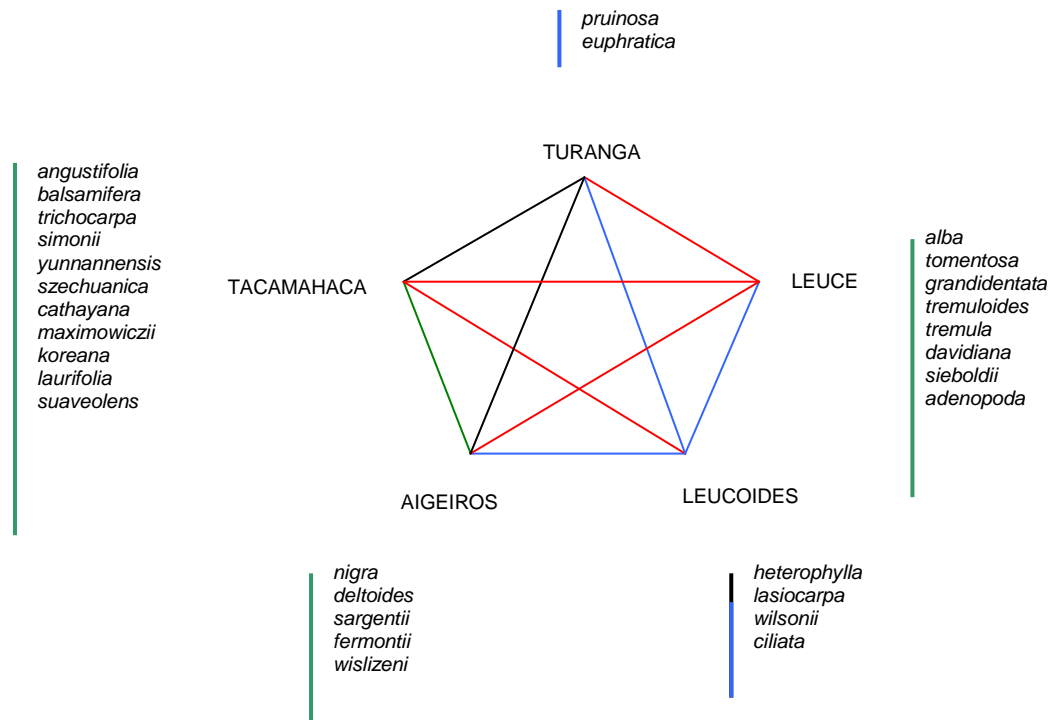


Figure 1.3.1. An illustration of possible hybrids in the *Populus* genus, both between the five sections (main picture), as well as between species within each section (vertical lines). Green lines indicate fertile crosses, black indicate incompatibility, red indicates difficult crosses, blue indicates no information available. Diagram adapted from http://www.na.fs.fed.us/spfo/pubs/silvics_manual/volume_2/Populus/Populus.htm.

During the 1920s, the first investigations into the *Populus* genome took place (Graf, 1921). In 1924 it was found to be comprised of 19 chromosomes (Harrison, 1924). The genome is small, relative to other trees (Taylor, 2002; Bradshaw *et al*, 2000). such as loblolly pine, which has a genome 40 times larger than that of *Populus* (Brunner *et al*, 2004). Sequencing of the genome of *Populus trichocarpa* ‘Nisqually-1’ has now been completed (Tuskan *et al*, 2006; <http://genome.jgi-psf.org/Poptr1/Poptr1.home>). The genome of *Populus trichocarpa* (410Mb) encodes more than 45, 000 putative protein coding genes (Tuskan *et al*, 2006).

1.4 Transcriptomics

1.4.1 Microarrays

Microarrays have become increasingly popular in recent years as a genomics tool for investigating the changes in gene expression that occur on a genome wide scale. Microarrays are used to determine transcript profiles of entire or partial genomes at a particular developmental stage or in response to an environmental stress or treatment. They have become useful for studying global gene expression profiles during plant development (Brinker *et al*, 2004) for example, to study the gene expression in cell wall biosynthesis in *Pinus taeda* (Whetten *et al*, 2001). They allow gene expression profiling following stimuli such as growth, metabolism, development, behaviour and adaptation of living systems to be investigated (Heath *et al*, 2002). The application of microarray technology allows the relative expression levels of many genes to be determined simultaneously with a high degree of sensitivity (Aharoni and Vorst, 2001).

1.4.1.1. History

Microarrays are principally a quick and relatively simple method for analysing gene expression. Their use can span many different scientific disciplines from medicine to ecology, allowing expression levels of genes that are important in growth, metabolism, development, behaviour and adaptation of living systems, to be investigated (Heath *et al*, 2002). Their use far exceeds simple gene expression analysis of comparing treatment and controlled samples: for example they also can be used for analysing DNA polymorphisms using Diversity Arrays Technology (DArT) (Jaccoud *et al*, 2001; Wenzl *et al*, 2004). Since their adolescence, the technologies involved in the production, implementation and analysis of microarrays have improved considerably.

1.4.1.2. Principles

A microarray consists of a number of lengths of DNA attached to a solid matrix. The process relies on complementary base pairing between the immobilised DNA on the slide and that of the sample. In accordance with conventional terminology, the immobilized cDNA on the substrate is referred to as the 'probe' whilst the extracted sample population in question is the 'target'. Following hybridisation the relative

abundance of the transcripts may be assessed by inspecting the intensity of the signal produced for each probe on the array.

1.4.1.3. Substrates

Nylon filter membranes are one type of substrate that may be used for microarray construction. Such arrays (termed ‘macroarrays’) are easy to manufacture and simple to use. However, with the continuing developments in microarray production, they are becoming less commonly used. One of the reasons for this is that the probe density on these membranes is low, thus providing the researcher with less information than may be gained by using an alternative substrate such as glass. Furthermore they require the use of radioactive targets and it is therefore not possible to conduct simultaneous hybridisations of different samples. Instead, the membrane needs to be stripped and re-hybridised in order to attain a full data set (this may be done up to a maximum of five times). In addition, the large volumes of reactants that are required for the hybridisations reduce the efficiency of the reaction.

Glass is generally the standard substrate of choice in microarray production given that it has many advantages over other substrates. One of its main advantages is that it permits the use of fluorescently tagged targets since it has low inherent fluorescence. Fluorescent dyes have a higher resolution than radioactive labels and therefore an increased spotting density on the slide is possible. This therefore provides a detailed picture of global expression. The use of fluorescent dyes also allows simultaneous hybridisations to be performed (a strategy not possible with radioactive labels). Glass is inert to high ionic strength buffers and when coated with substances such as poly-L-lysine, amino-silane or amino-reactive silane, the immobilization of DNA onto the surface of the slide is enhanced (Burgess *et al*, 2001). The coatings also enhance the hydrophobicity of the slides and limit the spread of deposited DNA on the surface (Duggan *et al*, 1999). Furthermore, since glass substrates are flat, rigid and transparent, the locations of the probes are easy to identify and thus images of high quality can be produced (Southern *et al*, 1999). Probes deposited onto substrates such as nylon do not follow the strict geometric patterning found on glass substrates (Duggan *et al*, 1999) and are therefore spotted at lower densities.

1.4.2 cDNA microarrays

There are two types of microarrays commercially available for gene expression studies; cDNA and oligonucleotide microarrays. cDNA microarrays are more commonly used since they are cheaper and easier to produce than oligonucleotide arrays, and they do not require full sequence information for probe production.

There are two categories into which the manufacture of a microarray may fall; 'synthesis' and 'delivery' (Schena *et al*, 1998). cDNA microarrays fall into the latter category (the 'synthesis' category is comprised of oligonucleotide microarrays, which will be discussed later in section 1.4.3). The material spotted onto cDNA microarrays is derived from library collections. They are amplified by PCR and following purification, they are deposited onto the substrate at known coordinates.

1.4.2.1. Experimental procedures

The experimental process of producing a cDNA microarray is illustrated in Figure 1.4.1. The process begins with a reverse transcription stage to generate cDNA copies of the original mRNA population. The two cDNA populations are labelled with two fluorescent dyes with differing absorption and emission spectra, either during (direct labelling) or following (indirect) the reverse transcription step. The most commonly used are the cyanine dyes; Cy3, which absorbs light at 552nm and emits at 568nm; and Cy5, which absorbs at 650nm and emits at 667 nm.

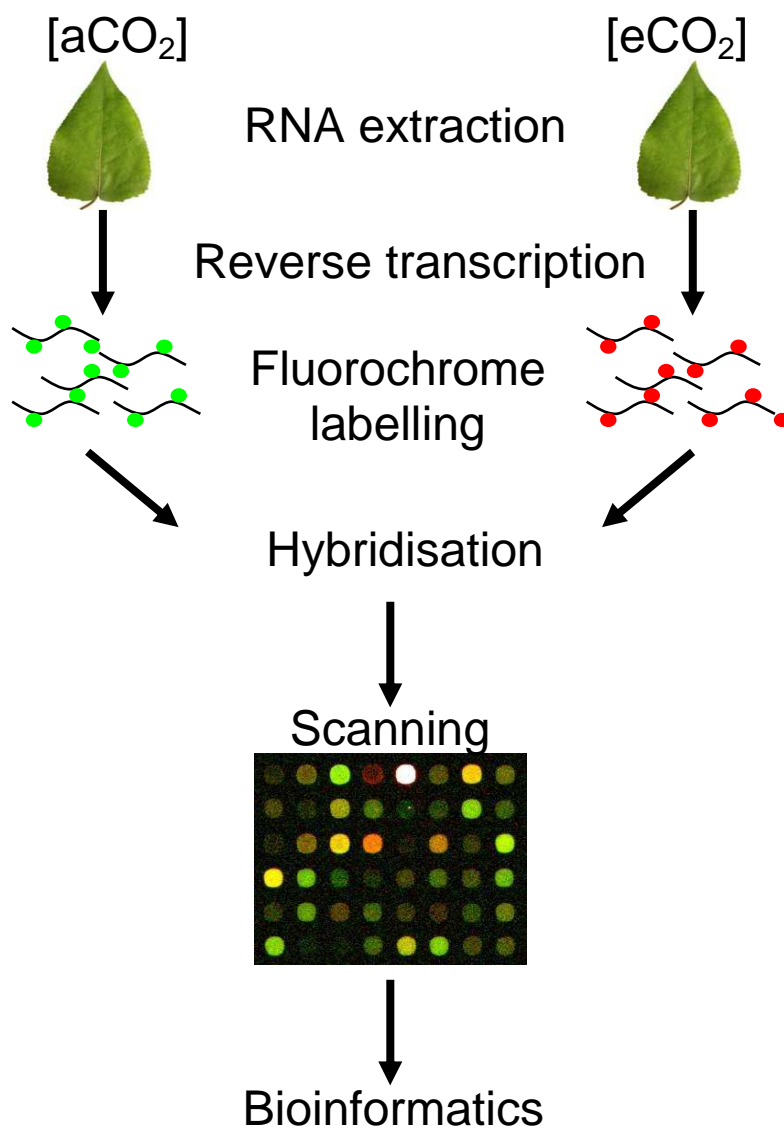


Figure 1.4.1. A schematic of the process of a cDNA microarray experiment. RNA is extracted from two sample populations, reverse transcribed and labelled with one of two fluorescent dyes. The samples are combined and hybridised onto a single array. Following hybridisation (commonly lasting approximately 14 hours) the slide is imaged. The resulting data files are then analysed.

The hybridisation phase of the experiment typically lasts for 14 hours. Commonly this is done using a hybridisation station where the samples are injected into a sealed chamber containing the slide. Alternatively, hybridisation may be carried out manually. The slides are washed and dried following hybridisation thus removing any unbound target material and preparing them for insertion into a laser scanner.

The resolution of the scanner is such that it examines each of the thousands of probes on the slide with a resolution of 5-10 μ m per pixel. This process relies on the different excitation wavelengths of the fluorescent dyes. Each spot on the array is exposed to the excitation wavelengths of the two dyes used in the reaction and the light emitted is recorded. These intensities are used to generate comparative expression ratios for each spot on the array.

Following scanning, the intensity data needs to be matched with the probe information. This process can be done using computer packages such as GenePix (Axon Instruments, Union City, California). In this program the files from the scans are loaded and falsely coloured (Cy5 is coloured red and Cy3 is coloured green). A grid is laid over the composite image from the two channels (i.e. Cy3 and Cy5). Within each grid are a number of circles which correspond to the number of probes in that area. The GenePix software is used to overlay the circles on the appropriate spots (a process made easier by the strict geometric regularity of the spots due to the robotic deposition of the probes). GenePix will 'flag' any spots considered inappropriate for further analysis e.g. saturated spots (where the intensity is skewed) or those where the foreground (i.e. spot) intensity is low. The median pixel intensity of the foreground data is used for further analysis. Information on the background intensity is gained from the middle 'valley' region between two adjacent spots.

1.4.2.2. Limitations associated with the use of cDNA microarrays

Due to the nature of microarray experiments, the results from one single experiment can provide information regarding the quantitative hybridisation data for thousands of probes. However microarrays may be considered as a 'closed system' and only the sequences that are represented on the arrays can be measured (Primrose and Twyman, 2006). Therefore the choice of EST collections that are spotted need to be suited to the purpose of the experiment. Furthermore, promoters, introns and intergenic sequences which play a role in gene regulation are not represented on cDNA microarrays (Mantripragada *et al*, 2004).

Another problem with microarrays is that abundant genes are often over-represented in cDNA libraries, whereas rarely expressed transcripts and those induced only under specific conditions are often missing, resulting in the possibility of overlooking some

important regulatory genes (Breyne and Zabeau, 2001). Furthermore, there may also be a problem with cross hybridisation on a microarray. Transcripts from genes that exhibit a high degree of sequence homology have the potential to cross hybridise on the slide (Breyne and Zabeau, 2001). Therefore array choice and EST selection needs to be considered carefully when designing experiments. The data also needs to be analysed with an understanding of the limitations of the technique.

1.4.3 Oligonucleotide microarrays

Oligonucleotide microarray production is an example of the 'synthesis' classification of technologies (as defined by Schena *et al*, 1998). Here, I will be concentrating on one particular type of oligonucleotide microarray (Affymetrix), since it is most applicable to my work.

Although expensive to produce, Affymetrix microarrays are distinctly advantageous since the probes are designed according to existing genomic sequence data. Therefore the only limitations on the experiment are the physical size of the array and the achievable lithographic resolution (Lipshutz *et al*, 1999). The probes are constructed *in situ* by rounds of nucleotide additions, a process made possible through the use of photolithography technology, developed by Steve Fodor and colleagues (Lipshutz *et al*, 1999).

1.4.3.1. Photolithography

The technique for oligonucleotide microarray production using photolithography is very simple (see Figure 1.4.2). The probes are designed *in silico* and the way in which they are produced ensures there is no risk of probe misidentification as there is with cDNA arrays (e.g. misidentified tube, PCR contamination etc). A silane reagent is added to the substrate (quartz) to provide hydroxylalkyl groups which act as initial synthesis sites (Heller, 2002). These sites are extended with linker groups protected with special photolabile protecting groups (Heller, 2002). Upon exposure to UV-light, the protecting group is removed, which allows nucleotides to bind. However, in order to construct probes of specified sequences photomasks are used which protect certain probe sites from the light. Upon exposure to light, the protecting group remains intact and the nucleotides cannot bind. However, the nucleotides do bind in the areas where the photomask was absent. The nucleotides that are used in this process all have

protective groups attached to the 5' end, allowing continual progression of probe production. On the next round of synthesis (i.e. for the next set of nucleotides), a new photomask is applied and the required protecting groups are removed from the forming probes in the appropriate positions. The nucleotide set (again attached to a photolabile group at the 5' end) is exposed to the slide and they bind where required. This process ensures that a specific set of probes can be made in a highly organised and coordinated manner.

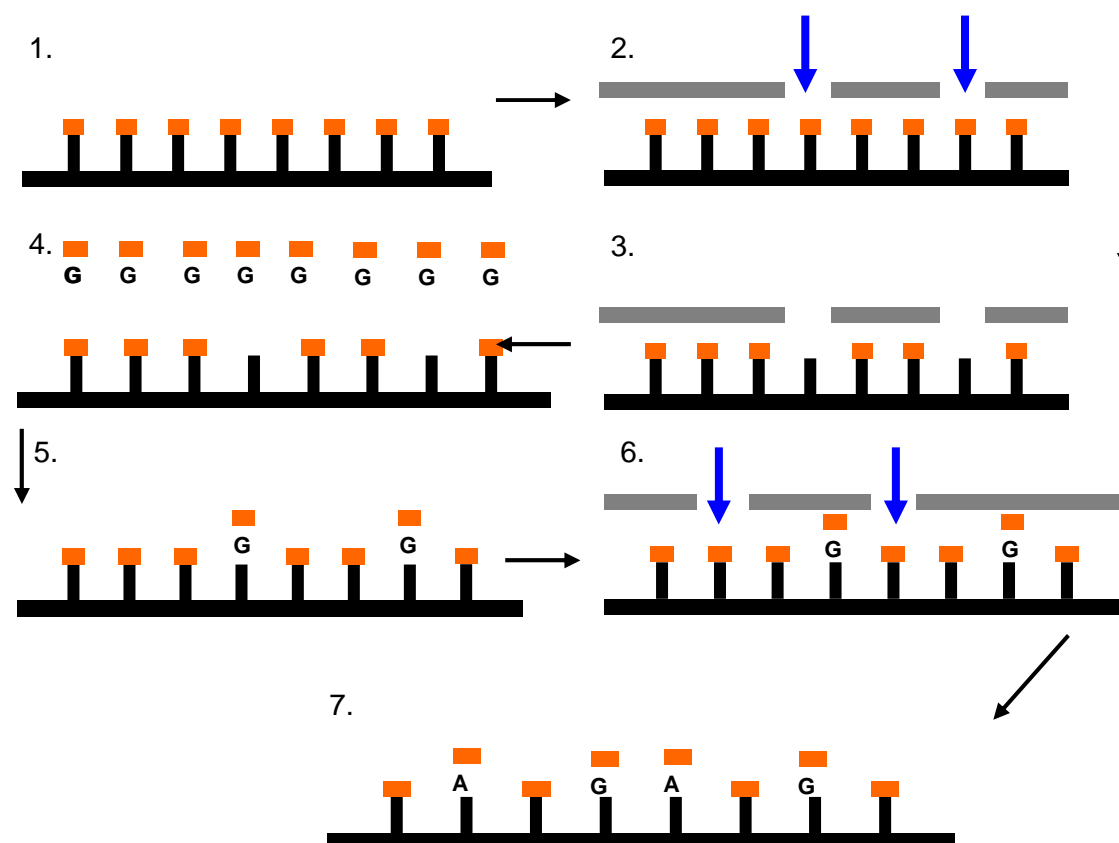


Figure 1.4.2. The construction of an oligonucleotide chip using photolithography. 1) Photolabile groups (orange boxes) protect the sites of probe synthesis from the light. 2) A photomask (grey box) is applied which causes some of the probe sites to be exposed to the light (illustrated by blue arrows). 3) The protective groups are removed upon light exposure. 4) Nucleotides attached to a protective group are applied to the surface (in this case guanine). 5) The nucleotides may only attach where there is no protective group. 6) A new photomask is applied to the surface, causing localised photodeprotection in the required positions. 7) A second set of nucleotides bound to protective groups are applied (in this case adenine). The probe sets continue to grow in this manner following continual rounds of synthesis. Diagram adapted from (Burgess *et al*, 2001).

Another important feature of oligonucleotide microarrays is the presence of ‘match’ and ‘mismatch’ probes which are used as a control to test for the specificity of the hybridisation signal. A set of probes are designed for each gene represented on the chip. Each probe represents a portion of that gene, and is generally 20-80mer long. In the case of both the *Arabidopsis* Affymetrix Genechip (ATH1) and the Poplar Affymetrix GeneChip, there are 11 probe pairs i.e. 11 paired ‘match’ and ‘mismatch’ probes of 23-mers. The difference between the match and mismatch pair is a single base change.

1.4.3.2. Experimental procedures

In contrast to cDNA microarrays (dual channel with competitive hybridisation reactions), Affymetrix oligonucleotide microarrays are ‘single channelled’ i.e. one sample is hybridised on a single slide while the comparative sample is hybridised on a second slide. Samples are compared *in silico* following the reactions. In this type of array, mRNA is extracted and reverse transcribed to produce first strand cDNA. This is followed by second strand cDNA synthesis. The resulting double stranded cDNA is cleaned and followed by *in vitro* transcription for linear amplification of each transcript. The antisense cRNA is labelled via the incorporation of biotinylated CTP and UTP. The biotinylated cRNA is cleaned and fragmented to produce products that are 200 nucleotides (or less) long. The labelled, fragmented cRNA is hybridised onto the chip (usually this takes approximately 16 hours). The chips are washed to remove unbound cRNA. The microarrays are stained using a Streptavidin-phycoerythrin (SAPE) solution. Fluorescence is amplified using biotinylated anti-streptavidin antibody solution mix and an additional aliquot of SAPE stain. The arrays are then scanned. The workflow for an oligonucleotide microarray experiment is illustrated in Figure 1.4.3 (Information from Upenn School of Medicine Microarray facility. <http://www.med.upenn.edu/microarr/> and Affymetrix <http://services.ifom-ieo-campus.it/Affymetrix/protocols.php>).

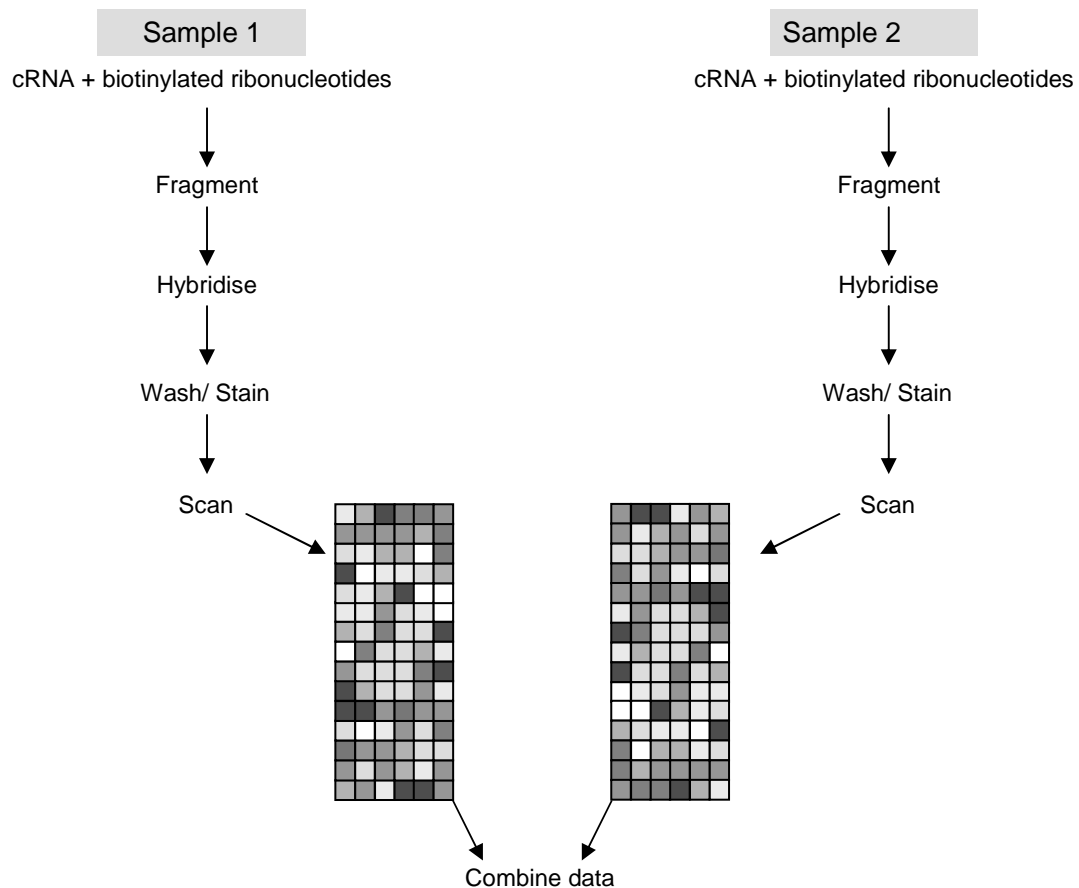


Figure 1.4.3. The generalised workflow for producing an oligonucleotide microarray. Following RNA extraction, the samples are reverse transcribed to produce first strand cDNA. Second strand cDNA is then produced and followed by in vitro transcription for the amplification of each transcript and the incorporation of biotinylated CTP and UTP. The cRNA is fragmented and hybridised. The microarrays are stained with Streptavidin-phycoerythrin stain solution and then washed to remove any unbound material. The chips are scanned and the data is analysed *in silico*. Diagram adapted from Primrose and Twyman, 2006.

One of the main problems with microarrays is that they only provide a picture of transcriptional changes and in some instances, changes at the protein level are not reflected by changes at the mRNA level (Donson *et al*, 2002) and therefore the results of microarray experiments need to be interpreted with caution. However, while there is widespread support for the notion that post-transcriptional events do have a role in modulating gene expression, it is generally accepted that the primary control for gene expression occurs at the transcriptional level (Donson *et al*, 2002).

1.4.4 Experimental design

The nature of microarrays is such that appropriate experimental design requires careful consideration. Regardless of the sample material to be tested, inaccuracies may be produced at several stages during the experiment e.g. sample handling, labelling efficiencies etc.

Appropriate design for microarray hybridisations are subject to some controversy. There is a trade-off between the number of arrays required (according to the experimental design) and cost. The expense of running an array experiment (either in-house or by service) has been a major hindrance to many experimental studies conducted to date. The most important consideration is producing enough data in order to satisfy the question or hypothesis, whilst keeping practical costs to a minimum.

Replication is an important consideration when designing an array experiment. In the context of microarray experiments, replication may refer to

- i) spotting genes multiple times on an array
 - ii) hybridising the RNA samples to multiple arrays
 - iii) using multiple samples to account for inherent biological variability
- (Kerr, 2003; Kerr and Churchill, 2001)

Technical replication ((i) and (ii) above) addresses the measurement error of the assay and act to reduce the uncertainty about gene expression in the particular samples being studied (Kerr, 2003). When designing an experiment it is important to remember that biological replication ((iii) above) is required in order to produce results regarding the population of interest (Kerr, 2003). However, increasing biological replication does present a problem: the number of arrays required and hence the cost of the experiment.

Pooling is a strategy used to reduce the number of arrays required for the experiment whilst still obtaining appropriate information to satisfy the question in hand. However, pooling RNA samples eliminates the possibility of assessing biological variation in the population since the effects will be masked by the presence of

multiple sample representatives (Kerr, 2003). Therefore if it is the response of individuals within a population that is to be investigated, pooling is deemed an inappropriate strategy. However, if the response across different populations was to be studied, pooling would be appropriate to give a global assessment of gene expression differences. There is an ‘in-between’ strategy where multiple independent pools from within a population could be studied (Kendzierski *et al*, 2003) called ‘composite sampling’.

1.4.4.1. Data analysis

The sensitivity of the microarray technique is such that thousands probes may be spotted onto a single array thus producing a detailed picture of expression differences between the two populations in question. Whilst the merits of such techniques are clear, there are also concomitant issues of dealing with vast datasets in order to extract transcripts that are significantly differentially expressed between the two populations.

The most desirable feature of a microarray experiment is the production of thousands of data points as a result of a single hybridisation, providing a ‘snapshot view’ of expression differences between the sample populations in question. However, this also presents a problem in the guise of data analysis. The sheer magnitude of a single microarray has led to a significant amount of research being dedicated to appropriate analysis techniques.

Microarray data analysis can be split into four categories; image analysis, normalisation, detection of differentially expressed transcripts and data mining (Wilson *et al*, 2003). Following image analysis and visual inspection (e.g. through the use of a program such as GenePix (discussed earlier in section 1.4.2)), the resulting data need to undergo some form of normalisation. Normalisation is essential in order to ensure that variations either between slides or on a single slide are minimal. Variations in an experiment can occur at many different stages such as hybridization and processing procedures or differences in scanner settings. Furthermore, differences due to the physical properties of the dyes, the efficiency of dye incorporation or simply unequal starting quantities of RNA cause variations across arrays (Quackenbush, 2001; Yang *et al*, 2002). Despite strict experimental procedures, many

of these stochastic effects cannot be controlled but must be corrected in order to produce meaningful data without the production of false positives.

Normalisation removes systematic variation which affects measured gene expression levels (Yang *et al*, 2002). There are many different types of normalisation procedures that may be performed on the data. The type of procedure chosen is strongly dependent upon the experiment and the desired comparisons that are to be made. Therefore a normalisation that is appropriate for one experiment may not necessarily be appropriate for another.

The results from a single microarray potentially provide data for thousands of different genes. Therefore the appropriate analysis of the data requires careful consideration. Whilst it is important to use an appropriate method so as to not allow the introduction of type I errors (wrongly defining a transcript as differentially expressed), it is also important not to allow type II errors (not reporting a differentially expressed transcript). Generally the analysis depends upon the experimental design and the method that is chosen should be deemed the most appropriate for answering the initial question.

The selection of differentially expressed transcripts provides a set of candidate genes for further downstream investigation. Historically, transcripts termed ‘differentially expressed’ were identified based on fold-change between the control and treated samples (generally a two-fold limit is acceptable). Other methods e.g. Analysis of Variance (ANOVA) have also been used.

The initial results from microarray data analysis will tell you that there are x number of transcripts that are differentially expressed between condition a and condition b . However, in most instances, it is important to understand the function of the genes that have been identified as well as their role within the biological system. Therefore, in order to further explore the data it is possible to use pathway analysis to ‘hone in’ on regions of interest. Two such pathway packages for analysing microarray data are freely available on the internet; MapMan (Thimm *et al*, 2004) and AraCyc (Muller *et al*, 2003). Both programs contain metabolic pathway maps and falsely colour the steps along the pathway according the microarray data that has been supplied. These tools

are particularly important where novel transcripts have been identified, and they provide a user-friendly system for identifying regions of interest for further, more in-depth study.

When appropriately analysed, microarrays generate information regarding gene expression differences between two or more sample populations. The magnitude of the technology allows the identification of novel transcripts to be uncovered. Furthermore, they have been used successfully in combination with other genomic studies (QTL) to identify genomic regions of interest in response to environmental perturbation. For example, differentially expressed transcripts identified by microarrays have been shown to collocate to regions of interest on the genome in drought (Street *et al*, 2006) and [eCO₂] (Rae *et al*, 2006) experiments in *Populus*.

1.4.5 Real time RT-PCR

The nature of microarrays is such that it permits a global screen of the samples in question, leading to the production of a list of candidate genes involved in the response. Due to the nature of conducting the microarray experiment, it is often deemed appropriate to check the results from the transcriptomic study independently (e.g. Taylor *et al*, 2005). A commonly used technique for such applications is quantitative real-time RT-PCR (qPCR).

qPCR is a technique that can be used to determine the relative or absolute expression levels of mRNA from different samples. This technique is becoming increasingly popular within the scientific community and has been used in a variety of applications in a range of species including mice (e.g. Tian *et al*, 2004) humans (e.g. Jordens *et al*, 2000) as well as in *Arabidopsis* (e.g. Charrier *et al*, 2002). qPCR is widely favoured due to its high sensitivity, since it permits the quantification of rare transcripts, or those that show only subtle changes in gene expression (Pfaffl, 2001).

1.4.5.1. Principles

The qPCR reaction takes place over a number of cycles. There are three main stages in each cycle; denaturation, annealing and extension. The primers used in the reaction are designed to replicate the target sequence of interest. The primers bind at the end of the target sequence and only the sequence between the primers are amplified. During

the denaturation step of the cycle, the reaction mixture is heated to 90°C in order to break the hydrogen bonds between the bases of the DNA. This results in the production of two single strands of DNA. During the annealing stage, the primers bind to the complementary target sequence. A temperature of 40-65°C is commonly used for the annealing reaction, although this depends on the size and base sequence of the primers.

The final stage in the cycle is the extension step. A DNA polymerase (eg Taq DNA polymerase) is required in order to make a copy of the target sequence. The DNA polymerase starts the synthesis of the DNA region at the position of the primers. The DNA polymerase facilitates the binding of the nucleotides that are free in solution (dNTPs) with the DNA, and requires magnesium chloride as a cofactor. The DNA polymerase is extracted from bacteria such as *Thermus aquaticus* (Taq), which are able to withstand high temperatures (up to 95°C). This property is extremely important due to the high denaturing temperature required at the beginning of each cycle, therefore eliminating the need to add fresh DNA polymerase after each cycle (Saiki *et al*, 1988), as was required for *E. coli*, the predecessor of *T. aquaticus* (Holland *et al*, 1991).

The qPCR technique is based on the detection and quantitation of a fluorescent reporter. There are three main types of fluorescent reporter; hydrolysis probes (e.g. TaqMan probes, molecular beacons and scorpions) hybridising probes, and DNA binding agents.

1.4.5.2. DNA binding agents

The DNA binding agents fall into two categories; intercalators (e.g. ethidium bromide) and minor groove binders (e.g. SYBR green). The experimental qPCR work in this report involved the use of the SYBR green reporter, and it is described here.

The use of SYBR green is a cheaper alternative to the other varieties of fluorescent reporters. It uses the modified DNA polymerase from *Thermus brockianus* (*Tbr*), which has been designed to accurately detect targets with low copy numbers in a shorter reaction time. SYBR green is specific for dsDNA only (it will not bind to ssDNA) and it fluoresces when bound to the amplified double-stranded target

sequence. The SYBR green works in a sequence independent manner, which therefore requires a melting curve to be produced which verifies whether a single product has been formed (Ririe *et al*, 1997; Lekanne Deprez *et al*, 2002). Without this post-qPCR analysis, there is a risk of generating a false positive result. SYBR green can be used to validate changes in expression between two samples for a number of different genes (although only one gene can be tested in each reaction). This requires specific primers to be used in the reaction.

The SYBR green molecule cannot bind during the denaturation and annealing phase of the cycle due to the presence of ssDNA. During the extension phase, the SYBR green molecule binds to the dsDNA and a fluorescence signal is observed. This process continues and the resulting total fluorescence detected is proportional to the concentration of the amplified product.

1.5 Proteomics

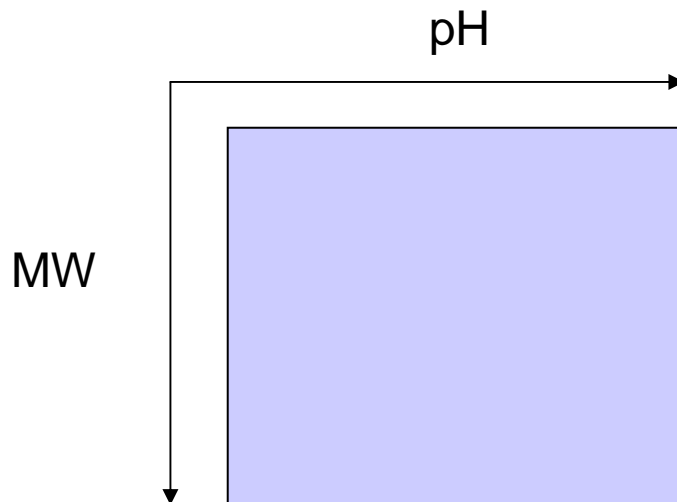
The technique of proteomics is used to investigate the PROTEin complement of the genOME (the proteome) and can be used to quantify protein levels in response to different experimental variables. The developing technology of proteomics is one tool that plant biologists will be able to use in order to further improve genomic data (Bolwell *et al*, 2004) and help confirm the functional identity of genes existing in the genome. Whilst the merits of transcriptomic studies are well documented, mRNA levels and protein levels are often not correlated (Mann, 1999). The study of the proteome is important for further understanding into the mechanisms underlying various biological processes, thus providing additional information to transcriptomic studies.

1.5.1 Principles and techniques

There are several different approaches for quantitative protein profiling, which fall into two main categories; gel-based and non-gel based. The most widely documented technique is a gel based approach which combines two widely used techniques; electrophoresis and mass spectrometry (Süle *et al*, 2004). In this approach, proteins are separated by the implementation of two-dimensional gel electrophoresis (hereafter referred to as 2-DE), where proteins are initially separated according to their isoelectric point in one dimension and by sodium dodecyl sulphate electrophoresis in

the 2nd dimension (O'Farrell, 1975). Following separation, the spots are excised from the gel, digested with trypsin and analysed by mass spectrometry (Figure 1.5.1).

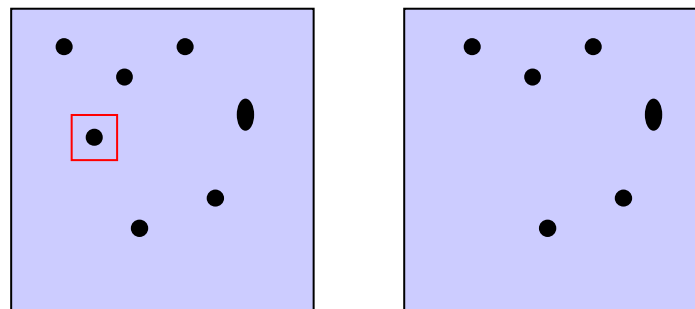
There are some disadvantages associated with the use of 2-DE gels such as the time taken to produce results as well as the degree of expertise required to produce a suitable gel (Quadroni and James, 1999). Furthermore, 2-DE gels are often not an appropriate technique for detecting some membrane proteins, very large or small proteins, or those that are either very acidic or very basic (Gygi *et al*, 1999). It is also apparent that this technique is not appropriate for detecting proteins present in low abundance, a problem known to be influenced by the type of fluorescent dyes used to stain the proteins (Jenkins and Pennington, 2001). For these reasons, non gel-based methods have recently been favoured, although there are as yet no reports of such techniques being used on plant material.



(a)

Condition 1

Condition 2



(b)

Figure 1.5.1. Proteomic strategies using 2-DE gels involve separating the proteins according to their pH and molecular weight (a). Following gel image acquisition (b) it is possible to identify proteins specific to either condition being tested (highlighted by the red square). These spots can be excised, digested with trypsin and the resulting peptides analysed using tandem mass spectrometry.

There are a number of non-gel based methods available, one of which is termed ICAT (Isotope Coded Affinity Tags). This technique works by labelling the proteins containing cysteine residues from two samples with ‘heavy’ (e.g. deuterium) or ‘light’ (e.g. hydrogen) isotopically labelled reagents. The ICAT reagent has three components. One is an affinity tag (biotin) which is used to selectively isolate proteins of interest (Tao and Aebersold, 2003). The second part is a linker to which the stable isotopes are attached and the third is a thiol specific reactive group (Gygi *et al*, 1999).

A similar approach to ICAT has recently been developed, termed iTRAQ (Isobaric Tags for Relative and Absolute Quantification) (Applied Biosystems, www.appliedbiosystems.com), which works on a similar principle, although it is specific for amine residues rather than cysteine residues (Ross *et al*, 2004; Zieske *et al*, 2006).

1.5.2 Peptide identification and analysis

Mass spectrometry (MS) is used to analyse the peptides thus permitting identification. Principally, MS measures the mass-to-charge ratio (m/z) of the peptide ions. There are different types of MS available, but they all have the same four components; an ionization source, mass analyser, ion detector and a data processor.

In order to identify the peptide using MS, they have to be converted to gas phase ions, either by Matrix Assisted Laser Desorption Ionisation (MALDI) or Electrospray Ionisation (ESI). In experiments where MALDI is used, each sample is placed onto a UV-absorbing matrix on a target plate. The target plate is pulsed with UV light causing the desorption of the analyte from the matrix and results in the production of singly protonated molecules. MALDI is usually teamed with a time-of-flight (TOF) mass analyser, which measures the time taken for the ions to reach a detector and thus the resulting mass-to-charge ratio can be calculated once the ions pass through the detector. The TOF is completed under vacuum and low pressure to ensure the ions do not collide with air molecules which would impede their movement.

In this section I shall focus on explaining ESI (as an ionisation source) and ion traps (as a mass analyser) only, since they are most relevant to my work. In contrast to MALDI, where a plate is used, the peptide samples for ESI are in acidic solution. Following chromatographic separation by HPLC (High Pressure Liquid Chromatography), the samples are loaded into a needle and a high positive voltage is applied. The protons from the acidic solution give the peptides a positive charge and the sample is discharged into a capillary in the form of droplets. The solvent evaporates in the capillary, leaving the protonated ions behind, which pass into the mass spectrometer (Figure 1.5.2).

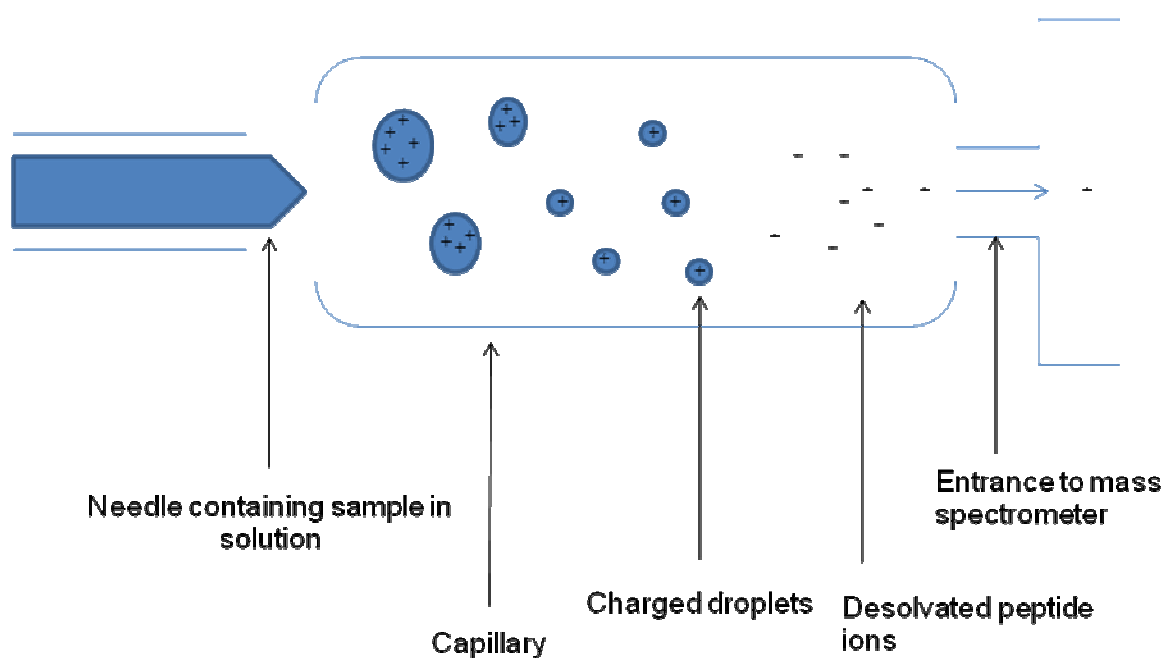


Figure 1.5.2. A generalised view of the processes associated with electrospray ionisation (ESI) to produce protonated ions for analysis by mass spectrometry. A voltage is applied to the needle containing the sample (in aqueous solution). Droplets of sample are dispelled into a capillary where the droplets split due to evaporation of the solution. This leaves protonated peptides which can then be analysed by mass spectrometry. The blue arrow indicates the path of the ions. Diagram adapted from Kinter and Sherman, (2000).

In order to analyse the samples produced from ESI, the protonated ions then pass into an ion trap (Figure 1.5.3). Here, the ions are held in a trap due to oscillating voltages. The mass analysis occurs by sequentially applying differing voltages which permit the exclusion of particular ions in an m/z dependent manner. The ions of particular m/z then pass into the detector for analysis.

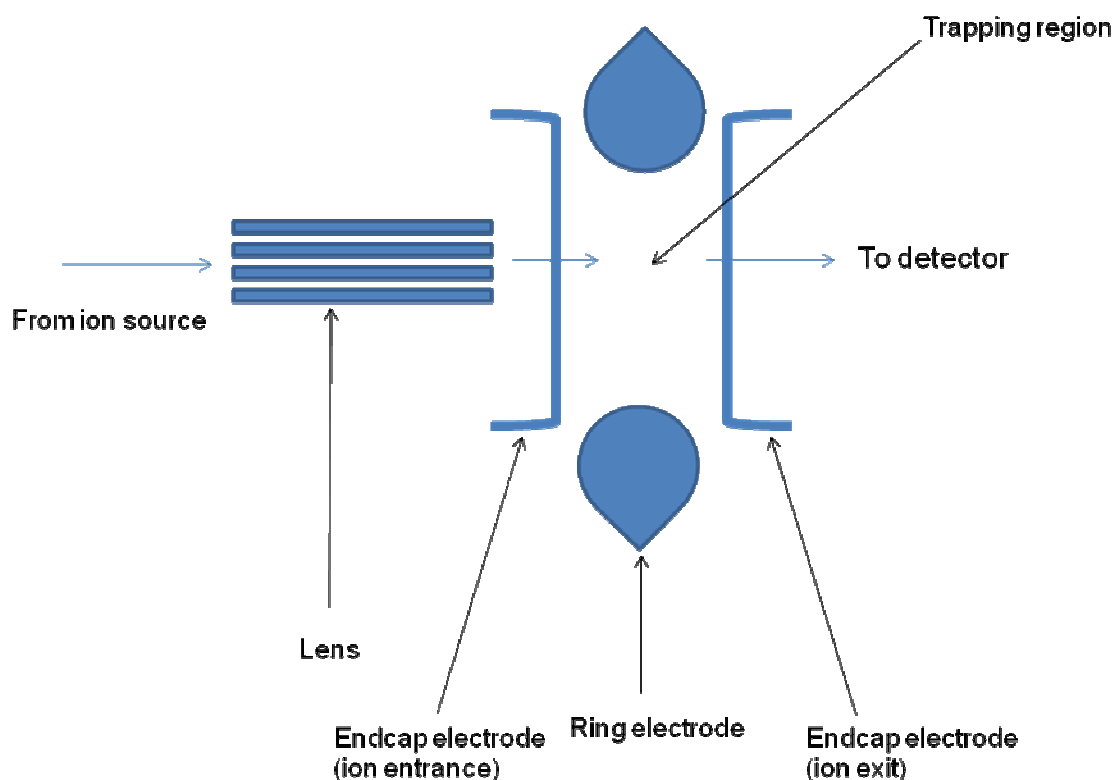


Figure 1.5.3. A generalised view of an ion trap mass analyser. The ions (e.g. from ESI) enter the system and are focussed by a number of lenses. The ions accumulate in the trapping region before being ejected from the endcap electrode into the detector. The blue arrow indicates the path of the ions. Diagram adapted from Kinter and Sherman (2000).

During the first stage of MS, a precursor ion is isolated. In order to gain sequence information from this ion, it must be further fragmented. This is usually completed in a process called Collision Induced Dissociation (CID). In order to fragment, the vibrational energy within the chemical bonds must exceed its strength (Arnott, 2001). In CID, the ions gain internal energy through collisions with an inert gas (usually helium). Low-energy CID causes fragmentation at amide bonds hence leading to the production of characteristic ions for that peptide (Arnott, 2001). The m/z for the fragmented ions are analysed by a second round of MS (hence tandem mass spectrometry or MS/MS). The resulting MS/MS data is then searched using protein databases for identification.

Similarly to microarrays, appropriate methods of quantitation are required in order to unravel the complex results produced from proteomic experiments thus permitting meaningful comparisons to be drawn between samples. There are a number of

databases that have been constructed to aid the interpretation of the results from the mass spectrometry data including MASCOT (Perkins *et al*, 1999), PepFrag (Qin *et al*, 1997), MS-Tag (Clauser *et al*, 1999), PeptideSearch (Mann and Wilm, 1994), SEQUEST (Eng *et al*, 1994) and Sherpa (Taylor *et al*, 1996). Furthermore, a centralised proteomics database has recently been created with the aim of sharing experimental data with other researchers (<http://bioinformatics.icmb.utexas.edu/OPD>) which will further encourage the use of proteomics for future research purposes. The Stanford Microarray Database (Sherlock *et al*, 2001) constitutes a similar scheme that has been set up to allow shared access of microarray data for further transcript analysis and resources for sharing protein data are likely to follow a similar route.

1.5.3 Applications

Proteomics has been successfully applied in *Arabidopsis* to study the proteins found in the cell wall (Chivasa *et al*, 2002). This information has been used to further knowledge regarding the cell wall in relation to plant growth and development. Many acknowledged cell wall proteins with known biological function, were identified in this experiment including expansins, glucanases and peroxidases. A number of previously unnamed proteins, with domains characteristic of cell wall proteins, were also identified. Similar results have also been found in alfalfa (Watson *et al*, 2004). The results of these experiments therefore illustrate that proteomics can provide a great deal of additional information regarding the function of various constituents of the cell and also demonstrate the potential for protein discovery by uncovering various constituents, which had previously gone undetected using other experimental procedures.

Proteomics has been used for protein profiling in *Arabidopsis* in response to [eCO₂] (using 2-DE), although only very small changes in the proteome were detected between the treatments (Bae and Sicher, 2004). It has also been used to detect in proteins in response to ozone in rice seedlings (Agrawal *et al*, 2002). With further developments to the technology, the use of proteomics in plant science in response to environmental changes may be realised.

1.6 Aims and hypotheses

The overall aim of the experiments detailed in this thesis was to understand how leaf development and growth is affected by CO₂. There were three avenues through which this was assessed; morphology, genes and proteins. The aims and objectives of each result chapter are given below;

Chapter 3. *Populus deltoides* and *P. trichocarpa* originate from contrasting environmental habitats. The aim of this experiment was to explore the different growth mechanisms adopted by these two species, which are the main subjects of this thesis.

Chapter 4. The aim of this experiment was to identify the effects of [eCO₂] on leaf growth and development in *P. deltoides* and *P. trichocarpa*. Given the fact that *P. deltoides* has numerous small cells (i.e. leaf size can largely be attributed to cell division) and *P. trichocarpa* has few large cells (i.e. leaf size attributed to cell expansion) it was hypothesized that the two species would respond differently to [eCO₂].

Chapter 5. Previous reports have indicated that leaf growth is stimulated by [eCO₂] in *Populus euramericana* grown at the EUROFACE facility in Italy. The aim of this experiment was to identify the transcripts involved in the response to [eCO₂] in *P. x euramericana*. It was hypothesized that transcripts involved in growth, such as cell cycle genes and cell wall transcripts would be up-regulated in [eCO₂].

Chapter 6. The aim of this experiment was to identify the effects of [eCO₂] on leaf growth and development in *P. deltoides*, *P. trichocarpa* and genotypes deemed to be ‘extreme’ in terms of yield (the genotypes were selected from the F₂ generation of the *P. deltoides* x *P. trichocarpa* cross). There were two hypotheses to be tested here. The first was that the two grandparental species (*P. deltoides* and *P. trichocarpa*) would respond differently to [eCO₂] in terms of leaf and cellular growth. Secondly, it was hypothesized that the two extreme groups would respond differently to [eCO₂]. It was predicted that the low-yielding genotypes would respond to a greater degree to [eCO₂] than the high-yielding genotypes.

Chapter 7. Previous experiments which aimed at identifying the transcripts that are differentially regulated as a result of [eCO₂] yielded some disappointing results (see Chapter 5). The aim of this experiment was to use two different types of microarray platform (cDNA and oligonucleotide) to identify transcripts that were affected by [eCO₂]. Again, it was predicted that transcripts involved in cell wall modification and cell cycle progression would be up-regulated in [eCO₂] but that this would be dependent upon the species.

Chapter 8. Two previous experiments have shown that there are few transcriptional differences between the leaves subjected to [eCO₂] and those subjected to [aCO₂]. For this reason the protein complement of the leaves of the two species was examined. It was hypothesized that there may be proteomic differences due to [eCO₂] as well as species differences between *P. deltoides* and *P. trichocarpa*.

CHAPTER 2

Materials and Methods

2.0 Overview

The following chapter outlines the general materials and methods used throughout this thesis. For each subsequent chapter, any specific technique or modification to an existing method is indicated within the materials and methods section of that chapter.

2.1 Phenotypic analysis

2.1.1 Leaf growth

Leaf images were captured using a Nikon digital camera. Each individual leaf was placed on a white background alongside a 1cm scale bar. The images were captured at a 90° angle to the plane of the paper, in order to reliably estimate the size and shape of the leaf. Throughout the experiments documented in this thesis, leaf one was defined as the first fully unfurled leaf (from the meristem). The dimensions of the leaves (length, width and area) were calculated using the 'Image J' program, which is freely available on the internet (<http://rsb.info.nih.gov/ij/>). Leaf length was measured from the point at which the petiole meets the leaf blade to the tip. Leaf width was measured at the widest point (Figure 2.1.1).

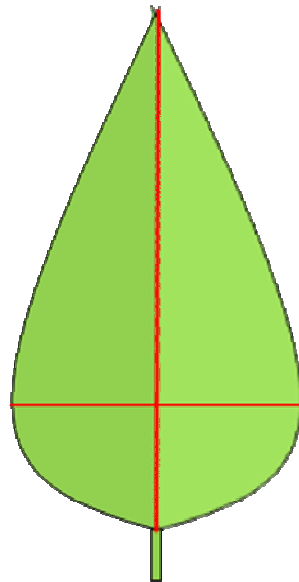


Figure 2.1.1. Leaf length was measured from the tip to the base, where the leaf meets the petiole (vertical red line). Leaf width was measured at the widest part of the lamina (horizontal red line). Leaf area was measured around the perimeter of the lamina only.

2.1.2 Leaf anatomy

Tissues sections were sampled into a fixative containing 3% (v/v) Gluteraldehyde and 0.1M (v/v) PB (provided by A. Page, University of Southampton). Each tissue section was harvested with a scalpel blade to a size of approximately 10x10mm. In each experiment where leaf anatomy was studied, the material was sampled from the second interveinal area of the leaf (where the first interveinal was the most basal (Figure 2.1.2). The material was sent to Anton Page (University of Southampton BioImaging Unit) for sectioning. The mounted samples were then visualised using a light microscope.

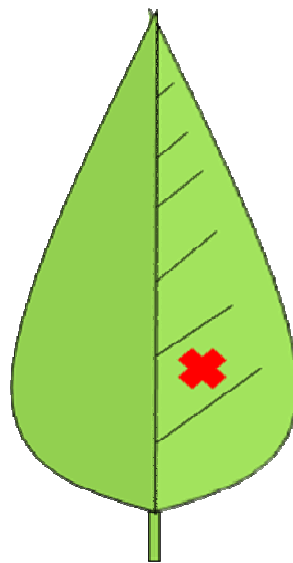


Figure 2.1.2. Material for leaf ultrastructure was sampled from the second interveinal area of the leaf (indicated by the red cross), where the first interveinal area was the most basal.

2.1.3 Specific leaf area (SLA)

The leaves selected for SLA measurements were picked from the tree and the circumference was recorded by drawing around the edge of the leaf onto a brown paper bag. The leaves were placed inside the paper bag and dried in an oven (80°C) for 48 hours. The leaves were weighed after they had been dried. The paper bags were scanned and the resulting JPEG files were imported into Image J in order to calculate the area of the leaf prior to drying. The SLA was calculated by the following formulae;

$$\text{SLA} = \text{leaf area} \div \text{leaf weight}$$

2.1.4 Cellular impressions

Epidermal imprints were captured according to the protocol proposed by Ferris and Taylor (1994). Clear nail varnish was painted onto a small section of leaf (approximately 10mmx10mm). The nail varnish was allowed to dry and a piece of sellotape was used to take the impression, which was then fixed onto a microscope slide (Ferris and Taylor, 1994). The cell images were captured at 200x magnification on a light microscope. The areas of the cells were analysed in 'Image J' and all measurements were taken in μm^2 . In total, ten cells were measured per image to determine an average cell size per leaf in each biological replicate. The average cell area and average leaf area were used to calculate the approximate number of cells in the leaf (leaf area \div average cell size = number of cells per leaf). Stomatal density was calculated by determining the size of the field of view and dividing it by the number of stomata in that area (and the same applied for trichome density).

2.1.5 Tree height

Tree heights were recorded using a measuring pole. The reading was taken from the base of the plant (soil level) to the meristem. Measurements were taken to the nearest cm.

2.2 RNA

2.2.1 Leaf samples

Leaves were sampled into individual pre-labelled foil bags and immediately flash frozen in liquid nitrogen. Where required, samples were transported on dry ice. The samples were stored at -80°C .

2.2.2 RNA extraction

RNA was extracted using the CTAB extraction method, adapted from Chang *et al*, (1993) by Street (2005) and Tucker (2006). One gram of leaf tissue was ground in liquid nitrogen using a pre-chilled pestle and mortar. After the leaf material had been ground to a fine powder, 15ml of pre-warmed (65°C) CTAB extraction buffer (2% CTAB (hexadecyl-trimethylammoniumbromid) (w/v), 2% PVP (polyvinylpyrrolidone) (w/v), 100mM Tris-HCl (v/v), 25mM EDTA (ethylenediamine tetraacetic acid) (v/v), 2M NaCl (v/v)) was added, along with 400 μl 2.67% (v/v) β -mercaptoethanol. After a brief period of incubation at 65°C , 15ml CHISAM

(Chloroform: Isoamyl alcohol, 24:1) was added to the material, which was then centrifuged (2000x g) for 20 minutes. The upper phase was transferred to a new vessel after which a further 15ml CHISAM was added and the sample re-centrifuged. The upper phase was transferred and precipitated at 4°C with 3ml of 10M lithium chloride overnight (approximately 18 hours).

The samples were centrifuged (9300x g for 30 minutes) at 4°C, to form a pellet which was dissolved in 700µl SSTE (11.7g 1M NaCl (w/v), 0.5% SDS (v/v), 10mM Tris-HCl (v/v) (pH 8.0), 1mM EDTA (v/v)), pre-warmed to 60°C. The sample was incubated for five minutes at 60°C after which 700µl CHISAM was added. After centrifugation (9300x g for ten minutes) the upper phase was transferred and the CHISAM step repeated. Two volumes (1.2ml) of 99.8% ethanol was added to the supernatant, which was allowed to precipitate for one hour (-80°C). After a further centrifugation (15,700x g for 30 minutes) at 4°C, the pellet was washed twice with 1ml 70% ethanol (v/v) and centrifuged (9300x g for two minutes) at 4°C following each one. The pellets were dried and re-suspended in 50µl DEPC-(diethylpyrocarbonate) treated water.

2.2.2.1 RNA quantification

The concentration of RNA was measured using the Nanodrop spectrophotometer (ND100, NanoDrop Technologies, Delaware, USA). The quality of the RNA was checked using either an RNA electrophoresis gel (see below) or the Agilent 2100 Bioanalyser (Agilent Technologies, Waldbronn, Germany) according to the manufacturer's instructions. The use of an electrophoresis gel or the bioanalyser is indicated in the materials and methods sections of the respective chapters of this thesis.

The RNA gels were prepared by making a 10x MOPS solution (41.9g MOPS, 6.8g sodium acetate, 2.6g EDTA in one litre of de-ionised (18Ω) water). The pH was adjusted to 7.0 using 1M NaOH. The gel was made by dissolving 1g of agarose in 100ml 1x MOPS in a microwave oven. The solution was cast and allowed to cool and set. 1µl of RNA was loaded onto the gel using 9µl 1xMOPS/ ethidium bromide mix (5µl ethidium bromide in 1ml 1x MOPS solution), and 2µl loading dye (glycerol: TE buffer (1:1) and Orange G). The gel was pre-run (100V) for ten minutes prior to

loading to remove any RNases from the sample wells. The gels were viewed using a UV-imager (Alpha Imager 1220 v5.04, Alpha Innotech Corporation).

2.3 Microarrays

2.3.1 POP2 microarrays

RNA was extracted from the leaves as described in section 2.2. The POP2 cDNA microarrays were used for this set of experiments as described in (Sterky *et al*, 2004). Each microarray consisted of 24,735 probes representing >100,000 ESTs. The ESTs represented on the microarrays were derived from 18 different tissues (Sterky *et al*, 2004).

The POP2 microarrays and associated reagents were provided by the Umeå Plant Sciences Centre (UPSC) in Sweden. The cDNA syntheses, microarray hybridisations, image and data analyses were all conducted at UPSC. The GeneSpring analyses were conducted at the University of Southampton.

2.3.1.1 cDNA synthesis

The cDNA syntheses began with 50µg of the extracted total RNA suspended in 9µl DEPC treated water. The RNA was denatured with 1µl of Oligo (dT)-anchor (5mg/ml) and the reaction was heated at 70°C for five minutes before being chilled on ice.

mRNA was reverse transcribed by the addition of the following reagents; 6µl 5x RT buffer, 7.4µl DEPC water, 3µl DTT (10mM) 0.6µl 50x dNTP mix (25 mM dATP, dCTP, dGTP, 20mM aa-dUTP, 5 mM dTTP), 1µl RNase inhibitor and 2µl Superscript II. The reaction was incubated at 42°C for 3 hours. The reverse transcription reaction was stopped by the addition of 10µl 0.5M EDTA, the RNA was degraded with 10µl 1M NaOH. Following incubation at 65°C for 15 minutes, 50µl 1M HEPES (pH 7.0) was added to neutralize the reaction.

The cDNA was purified using Microcon 30 columns (YM-30, Milipore, MA, USA) according to the manufacturer's instructions. The cDNA was eluted with 50µl dH₂O and the concentration was determined using the Nanodrop spectrophotometer

(NanoDrop Technologies, Delaware, USA). The samples were dried in a Speedvac (Savant, DNA SpeedVac) at 40°C for 60 minutes.

2.3.1.2 Probe labelling

The cDNA was re-suspended in 10µl 0.1M NaHCO₃ (pH 9.0). Mono-reactive NHS-ester Cy3 (PA23001 GE Healthcare, Uppsala, Sweden) and Cy5 (PA25001) were suspended in 85µl DMSO. 10µl of the re-suspended dye was then added to the cDNA. The samples were incubated at room temperature for two and a half hours.

The labelled samples were purified using GFX columns (GE Healthcare, Uppsala, Sweden). 500µl of Capture Buffer was added to each of the labelled samples, mixed, and then transferred to a column. Following centrifugation (13,800x *g* for 30s) the columns were washed three times using 600µl 80% ethanol, with intervening centrifugation stages between each wash. The columns were added to fresh eppendorf tubes following the washing stages. The samples were eluted twice using 35µl Elution Buffer (pre-warmed to 65°C), which was added to each column. The samples were centrifuged after each elution. The dye incorporation was measured on the Nanodrop spectrophotometer. The Cy3 labelled samples were combined with the corresponding Cy5 labelled samples (making a total of 140µl). The samples were dried in a Speedvac to 82µl.

2.3.1.3 Hybridisation

The hybridisations were conducted using an ASP (Automated Slide Processor, Lucidea ASP Hybridisation Station, Amersham-Pharmacia Biotech, Uppsala, Sweden). The pre-hybridisation of the microarray slides was initiated just prior to the dye purification stage.

To the labelled cDNA, a solution containing 25% Formamide, 5x SSC, 0.22% SDS, 1µl tRNA, and 0.42 µg Oligo-dA(80mer), was added. The samples were denatured at 95°C for two minutes and then chilled on ice for 30s. The samples were immediately injected into the ASP chambers. The pre-hybridisation buffer contained 50% Formamide, 5x SSC and 2.5x Denhart's solution. The slides were hybridised at 42°C for 13 hours. Wash buffer (WB) I consisted of 0.8x SSC, 0.03 % SDS; WB II

consisted of 0.2x SSC and WB III was 0.05x SSC, 2 mM KPO₄. Isopropanol (100%) was used to clean slides after washing.

2.3.1.4 Scanning

The arrays were scanned at four settings of increasing laser power and PMT (Laser power – 60, 80, 100, 100 %; PMT – 70, 70, 70, 80 %) at 10µm resolution, using a ScanarrayLite Microarray Analysis System scanner (PerkinElmer).

2.3.1.5 Image analysis

Spot data were extracted using GenePix (version 4.1 Pro, Axon Instruments Inc, California, USA). Settings for spot diameter resize feature were set to <75% and >150%. The CPI (Composite Pixel Intensity) was set to 300.

2.3.1.6 Data analysis

All the POP2 microarray data is publicly available (<http://www.upscbase.db.umu.se/>). Within the database, the data from Chapter 5 can be found under 'Experiment 0035', whilst that in Chapter 6 as 'Experiment 0085'.

The data output from GenePix was imported into UPSC-BASE for quality control and data analysis. Quality control was conducted using plug-ins, essential for analysis in UPSC-BASE (see Sjödin *et al*, 2006). Median foreground intensities were used in the analysis. Regression analysis was applied to the multiple scans to produce a unified dataset from which spot intensity data was extracted (Dudley *et al*, 2002). A stepwise normalisation process was used for data normalisation. Spots flagged as bad had a negative weighting factor of 0.1 applied to them. Data were filtered based on the A-value ($(\log_2 R + \log_2 G)/2$) to remove spots with low intensities in both channels.

B-statistics, implemented in the LIMMA package for R (Smyth and Speed 2003, Smyth 2004; <http://bioinf.wehi.edu.au/limma/>) and made available as a UPSC-BASE plug-in, were used to select genes with a high probability of differential expression. Bayesian statistics computes the probability of a gene being differentially expressed. A 'B-value' of zero equals a 50:50 probability of differential expression where as a B value of 3 represents approximately 95% certainty of differential expression ($\exp[3] / (1+\exp[3]) = 0.95$, or 95 %). B-values are automatically adjusted for multiple testing

with a FDR of 0.05. In the experiments described in Chapters 5 and 7 a B-value of zero was used as an arbitrary cut off for considering genes differentially expressed. Data was imported into GeneSpring 7 (Silicon Genetics, Redwood City, California) for subsequent analysis and visualisation.

2.3.2 PICME microarray

The PICME (Platform of Integrated Clone Management) microarrays consist of approximately 26,000 ESTs from a number of collections, including leaf and root libraries from *P. trichocarpa* x *P. deltoides*, wood libraries for *P. alba* x *P. tremula* and stress conditions from *P. euphratica* (www.picme.at).

The cDNA syntheses, microarray hybridisations, image and data analyses were all conducted at the University of Southampton.

The RNA was extracted using the modified maxi-CTAB extraction method (Chang *et al.*, 1993; Street, 2005; Tucker, 2006) as described in section 2.2.

2.3.2.1 cDNA synthesis

To the RNA sample (100µg in 15µl DEPC-treated water), 2 µl of anchored Oligo-(dT) was added. The sample was denatured at 65°C for ten minutes and chilled on ice. A master mix was prepared using 6µl 5x first strand buffer, 1µl 50x dNTP, 3µl DTT, 1µl RNase inhibitor, 1µl superscript III per reaction. 13µl of the mastermix was added to each sample and was incubated at 48°C overnight (approximately 16 hours). The reaction was stopped using 10µl 0.5M EDTA and the RNA was degraded with 10µl 1M NaOH with a subsequent incubation at 65°C for 15 minutes. Finally, 50µl 1M HEPES (pH 7.5) was added to neutralise the reaction.

The cDNA was cleaned using the Qiaquick columns (Qiagen). 500µl binding buffer was twice passed through a column and centrifuged at 15,700 \times g for one minute. Phosphate wash buffer was used (750µl for each of three washes) and the column was dried by centrifugation at 15,700 \times g for one minute. The cDNA was eluted twice in 30µl 0.1M NaHCO₃ by centrifugation at 15,700 \times g for one minute, making a final

elution of 60µl per sample. The concentration of cDNA was checked on the Nanodrop spectrophotometer.

2.3.2.2 Probe labelling

The cDNA was combined with an aliquot of Cy3 or Cy5 dye and incubated at room temperature in the dark for two and a half hours. Qiaquick columns (Qiagen) were used to clean the samples (three washes with 750µl of Buffer PE). The labelled cDNA was eluted twice in 50µl of elution buffer for each sample. The sample labelled with the Cy5 dye was eluted into the same vessel as the corresponding sample labelled with Cy3, making a total of 200µl. The dye incorporation and cDNA quantity results were obtained from the Nanodrop spectrophotometer.

2.3.2.3 Hybridisation

Each microarray slide was placed in a coplin staining jar containing pre-hybridisation buffer (formamide 50% (v/v), 5x SSC, 0.1% SDS (w/v), 0.1mg ml⁻¹ BSA). The slides were incubated at 42°C for one hour. Following incubation, the slides were removed and placed into a bath of WB III (0.2x SSC) for five minutes, a second bath with WBIII for a further five minutes, one 30 second wash in dH₂O, one minute in boiling dH₂O and one minute in 100% ethanol (pre-chilled to 4°C). The slides were centrifuged (3000 *x g*) and stored in a sealed tube until loading into the hybridisation station.

The samples were denaturated with 50µl formamide, 25µl DEPC water and 25µl hybridisation buffer was added to the labelled cDNA samples. The samples were heated at 95°C for one minute. The microarray slides were loaded into the HS400 hybridisation station (Tecan, Reading, UK) and washed for one minute with pre-hybridisation buffer (50% formamide (v/v), 5x SSC, 0.1% SDS (w/v) and 0.1mg ml⁻¹ BSA.) The prepared samples were then loaded and the slides were hybridised for 16 hours at 42°C with low agitation frequency. Following hybridisation, the slides were sequentially washed for one minute each with WB I (1x SSC, 0.2% SDS), WBII (0.1x SSC, 0.1% SDS), WB III (0.2x SSC), dH₂O, and ethanol (100%). The slides were finally dried using pure N₂ gas.

2.3.2.4 Scanning and image analysis

The slides were scanned using a Genetix Acquire Scanner (Genetix, Hampshire, UK). Each array was initially scanned at a resolution of 30µm in order to manually adjust the PMT voltage levels and balance the Cy3 and Cy5 channels. The slides were then scanned at a final resolution of 5µm according to the PMT settings deemed appropriate in the 30µm preview scan. The two .TIFF files (one for each of the two channels) were imported into GenePixPro 5.1 (Axon Instruments, Union City, California). The GenePix program and the associated GPR file for the PICME microarray were used to analyse the results of the scan. This was required in order to 'flag' bad spots (e.g. those that were saturated or abnormal) and to manually check for any deposits left on the slide following hybridisation (e.g. dust or salt). Following the automatic spot detection by GenePix and the manual check, the program was used to calculate the mean and median pixel intensity of each spot. The 'background' was calculated using the pixel information in the 'valley' between adjacent spots (Yang *et al*, 2001). The information for each slide was stored in a .GPR file for further analysis.

2.3.2.5 Data analysis

The data was normalised using locally weighted linear regression (LOWESS), which is a commonly used transformation in microarray studies (Quackenbush, 2002). B-statistics were again used for statistical analysis (see section 2.3.1.6). The normalised data was imported into GeneSpring 7 (Silicon Genetics, Redwood City, California) for subsequent analysis.

The raw data files for all of the microarray experiments are available on the appendix CD at the back of this thesis.

2.4 qPCR

Total RNA was extracted as described in section 2.2.

2.4.1 cDNA synthesis

Prior to cDNA synthesis, contaminating genomic DNA was digested using the TURBO DNase-free kit (Ambion). 0.1 volumes of DNase buffer and 1µl DNase were added to the sample. After 30 minute incubation at 37°C, a further 1µl DNase was added followed by a second incubation. 0.2 volumes of the inactivation reagent were added to the sample and the supernatant was removed after a centrifugation at 10,000 $\times g$ for one and a half minutes.

A mastermix containing 6µl 5x first strand buffer (250mM Tris-HCl (pH 8.3) (v/v); 375mM KCl (v/v); 15mM MgCl₂(v/v)), 3µl 0.1 M DTT (dithiothreitol), 1µl dNTP, 1µl RNase OUT and 1µl Superscript III per reaction was prepared for the cDNA synthesis. The RNA was incubated with 1µl oligo (dT)₂₀ primer at 70°C for five minutes after which 12µl of the prepared mastermix was added. The initial incubation was one hour at 50°C and the RNA was degraded using 3µl of 5M NaOH. The cDNA was cleaned using the QIAquick PCR Purification Kit (Qiagen) using 500µl buffer PB, 500µl buffer PE and an elution volume of 50µl buffer EB. The concentration of cDNA was measured on the NanoDrop spectrophotometer. The concentration of cDNA ranged from 2-10ng/µl.

2.4.2 Primer design

Primers were designed using the programme 'Beacon Designer 4.0'. A temperature gradient experiment was conducted in order to determine the best annealing temperature for the primers (data not shown).

2.4.3 qPCR reactions

In each 20µl reaction, 10µl Dynamo SYBR green mastermix (SYBR green, Finnzymes, GRI, Braintree, UK), 8.4µl DEPC treated water, 0.6µl primer mix containing 10 µM forward and reverse primers, and 1µl cDNA template, were added. All pipetting was conducted on ice.

2.4.4 Programme parameters

The plates were run on the DNA Engine Opticon 2 System (MJ Research). After the initial heating step of 95°C for ten minutes at the beginning of each run, the plates were run at 94°C for ten seconds for the denaturing step, annealed at 56°C (known to be the optimum temperature for the primers, data not shown) for 20 seconds and extended at 72°C for 20 seconds. A melting curve produced at the end of each run was used to check for secondary products (Ririe *et al*, 1997).

2.4.5 Data analysis

Data was analysed using the LinReg program. This approach is based upon linear regression in order to calculate the starting concentration of mRNA and the PCR efficiency of each sample. The ratios were calculated using the method outlined by (Pfaffl, 2001) (equation 1).

$$\text{Ratio} = \frac{(E_{\text{target}})^{\Delta CP_{\text{target}}(\text{control-sample})}}{(E_{\text{ref}})^{\Delta CP_{\text{ref}}(\text{control-sample})}}$$

Equation 1. The results from the qPCR data were analysed using the method proposed by (Pfaffl, 2001). Target= target sample, Ref= reference sample, E= PCR efficiency for the sample, ΔCP is the CP deviation of (control – sample) of the transcript, where CP is the point at which the fluorescence rises above the background levels (Pfaffl, 2001).

CHAPTER 3

Leaf development in two contrasting *Populus* species

3.0 Overview

The leaves of a plant represent adaptable appendages, which act as the main interface connecting the plant with its immediate environment. They are crucial to plant function since they determine overall productivity. This thesis mainly focuses on two phenotypically distinct *Populus* species; *P. deltoides* and *P. trichocarpa*. Prior to any experiments regarding environmental perturbation, it is important to understand how the two species grow under ambient conditions. This chapter outlines some general characteristics of the two species following spatial (i.e. developmental stage profile) and temporal growth measurements. By studying both leaf and epidermal cell profiles the results show that the two species have contrasting growth strategies. This suggests that it is likely the two species will respond differently to increased carbon availability in future studies into the effects of [eCO₂] on growth.

3.1 Introduction

The cellular characteristics of a leaf may be considered to be due to the influence and execution of the cell cycle. There are two contrasting theories that attempt to define the relationship between plant growth and the cell cycle. In the Cell Theory, cells are considered to be the ‘building blocks’ of the organism and growth therefore depends on the rate at which the cells are produced and the size they reach. Conversely, the Organismal Theory states that cell division is a consequence rather than a cause of growth (Beemster *et al*, 2006). In this scenario, cells are considered as ‘compartments in organismal space’ (Beemster *et al*, 2003). Neither theory alone adequately explains the link between the cell cycle and plant growth because they are so intricately linked (Beemster *et al*, 2003).

The dimensions of a leaf are dependent upon the number and the size of the cells of which it is comprised. Therefore the growth of a leaf can be considered to be the result of two tightly coordinated processes; cell expansion and cell production. The extent to which these processes contribute to final leaf area is dependent upon the species under scrutiny (Ferris *et al*, 2002).

The study of leaf growth in dicotyledonous plants presents a challenge when compared to a monocotyledonous plant, such as grass, for example. Here the cells are arranged into ‘files’ and can be segregated into ‘division’ and ‘elongation’ zones (Fiorani *et al*, 2000). In dicotyledonous plants however, growth is more heterogeneous, making detailed studies of growth rather more challenging (Fiorani and Beemster, 2006) although artificially partitioning leaves using a grid (Granier and Tardieu, 1998) or using leaf veins as boundary markers (Taylor *et al*, 2003) has been used successfully to calculate cellular growth rate (Fiorani and Beemster, 2006).

Populus deltoides and *Populus trichocarpa* represent two phenotypically distinct members of the *Populus* genus. *P. deltoides* (commonly known as the Eastern Cottonwood) is prevalent in the South East of the United States of America, whilst *P. trichocarpa* (commonly known as the Black Cottonwood) originates in the North West, with a range spanning from Alaska to California (Figure 3.1.1). These contrasting areas of natural distribution will inevitably expose the two species to different environmental conditions and stresses, and hence they will have adapted

different means by which to adapt to the local conditions. For example, they are known to have contrasting responses to water deficit (Street *et al*, 2006).

Along with the advantages associated with using two species with vast phenotypic differences in leaf development studies, *P. deltoides* and *P. trichocarpa* have also been successfully used to create an F₂ mapping population ('Family 331') (Bradshaw *et al*, 1994).

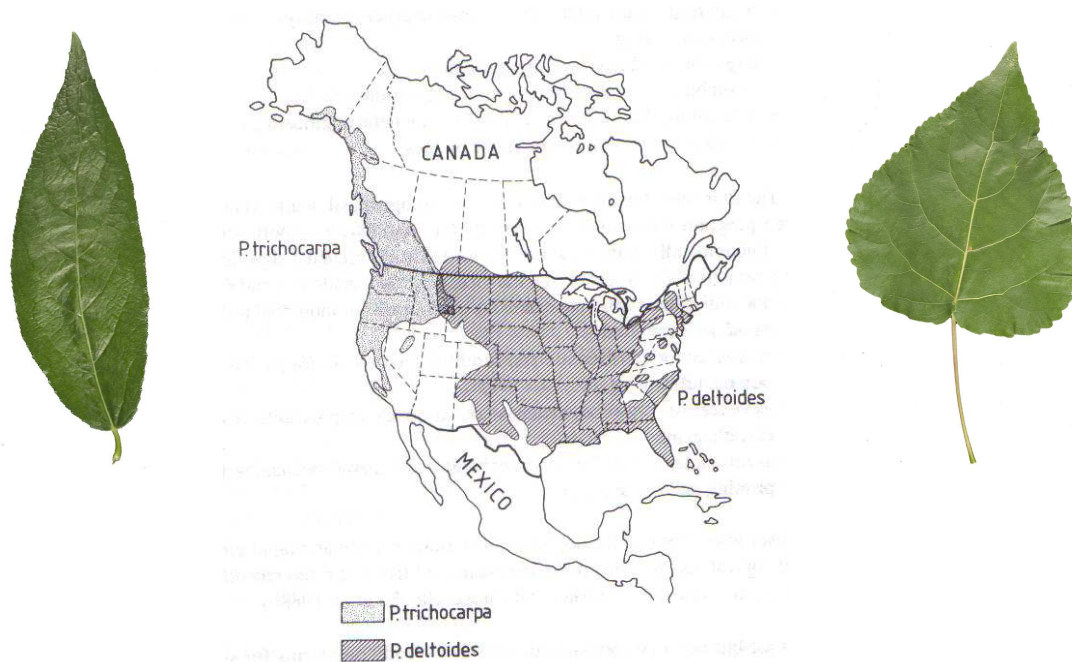


Figure 3.1.1. *P. trichocarpa* and *P. deltoides* originate from different regions of North America. Whilst *P. trichocarpa* is mainly distributed in the North West, *P. deltoides* is generally located in the South East of the country. The leaves of *P. deltoides* (right) and *P. trichocarpa* (left) are phenotypically distinct. The species distribution map was adapted from Ceulemans, (1990).

The aim of this thesis was to develop an understanding of leaf growth in relation to changing environmental conditions (i.e. [eCO₂]). *Populus trichocarpa* and *P. deltoides* represent two contrasting models in which to study leaf development. The aim of this experiment was to test the hypothesis that the growth strategies governing leaf size and shape were different in the two species (grown under normal climatic conditions) and consequently that they would be useful models for exploring the underlying responses to [eCO₂] in subsequent studies. In particular, the experiment focussed on the study of spatial and temporal leaf growth in the two species. The spatial differences in epidermal cell dimensions were discussed, rather than a detailed kinematic analysis of cellular growth in *Populus*, which was beyond the scope of this chapter.

3.2 Materials and Methods

In 2002, *Populus deltoides* and *Populus trichocarpa* hardwood cuttings were planted in the grounds of the Boldrewood campus at the University of Southampton. The trees were planted approximately 30 cm apart and were cut back after every year of growth.

During the growing season of 2004, four *P. deltoides* and four *P. trichocarpa* trees were randomly selected from the collection in order to obtain a profile of leaf growth. Photographic images of leaves one to ten (where age one was the first fully unfurled leaf from the shoot meristem and age ten was a mature leaf) were sampled and a small length of thread was tied around the petiole of the leaves to act as a marker to follow the progression of development over time. The first sets of photographs were collected on the 10th August 2004. The second sets of photographs were taken on the 13th August 2004.

Abaxial epidermal imprints of leaf ages one to ten from both species were sampled on the 13th August 2004. The cell images were captured on a Zeiss microscope.

3.3 Results

In order to investigate the growth characteristics of *P. deltoides* and *P. trichocarpa*, leaf images were captured at two different time-points to construct a spatial and temporal profile of growth, individual to each species. The images were collected from the youngest unfurled leaf (age one as defined on the first day of the experiment) to the mature leaves (the measurements were discontinued after age ten).

3.3.1 Leaf growth analysis

The results from the leaf area analysis of the two species are shown in Figures 3.3.1 and 3.3.2. The results in Figure 3.3.1 show that in *P. deltoides*, there was a significant difference in leaf size between the first and second measurements, in leaf ages one to four. This suggests that beyond age four, leaf growth slowed until maturity. In *P. trichocarpa* however, there was a significant difference in leaf size between the two time-points in ages one to three. It is worthy to note the differences in leaf size between the two species. The average leaf area in *P. deltoides* was generally much larger than *P. trichocarpa*. The maximal leaf area attained (incidentally at age eight in both species) in *P. deltoides* was approximately double that of *P. trichocarpa*.

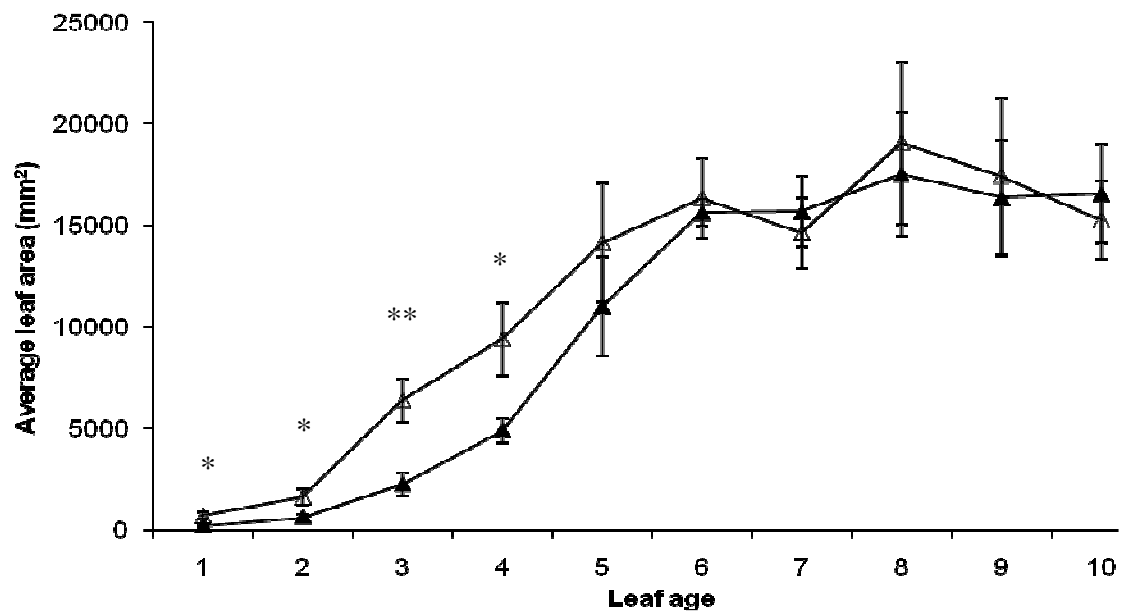


Figure 3.3.1. The average leaf area in *P. deltoides*. The leaves were tagged and photographed on the 10th August 2004 (solid triangles) and these same leaves were re-measured on the 13th August 2004 (open triangles). Leaf one was defined as the first fully unfurled leaf (i.e. the youngest leaf) on day one. The results of a one-way ANOVA are provided on the graph (* $p > 0.05$, ** $p > 0.01$) along with standard error bars. $n=4$.

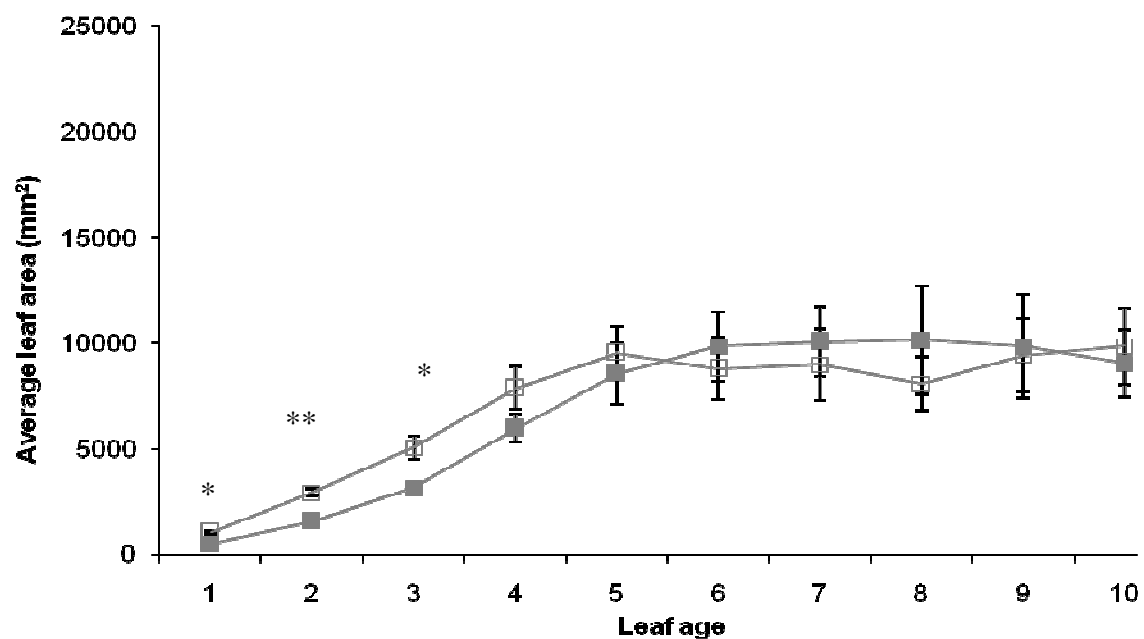


Figure 3.3.2. The average leaf area in *P. trichocarpa*. The leaves were tagged and photographed on the 10th August 2004 (solid squares) and these same leaves were re-measured on the 13th August 2004 (open squares). Leaf one was defined as the first fully unfurled leaf (i.e. the youngest leaf) on day one. The results of a one-way

ANOVA are provided on the graph (* $p > 0.05$, ** $p > 0.01$) along with standard error bars. $n=4$.

Figures 3.3.3 and 3.3.4 show the Absolute Growth Rates (AGR) and Relative Growth Rates (RGR) of leaves one to ten of the two species. The results indicate that there was a statistically significant difference between the two species at age three only, where the growth rate of *P. deltoides* was greater than *P. trichocarpa*. The average relative growth rate in *P. deltoides* was consistently greater in *P. deltoides* compared to *P. trichocarpa*. At leaf age three there was a statistically significant difference between the two species. In general, beyond age six the leaves of both species began to shrink.

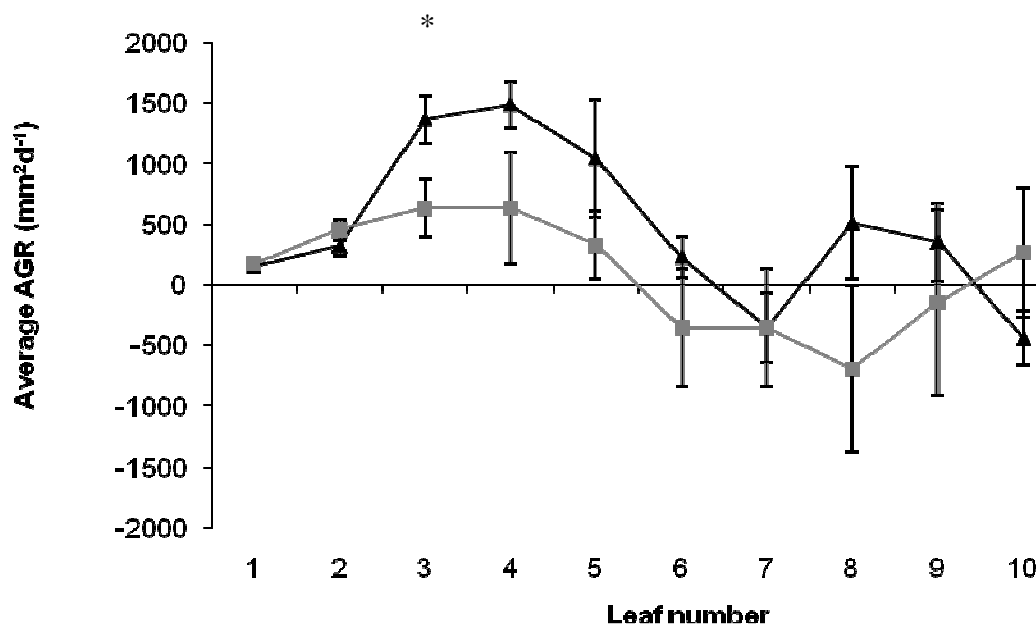


Figure 3.3.3. The average AGR of leaves one to ten in *P. deltoides* (black triangles) and *P. trichocarpa* (grey squares). Leaf one was defined as the first fully unfurled leaf from the meristem (i.e. the youngest leaf) on day one (10th August 2004) of the experiment. The results of a one-way ANOVA are provided on the graph (* $p > 0.05$) along with the standard errors. $n=4$.

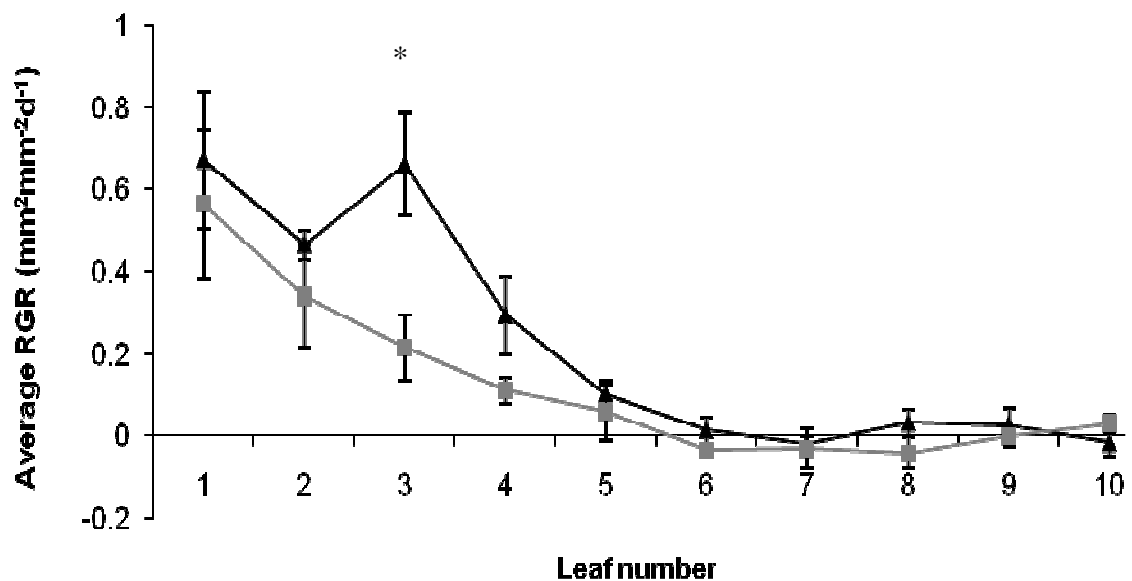


Figure 3.3.4. The average RGR of leaves one to ten in *P. deltooides* (black triangles) and *P. trichocarpa* (grey squares). Leaf one was defined as the first fully unfurled leaf from the meristem (i.e. the youngest leaf) on day one (10th August 2004) of the experiment. The results of a one-way ANOVA are provided on the graph (* $p > 0.05$) along with the standard errors. $n=4$.

3.3.2 Leaf shape index analysis

In conjunction with leaf area data, changes in leaf dimensions in the species over time were also calculated. The results from the analysis are shown in Figures 3.3.5 and 3.3.6. In *P. deltooides*, leaf shape dimensions were statistically significantly different in ages one to four. Beyond this age however, there were no differences between the data obtained on the two days, therefore suggesting that the leaves maintained a consistent shape. In *P. trichocarpa* however, there was a significant difference in length to width ratio in age one only. This suggests that whilst growth continued up to age three (see Figure 3.3.2), the leaves maintained their shape and therefore grew proportionally across the medio-lateral and proximo-distal axes.

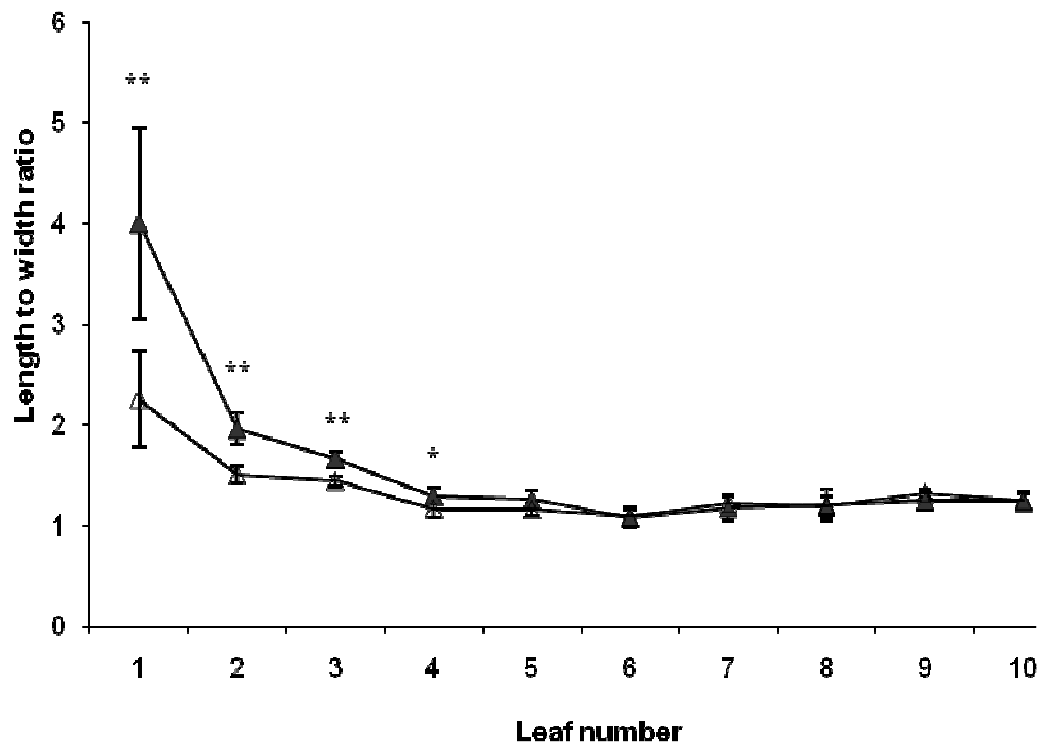


Figure 3.3.5. The average length to width ratio for each leaf age in *P. deltoides*. The length and width of the leaves were both measured in mm. The solid triangles show the results on day one of the experiment (10th August 2004) whilst the open triangles illustrate the results on day two (13th August 2004). The standard errors are provided on the graph along with the results of a one-way ANOVA (* $p > 0.05$, ** $p > 0.01$). $n=4$.

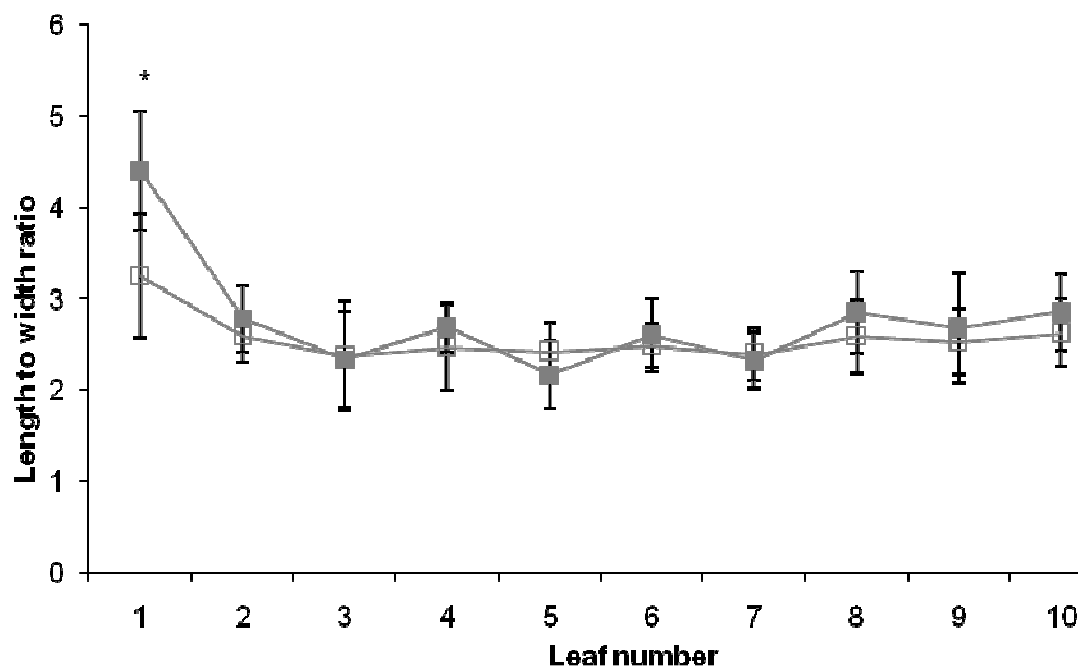


Figure 3.3.6. The average length to width ratio for each leaf age in *P. trichocarpa*. The length and width of the leaves were both measured in mm. The solid squares show the results on day one of the experiment (10th August 2004) whilst the open squares illustrate the results on day two (13th August 2004). The standard errors are provided on the graph along with the results of a one-way ANOVA (* $p < 0.05$). $n=4$.

3.3.3 Cell Growth Analysis

Abaxial epidermal cell impressions were sampled and analysed from leaves one to ten on day two of the experiment (13th August 2004) for *P. deltoides* and *P. trichocarpa*. There were a large number of trichomes in the young leaves of *P. trichocarpa* relative to the equivalent leaf age in *P. deltoides* (data not shown).

The results in Figure 3.3.7 illustrate the differences in cell area in *P. deltoides* and *P. trichocarpa*. The cells of *P. trichocarpa* were consistently larger than those of *P. deltoides* at each leaf age (and were statistically significantly different between the two species in the majority of leaf ages). The difference between the two species was most pronounced in the mature leaves. The results in Figure 3.3.8 show the approximate number of cells at each leaf age in the two species. The results indicated that *P. deltoides* consistently had a greater number of cells in the leaves in each age group. It can therefore be concluded that the two species attain final leaf areas in different ways. Whilst *P. deltoides* attains its leaf area primarily by cell production, cell expansion is more important in determining leaf size in *P. trichocarpa*.

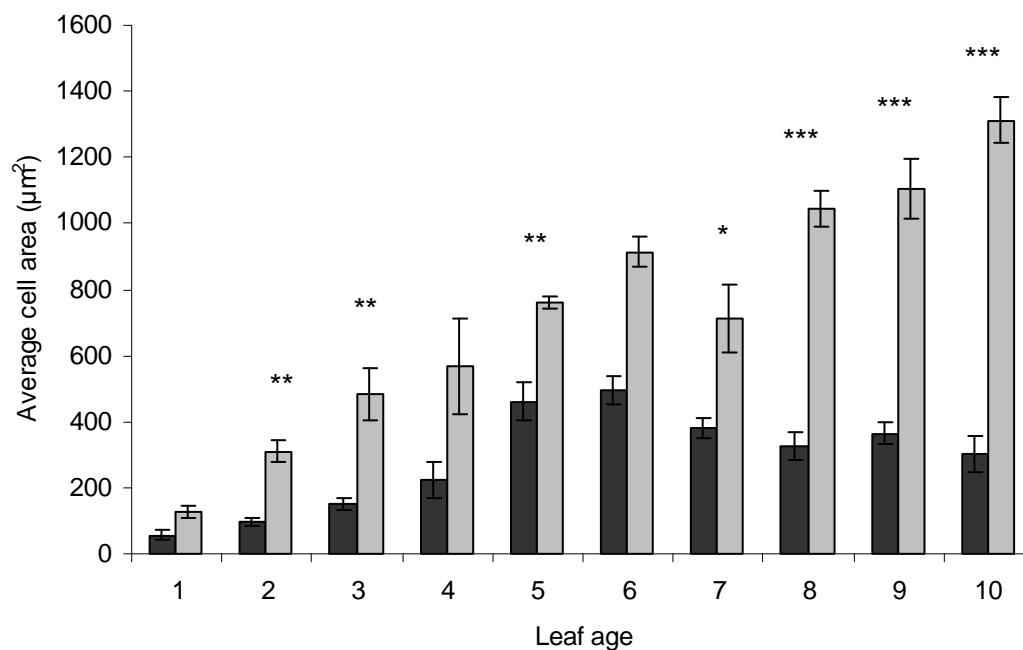


Figure 3.3.7. The average epidermal cell areas of leaf ages one to ten in *P. deltoides* (black bars) and *P. trichocarpa* (grey bars). The cell impressions were sampled on day two of the experiment (13th August 2004). Leaf one was defined as the first fully unfurled leaf on day one of the experiment (10th August 2004). The standard errors are shown on the graph. The results of a one-way ANOVA are shown on the graph (* $p > 0.05$, ** $p > 0.01$, *** $p > 0.001$). $n=40$.

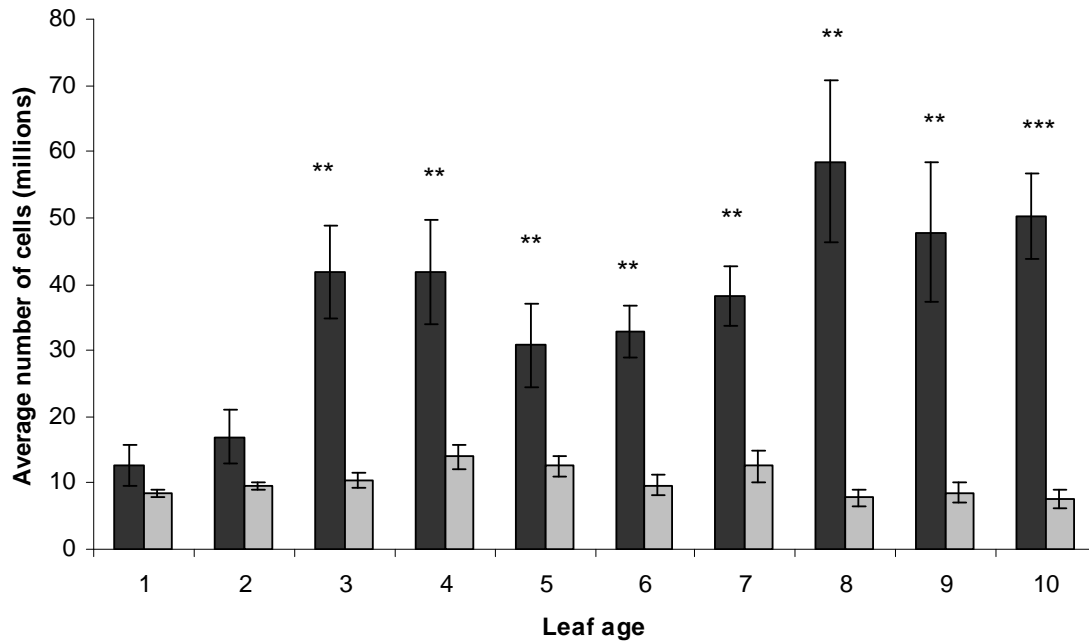


Figure 3.3.8. The average epidermal cell number per leaf of ages one to ten in *P. deltoides* (black bars) and *P. trichocarpa* (grey bars). The cell impressions were sampled on day two of the experiment (13th August 2004). Leaf one was defined as the first fully unfurled leaf on day one of the experiment (10th August 2004). Average epidermal cell number was calculated by dividing the leaf area by the average cell area for each biological replicate. The standard errors are shown on the graph. The results of a one-way ANOVA are shown on the graph (** $p > 0.01$, *** $p > 0.001$). $n=40$.

3.4 Discussion

Populus deltoides and *Populus trichocarpa* represent two phenotypically distinct tree species. The aim of this chapter was to provide some key information regarding how the leaves of these two species grow, both spatially (by building a profile of development for the leaves in chronological order) and temporally (by monitoring the growth at two points in time).

3.4.1 Leaf growth in *P. deltoides* and *P. trichocarpa*

Temporal changes in leaf growth were calculated for the two species by recording leaf dimensions at the beginning of the experiment, and repeating the measurement after three days. In *P. trichocarpa*, there was a significant difference in size for leaf ages one to three between the two time-points, suggesting that the leaves were still in the process of growing. However, in *P. deltoides*, there was a statistically significant

difference in leaf ages one to four. This difference between the two species may reflect differences in leaf maturation rate or leaf production rate.

There was a significant difference in growth rate between the two species at leaf age three (Figures 3.3.3 (AGR) and 3.3.4 (RGR)), where *P. deltoides* had a significantly higher growth rate compared to *P. trichocarpa*. The growth of *P. trichocarpa* leaves was declining at this point since there was no significant difference in temporal leaf growth at age four in this species. Once fully mature, the leaves of both species shrunk, (Figure 3.3.3 (AGR)). This happened more prematurely in *P. trichocarpa* (leaf age six), than *P. deltoides* (leaf age seven).

The availability of carbohydrates affects the growth and development of non-photosynthetically active tissues (or ‘sinks’), such as roots, seeds, internodes and young leaves (Kehr *et al*, 1998). The ‘sources’ are represented by photosynthetic tissues i.e. mature leaves, which act as net exporters of sucrose. The higher number of actively growing leaves in *P. deltoides* therefore suggests that there may have been a greater sink demand in this species than in *P. trichocarpa*. It has been estimated that leaves of dicotyledonous plants stop importing photosynthate and begin to export it when they are 30-60% expanded (Turgeon, 1989), which would have corresponded to leaves four to five in *P. deltoides* and two to five in *P. trichocarpa* (based on maximal leaf area data from day one).

By considering this result in the context of the theme of the thesis it is possible to imagine a difference in CO₂ response between the two species. Indeed, *P. trichocarpa* has been shown to respond to a greater degree to [eCO₂] than *P. deltoides* in an open-topped chamber experiment (Rae *et al*, 2006). Sucrose availability affects growth and could be considered as one of its limitations. Hence an increase in sucrose availability due to [eCO₂] exposure could affect the species differently due to the differing requirements for sugar (inferred from differing sink strengths) leading to altered growth. Furthermore it has previously been shown that the ratio of expanded to expanding leaves affects the response to [eCO₂] in *Populus* (Wait *et al*, 1999).

The rates of cell division and expansion at each stage in leaf formation contribute to final leaf shape (Tsukaya, 2003; Kim and Cho, 2006). During the maturation of *P.*

deltoides leaves, continued meristematic activity at the base contributes to the production of a wider leaf (Van Volkenburgh and Taylor, 1996). The investigation into differences in leaf shape was conducted by calculating leaf length to width ratios (the 'leaf shape index'). There was a significant difference in length to width ratio in the youngest studied leaf (age one) in *P. trichocarpa*. Beyond this age however, there was no difference in the leaf shape ratio over time. In *P. deltoides* however, there was a significant difference in temporal leaf shape at ages one, two, three and four. Since temporal growth in *P. trichocarpa* continued until leaf age three (Figure 3.3.2), the results suggested that this species maintained a constant shape over time by growing proportionally across the proximo-distal and medio-lateral axes. Conversely, temporal growth in *P. deltoides* was significantly different until leaf age four (Figure 3.3.1).

3.4.2 Cellular basis of growth in *P. deltoides* and *P. trichocarpa*

It has been hypothesized that the epidermal cell layer governs plant growth (Scheres, 2007). The growth restriction is in part due to the action of brassinosteroids (Savaldi-Goldstein, 2007), which cause a reduction in leaf expansion due to reduced cell proliferation in *Arabidopsis* mutants (Nakaya *et al*, 2002). This effect on plant growth therefore highlights the importance of a clear knowledge and understanding of cellular growth in the epidermal layer. The analyses of cellular growth in *P. deltoides* and *P. trichocarpa* indicated that the species used different strategies in order to attain final leaf size. By comparing Figures 3.3.7 and 3.3.8, it was clear that growth in *P. deltoides* could be attributed to cell production, whilst in *P. trichocarpa* it was due to cell expansion. This result has been shown in previous studies (e.g. Ridge *et al*, 1986). It has further been shown that in *P. deltoides* cell proliferation continued until the leaf was 80-90% of its final size whereas cell proliferation in *P. trichocarpa* ceased once the leaf was 10-20% of its final size and continued to grow by expansion (Van Volkenburgh and Taylor, 1996).

Cell expansion can be attributed in part to endoreduplication (Sugimoto-Shirasu and Roberts, 2003). Endoreduplication is the process by which cells enter the cell cycle and replicate the DNA and other cellular components but do not undergo mitotic division, hence causing the cells to expand. In this experiment it was shown that *P. trichocarpa* has much larger cells and therefore it could be hypothesized that this

species would have a higher ploidy level than *P. deltoides*. Using flow cytometry it would be possible to study the differences in ploidy level between the two species.

3.5 Conclusion

Despite the large amount of work that has been conducted on understanding the growth and development of leaves, there are still major gaps in our knowledge of the processes underlying the observed phenotype. The use of *Arabidopsis* is particularly useful for such studies due to its ease of propagation, short generation time, widespread availability and large genetic resources (AGI, 2000). However, a more detailed understanding of growth and development of an economically important species such as *Populus* is required (Jansson and Douglas, 2007). This was addressed in this chapter by characterising the growth of two species of *Populus* that form the basis of this thesis. The results provided clear evidence of mechanistic differences in epidermal cell growth between *P. deltoides* and *P. trichocarpa*, with the former using cell production and the latter using cell expansion, for leaf growth. Temporal changes in shape occurred in the youngest four leaves of *P. deltoides* but not *P. trichocarpa*, which maintained its proximo-distal/ medio-lateral growth ratio over time. The results suggest that early in development the underlying genetics is important, but during maturation the leaves are increasingly affected by the environment which tends to lead to greater variation between them. It is possible that the differential number of growing leaves in the two species will alter the source-sink balance and may thus affect downstream CO₂ responses.

CHAPTER 4

Phenotypic analyses of *P. deltoides* and *P. trichocarpa* grown in [eCO₂] using a FACE experimental system

4.0 Overview

FACE experiments are used to assess responses to [eCO₂] without the restrictions associated with controlled environment experimentation. Previous studies in have indicated that *Populus* is sensitive to increased [CO₂], although this is dependent upon species (Ferris *et al*, 2002; Rae *et al*, 2006; Rae *et al*, 2007).

Here, the newly constructed BangorFACE experimental field site was used to assess the growth response of two contrasting model *Populus* species (*P. deltoides* and *P. trichocarpa*) to [eCO₂]. The results indicated slight growth stimulation in *P. trichocarpa* following exposure to [eCO₂]. However, of particular interest were the results from the XET co-localisation assay. XET, an enzyme involved in cell wall loosening (Fry *et al*, 1992) and hence growth, has previously been suggested to be involved in the growth response to CO₂ (Ferris *et al*, 2001). In this experiment, the XET assay showed that activity was higher in FACE in *P. deltoides*, the species that attains its final leaf size by cell division. Furthermore, XET activity was reduced in [eCO₂] in *P. trichocarpa*, the species that attains final leaf size by cell expansion. The results presented do suggest a species-specific difference in response to FACE in terms of XET activity, but this needs further exploration with adequate controls in the assay.

4.1 Introduction

The concentration of atmospheric CO₂ has greatly fluctuated over geological time. The majority of plant species that are dominant in the current biosphere evolved in [CO₂] of less than 240ppm (Körner, 2006; Petit *et al*, 1999; Siegenthaler, 2005). The [CO₂] has been steadily rising over the past 200 years due to anthropogenic activities such as fossil fuel combustion. The concentration in the atmosphere is currently 380ppm (The Carbon Dioxide Research Group (<http://cdrg.ucsd.edu/maunaloa.html>)) but is projected to reach 550ppm by the middle of this century (Prentice *et al*, 2001). The change in the composition of the atmosphere is likely have a dramatic effect on terrestrial life if it continues at its current rate. Investigations to assess changes in plant growth and habit are required in order to understand the changes that may occur under the projected climatic conditions.

Trees represent a significant carbon sink for the increasing [CO₂] in the atmosphere and have been proposed as an alternative (carbon neutral) energy resource. Therefore there has been a surge in research to investigate the use of trees to mitigate the effects of [eCO₂] by carbon assimilation, particularly in species belonging to the model *Populus* genus (Taylor *et al*, 2002).

There have been numerous previous studies investigating the effects of [eCO₂] on plant growth. For example, leaf area (Ferris and Taylor 1994; Gardner *et al*, 1995; Tricker *et al*, 2004; Taylor *et al*, 2003), leaf area index (LAI) (Liberloo *et al*, 2005; Norby *et al*, 1999) and leaf production (Radoglou and Jarvis, 1990) are all stimulated in [eCO₂]. Furthermore, below-ground biomass is stimulated (Calfapietra *et al*, 2003; Lukac *et al*, 2003) and bud set and senescence have often been reported to be delayed in [eCO₂] (Taylor *et al*, 2008). However, there are reports that have shown that [eCO₂] has no effect on plant growth (e.g. Asshoff *et al*, 2006; Norby *et al*, 2003). For example, in a study of four C₃ annuals it was found that the most efficient use of CO₂ occurred at current atmospheric concentrations. In this study there was a general reduction in leaf area and dry mass at higher concentrations of CO₂ (90µmol mol⁻¹ above current atmospheric [CO₂]) (Bunce *et al*, 2001). It is likely that growth responses to [eCO₂] reflect the underlying conditions of the experiment (Körner, 2006).

Investigations into the long-term growth responses of trees cannot be conducted under controlled environment conditions, mainly due to the size limitation. The use of FACE experiments can avoid the limitations of enclosure methods (McLeod and Long, 1999) and they are widely accepted as an appropriate means of assessing whole ecosystem responses to changes in atmospheric $[\text{CO}_2]$ (Miglietta *et al*, 2001). One such FACE experiment was recently constructed at the Henfaes Research Centre in Bangor, North Wales (www.bangorface.org.uk) which aims to assess carbon sequestration potential of a mixture of native tree species.

The overall aim of this experiment was to determine the morphological responses of *P. deltoides* and *P. trichocarpa* to $[\text{eCO}_2]$ by using the BangorFACE experimental field site. Whilst the focus of the experiment concentrated on leaf growth, other variables that could be affected by $[\text{eCO}_2]$ (e.g. tree height), were also measured. Leaf growth represents an important aspect of plant development and survival, since it inevitably affects overall productivity. It has been proposed that the XET enzyme alters the composition of the cell wall and promotes cell wall loosening and growth (Fry *et al*, 1992). Furthermore, it has been proposed that stimulation in leaf area as a result of growth in $[\text{eCO}_2]$ is associated with the XET group of cell wall loosening enzymes (Ferris *et al*, 2001; Gardner *et al*, 1995). There is little direct evidence to show that XETs are directly involved in the CO_2 response and hence in this experiment XET activity was quantified in the two species in order to assess species and treatment differences.

4.2 Materials and Methods

4.2.1 The BangorFACE experimental field site

The BangorFACE field site is a 2.36 hectare plantation which was planted in March 2004. Each of the eight experimental rings (four [eCO₂] and four [aCO₂] (Figure 4.2.1)) are 8m in diameter. The FACE technology (Figure 4.2.2) used for CO₂ exposure is identical to that at EUROFACE (Miglietta *et al*, 2001).

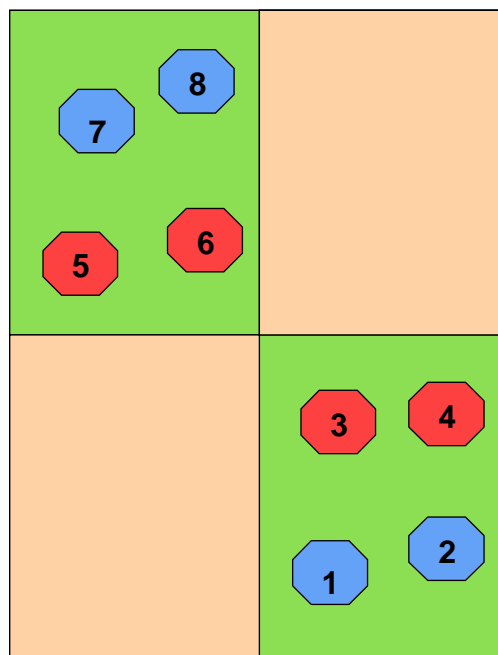


Figure 4.2.1. There are eight experimental rings at the BangorFACE site, which are split between two fields. Each hexagon represents one of the rings. The blue hexagons represent those exposing the plants to [aCO₂], whilst the red represents those grown in [eCO₂]. The positions of the hexagons on the diagram represent the approximate positions of the rings at the site.

Growing within the rings are birch (*Betula pendula*), alder (*Alnus glutinosa*) and beech (*Fagus sylvatica*) trees. Each tree is planted 80cm away from the nearest neighbour. There is a 10m ‘buffer’ surrounding each ring, consisting of beech, alder and birch trees, again planted at 80cm distances. The remainder of the plantation is comprised of a mixture of chestnut, oak, sycamore and ash, as well as beech, alder and birch trees.



Figure 4.2.2. One of the FACE rings at the BangorFACE site. The CO₂ is released from pipes around the middle of the main infrastructure. Each ring has a CO₂ monitoring system.

During the 2005 growing season (April to October) the average [CO₂] in the FACE rings during the day was 571.69ppm (± 57.72) and at night was 403.92ppm (± 69.01). The average monthly rainfall during this period was 2.4mm and the average monthly air temperature was 13.9 °C (M. Lukac, pers comm).

4.2.2 Measurements

On the 3rd May 2004, rooted stock of 32 *P. trichocarpa* and 32 *P. deltoides* trees were transported to the field site where they were planted into individual 20 litre tubs containing John Innes (#3) potting compost. Each plant was thoroughly watered after potting. In total, four plants of each species were placed into each of the eight rings. The pots were distributed as evenly as possible within the rings. A visual assessment at the end of the experiment showed that the plants were not root-restricted in the pots, which would have affected the response to eCO₂.

The height of each tree was measured on the 2nd August 2005. The leaves (ages one to nine) were photographed on 2nd August 2005 and 3rd August 2005 in order to assess size and shape. Cell impressions were taken from the abaxial surface of leaf ages two, five and nine. For leaf ages five and nine, cell imprints were sampled from seven abaxial interveinal areas (from base to tip). The images of the cell impressions were

obtained using a Nikon microscope. To study leaf anatomy, tissue from leaf age three (exposed to [aCO₂] or [eCO₂]) were sampled into fixative. The material was sent to Anton Page (University of Southampton Bioimaging Unit) for sectioning. The samples were then visualised using a Nikon microscope.

4.2.3 Endogenous XET activity

The endogenous XET activity was detected using fluorescently labelled oligosaccharides, a kind gift from S. Fry (University of Edinburgh). The material was sampled from leaf age three of *P. deltoides* and *P. trichocarpa* exposed to either [aCO₂] (ring 7) or [eCO₂] (ring 5).

The XET activity was localised using a xyloglucan oligosaccharide sulphorhdamine conjugate (XLLG-SR, a fluorescent acceptor, see Figure 4.4.1). Leaf material (ten 25 mm² sections) from the second interveinal area of the leaf (where interveinal one was defined as the most basal) was sampled directly into 100µl buffer (90µM XLLG-SR, 25mM MES buffer, pH5.6) and placed in cold storage for transportation. The material was stored in the buffer for one week (in the dark at 4°C). The material was vacuum infiltrated using a 1ml syringe after which the material and buffer were transferred to a new vessel and kept in the dark for two hours. The material was washed twice with 70% (v/v) ethanol and stored in the dark at 4°C for further analysis.

Three sections of tissue (per species per treatment) were mounted onto a microscope slide using 70% (v/v) ethanol and a non-silicated coverslip. The samples were sealed by applying silicon glue to the edge of the coverslip, which was then irradiated with UV-light to seal it in place. The images were captured using the Confocal Laser Scanning Microscope using the same zoom and gain settings for each image. The 'Metamorph' software package was used for data analysis, allowing the quantification of fluorescence in terms of the number of red pixels in the image as a proportion of the total number of pixels. This technique has previously been reported for lettuce tissue (Wagstaff *et al*, 2008).

4.3 Results

4.3.1 Above-ground growth

The results suggest that above-ground growth was stimulated in response to [eCO₂] in *P. trichocarpa*, since tree height was statistically significantly different between the two conditions (Figure 4.3.1). Furthermore, leaf production was also stimulated in this species as shown by the significant increase in leaf number in [eCO₂] (Figure 4.3.2). However, the growth of *P. deltoides* did not differ between [aCO₂] and [eCO₂] since there were no statistical differences in tree height (Figure 4.3.1) or leaf number (Figure 4.3.2).

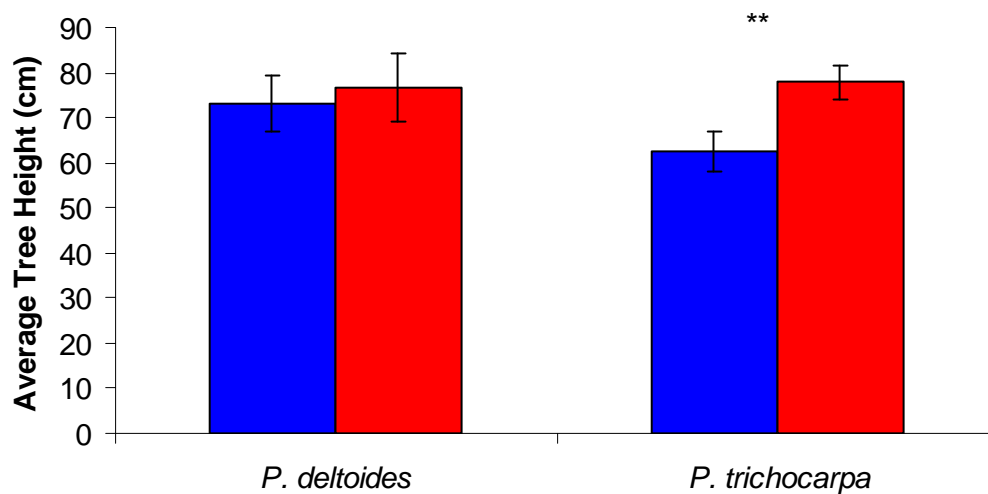


Figure 4.3.1. The average height of *P. deltoides* and *P. trichocarpa* exposed to [aCO₂] (blue bar) or [eCO₂] (red bar). Standard error bars are presented on the figure. The results of a one-way ANOVA post-hoc Dunnetts comparison test for [eCO₂] are also given on the graph. (**= p<0.01). n=4.

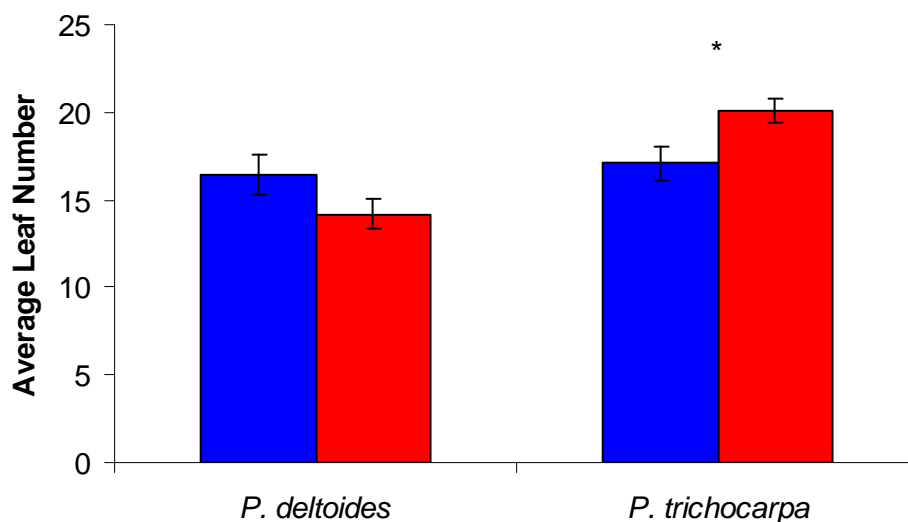


Figure 4.3.2. The average number of leaves of *P. deltoides* and *P. trichocarpa* exposed to [aCO₂] (blue bar) or [eCO₂] (red bar). Standard error bars are presented on the Figure. The results of a one-way ANOVA post-hoc Dunnetts comparison test for [eCO₂] are also given on the graph. (* = $p < 0.05$). $n=4$.

Leaf area was stimulated in ages one and four in *P. deltoides* (Figure 4.3.3). Beyond this age there was a general reduction in leaf area although this was not statistically significant. In *P. trichocarpa*, leaf area was statistically significantly different in ages one, two and three. Leaf area was generally reduced in [eCO₂] in young leaf ages of this species, but stimulated in the mature leaves.

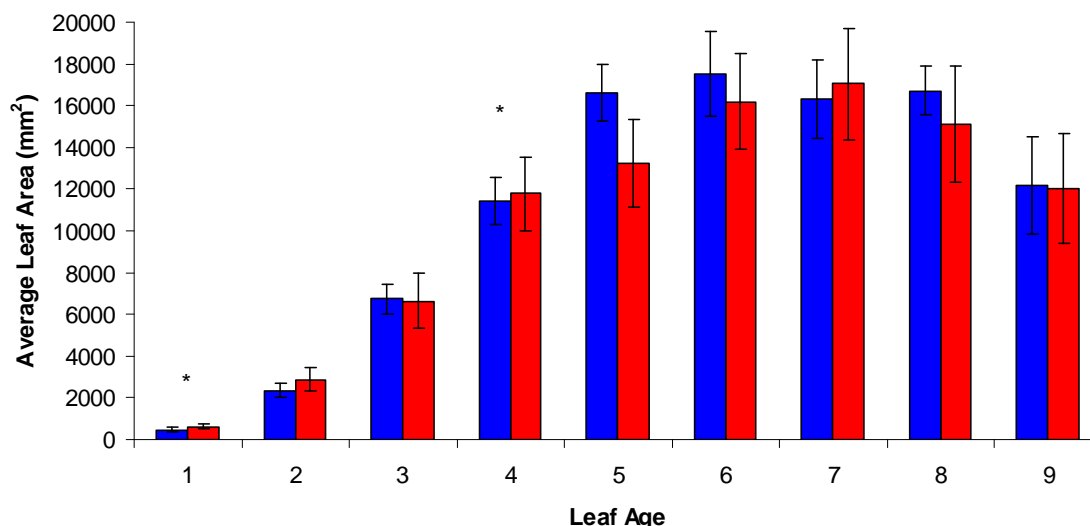


Figure 4.3.3. The average leaf area of *P. deltoides* exposed to either [aCO₂] (blue) or [eCO₂] (red). Leaf one was defined as the first fully unfurled leaf (i.e. the youngest leaf) on day one of the experiment (2nd August 2005). The results of a one-way ANOVA post-hoc Dunnetts comparison test for [eCO₂] are also given on the graph. (*= p<0.05). Standard error bars are shown. n=4.

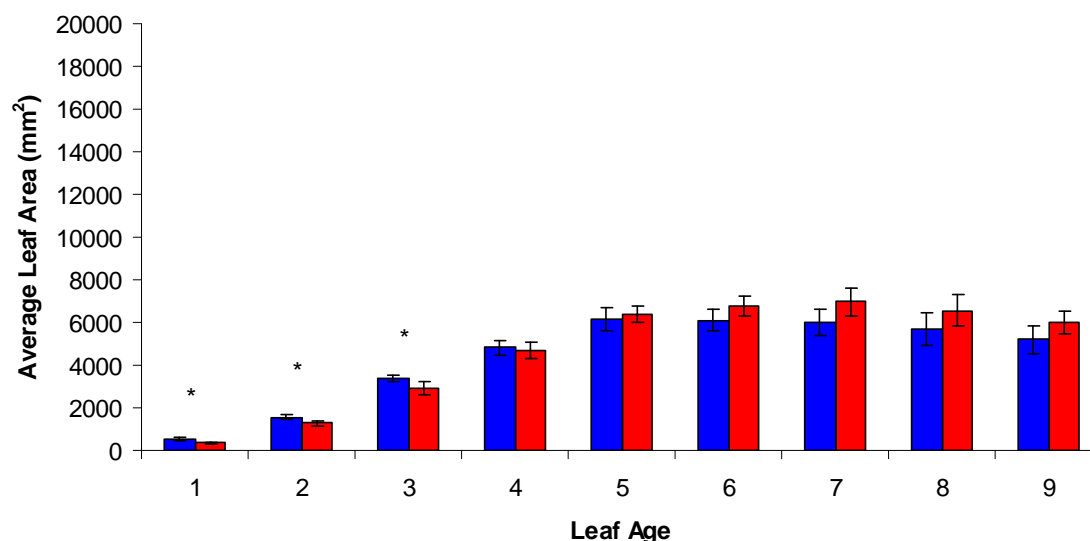


Figure 4.3.4. The average leaf area of *P. trichocarpa* exposed to either [aCO₂] (blue) or [eCO₂] (red). Leaf one was defined as the first fully unfurled leaf (i.e. the youngest leaf) on day one of the experiment (2nd August 2005). The results of a one-way ANOVA post-hoc Dunnetts comparison test for [eCO₂] are also given on the graph. (*= p<0.05). Standard error bars are shown. n=4.

Populus deltoides showed no response to [eCO₂] in terms of SLA in any of the three age categories that were sampled (Figure 4.3.5). However, there was a significant decrease in SLA in the young leaves of *P. trichocarpa* in response to [eCO₂] (Figure 4.3.6).

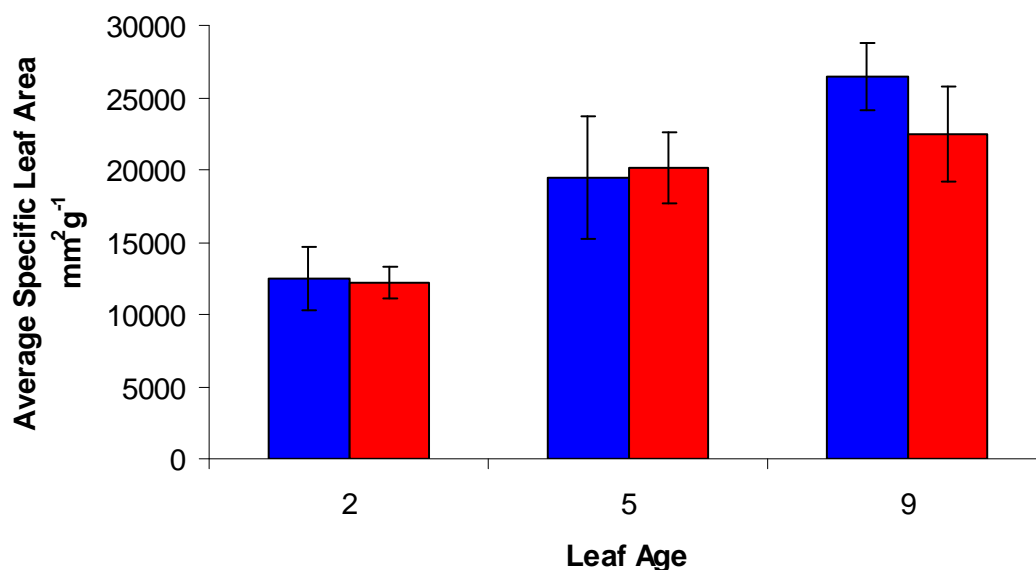


Figure 4.3.5. The SLA of *P. deltoides* exposed to either [aCO₂] (blue) or [eCO₂] (red). SLA was measured for leaf ages two, five and nine, where leaf one was defined as the first fully unfurled leaf (i.e. the youngest leaf) on day one of the experiment (2nd August 2005). A one-way ANOVA post-hoc Dunnetts comparison test for [eCO₂] was conducted but there were no statistically significant differences between treatments at any of the leaf ages. Standard error bars are shown. n=4.

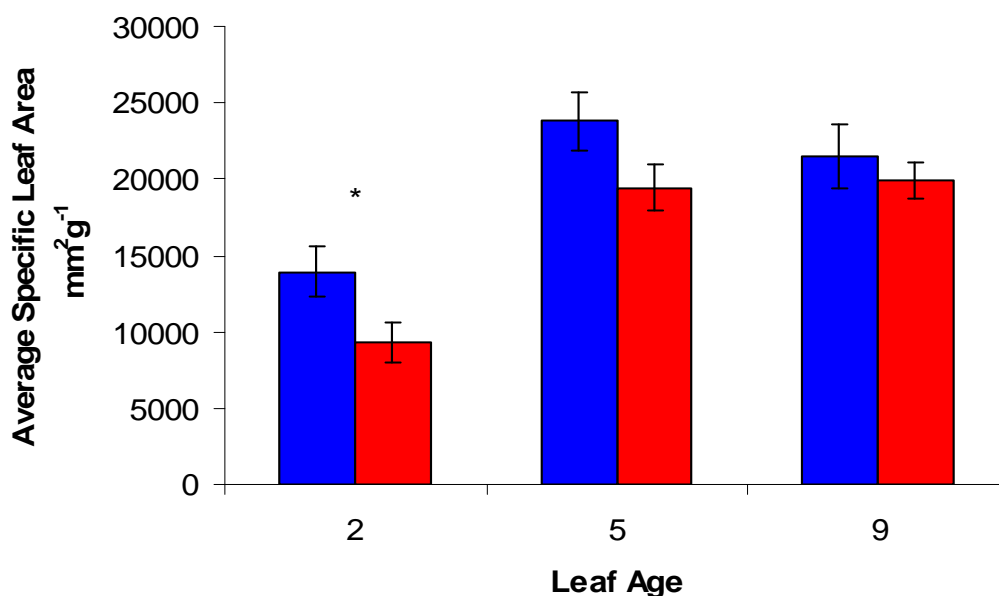


Figure 4.3.6. The SLA of *P. trichocarpa* exposed to either [aCO₂] (blue) [eCO₂] (red). SLA was measured for leaf ages two, five and nine, where leaf one was defined as the first fully unfurled leaf (i.e. the youngest leaf) on day one of the experiment (2nd August 2005). The results of a one-way ANOVA post-hoc Dunnetts comparison test for [eCO₂] are also given on the graph. (* = p<0.05). Standard error bars are shown. n=4.

4.3.2 Cellular analyses

There was no significant treatment effect on epidermal cell area in any of the three leaf ages in *P. deltoides* (Figure 4.3.7) or *P. trichocarpa* (Figure 4.3.8).

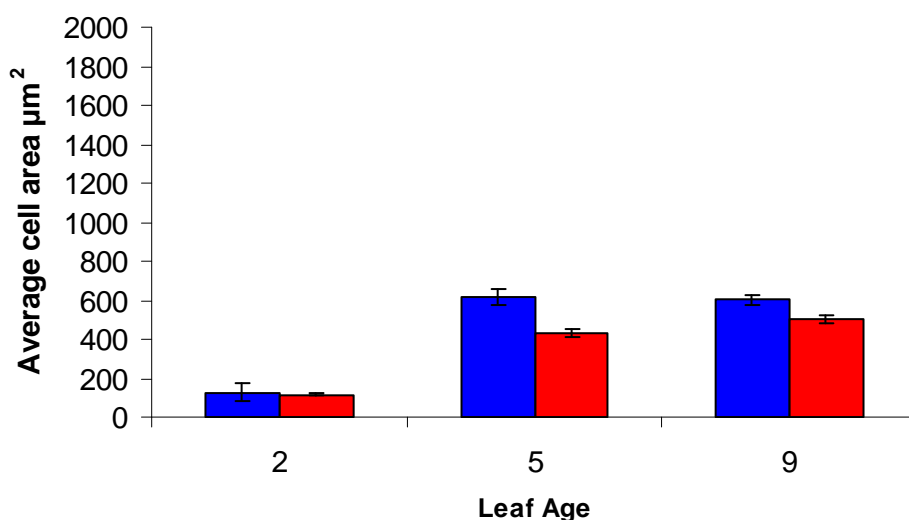


Figure 4.3.7. Average epidermal cell area in *P. deltoides*. Blue bars represent the results from [aCO₂] and red bars represent results from [eCO₂]. The cell area was measured for leaf ages two, five and nine, where leaf one was defined as the first fully unfurled leaf (i.e. the youngest leaf) on day one of the experiment (2nd August 2005). A one-way ANOVA post-hoc Dunnetts comparison test for [eCO₂] was conducted but there were no statistically significant differences between treatments at any of the leaf ages. Standard error bars are shown. n=20.

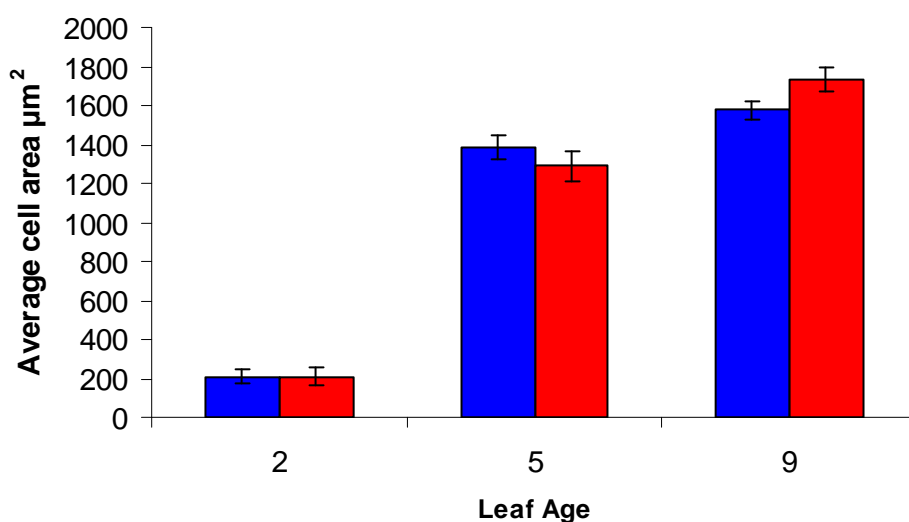


Figure 4.3.8. Average epidermal cell area in *P. trichocarpa*. Blue bars represent the results from [aCO₂] and the red bars represent the results [eCO₂]. The cell area was measured for leaf ages two, five and nine, where leaf one was defined as the first fully unfurled leaf (i.e. the youngest leaf) on day one of the experiment (2nd August 2005).

A one-way ANOVA post-hoc Dunnetts comparison test for [eCO₂] was conducted but there were no statistically significant differences between treatments at any of the leaf ages. Standard error bars are shown. n=20.

The average interveinal cell area remained constant across the lamina of *P. deltoides*. The cell area of *P. trichocarpa* was consistently higher in [eCO₂] across the lamina of mature leaves than ambient mature leaves or semi-mature leaves (data not shown). There was no significant treatment effect for average epidermal cell number in any leaf age of *P. deltoides* (Figure 4.3.9) or *P. trichocarpa* (Figure 4.3.10).

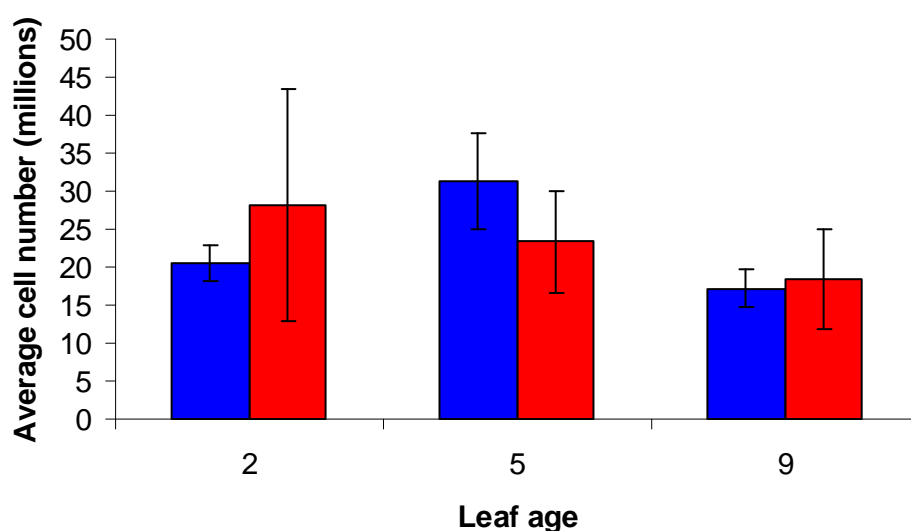


Figure 4.3.9. The average number of epidermal cells per leaf in *P. deltoides* exposed to [aCO₂] (blue) or [eCO₂] (red). The number of cells was calculated for leaves two, five and nine only (where leaf one was defined as the first fully unfurled leaf (i.e. the youngest leaf). A one-way ANOVA post-hoc Dunnetts comparison test for [eCO₂] was conducted but there were no statistically significant differences between treatments at any of the leaf ages. Standard error bars are shown.

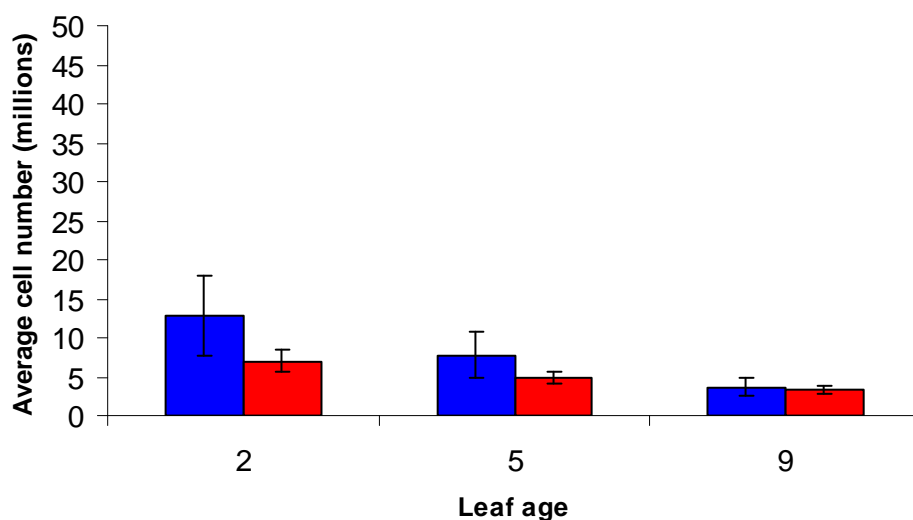


Figure 4.3.10. The average number of epidermal cells per leaf in *P. trichocarpa* exposed to [aCO₂] (blue) or [eCO₂] (red). The number of cells was calculated for leaves two, five and nine only (where leaf one was defined as the first fully unfurled leaf (i.e. the youngest leaf)). A one-way ANOVA post-hoc Dunnetts comparison test for [eCO₂] was conducted but there were no statistically significant differences between treatments at any of the leaf ages. Standard error bars are shown.

4.3.3 Leaf anatomy

The results from the leaf anatomy studies showed cell production was influenced by increased carbon availability in the young leaves of *P. trichocarpa* (Figure 4.3.11). This figure clearly shows large intercellular spaces in the mesophyll layer of *P. trichocarpa* grown under ambient atmospheric conditions. The intercellular air spaces were lacking in *P. trichocarpa* exposed to [eCO₂] and increased cell production was clearly visible and led to an increase in leaf thickness. Conversely, there was no apparent effect of [eCO₂] in *P. deltoides*.

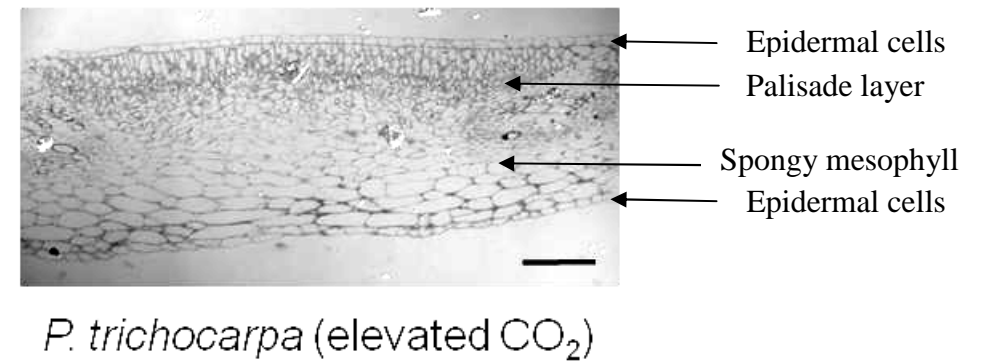
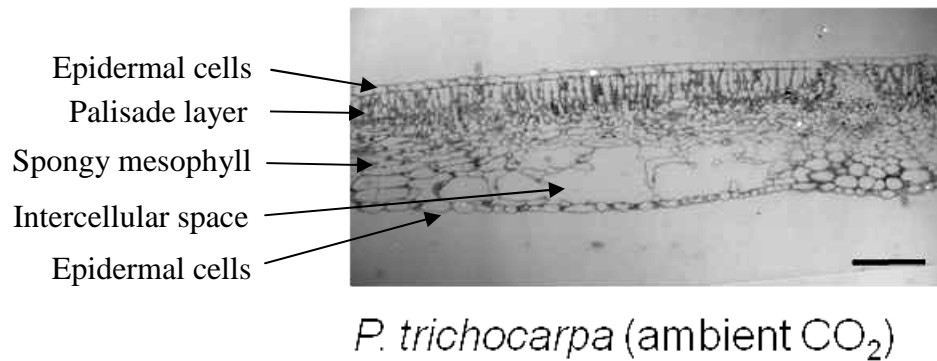
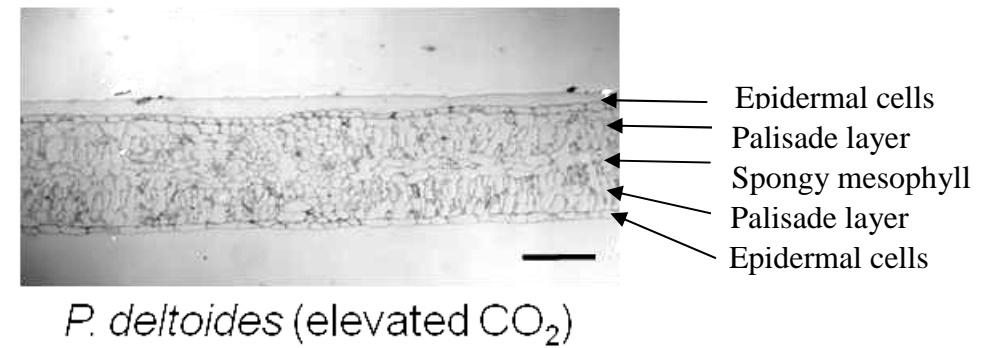
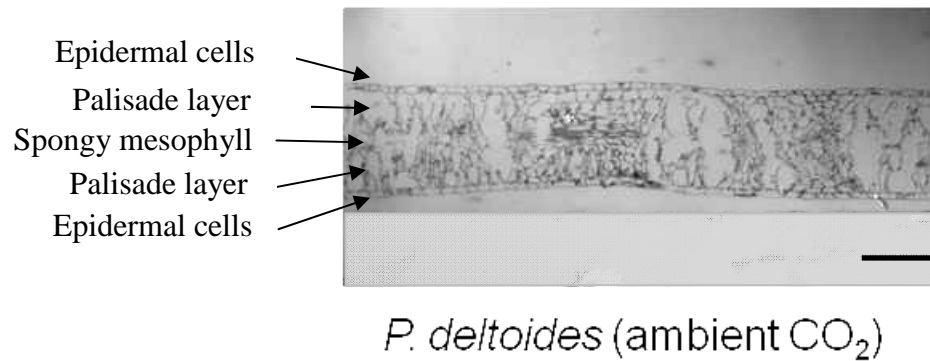


Figure 4.3.11. Cross sections of *P. deltoides* and *P. trichocarpa* exposed to [aCO₂] or [eCO₂]. The material for the cross sections were collected from leaf age three in rings five ([eCO₂]) and seven ([aCO₂]). The scale bar represents 100µm. The cross sections were produced by Dr Anton Page, University of Southampton.

4.3.4 XET co-localisation

Endogenous XET activity was quantified using Sulphorhodamine conjugates of xyloglucan oligosaccharides. The images were captured using a confocal laser scanning microscope, and the results were quantified using the software programme 'MetaMorph'. From purely a visual assessment (Figure 4.3.12), it was clear that there was a species difference in XET activity, regardless of treatment.

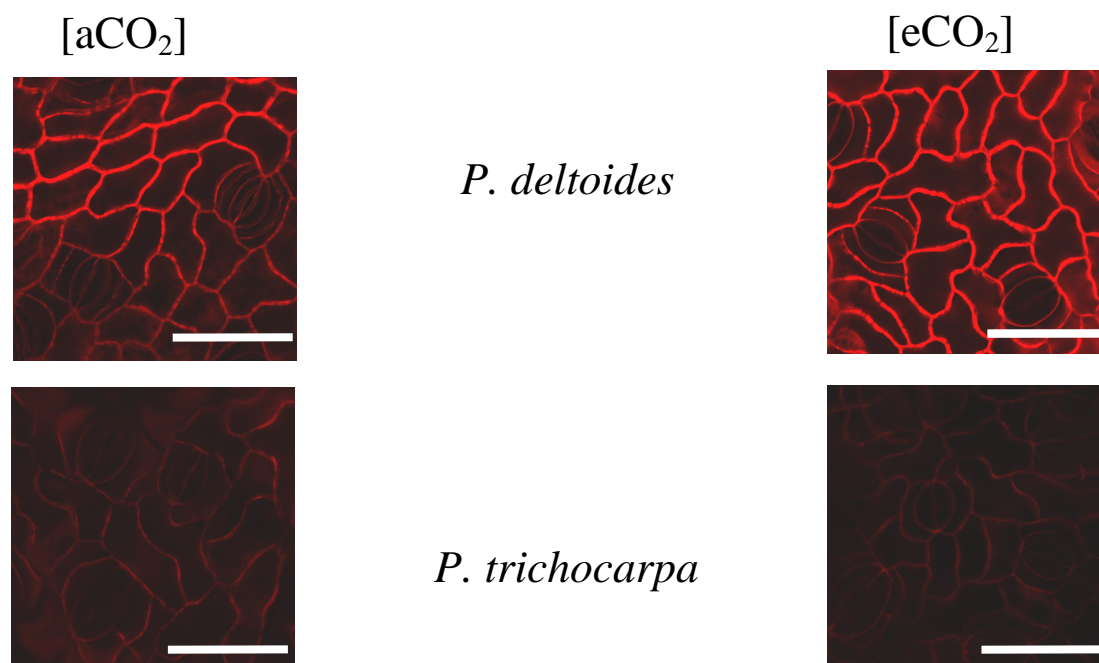


Figure 4.3.12. Examples of images captured on the Confocal Laser Scanning Microscope in order to quantify XET activity in *P. deltoides* and *P. trichocarpa* exposed to [aCO₂] or [eCO₂]. The samples were collected from leaf age three from both species (where leaf one was defined as the first fully unfurled leaf). The images were captured from the centre of the tissue sample. Each white bar represents 50μm.

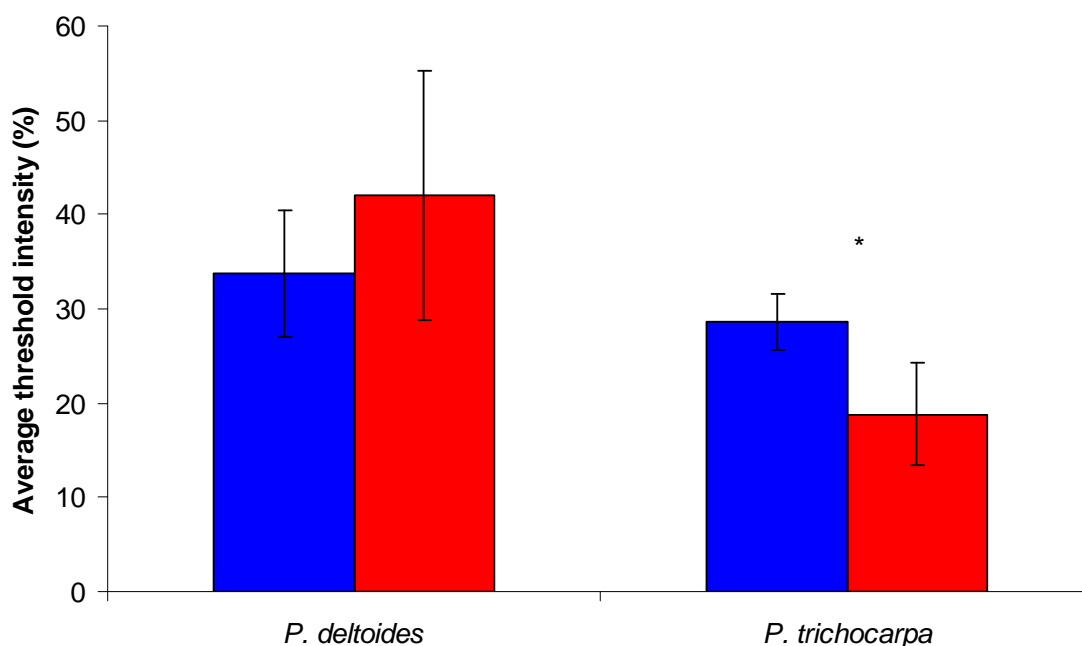


Figure 4.3.13. The XET activity was quantified by expressing the number of red pixels as a percentage of the total number of pixels in the image. This analysis was conducted using the ‘MetaMorph’ software. The figure shows the results from leaf age three of *P. deltoides* and *P. trichocarpa* exposed to either [aCO₂] (blue bars,) or [eCO₂] (red bars). A one-way ANOVA was conducted on the data (*= p<0.05). Standard error bars are shown on the graph. n=6.

The quantification of the results of the XET assay (Figure 4.3.13) was conducted in ‘MetaMorph’ by measuring the number of red pixels as a percentage of the total number of pixels in the image, as has been done previously with this assay (Wagstaff *et al*, 2008). The results show that there was a significant difference between the treatments in *P. trichocarpa*, but not in *P. deltoides*. However, there were greater levels of XET activity in [aCO₂] in *P. trichocarpa*. Whilst this is the first time this assay has been done in these two species when exposed to [eCO₂] the results need to be interpreted with caution. Since there was no control tissue (i.e. buffer with no fluorophore) it would be unwise to rule out the possibility of autofluorescence contributing to the data.

4.4 Discussion

Leaves are important for determining light interception, carbon gain and water use efficiency, and are hence linked to overall productivity. Leaf area is a trait that is correlated with biomass production (Rae *et al*, 2004). Additionally, traits including leaf longevity, leaf thickness and the degree of efficiency in biomass partitioning between leaves and stems also influence the relationship between leaf area and biomass (Tharakan *et al*, 1998). Using the FACE facility in Bangor, North Wales, it was possible to expose *P. deltoides* and *P. trichocarpa* to [eCO₂] predicted for 2050.

The growth characteristics of *Populus* have resulted in its status as a biomass crop candidate (Taylor *et al*, 2002). However, the growth mechanisms adopted by *Populus* species grown in [eCO₂] are still not fully understood. Physiological and morphological responses to [eCO₂] have been characterised in a number of different species in FACE experiments (Ainsworth and Long, 2005). Here two species with contrasting growth strategies were used as a tool to help further our knowledge into the response to [eCO₂]. To the best of our knowledge this is the first time that any growth analysis has been conducted on these two species using FACE.

4.4.1 Leaf growth in [eCO₂]

Leaf growth in [eCO₂] is a plastic process (Taylor *et al*, 2005). In general, plant growth in [eCO₂] was observed to be slightly stimulated. Plant height was stimulated in *P. trichocarpa* under FACE conditions. A similar response to [eCO₂] in terms of tree height has been reported in other FACE experiments (Ainsworth and Long, 2005). However, there was no such stimulation in *P. deltoides* in the FACE experiment. The young *Populus* leaves were affected by [eCO₂], which may due to the initial RGR of the leaves. For example, at the EUROFACE site, stimulation in leaf area and biomass in [eCO₂] was attributed to an initially higher RGR (Liberloo *et al*, 2004). The RGR of young leaves is greater in *P. deltoides* than *P. trichocarpa* (chapter 3), which may explain the stimulation in leaf area in *P. deltoides* but not *P. trichocarpa*.

A number of previous studies have shown that SLA is reduced in leaves grown in [eCO₂] (e.g. Tricker *et al*, 2004), which reflects the higher starch content (Walter *et al*, 2005), which may cause an overall enhancement of canopy respiration (Barron-Gafford *et al*, 2005). However, in this study SLA was unaffected by FACE. SLA has

also been shown to be unaffected by [eCO₂] in EUROFACE (Gielen *et al*, 2001), although a slight reduction in SLA was apparent in *P. trichocarpa* only.

The anatomical analysis of leaf structure indicated the distinct differences between the two species. *P. deltoides* possess a double palisade layer, a character absent in *P. trichocarpa*. The intracellular airspaces in *P. trichocarpa* give the abaxial sides of the leaves their characteristic white appearance (Van Volkenburgh and Taylor, 1996). The leaf cross sections in Figure 4.3.11 show an apparent reduction in the number of intracellular airspaces in *P. trichocarpa* under [eCO₂]. This could be due to enhanced cell production, which has been reported to be stimulated in epidermal cells in response to [eCO₂] (Taylor *et al*, 2003). However, this contrasts with aspen where [eCO₂] caused the intercellular air space volume in the mesophyll to increase (Oksanen *et al*, 2001). There was no apparent effect of [eCO₂] on the anatomy of the leaves of *P. deltoides*.

4.4.2. Leaf epidermal cell characteristics following exposure to FACE

Elevated CO₂ causes an increase in TNC (total non-structural carbohydrate) in leaves, which enhances cell expansion (Rae *et al*, 2006; Taylor *et al*, 1994) and production (Masle, 2000). In *P. x euramericana*, epidermal cell area and number are sensitive to [eCO₂] in young leaves, whereas only cell number is significantly different in [eCO₂] in mature leaves (Taylor *et al*, 2003). Furthermore, in *P. x euramericana* and *P. nigra*, epidermal cell size is increased in [eCO₂] (Tricker *et al*, 2004). In this experiment however, there was no statistical significant difference in cell size or number in response to [eCO₂] at any of the leaf ages studied.

Leaves exhibit heterogenous spatial growth patterns across the surface of the lamina (Matsubara *et al*, 2006; Walter *et al*, 2005). Since it therefore must be assumed that cell size is heterogeneous across the lamina, it is necessary to sample from across different areas of the leaf; from the base to the tip. There was no spatial difference in cell area in *P. deltoides* across the leaf lamina in [aCO₂]. Similarly, there were no spatial differences in epidermal cell area in *P. deltoides* in a study conducted by Matsubara *et al*, (2006). In leaf nine of *P. trichocarpa* there was a difference between [aCO₂] and [eCO₂], with the biggest variation at ‘interveinal five’. Increasing cell cycle activity in the basal areas of expanding leaves has been shown in *Arabidopsis*

(Donnelly *et al*, 1999) and previous reports on the CO₂ response have shown that the basal areas of the leaf were particularly affected (Taylor *et al*, 2003), but this was not shown here.

4.4.3. XETs and [eCO₂]

Xyloglucans are a major constituent of the primary cell wall of higher plants. The xyloglucan chains play a role in maintaining the structure of the wall by tethering adjacent cellulose microfibrils together. In order for the cell to grow, the constraint placed upon the microfibrils by the xyloglucan tethers must be overcome. The XETs are involved in this process (Fry *et al*, 1992). The XETs cleave the xyloglucan chains (which represent the ‘donor’ substrates). They create an extended chain by synthesizing a new bond between the donor substrate and another xyloglucan chain (the ‘acceptor’ substrate). This arrangement thus permits the cells to increase in size in an organised and controlled manner. In this experiment, XET activity was quantified in young growing (age three) leaves of both species. The sulphorhodamine conjugates of xyloglucan oligosaccharides (XGO-SRs) were the ‘acceptor’ substrates and the xyloglucan chains were the ‘donor’ substrates. The donor substrates were cleaved in the presence of XET, allowing a bond to form between the donor and acceptor substrate. The XGO-SR therefore became incorporated into the cell wall and the product was detectable due to the presence of the fluorescent moiety (Fry, 1997; Vissenberg *et al*, 2000) (Figure 4.4.1).

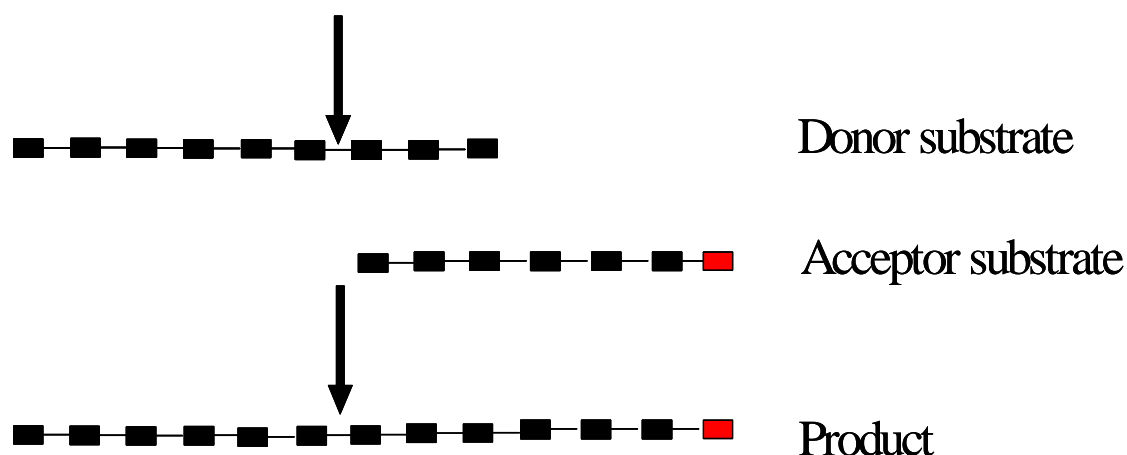


Figure 4.4.1. A diagrammatic representation of the XET co-localisation assay. The xyloglucan chains within the cell wall act as the ‘donor substrate’. The chains are cleaved due to the action of XET’s. Sulphorhodamine conjugates of xyloglucan oligosaccharides act as the ‘acceptor’ substrates. New bonds are formed between the recently cleaved donor substrate and the acceptor substrate due to the action of the XET’s. The product of this union can be visualised due to the incorporation of the fluorescent moiety (represented by the red blocks on the diagram). The arrows represent the action of the XET’s. Figure adapted from (Fry, 1997).

It has been postulated that $[eCO_2]$ causes a decrease in cell pH (Ferris *et al*, 2001), which would therefore comply with the acid growth theory of leaf development (Rayle and Cleland, 1992). Previous experiments to investigate the effects of elevated CO_2 in *Populus* have indicated that xyloglucan endotransglycosylases (XETs) are key candidates for the observed growth difference between leaves grown under ambient and elevated $[CO_2]$ (Ferris *et al*, 2001; Gardner *et al*, 1995). Furthermore, high levels of XET are known to correlate with low pH (Okamoto-Nakazato, 2000) thus complying with the acid growth theory. This all therefore suggests that XETs play an important role in leaf growth and development in $[eCO_2]$.

The results from this assay indicated that in *P. deltoides* there was a slight increase in XET activity in $[eCO_2]$ (non-significant) as assessed by the co-localisation assay. In *P. trichocarpa*, there was a significant difference in activity between ambient and elevated $[CO_2]$, with cells in $[aCO_2]$ displaying higher XET activity. The leaf area of *P. trichocarpa* (age 3) was greater in $[aCO_2]$ (see Figure 4.3.4), and hence may be a reflection of the higher XET activity observed in this species in $[aCO_2]$ conditions. This however contradicts with the theory that $[eCO_2]$ causes a decrease in pH which is correlated with high XET activity.

The difference in activity between the species may be due to differences in cell size. The quantification was based upon the set window of the image, rather than on a cell-by-cell basis. Therefore the larger cell size of *P. trichocarpa* may have resulted in the XET activity of this species being underrepresented. Furthermore, there may be differences between the two species' in terms of the ability of the substrate to penetrate the tissue. The images were collected from the middle of the tissue section but differences in the accessibility of the tissue may have influenced the quantification. In short, the merits of conducting such an assay are clear when considering the influence of [eCO₂] on cell growth. However, the results presented here need to be interpreted with caution. It would be wise to repeat such an exercise using an adequate control as a reference point.

4.4.4 The CO₂ response

A meta-analysis of the results collected from across 12 different FACE experiments has shown that the magnitude of the response to [eCO₂] varies between species, growing seasons and experimental conditions (Ainsworth and Long, 2005). The results from this experiment showed modest growth stimulation in [eCO₂] in *P. trichocarpa*, but not *P. deltoides*.

P. trichocarpa has previously been shown to respond to a greater degree to [eCO₂] than *P. deltoides* in an open-topped chamber experiment (Rae *et al*, 2006). *P. trichocarpa* showed a greater growth stimulation in terms of leaf area, petiole length, leaf number, leaf extension, leaf expansion, leaf width and leaf length in this experiment (Rae *et al*, 2006). However, it was clear from the trees growing at the BangorFACE field site that the conditions favoured the growth of *P. trichocarpa*. *Populus deltoides* originates from warm climates of the eastern United States and therefore the growing environment of the field site was unfavourable. The contrasting climatic origins of the two species suggest that future experiments aimed at unravelling detailed mechanistic processes involved in leaf growth and development of the two species should focus on the use of experimental conditions that are less liable to large environmental fluctuations. Under such conditions the growth of one or the other species would not be favoured.

4.5 Conclusion

In general, above-ground plant growth was slightly stimulated in [eCO₂], although this was dependent upon many factors. It is likely that environmental influences greatly affect CO₂ growth responses. The natural climatic conditions of each species are very different, and it is likely that the responses of the two species reflected these differences.

The activity of the cell wall loosening enzyme XET was assessed in both species exposed to ambient atmospheric conditions and FACE. The results confirm that it is likely that XET is involved in cell wall loosening and leaf growth in [eCO₂]. The slight increase in XET activity in [eCO₂] in *P. deltoides*, suggests that stimulated cell expansion could be important in the leaf growth response. There was no such increase in *P. trichocarpa*.

CHAPTER 5

The transcriptome of *Populus* following exposure to [eCO₂] using a FACE experimental system

5.0 Overview

Many previous studies have focussed on the morphological and physiological responses of plants to [eCO₂]. Here I have used cDNA microarrays to conduct a study on the transcriptome of *Populus* exposed to [eCO₂]. Two different cDNA microarray platforms were used, and a qPCR experiment was conducted in order to confirm the differences in expression observed between the two conditions.

Few studies have previously attempted to quantify gene expression studies in trees exposed to [eCO₂]. However, in agreement with those that have been conducted, there were found to be very few transcripts that demonstrated large differences in expression between the two treatments.

The species selected for this study was *P. x euramericana* (*P. deltoides* x *P. nigra*), grown at the EUROFACE site in central Italy. Previous studies have indicated that this species is highly responsive to [eCO₂], but here it was concluded that these changes are not represented at the gene expression level.

5.1 Introduction

The concentration of greenhouse gases in the atmosphere have increased markedly since 1750 (IPCC, 2007). In particular the concentration of CO₂ has risen from 280ppm in the pre-industrial era to 379ppm in 2005 (Prentice *et al*, 2001; IPCC, 2007), representing an increase of 74%. The rise of atmospheric [CO₂] is positively correlated with the changes in industrial CO₂ emissions (Keeling *et al*, 1995). Under predicted climatic scenarios the concentration of CO₂ will reach 550ppm by the middle of this century. This concentration has been used as a target value in many CO₂ experiments, thus providing a realistic model for studying growth and development.

Forest trees represent a significant carbon sink (Myneni *et al*, 2001) therefore an evaluation of the potential of forest trees to sequester carbon under future climatic scenarios is necessary. For example, European forests have been estimated to sequester 363 Tg C m⁻²y⁻¹ (Falge *et al*, 2002). FACE experiments allow a unique chance to study physiological responses to [eCO₂] at the ecosystem level. This provides an ideal situation to study the response of trees to [eCO₂] since the experiment could potentially be used for many years of study.

Numerous studies have been conducted on the morphological and physiological responses of [eCO₂] on plant development and the general consensus is that growth is stimulated under such conditions. Reports on the responses to [eCO₂] exposure include increased photosynthesis (Moore *et al*, 1999), decreased respiration (Volin and Reich, 1996), increased water use efficiency (Tjoelker *et al*, 1998), stimulated above-(Norby *et al*, 1999) and below-(King *et al*, 2001) ground growth. However, the response to [eCO₂] is also dependent upon time scale of exposure. It is known that prolonged growth in [eCO₂] causes an acclimatory response to the stimulus. This is most commonly observed by a reduction in photosynthesis (Drake *et al*, 1997) and its associated proteins (Webber *et al*, 1994). Furthermore, this reduction in photosynthetic activity has been reflected by reduced expression of transcripts encoding genes involved in photosynthesis (e.g. Cheng *et al*, 1998). Acclimation has been suggested to occur within days to weeks of exposure (Moore *et al*, 1999).

Ecological genomics (Feder and Mitchell-Olds, 2003) is a discipline aimed at coalescing ecology and molecular biology in order to provide an understanding of the

function and variation of genes that are important within an ecological context (Ouborg and Vriezen, 2006). Such information is necessary in order to comprehend the morphological and physiological changes that occur. Additionally, such an understanding is particularly important for adaptive traits that are relevant to productivity (Taylor *et al*, 2005).

Modifications in gene expression can occur rapidly in response to many environmental changes (Howe and Brunner, 2005). The use of genetic profiling techniques such as microarrays provides a means of studying such changes. However, there have been few investigations into the genetic changes that underlie responses to [eCO₂]. With the publication of the *Populus* genome sequence (Tuskan *et al*, 2006) and the availability of poplar microarrays (Sterky *et al*, 2004), it is now possible to determine global changes in gene expression for trees grown in enriched CO₂ conditions. The results from such experiments will potentially provide candidate genes that are important in determining growth and development under future climatic conditions. Furthermore, this resource can potentially unveil some novel transcripts involved in the response to increased [CO₂], as well as confirming speculative candidates proposed in previous experiments (e.g. xyloglucan endotransglycosylases (Ferris *et al*, 2001) (Chapter 4)).

The content of the following chapter reports a set of investigations into the changes that occur at the transcript level in response to [eCO₂] in *P. x euramericana*, grown at the EUROFACE site (www.unitus.it/euroface). Previous studies conducted at EUROFACE have shown that *P. x euramericana* (*P. deltoides* x *P. nigra*) is highly responsive to [eCO₂] (Taylor *et al*, 2003; Ferris *et al*, 2001) in terms of leaf growth. It was for this reason that the study focussed on this species. A qPCR experiment was also conducted in order to confirm some of the changes in transcript levels that were observed from the results from the microarrays. The aim of the investigation was to determine changes in gene expression and identify candidate genes important for leaf growth and development in *Populus* under future predicted climatic scenarios. Transcriptomics was conducted on two leaf ages (defined as ‘young’ and ‘semi-mature’) in order to assess the effect of [eCO₂] on leaf development. The results presented in this chapter have been published (Taylor *et al*, 2005).

5.2 Materials and Methods

5.2.1 The EUROFACE experimental system

The EUROFACE site is located in central Italy, in the province of Viterbo (Tuscania, 42°22'N, 11°48'E). In total there are six experimental plots located 120m apart on the 9 Ha site. Three of the six rings are exposed to FACE (Figure 5.2.1a). Each octagonal plot is 30m x 30m and split into 2 halves by a 1m deep resin-glass barrier to allow for different fertilisation treatments. During the 2004 growing season, a total of 290 Kg Ha⁻¹ ammonium nitrate fertiliser was supplied over a period of 22 weeks from 23rd April 2004 to 17th September 2004.

Each half of the experimental plot is further split into three subsections containing *P. alba* L., (Clone 2AS-11), *P. nigra* L., (Clone Jean Pourtet) and *P. x euramericana* (Dode) Guinier (*P. deltoides* x *P. nigra*, clone I-214) (Figure 5.2.1b). The trees are planted 1m from the nearest neighbour. The entire plantation is drip irrigated with 6-10 mm water per day during the growing season.

The design for the FACE system is described by (Miglietta *et al*, 2001). Pure CO₂ is released from jets through laser-drilled holes in the horizontal polyethylene pipes that form the octagonal shape of the FACE ring. The target [CO₂] for the three FACE rings (rings one, four and five) is 550ppm. The remaining three rings (two, three and six) are subjected to ambient atmospheric [CO₂]. The elevated [CO₂] measured at one minute intervals was found to be within 20% of this target concentration 89.4% of the time during the 2002 growing season, and 72.2% of the time during the 2003 growing season (Liberloo *et al*, 2005). The [eCO₂] treatment is supplied from bud burst (March/April) until leaf fall (November).

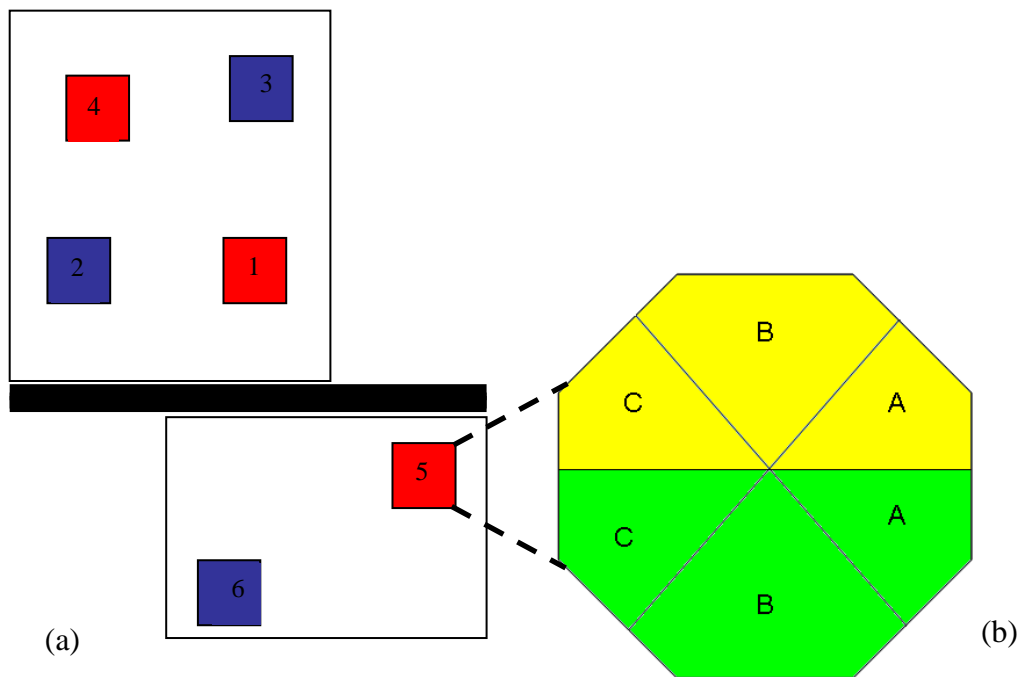


Figure 5.2.1. (a) A plan of the EUROFACE site in Italy. The two sites are separated by a small road (indicated by the solid black line). Red squares represent the FACE rings which expose the trees to 550ppm CO₂. Blue squares represent the [aCO₂] rings. (b) An example of one of the six experimental rings at the EUROFACE site. The plot is divided into six, with one of three species (A= *P. alba*, B= *P. nigra* or C= *P. x euramericana*) grown in each division. Each plot is split in two, where one half receives nitrogen treatment (represented in green) and the other half does not (represented in yellow). Diagram adapted from Gielen *et al* (2003).

5.2.2 Leaf samples and RNA extractions

In total, three sampling campaigns took place during the 2004 growing season (20th June 2004, 3rd August 2004 and 31st August 2004). Leaf ages three ('young') and six ('semi-mature') of *P. x euramericana* were sampled from the three ambient and three elevated CO₂ rings, and from the two nitrogen treatments within each ring. It is worthy to note that upon sample selection, leaf age 'one' was defined as the first fully unfurled leaf from the meristem. The samples were harvested from four biological replicates under each condition.

The RNA extractions were performed on leaf ages three and six, sampled from the EUROFACE site from all three time-points during the 2004 growing season. The

concentration of RNA was assessed using the Nanodrop spectrophotometer and the quality was checked using the Bioanalyser.

5.2.3 POP2 microarrays

5.2.3.1 Experimental design

Microarrays were conducted on pooled samples (for ages three and six) from the three sampling time points in the 2004 growing season using the samples from the ambient nitrogen treatment. The pools consisted of four biological replicates from each of the rings for each leaf age at the three time-points. The pools included samples taken from across the sampling time points in order to determine the overall effect of increased [CO₂] on the *Populus* transcriptome. The ‘elevated’ pools consisted of samples collected from rings one and four only, whilst the ‘ambient’ pools consisted of leaves collected from rings two and three only.

In total, eight POP2 microarrays (including dye swaps) were hybridised using the *P. x euramericana* samples from the pools from the 2004 growing season (Table 5.2.1). The design of the microarrays is given in Figure 5.2.2.

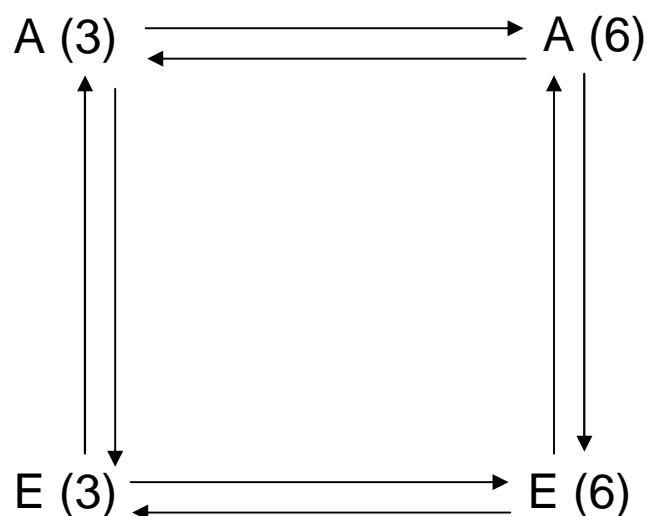


Figure 5.2.2. The POP2 microarray experiment was designed to compare both treatment ([aCO₂] or [eCO₂]) and developmental age. A= ambient [CO₂] pool (representing replicates from rings two and three only) E= elevated [CO₂] pool (from rings one and four only). The number in brackets indicates the developmental age of the leaf (3= ‘young’, 6= ‘semi-mature’).

Number	Cy3 Channel	Cy5 Channel
1	Age 3, Ambient	Age 6, Ambient
2	Age 6, Ambient	Age 3, Ambient
3	Age 3, Elevated	Age 6, Elevated
4	Age 6, Elevated	Age 3, Elevated
5	Age 3, Ambient	Age 3, Elevated
6	Age 3, Elevated	Age 3, Ambient
7	Age 6, Ambient	Age 6, Elevated
8	Age 6, Elevated	Age 6, Ambient

Table 5.2.1. In total eight POP2 microarrays were conducted on the samples from EUROFACE. The samples on each array are given in the table according to the design of the experiment shown in Figure 5.2.2. The dye used to label each sample is indicated in the table.

5.2.4 qPCR

The qPCR was performed on individual RNA samples (from the ambient nitrogen treatment, sampled on 3rd August 2004), previously used to make the RNA pools hybridised on the POP2 microarrays.

5.2.4.1 Primer design

From the results of the microarray experiment, primers were designed for five of the genes identified as being significantly differentially expressed between the treatments. The control gene used was a ribosomal protein (PU00602).

The primers used for the RT-PCR were;

(1) *PYRUVATE KINASE* (PU06984)

Forward; 5'-CACCTTCTCTCCGAAACTCATC-3'

Reverse; 5'-CGCTCCAGTTCCGTTGTTG-3'

(2) *RAS-RELATED GTP BINDING PROTEIN* (PU12448)

Forward; 5'-TGGTGCTGATTGTTGTGTCC-3'

Reverse; 5'-GGAAATTCTCTGGGTCTGAAGG-3'

(3) *RUBISCO SSU* (PU11281)

Forward; 5'-ATCTCACAGAGCAGGAATTGG-3'

Reverse; 5'-AGTAGCGTCCATCATAGTACC-3'

(4) *GDSL-MOTIF LIPASE/ HYDROLASE* (PU27165)

Forward; 5'-TGGAGTACTTCGAGCAATACC-3'

Reverse; 5'-CCGCCGACTGTAATGAGG-3'

(5) *ENDOXYLOGLUCAN TRANSGLYCOSYLASE* (PU20530)

Forward; 5'-TTCCTCTCCACGTCTCTGC-3'

Reverse; 5'-GATAGCCCTCCCTCCATCG-3'

Two primers and the control gene were run on each of the 96-well plates. Four technical replicates were run per biological replicate on each plate. The programme LinRegPCR was used for the analysis of the PCR data. This method was used as an alternative to the more conventional 'Ct approach' since it does not assume that all the samples have an equal efficiency for the amplicon (Ramakers *et al*, 2003).

5.2.5 PICME microarrays

5.2.5.1 Experimental design

The RNA was extracted from the POPFACE leaves (young and semi-mature) sampled on 3rd August 2004. The concentration of RNA was checked using the nanodrop spectrophotometer, and quality was checked by running a 1% agarose gel. The experimental design for the PICME microarray experiment is shown in Figure 5.2.3.

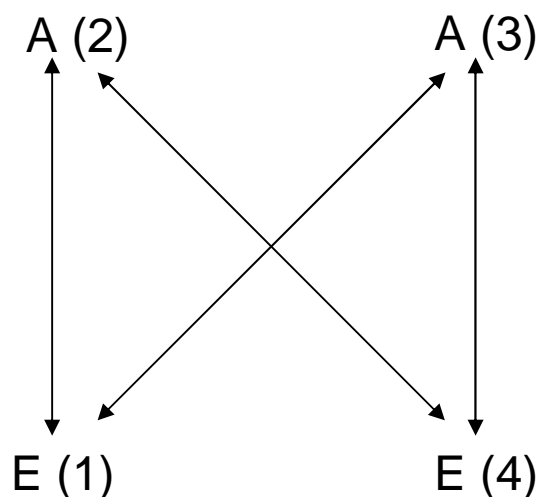


Figure 5.2.3. Experimental design for the PICME microarrays for the transcript analysis of semi-mature leaves exposed to [aCO₂] and [eCO₂]. The experiment was designed to compare samples obtained from the four experimental rings (numbers in brackets denote the ring number from the EUROFACE site. Rings one and four= FACE; rings two and three= [aCO₂].)

5.3 Results

5.3.1 POP2 microarrays

All eight microarray hybridisations (according to the design in Figure 5.2.2) were successful. The results of the age comparisons (young: semi-mature in [aCO₂] or [eCO₂]) are shown in Figure 5.3.1. The results of the CO₂ comparisons ([eCO₂]: [aCO₂] in young or semi-mature leaves) are shown in Figure 5.3.2.

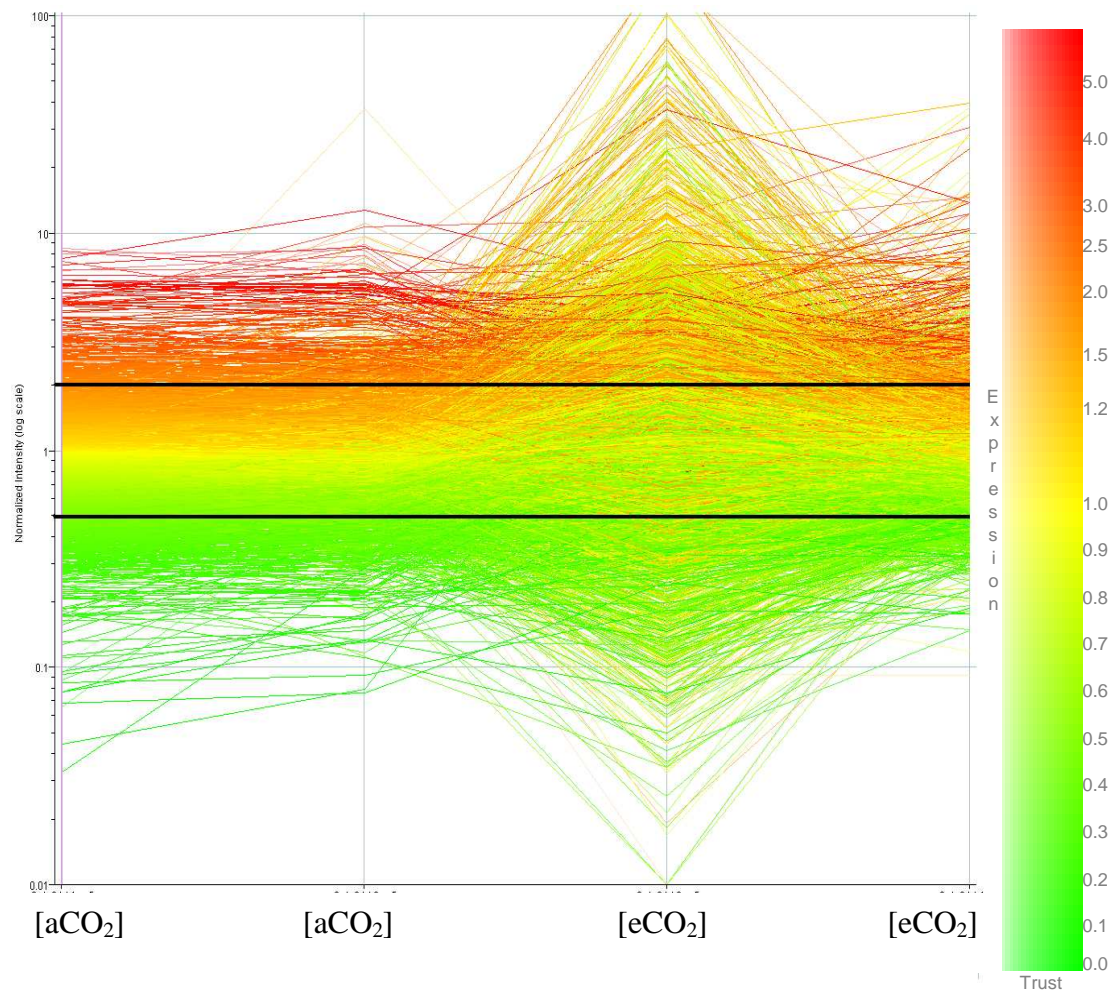


Figure 5.3.1. The expression ratios (young: semi-mature) of the four microarrays from [aCO₂] and [eCO₂] are illustrated on the graph. One line represents one EST. The colour bar indicates the level of expression for each of the genes (yellow= no change in expression; green= down-regulation; red= up-regulation). The diagram only illustrates the results from the ESTs whereby they were present in all four of the microarrays. The black line represents a two-fold change in expression. Each vertical line represents a single hybridisation. The two vertical lines on the left represent leaves grown in [aCO₂] and on the right are those exposed to [eCO₂].

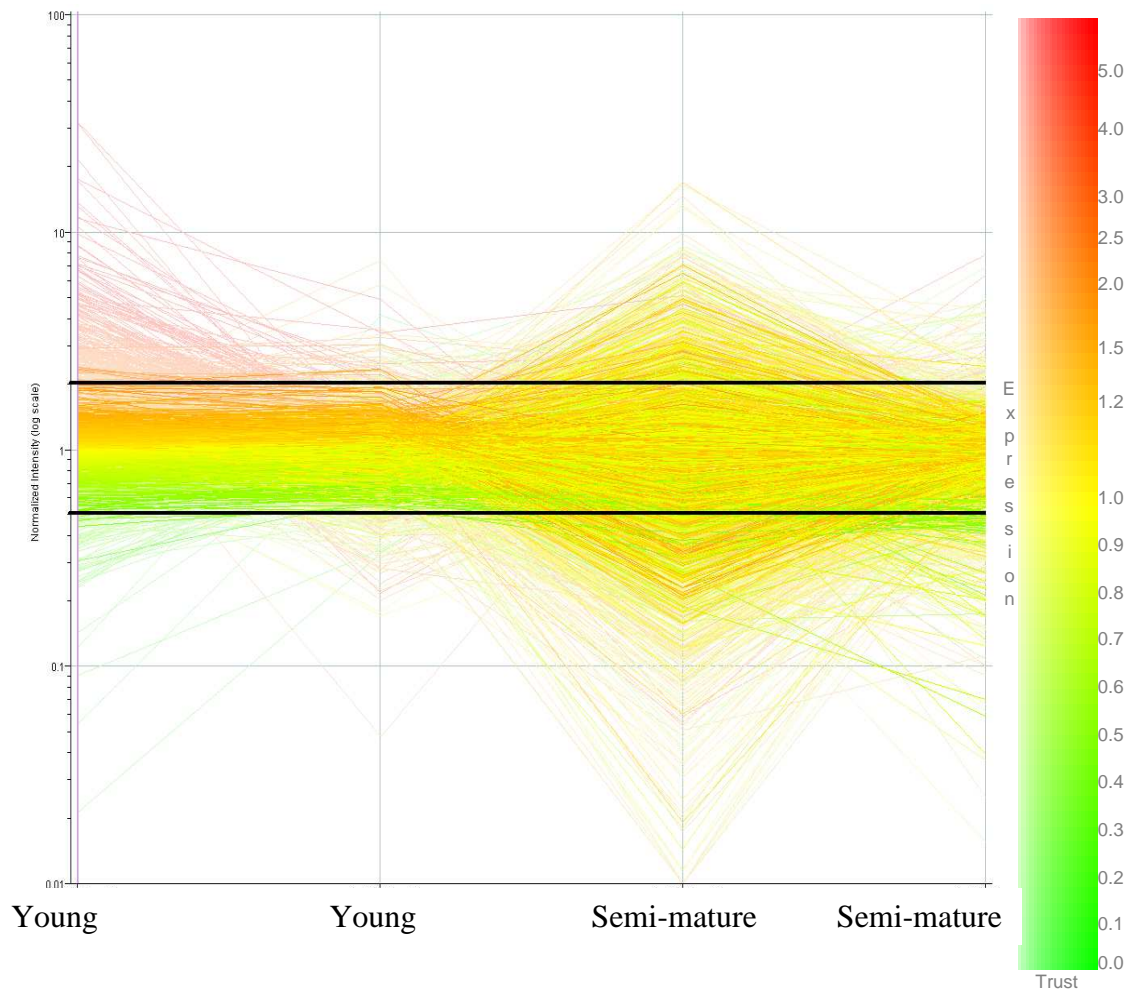


Figure 5.3.2. The expression ratios ($[eCO_2]:[aCO_2]$) from the four microarrays for the young and semi-mature leaves. One line represents one EST. The colour bar indicates the level of expression for each of the genes (yellow= no change in expression; green= down-regulation; red= up-regulation). The diagram only illustrates the results from the ESTs whereby they were present in all four of the microarrays. The black line represents a two-fold change in expression. Each vertical line represents a single hybridisation. The two vertical lines on the left represent young leaves and those on the right represent the semi-mature leaves.

The hybridisations of age comparisons showed the greatest expressional differences (Figure 5.3.1) whilst there was little difference in gene expression in the $[CO_2]$ comparisons in either the young or semi-mature leaves (Figure 5.3.2).

The results from the microarray hybridisations were analysed and filtered in GeneSpring. By considering the age comparisons only (those that showed the greatest differences in gene expression) there were a total of 178 transcripts that were

consistently two-fold up-(85) or down-(93) regulated in young leaves in ambient and elevated [CO₂].

5.3.1.1 Gene ontology

Venn diagrams were constructed in GeneSpring in order to identify differentially expressed transcripts in the age (Figure 5.3.3 and 5.3.4) and [CO₂] (Figure 5.3.5 and 5.3.6) comparative hybridisations. The GO information corresponding to the transcripts in each section of the Venn diagrams are indicated in each figure.

Generally, the ontology information implied that only very subtle differences in the functions of transcripts that were differentially regulated in the age comparison hybridisations. In the [CO₂] comparisons, transcripts involved in plant physiology were up-regulated in [eCO₂] in young leaves. Transcripts involved in development were up-regulated in young leaves grown in FACE, but not in ambient conditions (Figure 5.3.4) therefore suggesting the development process is promoted in trees grown in [eCO₂]. However, rather surprisingly the transcripts involved in growth were down-regulated (in young leaves) in [eCO₂]. The two transcripts commonly down-regulated in [eCO₂] in young and semi-mature leaves were (PU05929) an expressed protein and (PU24862) corresponding to a double-stranded RNA-binding domain.

Age comparison

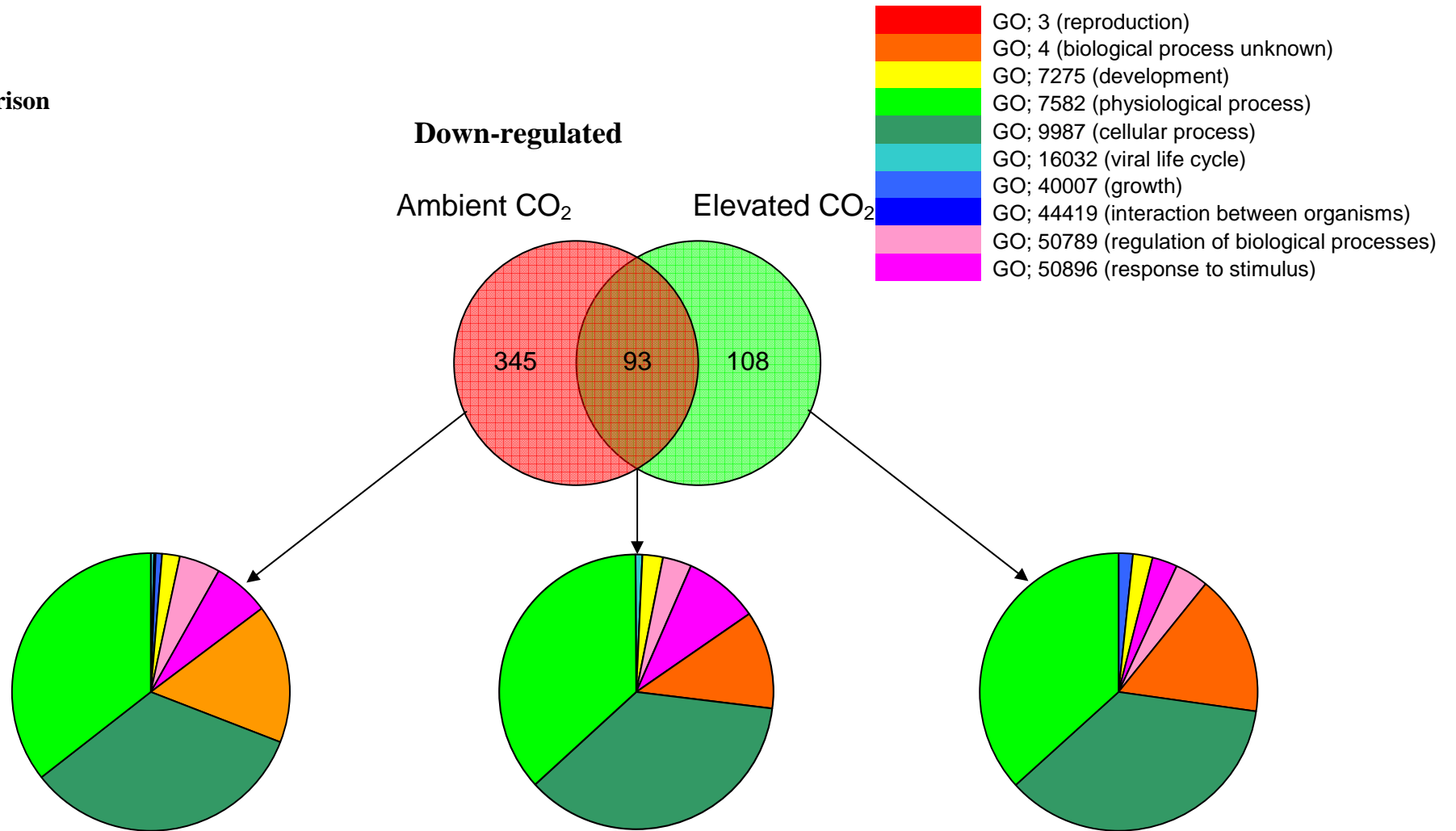


Figure 5.3.3. A Venn diagram constructed using GeneSpring, illustrating the results from the POP2 microarray experiments. The diagram shows the transcripts that were two-fold (or more) down-regulated in young leaves in ambient and elevated [CO₂] growth conditions. The numbers in the diagram represent the number of transcripts that were uniquely down-regulated in [aCO₂] (red), uniquely down-regulated in young leaves in [eCO₂] (green), or commonly down-regulated in [aCO₂] and [eCO₂] (middle section). Beneath the Venn diagram are pie charts representing the GO categories into which the transcripts within the designated section of the Venn diagram falls. The GO key is located in the upper right hand corner of the figure.

Age comparison

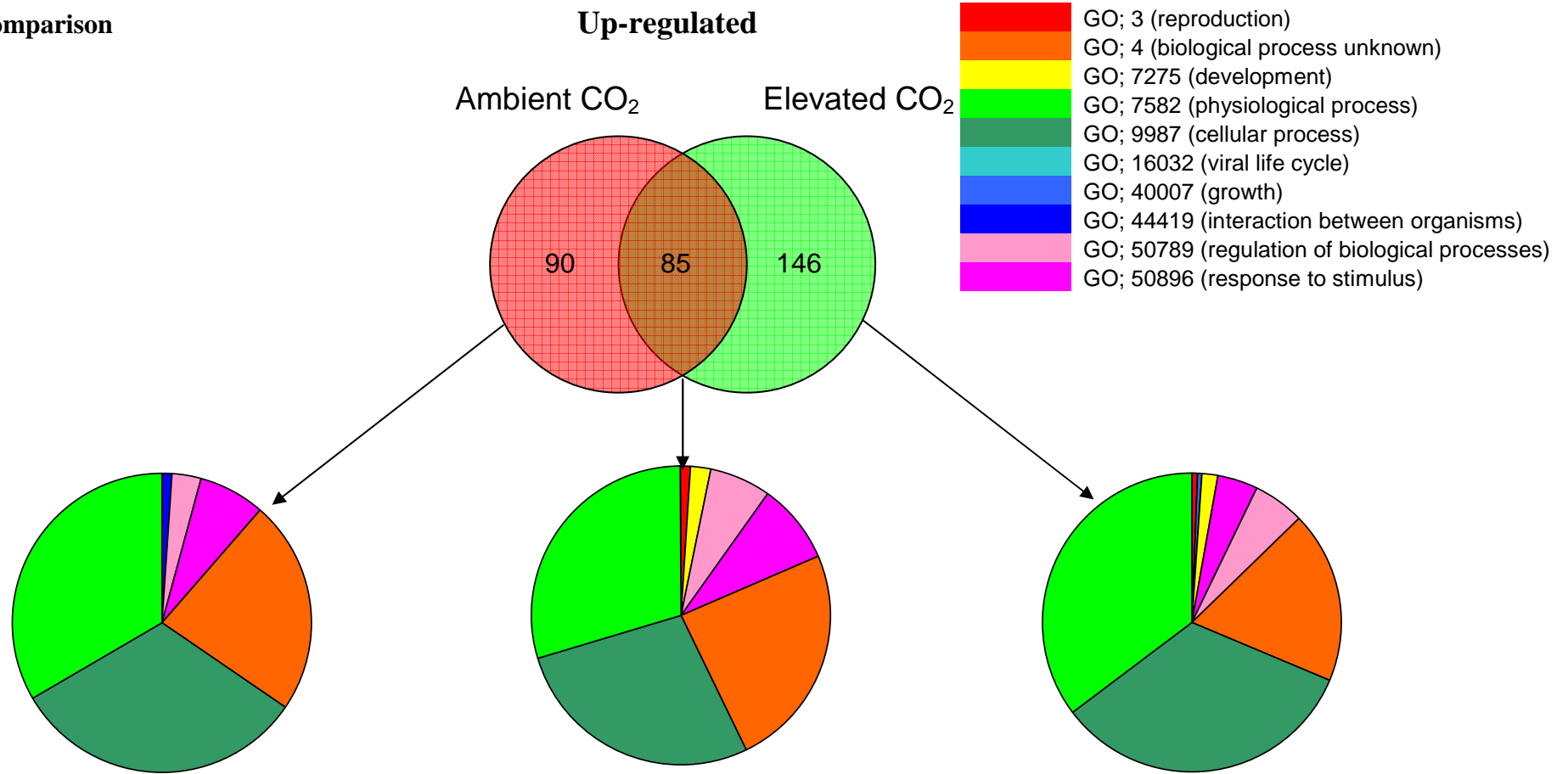


Figure 5.3.4. A Venn diagram constructed using GeneSpring, illustrating the results from the POP2 microarray experiments. The diagram shows the transcripts that were two-fold (or more) up-regulated in young leaves in ambient and elevated [CO₂] growth conditions. The numbers in the diagram represent the number of transcripts that were uniquely up-regulated in [aCO₂] (red), uniquely up-regulated in young leaves in [eCO₂] (green), or commonly up-regulated in [aCO₂] and [eCO₂] (middle section). Beneath the Venn diagram are pie charts representing the GO categories into which the transcripts within the designated section of the Venn diagram falls. The GO key is located in the upper right hand corner of the figure.

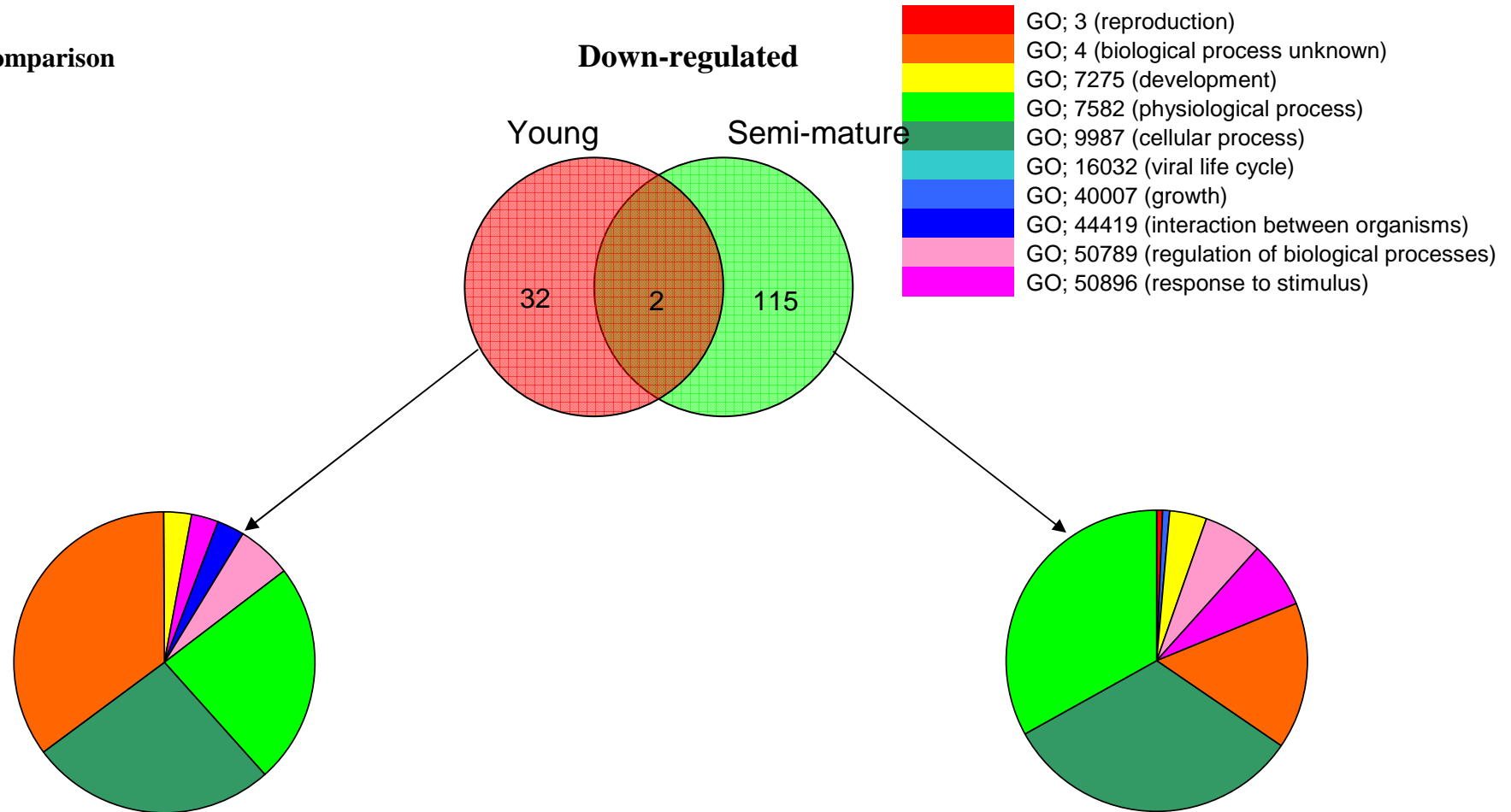
CO₂ comparison

Figure 5.3.5. A Venn diagram constructed using GeneSpring, illustrating the results from the POP2 microarray experiments. The diagram shows the transcripts that were two-fold (or more) down-regulated in [eCO₂] in young and semi-mature leaves. The numbers in the diagram represent the number of transcripts that were uniquely down-regulated in [eCO₂] in young leaves (red), uniquely down-regulated in [eCO₂] in semi-mature leaves (green), or commonly down-regulated in young and semi-mature leaves (middle section). Beneath the Venn diagram are pie charts representing the GO categories into which the transcripts within the designated section of the Venn diagram falls. The GO key is located in the upper right hand corner of the figure.

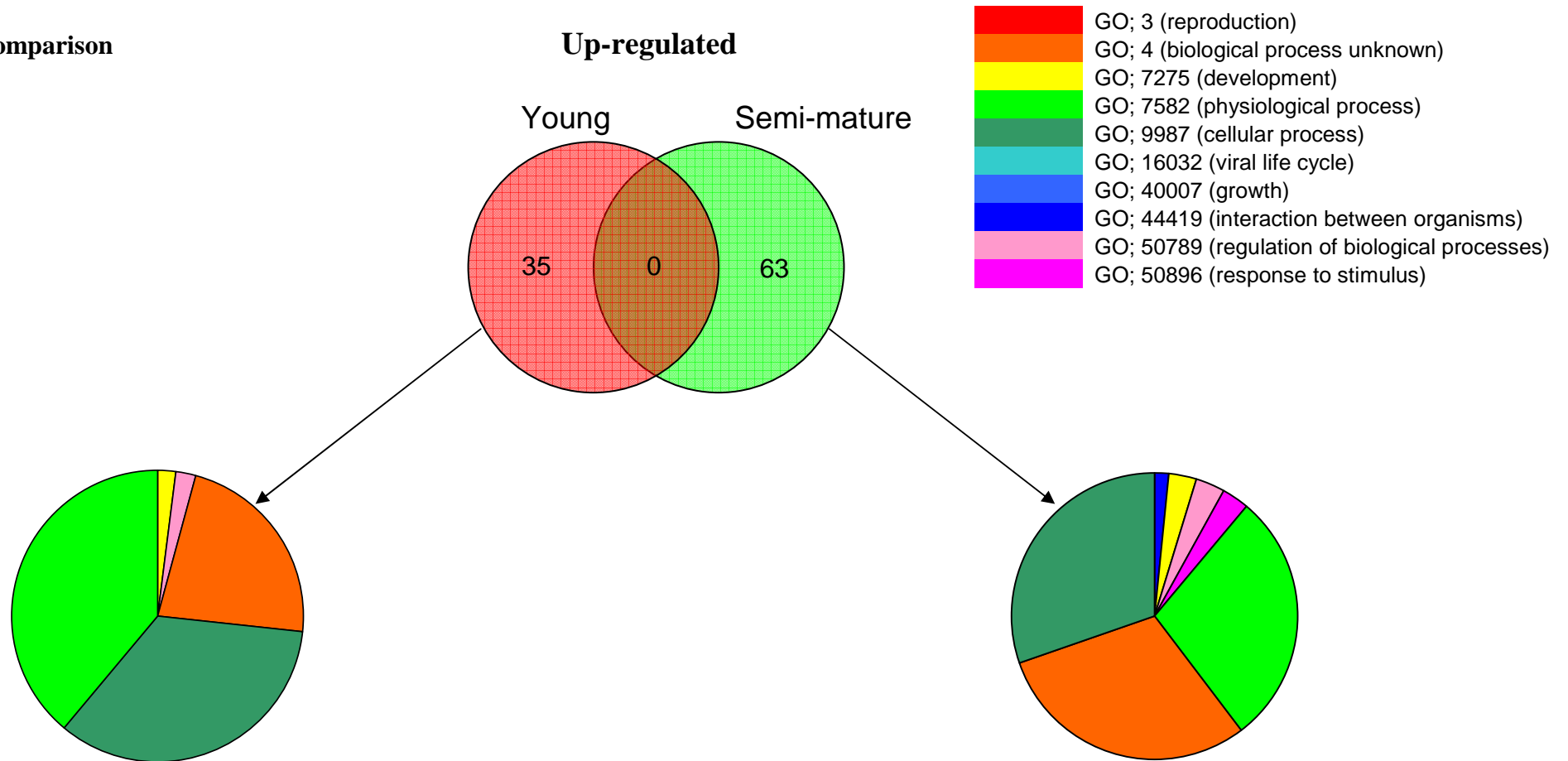
CO₂ comparison

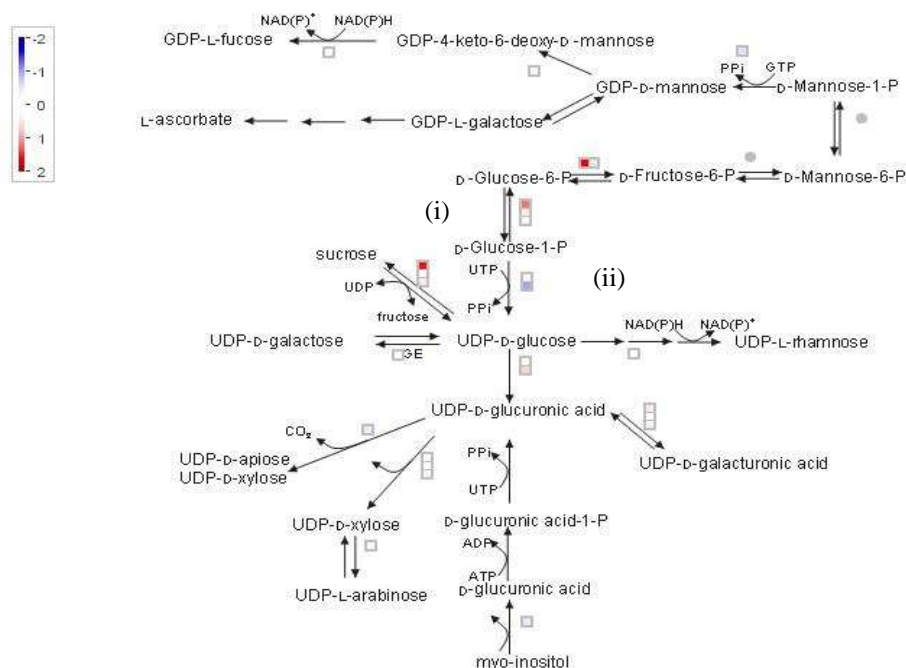
Figure 5.3.6. A Venn diagram constructed using GeneSpring, illustrating the results from the POP2 microarray experiments. The diagram shows the transcripts that were two-fold (or more) up-regulated in [eCO₂] in young and semi-mature leaves. The numbers in the diagram represent the number of transcripts that were uniquely up-regulated in [eCO₂] in young leaves (red), uniquely up-regulated in [eCO₂] in semi-mature leaves (green), or commonly up-regulated in young and semi-mature leaves (middle section). Beneath the Venn diagram are pie charts representing the GO categories into which the transcripts within the designated section of the Venn diagram falls. The GO key is located in the upper right hand corner of the figure.

5.3.1.2. Pathway analysis

All of the expression data from the POP2 microarrays were imported into the pathway mapping software 'MapMan' (Thimm *et al*, 2004) (freely available for download from the internet; <http://gabi.rzpd.de/projects/MapMan/>). Of particular interest was the pathway indicating the formation of cell wall precursors, since alterations in cell wall properties are thought to be involved in the CO₂ response. There were surprisingly few transcripts involved in the formation of cell wall precursors that were differentially regulated in either leaf age. Generally, there was an up-regulation of transcripts involved in the biosynthesis of cell wall precursors in young leaves and down-regulation in semi-mature leaves (Figure 5.3.7).

The production of UDP-glucose is particularly important in the context of leaf growth and development since it is required for cellulose biosynthesis. In young leaves, there was an up-regulation in the pathways converting sucrose to UDP-glucose (by sucrose synthase (SUSY) (i)), but down-regulation of UDP-glucose pyrophosphorylase (UGPase (ii)), an enzyme that converts glucose-1-phosphate to UDP-glucose.

Young leaves



Semi-mature leaves

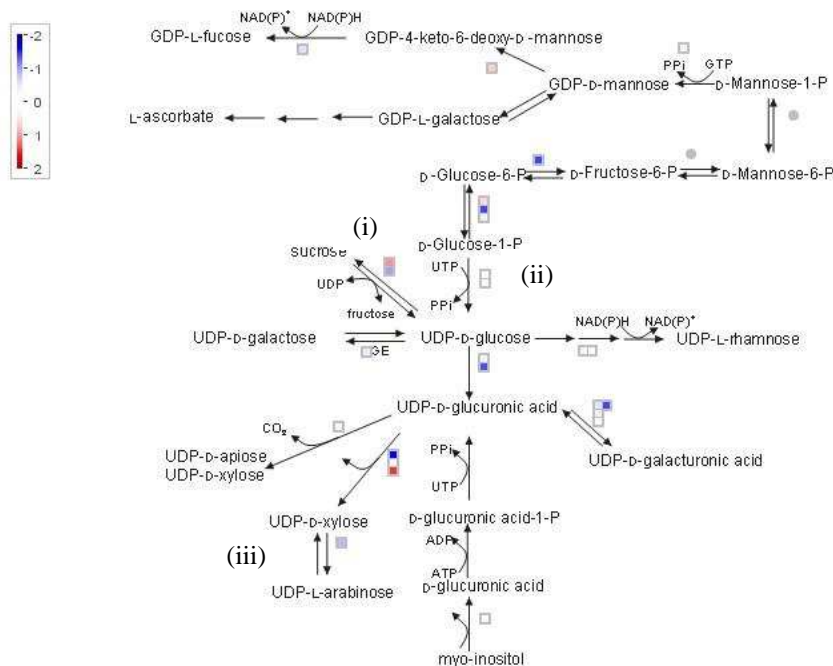


Figure 5.3.7. The cell wall precursor pathway obtained from Mapman using the expression data from the POP2 microarrays. The squares represent transcripts that were up-(red) or down-(blue) regulated in [eCO₂] in young (top pathway) or semi-mature leaves (bottom pathway). The colour strength corresponds to expression level according to the key, where red=up-regulated in [eCO₂] and blue=down-regulated in [eCO₂]. According to the key, a value of -2 represents two-fold down-regulation and +2 represents two-fold up-regulation. (i) represents SUSY, (ii) represents UGPase and (iii) represents UDP-D-xylose 4-epimerase.

5.3.2 qPCR

The microarray data was analysed using B-statistics. The transcripts with B-statistic values greater than 0 (representing a 50:50 chance of differential expression), were selected for further analysis. In young leaves, 8 transcripts had a B-statistic value greater than 0, whereas in semi-mature leaves there were 31 (appendix 1 from Taylor *et al.*, 2005). From these 39 differentially expressed transcripts, five were selected for confirmation using qPCR. The five transcripts were *GDSL-MOTIF LIPASE/HYDROLASE*, *ENDOXYLOGLUCAN TRANSFERASE*, *RAS-RELATED GTP BINDING PROTEIN*, *PYRUVATE KINASE* and *RUBISCO SSU*. The microarray data showed that the *GDSL-MOTIF LIPASE/HYDROLASE* and *ENDOXYLOGLUCAN TRANSFERASE* transcripts were up-regulated in response to [eCO₂] in young leaves (Figure 5.3.8 (i) and (ii) respectively). The *RAS-RELATED GTP BINDING PROTEIN*, and *PYRUVATE KINASE* transcripts were down-regulated in response to [eCO₂] in semi-mature leaves (Figure 5.3.8 (iii) and (iv) respectively).

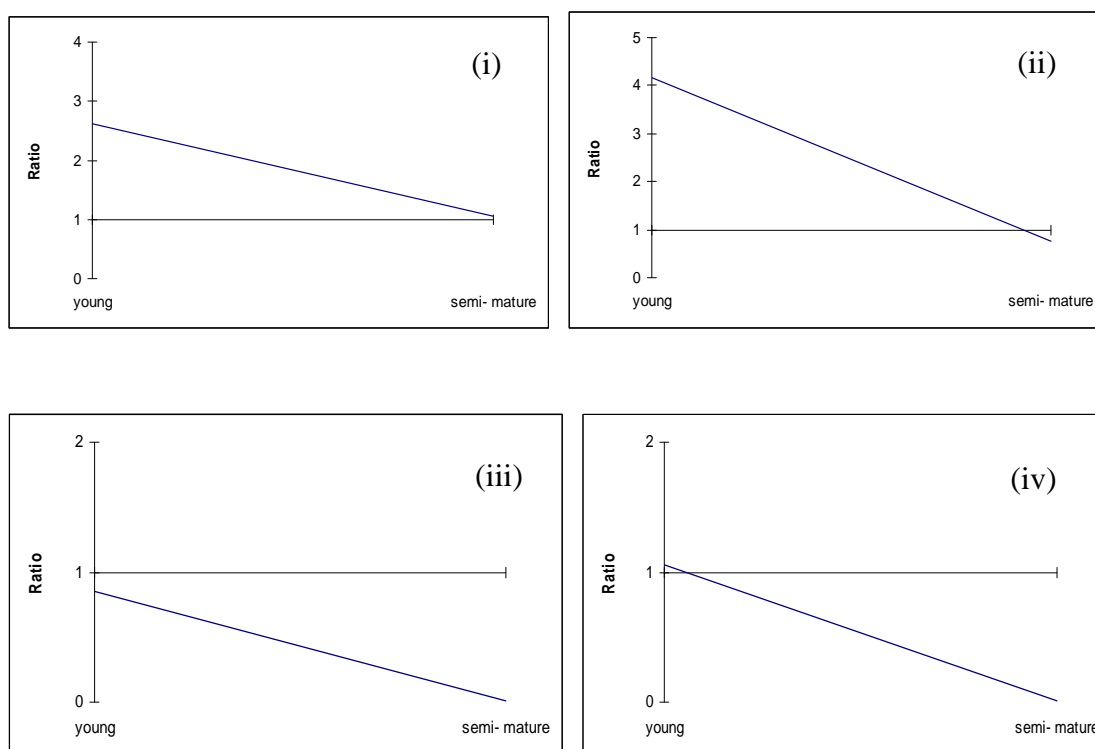


Figure 5.3.8. The expression ratios ([eCO₂]: [aCO₂]) from the POP2 microarray results for (i) *GDSL-MOTIF LIPASE/HYDROLASE* (PU27165), (ii) *ENDOXYLOGLUCAN TRANSFERASE* (PU20530), (iii) *RAS-RELATED GTP BINDING PROTEIN* (PU12448) and (iv) *PYRUVATE KINASE* (PU06984).

The microarray results for the *RUBISCO SSU* are shown in Figure 5.3.9. The results showed that the expression of *RUBISCO SSU* was up-regulated in [eCO₂] in young leaves and down regulated in semi-mature leaves. The results in Figures 5.3.8 and 5.3.9 clearly show the age dependency of expression levels due to CO₂ exposure.

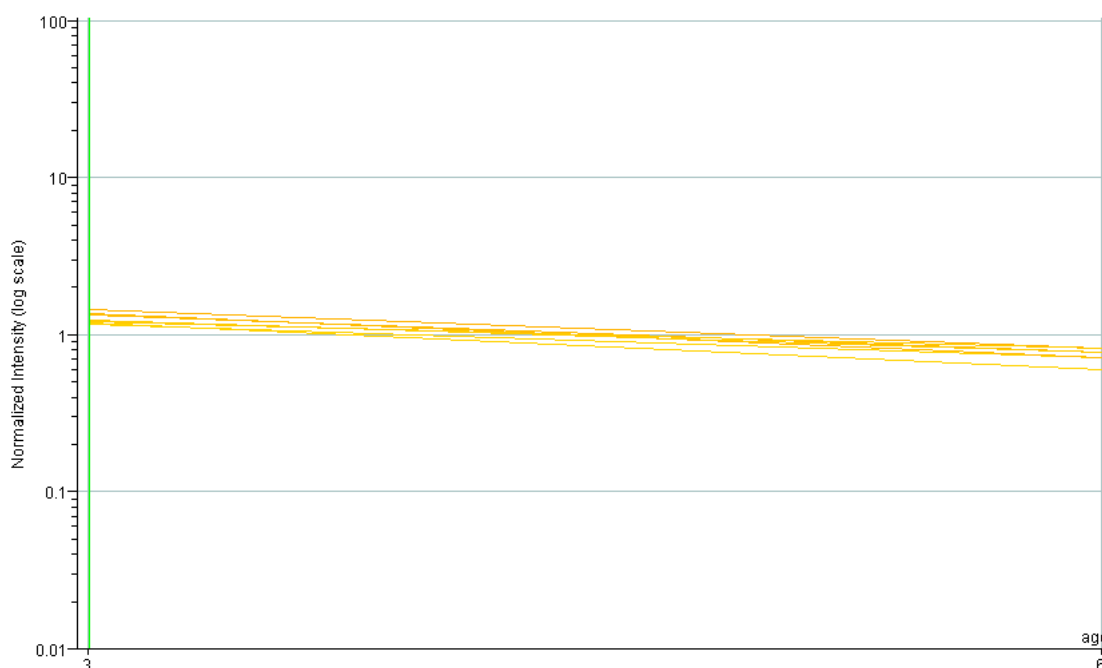


Figure 5.3.9. The average expression ratio of elevated CO₂: ambient CO₂ samples for the young (age 3) and semi-mature (age 6) leaves for the *RUBISCO SSU* (PU11281). One line represents one EST.

The qPCR results for the expression ratios ([eCO₂]: [aCO₂]) of the candidate genes in young leaves is given in Figure 5.3.10, along with the microarray results from those candidates. The *GDSL-MOTIF LIPASE/HYDROLASE* was up-regulated in response to [eCO₂] in both the microarrays and the qPCR. Similar trends in expression levels were also true for the *RAS-RELATED GTP BINDING PROTEIN* and *PYRUVATE KINASE*. The results for *ENDOXYLOGLUCAN TRANSFERASE* however, were contrasting between the qPCR and the microarrays. Whilst the microarray results indicated that *ENDOXYLOGLUCAN TRANSFERASE* was up-regulated in young leaves in response to [eCO₂], it was down-regulated according to the qPCR data.

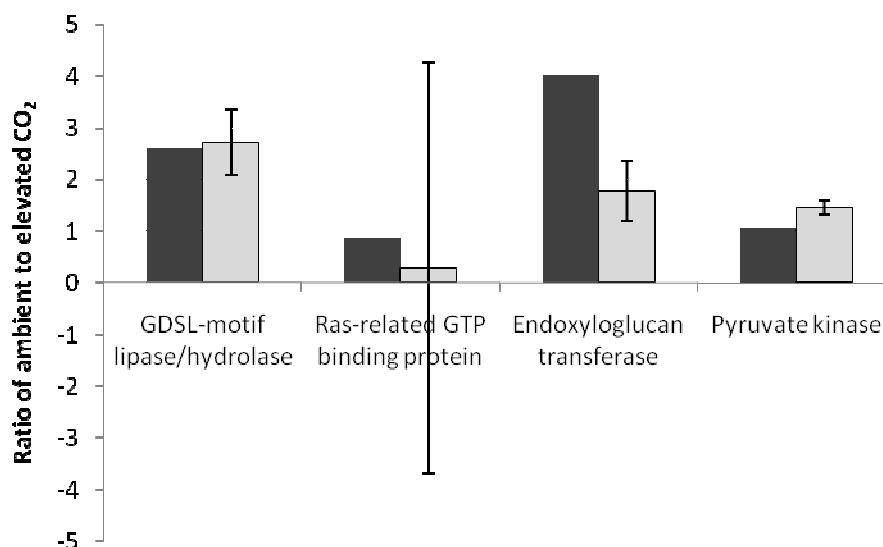


Figure 5.3.10. The graph illustrates the average expression ratio ($[eCO_2]: [aCO_2]$), for four of the selected candidate genes in young leaves of *P. x euramericana*. The results from the microarrays (black bars) and qPCR (grey bars) for the *GDSL-MOTIF LIPASE/ HYDROLASE*, *RAS-RELATED GTP BINDING PROTEIN*, *ENDOXYLOGLUCAN TRANSFERASE* and *PYRUVATE KINASE* transcripts are shown. Standard error bars are indicated on the graph.

The results for the average expression ratio of *RUBISCO SSU* in response to $[eCO_2]$ however, were very similar between the microarrays and the qPCR data (Figure 5.3.11). Both sets of results indicated that *RUBISCO SSU* expression was up-regulated in young leaves in response to $[eCO_2]$.

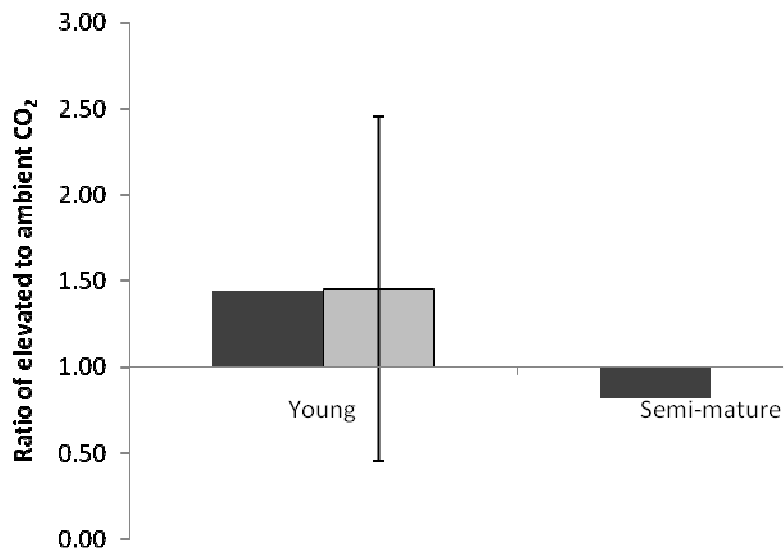


Figure 5.3.11. The microarray (black bars) and qPCR (grey bars) results for the average fold change in *RUBISCO SSU* expression levels in *P. x euramericana* in response to [eCO₂]. The qPCR was conducted on young leaves only, but the microarray results from young and semi-mature leaves are presented. Standard error bars are shown on the graph.

5.3.3 PICME microarrays

The results from the four PICME microarrays are displayed in Figure 5.3.12. By averaging across the replicates, there were 100 ESTs that were two-fold (or more) down-regulated in [eCO₂] and 62 that were up-regulated.

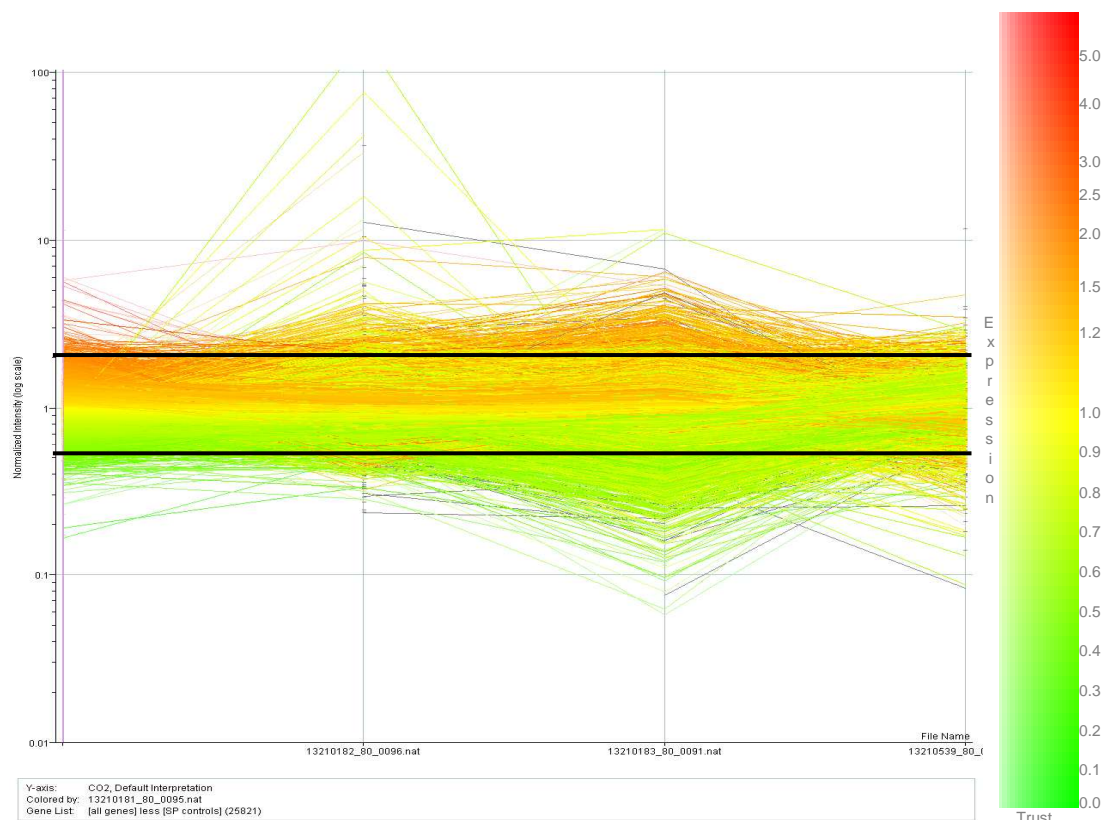


Figure 5.3.12. The average fold change in response to [eCO₂] in *P. x euramericana*. The results from the four PICME microarrays are presented here, where each vertical line represents one microarray. The black lines represent two fold up-regulation (upper line) or two fold down-regulation (lower line) in response to [eCO₂]. One line represents one EST. The colour bar indicates the level of expression for each of the genes (yellow= no change in expression; green= down-regulation; red= up-regulation).

Similarly to the results from the POP2 microarrays, there were relatively few large expressional differences as a result of CO₂ exposure. In total there were five and three transcripts that were two-fold or more up-or down-regulated (in 3/4 hybridisations) as a result of CO₂ exposure in semi-mature leaves of *P. x euramericana* respectively (Table 5.3.1).

Gene model	Expression	Annotation
estExt_fgenes4_kg.C_LG_IX0046 (PtaC0022F9F0911)	0.38	Osmotin-like protein precursor
estExt_fgenes4_kg.C_LG_IX0046 (R35H06)	0.38	Osmotin
estExt_fgenes4_kg.C_LG_IX0046 (P0000300023E11)	0.44	Osmotin-like protein
estExt_fgenes4_pm.C_LG_I0645 (PtaXM0025D11D1107)	1.68	Triose phosphate
estExt_Genewise1_v1.C_LG_X5306 (PtaXM0025G3G0313)	1.65	-
grail3.0242000102 (PtaXM0025H3H0315)	1.67	Calcyclin binding protein-like
gw1.I.15.1 (PtaXM0025B7B0703)	1.60	Glycine-rich RNA-binding protein
gw1.VIII.2932.1 (PtaXM0025B3B0303)	1.67	-

Table 5.3.1. The results from the PICME microarrays showing the transcripts that were two-fold (or more) up-or down-regulated in response to [eCO₂] in 3 of the 4 microarrays. The gene model is shown, along with the average fold change (across all four arrays) and the annotation. The figures in brackets represent the identifier on the PICME microarray.

The results from the two microarray platforms (PICME and POP2) were compared in order to identify transcripts that were consistently expressed. Using the transcripts that were two-fold (or more) up-or down-regulated from each of the two platforms, the data was aligned using the gene model as a reference point. In total there were five gene models that demonstrated consistent two-fold up- or down-regulation across arrays (Table 5.3.2). The POP2 microarray represents 16,651 gene models, whilst the PICME microarray represents 9,567. The fact that only five gene models were consistently regulated across the two platforms is rather surprising given the fact that there were 6,322 gene models found in both the POP2 and PICME microarrays. In some cases the expression levels were inconsistent within (e.g. PICME, gene model estExt_fgenes4_pg.C_280066) and between (e.g. gene model eugene3.00050346) platforms. However, there was correspondence between the platforms in one instance (e.g. gene model grail3.0046017801).

Gene model	Platform	Expression	Annotation
estExt_fgenes4_pg.C_280066	PICME	0.48	Sucrose synthase
estExt_fgenes4_pg.C_280066	PICME	0.25	Sucrose synthase
estExt_fgenes4_pg.C_280066	PICME	2.19	Sucrose synthase
estExt_fgenes4_pg.C_280066	POP2	0.25	Sucrose synthase
estExt_Genewise1_v1.C_410611	PICME	0.43	Bark storage protein
estExt_Genewise1_v1.C_410611	POP2	2.84	Bark storage protein
eugene3.00050346	PICME	0.44	Expressed protein
eugene3.00050346	POP2	3.72	Expressed protein
grail3.0046017801	PICME	0.49	Extensin-like protein
grail3.0046017801	POP2	0.38	Extensin-like protein
grail3.0147002801	PICME	2.54	Zinc finger protein
grail3.0147002801	POP2	0.29	Zinc finger protein

Table 5.3.2. The ESTs that were (on average) two fold (or more) up-or down-regulated in [eCO₂] in semi-mature leaves of *P. x euramericana*. The two cDNA platforms (PICME and POP2) were compared in order to identify transcripts that were consistently differentially regulated. The consistent gene models, along with the platform type, expressional fold change and annotation are provided in the table.

5.4 Discussion

The aims of ecological genomics are four-fold; (i) to elucidate the mechanisms of adaptation; (ii) to investigate the mechanistic causes of phenotypic variation; (iii) to identify genetic targets of selection and (iv) to understand the mechanisms leading from environmental cues to observed phenotypic response (Ouborg and Vriezen, 2006). In ecological genomic experiments, microarrays are considered to be an appropriate method for investigating gene expression under conditions of environmental perturbation (Gibson, 2002). This study represents one of the first ecological genomic approaches to understanding the genetic basis of adaptation in *Populus* grown in [eCO₂].

The growth responses of plants in [eCO₂] at the morphological and physiological levels are widely documented. It is generally accepted that [eCO₂] stimulates growth, although disparities do exist, and stimulation is often dependent upon the experimental conditions (Körner, 2006). The use of microarrays permits the study of the expression of thousands of transcripts in response to an environmental treatment. In this experiment, microarrays were used to determine transcripts with differential expression levels in ambient and elevated CO₂ concentrations in order to identify candidate genes important for leaf growth under altered atmospheric conditions.

Previous experiments on *P. x euramericana* from the EUROFACE site have shown that leaf growth is stimulated in response to [eCO₂] (Tricker *et al*, 2004, Taylor *et al*, 2003, Ferris *et al*, 2001). It is therefore rather surprising that relatively few transcripts were shown to be differentially expressed between [aCO₂] and [eCO₂] in this microarray experiment. It is possible that this is because this was a long term experiment. It is highly probable that the results would not be replicated in a short term exposure experiment.

5.4.1 [eCO₂] and cell wall modifications

As discussed in Chapters 1 and 4, changes in leaf growth in [eCO₂] are likely to be due to modifications to the integrity of the cell wall. The POP2 microarray results demonstrated a strong age dependence of the expression of a putative cell wall modifier. In young leaves, there was an increase in the expression of *ENDOXYLOGLUCAN TRANSFERASE* as a result of FACE exposure. This enzyme is

involved in incorporating xyloglucan into the cell wall and hence involved in leaf growth and development (Fry *et al*, 1992). This concurs with previous data collected from EUROFACE where cell wall extensibility increased, along with levels of xyloglucan endotransglycosylases in response to [eCO₂] in all three *Populus* species studied (Ferris *et al*, 2001). Furthermore microarray experiments conducted on samples of *P. deltoides* grown in the Biosphere 2 Laboratory (Walter and Lambrecht, 2004) also identified both *ENDOXYLOGLUCAN TRANSFERASE* and *XYLOGLUCAN ENDOTRANSGLYCOSYLASE* transcripts as being differentially expressed in response to [eCO₂] (Druart *et al*, 2006). Similarly, *XYLOGLUCAN ENDOTRANSGLYCOSYLASE* was also up-regulated in *Populus tremuloides* exposed to [eCO₂] at AspenFACE (Gupta *et al*, 2005). This therefore provides further evidence that these are important candidates in determining leaf growth in response to CO₂ treatment.

5.4.2 Cellulose biosynthesis and the cell wall

Cellulose is the major polysaccharide found in the plant cell wall, and is considered to be the most abundant biopolymer on Earth (Saxena and Brown Jr, 2005). SUSY is an enzyme involved in the catabolism of sucrose, producing fructose and UDP-glucose, which is required for the biosynthesis of cellulose. Current models suggest that SUSY channels UDP-glucose to the cellulose synthase (CESA) rosette complex in the plasma membrane where the glucose monomers are polymerised and UDP-is recycled back to SUSY (Joshi *et al*, 2004). It has been suggested that the membrane-associated KORRIGAN (KOR) cellulase edits the glucans chains that are produced (Sato *et al*, 2001). A comparison of the PICME and POP2 microarray data highlighted *SUSY* as consistently down-regulated in semi-mature leaves of *P. x euramericana* grown in FACE. This suggests a concomitant reduction in cellulose biosynthesis in [eCO₂].

The results from the pathway analysis showed that the response to [eCO₂] in terms of the genes involved in the formation of the major components of the cell wall was dependent upon the age of the leaf. The reduction in cell wall loosening activity (as assessed by the *ENDOXYLOGLUCAN TRANSFERASE* expression) over developmental time, and the reduction in *SUSY* expression levels in semi-mature leaves (no information was available regarding the young leaves for this particular gene model (estExt_fgenes4_pg.C_280066)) leads to the interpretation that the older leaves

were less responsive to [eCO₂] and that development was completed faster in trees grown in FACE. Furthermore, the expression of cell wall proteins such as extensin were also reduced in [eCO₂] in semi-mature leaves (and consistently across two microarray platforms (Table 5.3.2)). However, expression of UGPase, another enzyme that catalyses the production of UDP-glucose (from glucose-1-phosphate) was reduced in young leaves. This perhaps reflects the dual role of UGPase in sucrose metabolism, since its expression leads to increased sucrose generation in source tissues and a reduction in sinks (Coleman *et al*, 2006).

UDP-glucuronate (or UDP-glucuronic acid) is a precursor molecule which can be converted into different sugar products including UDP-xylose and UDP-arabinose. UDP-L-arabinose is the precursor of L-arabinose, a major constituent of cell wall polymers including pectins and hemicellulose. The gene encoding the UDP-D-xylose 4-epimerase enzyme, involved in the conversion of xylose to arabinose, was also down-regulated in semi-mature leaves exposed to FACE. This further confirms the previous notion that the production of cell wall components in semi-mature leaves of FACE-grown plants is down-regulated. The general up-regulation of transcripts involved in the production of cell wall precursors in young leaves and subsequent down-regulation in semi-mature leaves leads to a scenario where it is possible to imagine an altered ontogenic pattern of development in an [eCO₂] environment.

5.4.3 Acclimatory response

The quantitative RT-PCR results confirmed the microarray transcript data for Rubisco SSU, indicating a 1.45 fold up-regulation of this gene in response to [eCO₂] in young leaves. The increase in Rubisco transcript abundance in [eCO₂] suggests an increase in photosynthesis under such conditions, which has been observed in previous reports (e.g. (Drake *et al*, 1997; Ainsworth and Long, 2005)). The results from POP2 presented here indicate a greater competence for photosynthesis in the young leaves of *P. x euramericana* in [eCO₂] conditions (Taylor *et al*, 2005). The acclimation response to [eCO₂] is associated with a reduction in Rubisco activity and protein levels (Moore *et al*, 1998). The results here therefore suggest that the trees are not acclimated are still responding to CO₂ enrichment.

In the POP2 microarrays, the transcript encoding the *GDSL-MOTIF LIPASE/HYDROLASE* family protein (PU27165) was identified as significantly differentially expressed in response to [eCO₂] in young and semi-mature leaves. This transcript is involved in lipid metabolism and has also been shown to be differentially expressed between young and mature leaves of *P. deltoides* during the period of maximal growth rate in the circadian cycle (Matsubara *et al*, 2006).

5.4.4 Genomic regions of interest

QTL analysis is a useful technique for identifying genomic regions involved in controlling a particular trait of interest e.g. leaf area. QTL analysis has been used in previous experiments with *Arabidopsis* recombinant inbred lines (RILs) and a pedigree *Populus* mapping population (Family 331) exposed to [eCO₂]. This study illustrated the existence of conserved genomic regions controlling trait response to [eCO₂], thus implying a degree of genome synteny (A Rae, unpublished data). Using a combination of QTL analysis and transcriptomics, it is possible to identify important regions of the genome involved in controlling the trait under the different conditions. Using this approach in a *Populus* mapping population (*P. deltoides* x *P. trichocarpa*) it has been possible to identify the genomic regions important for leaf growth under ambient and elevated CO₂ conditions (Rae *et al*, 2006) and drought (Street *et al*, 2006). A number of the differentially expressed transcripts identified by the POP2 microarrays described here were shown to collocate to response QTL reported by Rae *et al* (2006). For example, on LGXII two transcripts identified by the POP2 microarrays, PU05763 (*POLCALCIN*, putative calcium binding pollen allergen) and PU06463 (60S *RIBOSOMAL PROTEIN*), collocate with two response QTL for leaf area (one for young and one for mature leaves) (Rae *et al*, 2006). This therefore suggests that this genomic region is particularly important in the response to [eCO₂] in *Populus*.

5.4.5 Small changes in gene expression

Leaf growth and development under [eCO₂] may be considered as a ‘plastic’ process (Taylor *et al*, 2005) and microarrays can be regarded as a way of studying phenotypic plasticity in plants. However, the results from two independent sets of microarrays have shown that there are few large changes in transcript expression in *P. x euramericana* in response to FACE treatment. Small changes in gene expression in response to CO₂ have also been reported in other experiments, including AspenFACE

(Gupta *et al*, 2005), SoyFACE (Ainsworth *et al*, 2006) and in the Biosphere 2 experiment (Druart *et al* 2006). However, QTL analysis has shown that of the transcripts that were identified in the POP2 experiment, a number of them collocate to genomic regions important for governing various aspects of leaf growth such as leaf area (Rae *et al*, 2006). Taking these results into account, I would therefore suggest that the responses observed at the phenotypic and physiological level that have previously been reported in *P. x euramericana* are an effect of small subtle changes in expression having an additive effect on growth.

Other studies of *Populus* gene expression changes in response to environmental change have shown rather substantial differences between the control and treated samples, e.g. drought (Street *et al*, 2006), ozone (J. Tucker, 2006) and UV-B (G. Emiliani, 2006). The commonality between these experiments is that they each represent a plant stress. The metabolite and transcript profiles of *Arabidopsis* grown under [eCO₂] at SoyFACE have shown that growth under FACE induces greater expression of stress-related genes than controlled environment experiments (Li *et al*, 2006; Miyazaki *et al*, 2004) but also confirm that there are generally only small changes in gene expression in response to [eCO₂]. However, it should not be claimed that CO₂ is a 'stress' *per se* since it is more akin to a 'fertiliser'. The CO₂ is utilised for photosynthesis in order to produce the sugars required for growth and development. Therefore it can be speculated that it is unlikely that large changes in gene expression would occur in response [eCO₂] because the plant is undertaking all of its normal physiological functions, and has acclimated to the conditions. In contrast, following exposure to a stress such as ozone, substantial changes in gene expression would be expected in order for the plant to produce the required defences, and ultimately to survive.

One of the main problems with microarrays is that they only provide a picture of what is occurring at the transcriptional level, and in some instances changes at the protein level are not reflected by changes at the mRNA level (Donson *et al*, 2002). Furthermore, abundant genes are often over-represented in cDNA libraries whereas rarely expressed transcripts and those induced only under specific conditions are often missing (Breyne and Zabeau, 2001). Therefore important regulatory genes may be overlooked. In addition, there may also be a problem with cross hybridisation on a microarray. Transcripts from genes that exhibit a high degree of sequence homology

have the potential to cross hybridise to targets on the microarray (Breyne and Zabeau, 2001).

Pooling samples is a way in which it is possible to identify differentially expressed transcripts whilst keeping experimental costs down. This strategy assumes that the expression of mRNA is close to the average expression from the individual samples (Shih *et al*, 2004). A number of studies have investigated the pooling strategy in microarray experimental design (e.g. Kendzierski *et al*, 2005; Zhang and Gant, 2005). In this experiment there was no indication of biological variation since the relative contributions of each biological replicate to the pool was not measured. However, since the aim of the experiment was to identify differentially expressed transcripts using a global screen, this approach was deemed to be an appropriate strategy.

5.4.6 Future directions

A further complication with transcript profiling in trees exposed to FACE is the concentration of CO₂ at which the plants are grown. The FACE system exposes trees to 550ppm CO₂, which represents the predicted concentration for the year 2050. This concentration may be too low to identify any large changes in gene expression levels in leaves. In studies by Druart *et al* (2006), *P. deltooides* was exposed to ambient, 800 or 1200ppm [CO₂]. The studies showed that more transcripts were significantly differentially expressed at the higher concentration of CO₂ in both leaves and stems. At 800ppm, relatively few transcripts were differentially expressed between the treatments, (reiterating the results presented here) but the number increased under the higher [CO₂].

Future research into transcriptomics in plants exposed to [eCO₂] can take two different routes. The first is to identify any transcripts that are likely to be differentially expressed according to current climatic models, such as the proposed concentration of CO₂ in 2050. This has the obvious application of providing the community with an idea of how plants will grow and develop under future climatic conditions. Alternatively, the second route is to identify CO₂ responsive genes by exposing the trees to very high concentrations that are unlikely to be experienced for the foreseeable future. Whilst both approaches have advantages, the current research is generally focused on the former since it is an issue that it is likely we will have to face within the

next 50 years. Furthermore, the results of such studies may help to encourage a change in the legislation regarding anthropogenic CO₂ emissions worldwide.

5.5 Conclusions

The effects of [eCO₂] on many physiological processes are now well known, although they are known to be affected by the species studied, length of exposure and the type of experimental system used. The experiments described here were one of the first examples of transcript profiling in *Populus*. Using two microarrays derived from different EST collections, it was clear that CO₂ does not induce large changes in gene expression. This result has also been confirmed in independent experiments using FACE facilities (e.g. Gupta *et al*, 2005; Ainsworth *et al*, 2006; Miyazaki *et al*, 2004) or controlled environments (e.g. Druart *et al*, 2006). It is reasonable to suggest that either there are few substantial changes in response to [eCO₂] or microarrays are not the most appropriate method to detect them. Microarrays are an extremely useful tool to provide an overview of transcriptional changes and are a good starting point for further studies, but they may not be the most appropriate technique for detecting changes in response to [eCO₂].

CHAPTER 6

Phenotypic analyses of selected *Populus* genotypes exposed to [eCO₂] using Closed Topped Chambers

6.0 Overview

There are many studies that have been conducted to investigate plant growth responses to [eCO₂]. The experiment described in this chapter was conducted in a set of closed topped chambers (CTCs), and the trees were exposed to the [CO₂] predicted for 2050.

Growth was assessed in selected members of the F₂ generation of the *Populus* F₂ mapping population, Family 331, as well as in the two F₁ genotypes and the original grandparental species, *P. deltoides* and *P. trichocarpa*. The F₂ genotypes were selected based upon their extreme polarity in terms of yield. The results showed that the low-yielding genotypes responded to a greater degree to [eCO₂] than the high-yielding genotypes.

The results from *P. deltoides* and *P. trichocarpa* showed that the two species respond to [eCO₂] to different magnitudes, with the response highly dependent upon the stage of leaf ontogeny. The samples from this experiment were used for subsequent transcriptomic and proteomic studies, described in Chapters 7 and 8 respectively.

6.1 Introduction

The latest report from the Intergovernmental Panel on Climate Change has stated that the global increases in CO₂ concentration are primarily due to fossil fuel combustion and land-use change (IPCC, 2007). Furthermore, the report also suggests that it is ‘very likely’ that the observed increase in global average temperature is due to such increases in anthropogenic greenhouse gas emissions (IPCC, 2007).

An understanding of plant growth and development is imperative in order to recognise the adaptive significance of traits which will ultimately affect the competitive ability of a plant in a changing global climate. Above-ground growth is generally stimulated in response to increased carbon availability (e.g. Curtis and Wang, 1998). However, there are still many unanswered questions relating to the development of plants in future atmospheric environments. One question of distinct relevance, particularly on a commercial and economic scale, relates to that of plant yield. In future environments will high yielding crops respond to the increased carbon availability in the atmosphere, or will low yielding species flourish? This has further implications with regards to the crops that are planted for use as carbon neutral energy resources.

In order to address such questions requires the use of individuals from the same genetic background, but which display differential characteristics. Family 331 (Bradshaw and Stettler, 1993) is an F₂ mapping population derived from a paternal *P. deltoides* individual and a maternal *P. trichocarpa* individual (Figure 6.1.1). Previous experiments have investigated the response of the whole population to [eCO₂], and it was shown that both above-and below-ground biomass was stimulated when grown in an enriched CO₂ environment (Rae *et al*, 2007). However, the response differed significantly between the members of the F₂ population (Rae *et al*, 2007). Therefore this divergent population is an important tool to enable mechanisms underlying the response to [eCO₂] to be investigated.

The selection of genotypes demonstrating ‘extreme’ phenotypic behaviour (for example maximal or minimal leaf area) is an accepted approach for understanding the genetic basis of the trait in question (Borevitz and Nordberg, 2003; Borevitz and Chory, 2004). The use of F₂ genotypes, which exhibit trait segregation within the population, will further permit important biological questions to be addressed.

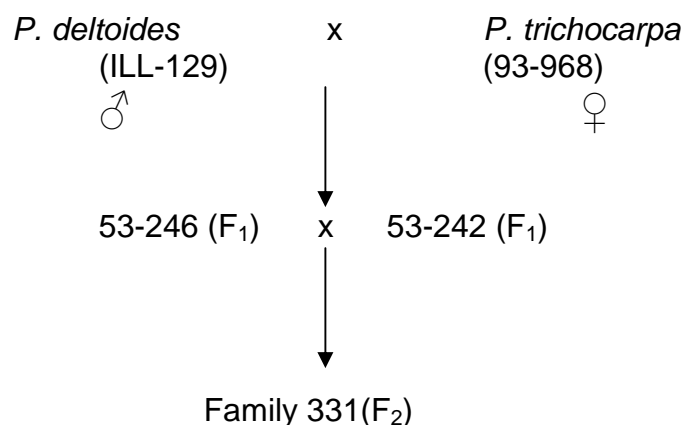


Figure 6.1.1. Family 331 was derived from a cross between *P. deltoides* (paternal) and *P. trichocarpa* (maternal). Two of the resulting F₁ genotypes ('246' and '242') were crossed to produce the F₂ generation (Bradshaw and Stettler, 1993).

The aim of this experiment was to assess the growth characteristics of *Populus* in future predicted CO₂ environments through the use of highly divergent individuals of a pedigree population. The leaf growth of the two phenotypically distinct 'grandparental' species, *P. deltoides* and *P. trichocarpa*, were monitored during the growing season, as well as the two F₁ genotypes derived from this cross, and a selection of genotypes from the F₂ population. The F₂ genotype selections were based upon yield (biomass) data collected from the population in a previous experiment.

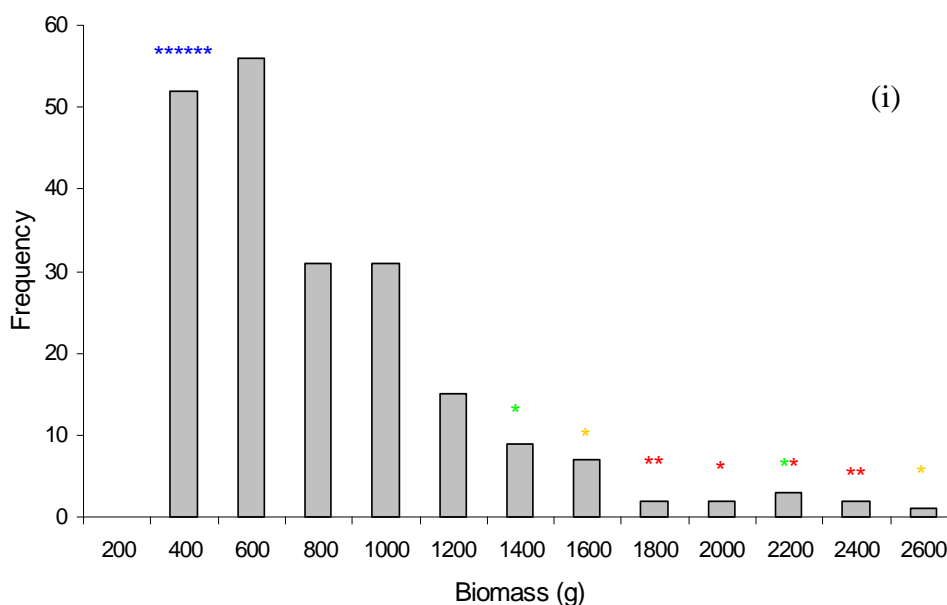
Previous experiments (e.g. Rae *et al*, 2007; Ferris *et al*, 2002) have demonstrated variable responses to [eCO₂] amongst members of the population. However, this is the first detailed study of leaf development, which focuses on selected members of the population.

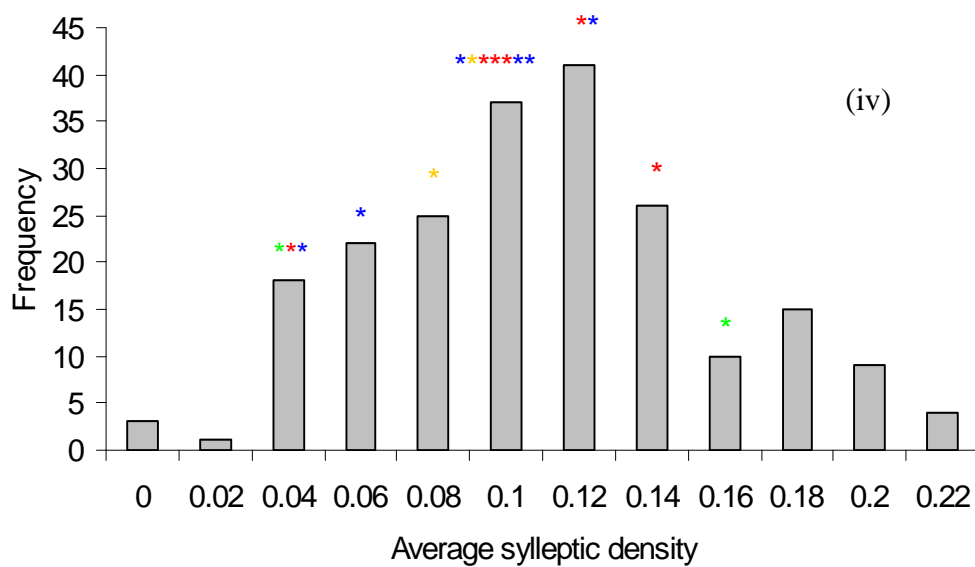
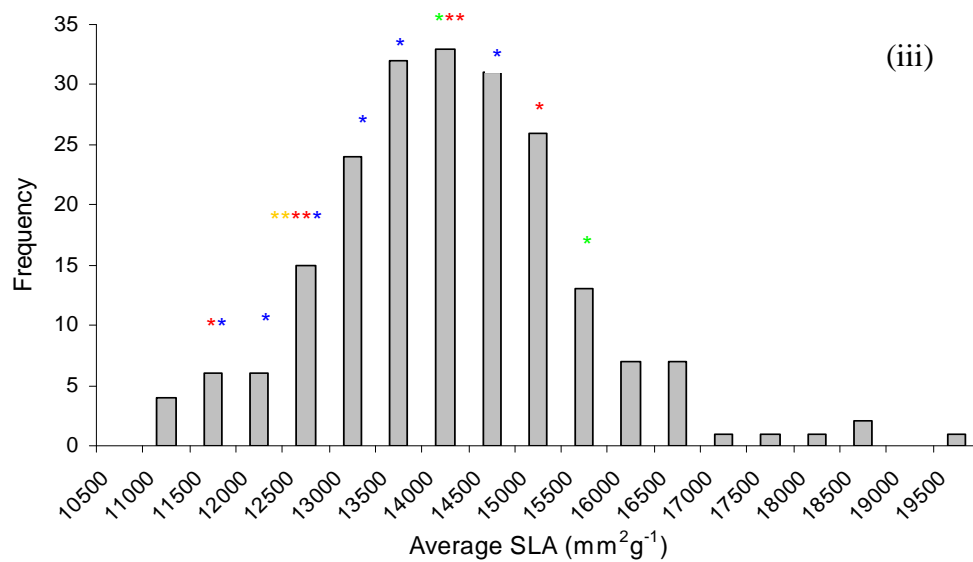
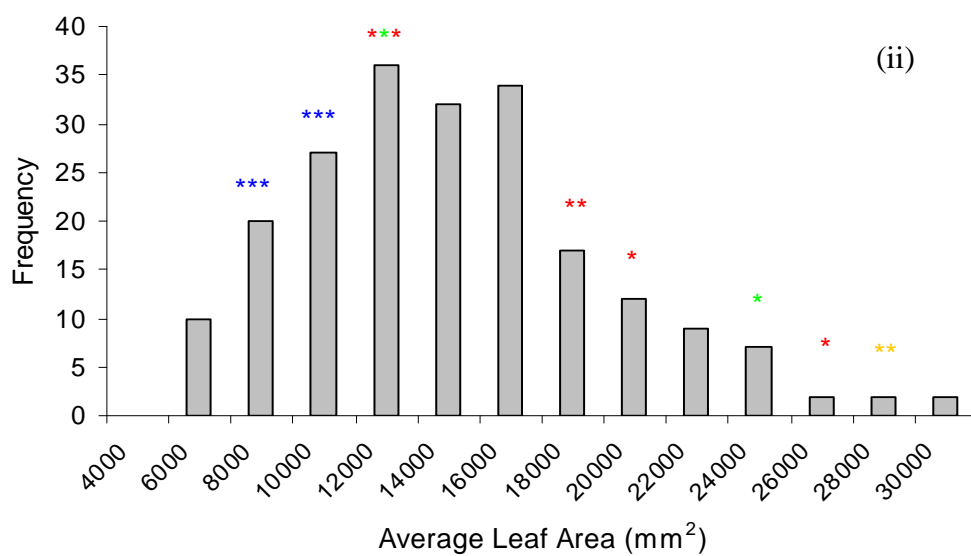
6.2 Materials and Methods

The genotype selections were based upon biomass data obtained as a part of the EU ‘Popyomics’ project (<http://www.soton.ac.uk/~popyomic/>). Part of this project involved measuring the growth traits of Family 331 members.

6.2.1 Genotype selection

The UK trait data from the Popyomics project has been published (see Rae *et al*, 2007) and was used here to select the extreme genotypes based on their biomass. The data was ranked according to biomass, and from this list six ‘high’ and six ‘low’ extreme genotypes were selected. (It is important to note that the genotype selection was also based upon cutting availability and quality.) For each trait, the results from the six high genotypes were grouped into one extreme category and the six low genotypes into another, and a one-way ANOVA was used to interpret the data. The results from the Popyomic’s data from the UK trials for various growth traits are shown in Figure 6.2.1. The results for each trait for each genotype in the data set are indicated alongside the corresponding category on the graph, in order to illustrate the different growth characteristics of the selected genotypes.





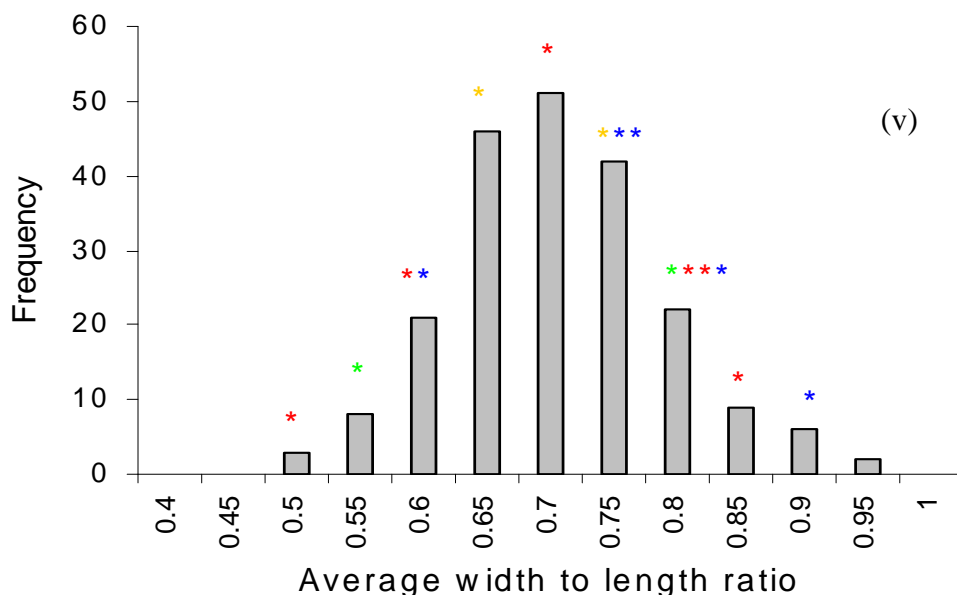


Figure 6.2.1. Frequency histograms showing the results for leaf area, SLA, leaf shape index (width: length) and sylleptic density in Family 331. The data was collected in the UK as part of the EU Popyomics project data and published in Rae *et al*, (2007). The genotypes were selected based on the biomass data (i). Each star represents the result for one of the selected genotypes. Blue stars= low biomass extremes, red stars= high biomass extremes, green stars= grandparents (*P. deltoides* or *P. trichocarpa*), yellow stars= parents (genotype 242 or 246). A one-way ANOVA was conducted on the results to check for statistical differences between the two extreme groups (high and low biomass) for each trait.

There was a statistically significant difference between the extreme groups for biomass ($p < 0.001$) and leaf area ($p < 0.001$) only. The remaining three traits that were tested (width: length, SLA and sylleptic density) were not significantly different between the groups.

6.2.2 Experimental design

On 22nd May 2006, the *Populus* cuttings were planted into the 16 chambers at the Forestry Commission field site, Headley, UK (51°07'N, 0°50'W). The chambers had been prepared for planting by removing all weeds and by digging hop waste into the soil for nutrition. Furthermore, the chambers were sprayed with fungicide and insecticide prior to experimentation.

The general design for the planting is given in Figure 6.2.2. Each chamber was split into two halves. One half contained the ‘grandparents’ of the population (*P. deltoides* and *P. trichocarpa*), and the F_1 genotypes (‘242’ and ‘246’), and the other contained the selected extreme F_2 genotypes (either high or low in a single chamber). In each chamber, the genotypes were assigned a position in the appropriate segment using a random number generator (www.random.org).

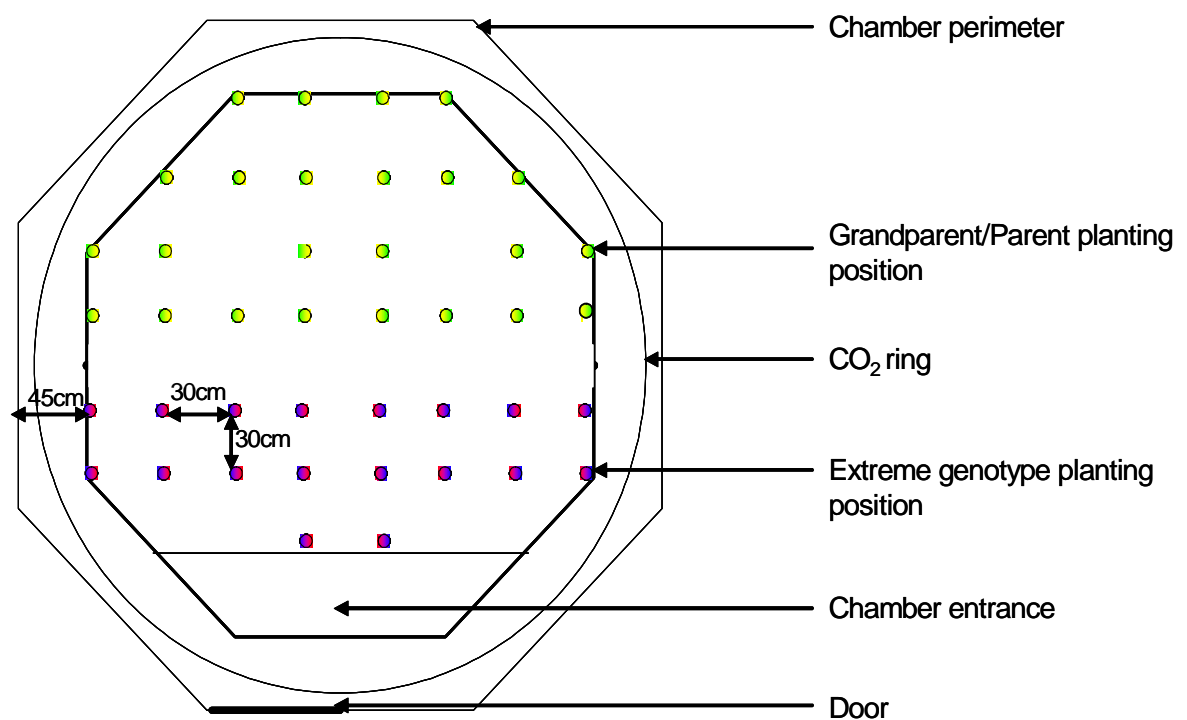


Figure 6.2.2. The general design plan for each chamber in the experiment. Each spot represents one planting position. The cuttings were planted 30cm from the nearest neighbour. The green/ yellow spots indicate the positions for the ‘grandparents’ and ‘parents’ respectively. The red/ blue spots indicate the positions for the high extremes or the low extremes in a chamber (high and low extremes were not grown in the same chamber.)

The chambers were ventilated as described in Ferris *et al*, 2002. The average [CO₂] was 387 ± 52 ppm ([aCO₂]) and 485 ± 100 ppm ([eCO₂]). The CO₂ exposure began on the 5th July 2006.

6.2.3 Phenotyping

6.2.3.1 *P. deltoides*, *P. trichocarpa* and the F₁ genotypes

A timeline representing sampling dates is shown in Figure 6.2.3. On the 17th August 2006 (90 days after planting (DAP) and 43 days following exposure to [eCO₂] (DFE)) the youngest fully unfurled leaf of each tree was tagged using a length of wool tied loosely around the petiole. This was defined as leaf one. Photographs of every tagged leaf were taken on the 17th, 21st, 24th, 28th, 31st August, and the 2nd, 4th and 7th September 2006 in order to construct a temporal growth profile. On the 17th August 2006, leaf ages two to ten (where the tagged leaf was age one) were also photographed in order to construct a spatial profile of leaf development. On the 24th August 2006 (50 DFE), one mature leaf was sampled for SLA as described in Chapter 2.

Adaxial and abaxial epidermal imprints were sampled on the 17th August 2006 according to the methodology described in Chapter 2. In total, four biological replicates of each genotype were sampled in a profile (i.e. leaves 2 to 10).

The material to study leaf anatomy was sampled on the 24th August 2006, according to the methodology described in Chapter 2. Small sections of tissue were sampled from the 2nd interveinal area (where the 1st was the most basal area) of a young and mature leaf. The samples were collected from chambers one ([eCO₂]) and two ([aCO₂]) only.

6.2.3.2 F₂ yield extreme genotypes

Photographs of the leaves were taken on the 19th, 24th, 26th, 28th, 31st August and the 2nd, 4th and 8th September 2006. The leaf above the tagged one was sampled at each time-point because on the date of the first sampling of biomass extremes (19th August 2006 (45 DFE)) the tagged leaf was no longer the youngest unfurled (which was the definition of 'leaf one' for grandparents and F₁ genotypes). The leaf above the tagged one represented the first fully unfurled leaf in the case of every biological replicate for each genotype.

6.2.3.3 All genotypes

Tree height and diameter were recorded for every individual on four occasions during the growing season (16th, 23rd and 30th August 2006). Diameter was recorded 30cm from ground level with a set of digital callipers. Only trees that had not had a leaf profile sampled (where the SAM was removed) were measured.

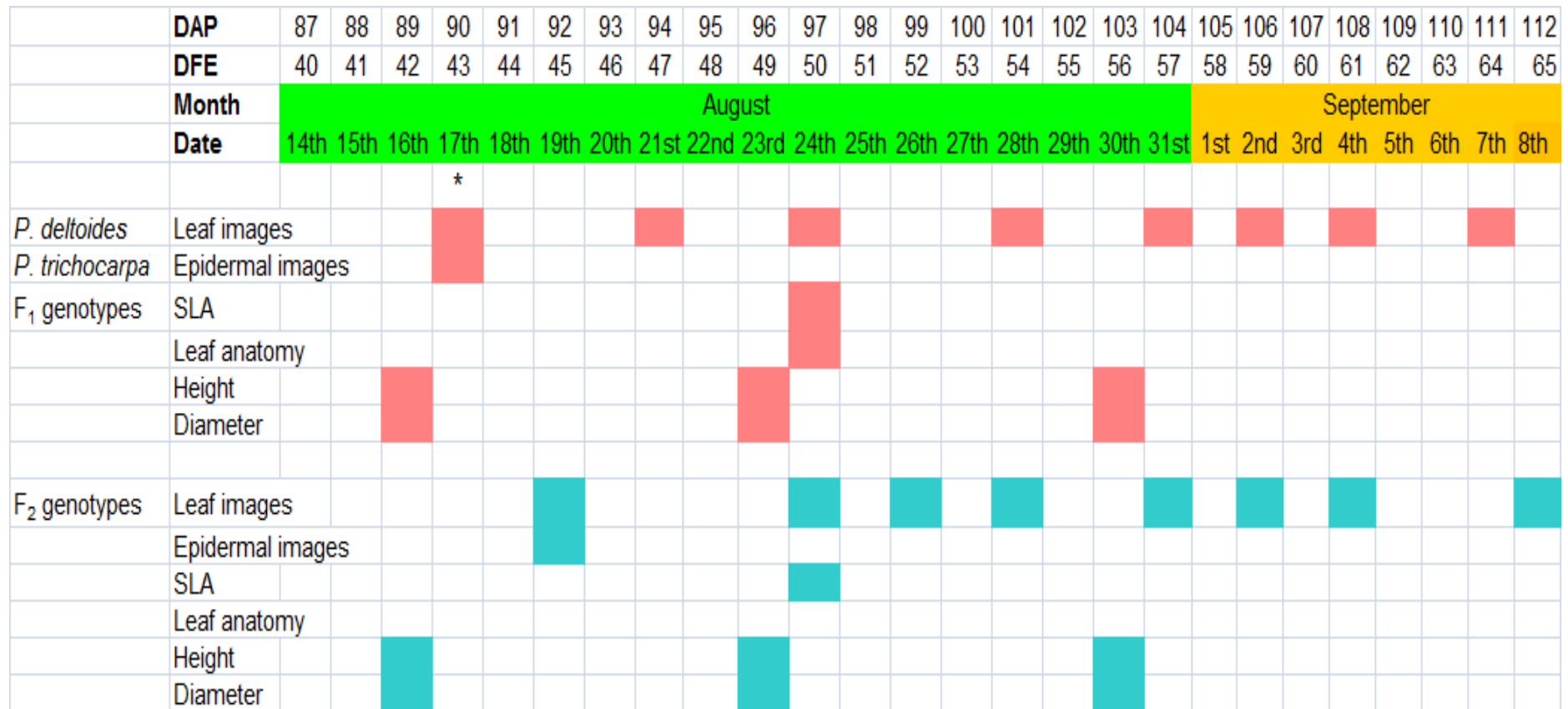


Figure 6.2.3. A timeline representing sampling dates during the course of the experiment. The diagram shows the time scale in terms of DAP (Days After Planting), DFE (Days Following Exposure (to [eCO₂])) and calendar days. The pink squares in the top part of the chart represent the times at which *P. deltoides*, *P. trichocarpa* and the two F₁ genotypes (242 and 246) were sampled. The blue squares in the lower part of the diagram represent the times when the extreme biomass (F₂) genotypes were sampled. The star represents the date at which the spatial profile was sampled for *P. deltoides* and *P. trichocarpa* for the transcriptomic and proteomic analyses (see chapter 7 and 8 respectively).

6.3 Results

6.3.1 Spatial analyses of *P. deltoides* and *P. trichocarpa*

In order to investigate the spatial response of *P. deltoides* and *P. trichocarpa* to [eCO₂], a ‘growth profile’ was constructed at a single time-point during the experiment. This involved collecting data from a set of chronologically ordered leaves from a group of randomly selected individuals. Leaf one was defined as the first fully unfurled leaf at the beginning of sampling when these profiles were collected (17th August 2006).

6.3.1.1 Leaf growth analyses

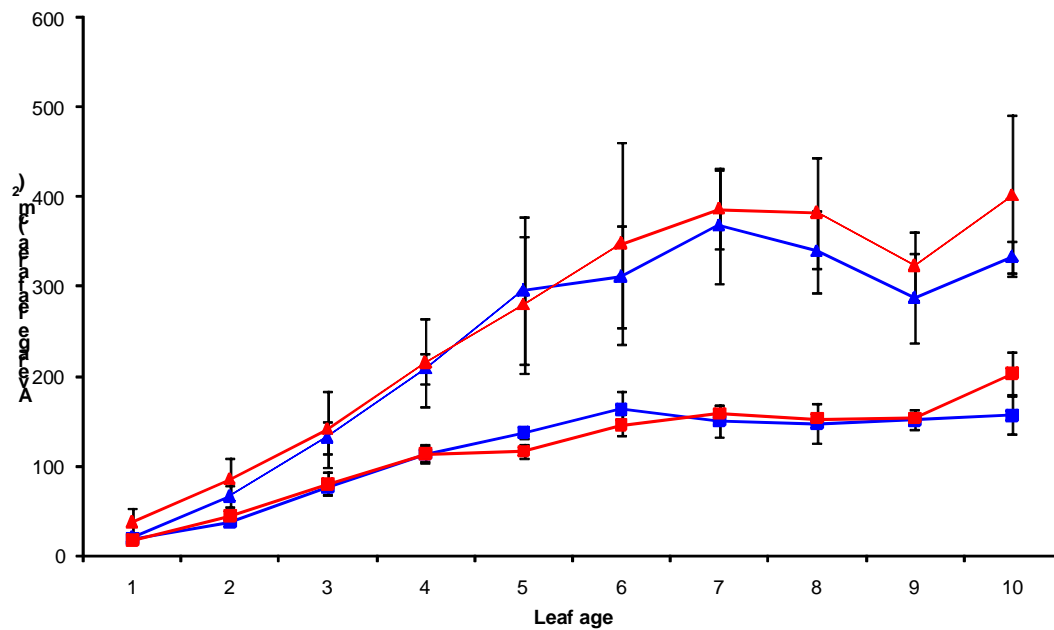
The percentage change in leaf area (Table 6.3.1) showed that growth was stimulated in young leaves exposed to [eCO₂] (particularly in *P. deltoides*), and that this response generally reduced with leaf age. However, there was no statistically significant treatment effect on leaf area ($F_{1,97}=1.31$ $p<0.05$) (Figure 6.3.1).

Leaf area	<i>P. deltoides</i>	<i>P. trichocarpa</i>
Leaf age	% change in leaf area	% change in leaf area
1	80.3	-7.97
2	28.9	21.15
3	6.90	4.80
4	2.86	0.40
5	-5.34	-15.49
6	11.86	-10.98
7	4.94	5.33
8	12.69	3.67
9	12.45	0.97
10	20.59	30.17

Table 6.3.1. The average leaf area was used to calculate the percentage changes according to the following equation;

$$\frac{\text{Leaf area ([eCO}_2\text{)]}-\text{Leaf area ([aCO}_2\text{)]}}{\text{Leaf area ([aCO}_2\text{)]}} \times 100$$

Leaf ‘1’ was defined as the youngest fully unfurled leaf from the shoot meristem on day one of the experiment.



Treatment	0.256 n.s
Species	0.000***
Age	0.000***
Treatment x Species	0.391n.s
Treatment x Age	0.988n.s
Species x Age	0.000***
Treatment x Species x Age	1.000n.s

Figure 6.3.1. The average leaf area of *P. deltoides* (triangles) and *P. trichocarpa* (squares) under ambient (blue) or elevated (red) [CO₂]. The data was collected on the first day of the experiment (17th August 2006). Standard error bars have been omitted from the graph for clarity. The results of a three-way ANOVA are provided underneath the graph (***p<0.001; ns= not significant). n=6.

Leaf shape index (i.e. length to width ratio) was generally reduced following growth in [eCO₂] (Table 6.3.2). The ratio was consistently greater in all leaf ages in *P. trichocarpa* in ambient than elevated CO₂ (i.e. a larger index equates to longer, thinner leaves, whilst a reduced index suggests shorter, wider leaves) ($F_{1,97}=1050.20$ $p<0.001$).

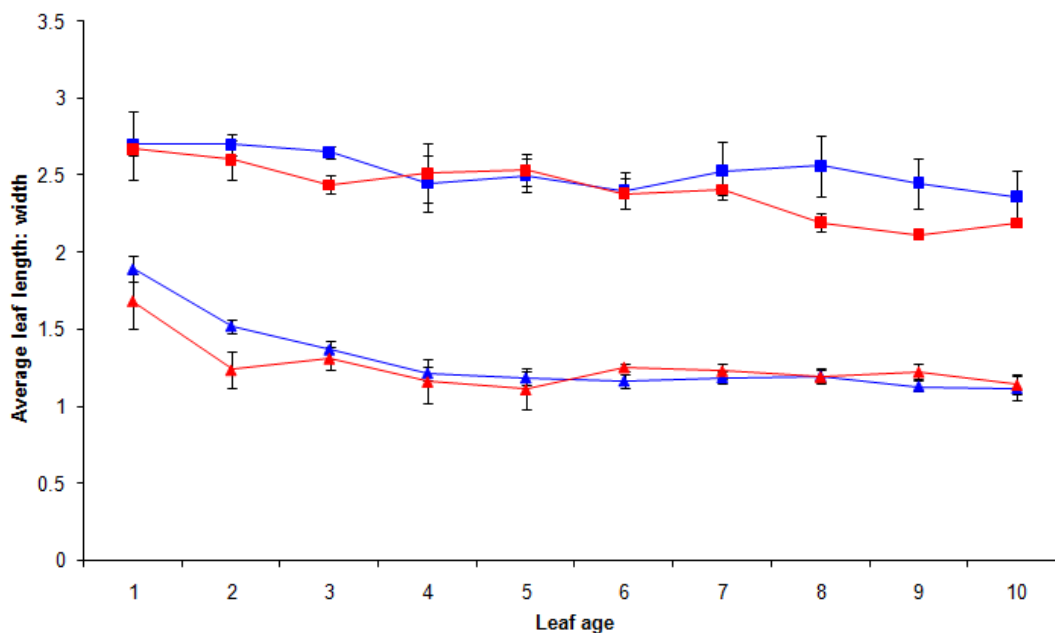
6.3.1.2 Leaf shape index

	<i>P. deltoides</i>	<i>P. trichocarpa</i>
Leaf age	% change in leaf l:w	% change in leaf l:w
1	-11.20	-0.87
2	-18.65	-3.67
3	-4.14	-8.03
4	-4.26	2.73
5	-6.09	1.40
6	7.80	-0.84
7	3.71	-4.84
8	-0.24	-14.42
9	8.34	-13.77
10	2.38	-7.21

Table 6.3.2. The average percentage change in leaf length to width ratio in *P. deltoides* and *P. trichocarpa*. The percentage change was used calculated according to the following equation;

$$\frac{\text{Leaf l:w ([eCO}_2\text{)]}-\text{Leaf l:w ([aCO}_2\text{)]}}{\text{Leaf l:w ([aCO}_2\text{)]}} \times 100$$

In *P. deltoides*, the leaf shape index was particularly affected by increased carbon availability in young leaves. The young leaves grown in [eCO₂] had, on average, a lower length to width ratio than those grown in [aCO₂]. However, this difference declined over developmental time (Figure 6.3.2).

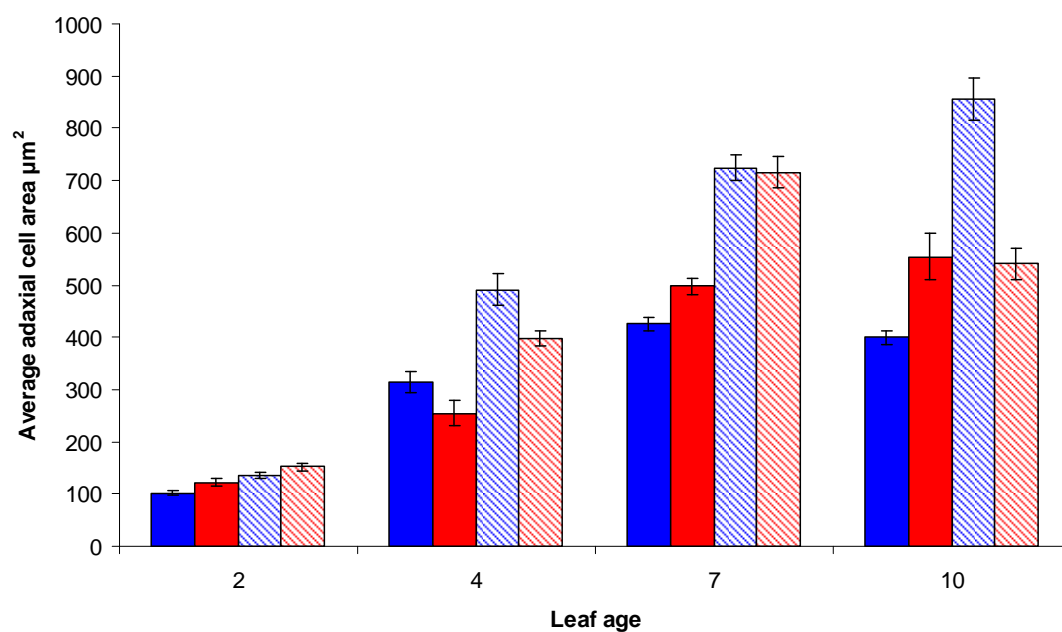


Treatment	0.025*
Species	0.000***
Age	0.000***
Treatment x Species	0.262 ns
Treatment x Age	0.890 ns
Species x Age	0.281 ns
Treatment x Species x Age	0.492 ns

Figure 6.3.2. The leaf length to width ratios of *P. deltoides* (triangles) and *P. trichocarpa* (squares) grown under ambient (blue) or elevated (red) [CO₂]. The data was collected on the first day of the experiment (17th August 2006). Error bars have been omitted for clarity. The results of a three-way ANOVA is given below the graph (*p<0.05; ***p<0.001; ns= not significant). n=6.

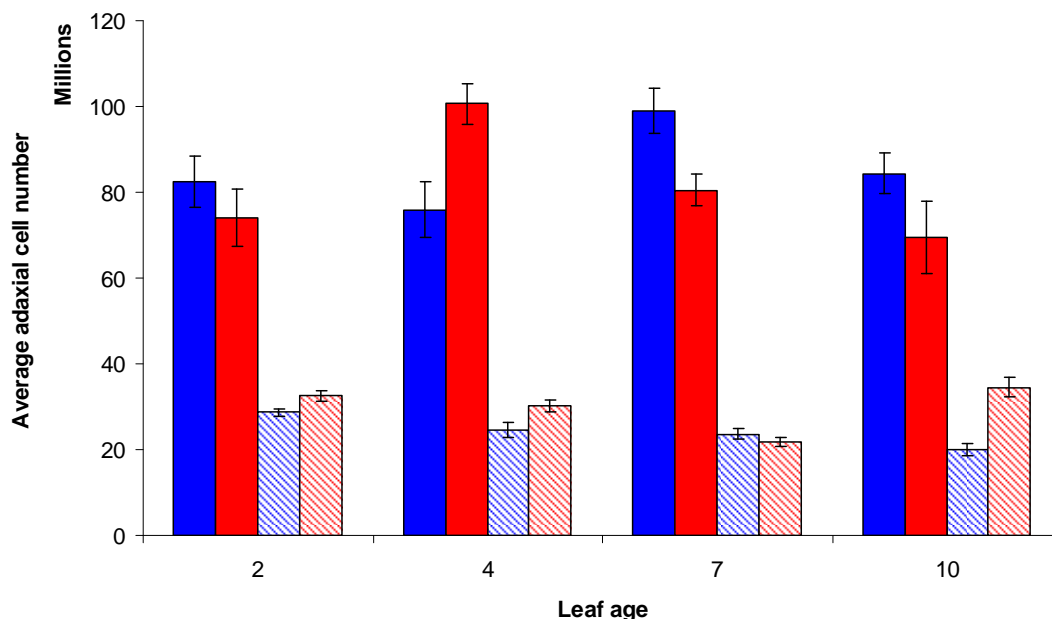
6.3.1.3 Cell growth analyses

Cell impressions were sampled from the growth profile trees and used to calculate average cell area and to estimate cell number per leaf. Adaxial cell area was stimulated by [eCO₂] in the mature leaves of *P. deltoides*, but reduced in *P. trichocarpa*. Similarly, abaxial cell area was stimulated in *P. deltoides* but reduced in the mature leaves of *P. trichocarpa*. Adaxial cell area and abaxial cell number were significantly affected by CO₂ treatment (Figures 6.3.3 and 6.3.6 respectively).



Treatment	0.025*
Age	0.000***
Species	0.000***
Treatment x Age	0.000***
Treatment x Species	0.000***
Age x Species	0.000***
Treatment x Age x Species	0.000***

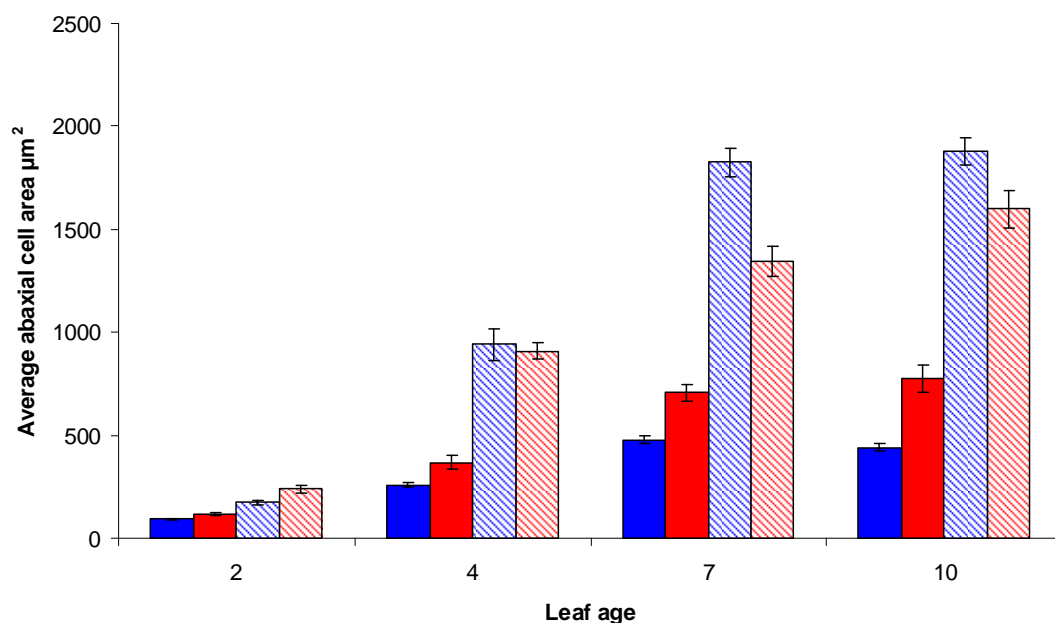
Figure 6.3.3. The average adaxial epidermal cell area at the first time-point (17th August 2006). The impressions were taken from the growth profile trees. The solid blocks represent the results for *P. deltoides* whilst the hatched blocks represents *P. trichocarpa*. Blue bars indicate growth in [aCO₂] and red bars indicate growth in [eCO₂]. The results of a three-way ANOVA is given below the graph (*p<0.05; ***p<0.001; ns= not significant). n=60.



Treatment	0.824	ns
Age	0.549	ns
Species	0.000***	
Treatment x Age	0.007**	
Treatment x Species	0.071	ns
Age x Species	0.022*	
Treatment x Age x Species	0.020*	

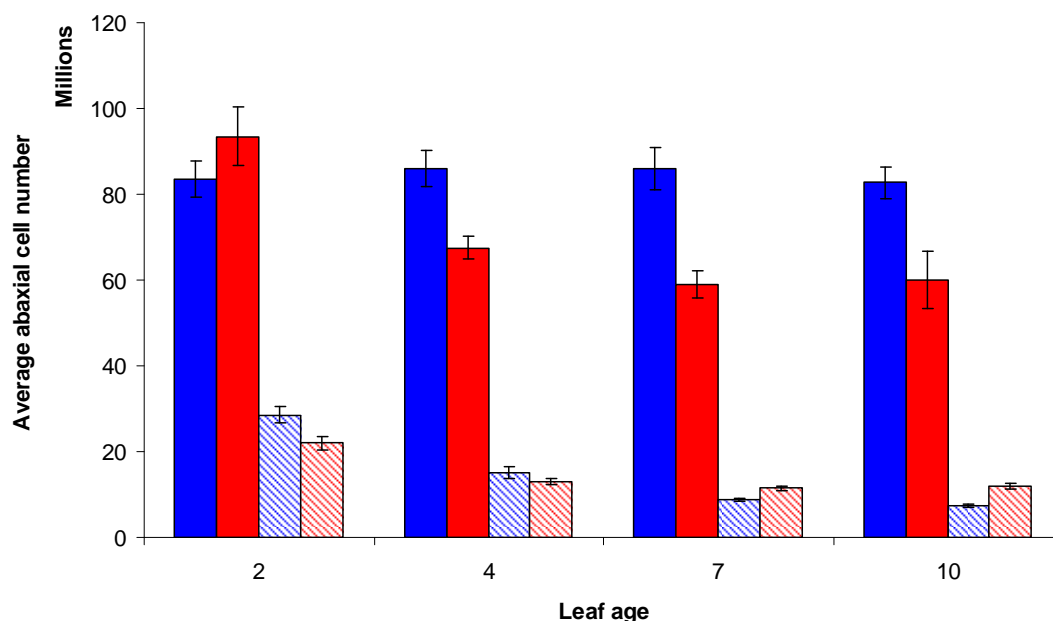
Figure 6.3.4. The average adaxial epidermal cell number at the first time-point (17th August 2006). The impressions were taken from the profile trees. The solid blocks represent the results for *P. deltoides* whilst the hatched blocks represents *P. trichocarpa*. Blue bars indicate growth in [aCO₂] and red bars indicate growth in [eCO₂]. The results of a three-way ANOVA is given below the graph. (*p<0.05; **p<0.01; ***p<0.001; ns= not significant).

As would be expected, there was a significant species difference in terms of adaxial ($F_{1,522} = 190.64$ $p < 0.001$) and abaxial ($F_{1,624} = 851.91$ $p < 0.001$) cell area, and adaxial ($F_{1,522} = 431.39$ $p < 0.001$) and abaxial ($F_{1,624} = 870.74$ $p < 0.001$) cell number. Elevated [CO₂] reduced adaxial cell area in *P. trichocarpa*, but generally stimulated it in *P. deltoides*, and this pattern was repeated on the abaxial surface. Treatment had no effect on adaxial cell number (Figure 6.3.4) or abaxial cell area (Figure 6.3.5). However, there was a general reduction in abaxial cell number in *P. deltoides* as a result of treatment (ages 4, 7 and 10) but a slight stimulation in ages 7 and 10 in *P. trichocarpa*.



Treatment	0.898 ns
Age	0.000***
Species	0.000***
Treatment x Age	0.029*
Treatment x Species	0.000***
Age x Species	0.000***
Treatment x Age x Species	0.000***

Figure 6.3.5. The average abaxial epidermal cell area at the first time-point (17th August 2006). The impressions were taken from the profile trees. The solid blocks represent the results for *P. deltoides* whilst the hatched blocks represents *P. trichocarpa*. Blue bars indicate growth in [aCO₂] and red bars indicate growth in [eCO₂]. The results of a three-way ANOVA is given below the graph (*p<0.05; ***p<0.001; ns= not significant). n=60.



Treatment	0.000***
Age	0.000***
Species	0.000***
Treatment x Age	0.087 ns
Treatment x Species	0.001***
Age x Species	0.995 ns
Treatment x Age x Species	0.000***

Figure 6.3.6. The average abaxial epidermal cell number at the first time-point (17th August 2006). The impressions were taken from the profile trees. The solid blocks represent the results for *P. deltoides* whilst the hatched blocks represents *P. trichocarpa*. Blue bars indicate growth in [aCO₂] and red bars indicate growth in [eCO₂]. The results of a three-way ANOVA are given below the graph (***p<0.001; ns= not significant).

The results imply that increased carbon supply caused an increase in adaxial and abaxial cell area in *P. deltoides* by the process of cell expansion. No such stimulation was observed in *P. trichocarpa*, where adaxial and abaxial cell areas were reduced by treatment (in ages 4, 7 and 10). CO₂ enrichment did not promote cell division in the maturing leaves of *P. deltoides* and this was particularly true in the abaxial surface (Figure 6.3.6). The results show that *P. deltoides* responded more to [eCO₂] by promoting cell expansion.

Stomatal density was not affected by CO₂ treatment in *P. trichocarpa* ($F_{1,144}=0.75$, $p<0.01$) but in *P. deltoides*, stomatal density increased in response to treatment

($F_{1,117} = 10.84$ $p < 0.001$). Stomatal density was consistently higher on the abaxial surface (Table 6.3.3).

Trichome density was not affected by treatment ($F_{1,144} = 0.97$ $p < 0.01$) in *P. trichocarpa*. The density was consistently highest in the youngest leaves (in both the adaxial and abaxial leaf surfaces) and reduced with leaf age, therefore suggesting that trichome production ceased with leaf maturation (Table 6.3.4).

Age	Surface	<i>P. deltoides</i>			<i>P. trichocarpa</i>		
		Stomata per mm ² [aCO ₂]	se	Stomata per mm ² [eCO ₂]	se	Stomata per mm ² [aCO ₂]	se
3	Abaxial	273.0	32.5	190.3	21.8	289.9	31.1
4	Abaxial	212.7	9.5	237.5	22.5	211.5	17.8
5	Abaxial	190.3	10.3	203.3	15.2	171.1	8.3
6	Abaxial	182.7	9.9	193.0	16.3	150.6	7.2
7	Abaxial	174.6	10.9	157.3	5.2	132.7	7.3
8	Abaxial	195.0	6.7	158.4	12.6	120.7	8.5
9	Abaxial	193.4	8.8	165.4	11.8	125.6	3.9
10	Abaxial	181.6	8.5	161.7	16.4	113.9	5.1
3	Adaxial	177.4	21.5	159.9	19.5	0.0	0.0
4	Adaxial	158.8	25.2	99.9	50.3	0.0	0.0
5	Adaxial	148.5	4.3	119.0	28.3	0.4	0.4
6	Adaxial	125.4	9.5	138.7	13.1	0.0	0.0
7	Adaxial	120.0	10.4	102.9	19.0	0.0	0.0
8	Adaxial	133.1	8.7	118.0	15.8	0.4	0.4
9	Adaxial	136.8	6.7	98.9	21.1	1.3	0.8
10	Adaxial	124.6	5.3	107.2	18.5	1.2	0.8
Treatment		0.001***				Treatment	0.389 ns
Surface		0.000***				Surface	0.000***
Age		0.000***				Age	0.000***
Treatment x Surface		0.653 ns				Treatment x Surface	0.381 ns
Treatment x Age		0.331 ns				Treatment x Age	0.943 ns
Surface x Age		0.709 ns				Surface x Age	0.000***
Treatment x Surface x Age		0.144 ns				Treatment x Surface x Age	0.949 ns

Table 6.3.3. The average stomatal density in the abaxial and adaxial surfaces of *P. deltoides* and *P. trichocarpa* grown in either ambient or elevated CO₂. The standard errors are provided in the table and the results of a three-way ANOVA (for each species) are also shown (***p<0.001; ns= not significant).

<i>P. trichocarpa</i>					
Age	Surface	Trichomes per mm ² [aCO ₂]	se	Trichomes per mm ² [eCO ₂]	se
3	Abaxial	19.3	1.2	10.7	3.1
4	Abaxial	9.6	1.7	20.7	2.5
5	Abaxial	10.4	1.5	13.7	1.1
6	Abaxial	11.2	1.4	12.8	1.0
7	Abaxial	9.8	0.8	12.7	2.4
8	Abaxial	11.3	1.3	9.0	1.5
9	Abaxial	8.0	1.2	10.0	1.8
10	Abaxial	9.2	1.2	12.8	1.2
3	Adaxial	28.1	5.2	23.4	1.3
4	Adaxial	14.9	2.6	17.7	2.7
5	Adaxial	9.5	1.7	15.8	1.9
6	Adaxial	15.3	5.7	8.6	1.8
7	Adaxial	11.1	2.2	8.6	5.1
8	Adaxial	11.0	0.6	8.6	1.6
9	Adaxial	7.9	2.2	13.8	0.9
10	Adaxial	8.3	1.5	8.6	1.9

Treatment	0.326	ns
Surface	0.111	ns
Age	0.000***	
Treatment x Surface	0.251	ns
Treatment x Age	0.000***	
Surface x Age	0.001***	
Treatment x Surface x Age	0.208	ns

Table 6.3.4. The average trichome density in the abaxial and adaxial surfaces of *P. trichocarpa* grown in either ambient or elevated CO₂. The standard errors are provided in the table and the results of a three-way ANOVA are also shown (***p<0.001; ns= not significant). Note; Trichomes were not present in either the abaxial or adaxial surfaces of *P. deltoides*.

6.3.1.4 Leaf anatomy

Basal sections of both young and semi-mature leaves were sampled for subsequent cellular analyses of transverse sections (Figure 6.3.7 (young leaves) and Figure 6.3.8 (mature leaves)). The young and mature leaves of *P. trichocarpa* demonstrated an increase in leaf thickness as a result of CO₂ exposure. The results suggest that in *P. trichocarpa*, cell production was stimulated in the dorsio-ventral direction. There was no apparent stimulation in growth in *P. deltoides*, although the young leaves of F₁ genotype '242' were affected by CO₂ exposure by demonstrating a subtle increase in leaf thickness (Figure 6.3.7).

Young leaves

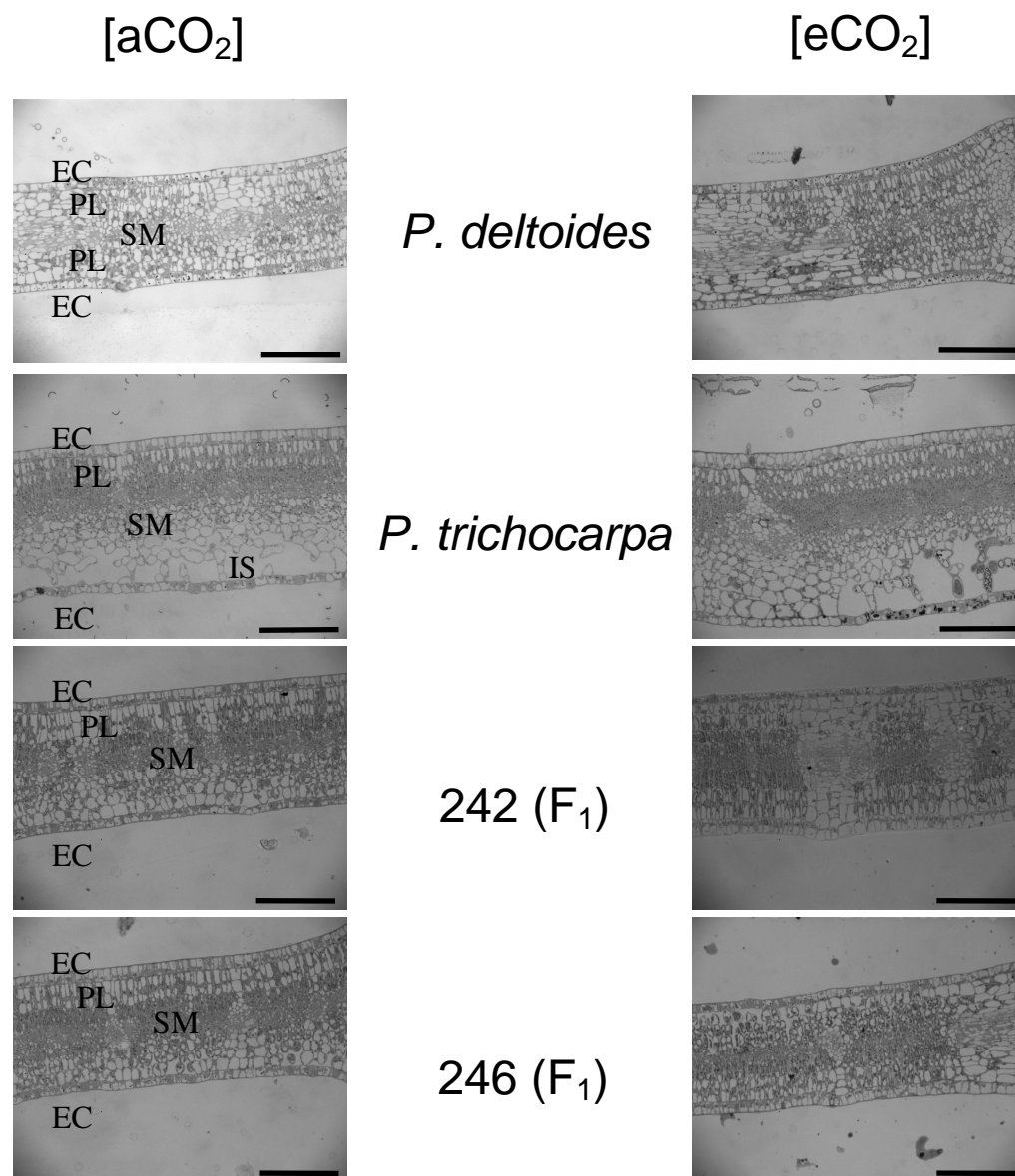


Figure 6.3.7. The transverse sections of young leaves of *P. deltoides*, *P. trichocarpa*, and the two F₁ genotypes '242' and '246'. The black bars represent a 100µm scale bar. Each picture in the diagram is representative of replicates within the genotype/treatment category. EC= epidermal cell layer; PL=palisade layer; SM= spongy mesophyll layer; IS= intercellular space.

Mature leaves

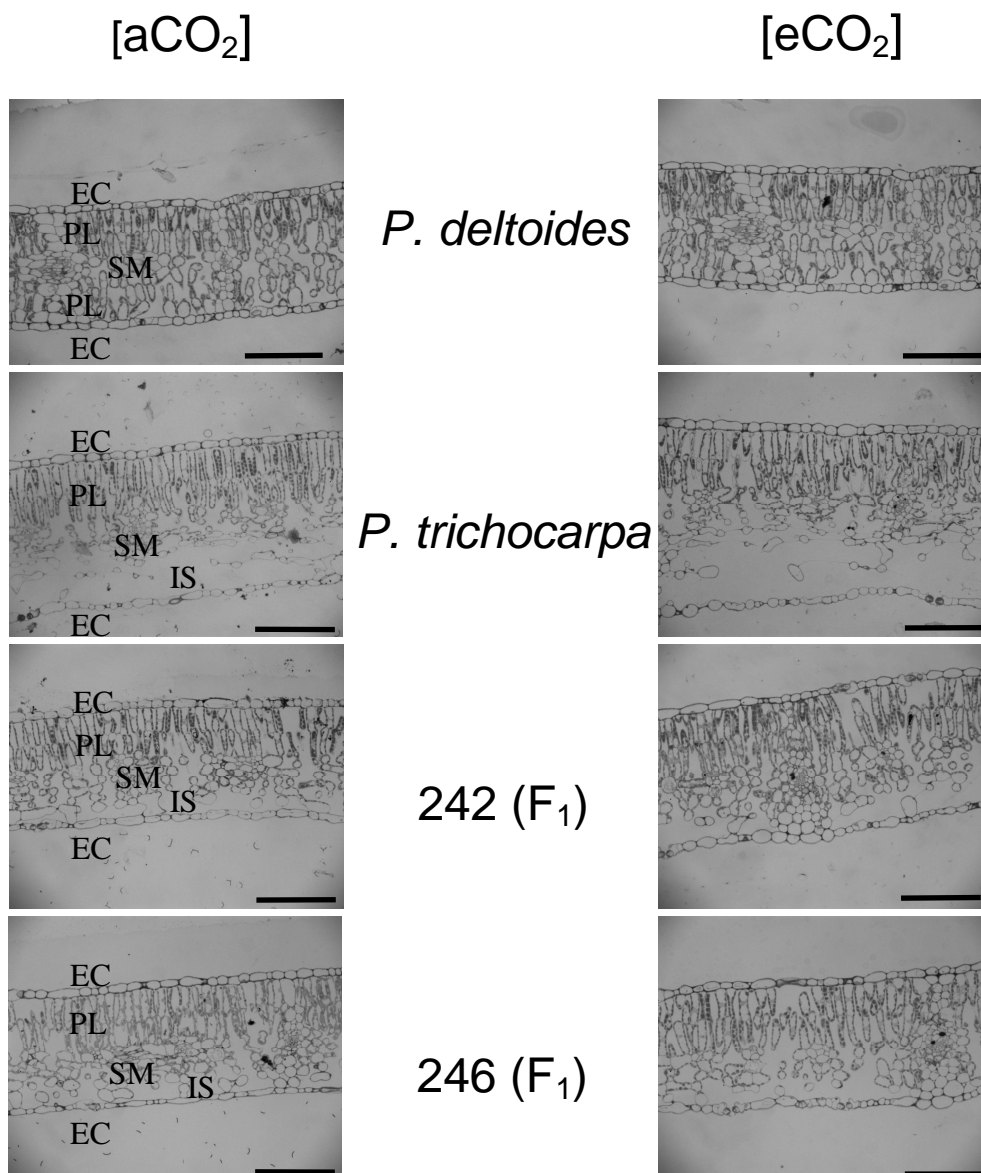


Figure 6.3.8. The transverse sections of mature leaves of *P. deltoides*, *P. trichocarpa*, and the two F₁ genotypes '242' and '246'. The black bars represent a 100µm scale bar. Each picture in the diagram is representative of replicates within the genotype/treatment category. EC= epidermal cell layer; PL=palisade layer; SM= spongy mesophyll layer; IS= intercellular space.

6.3.2 Temporal analyses of *P. deltoides* and *P. trichocarpa*

6.3.2.1 Leaf growth analyses

Along with a spatial profile of development in response to CO₂ treatment (section 6.3.1) a temporal profile was also measured in order to determine the response of individually tagged leaves to [eCO₂] during their growth period. This involved tagging a young leaf on the first day of the experiment and tracking its development by taking repeated growth measurements over time. The results for *P. deltoides* and *P. trichocarpa* are shown in Figure 6.3.9, Figure 6.3.10 and 6.3.11.

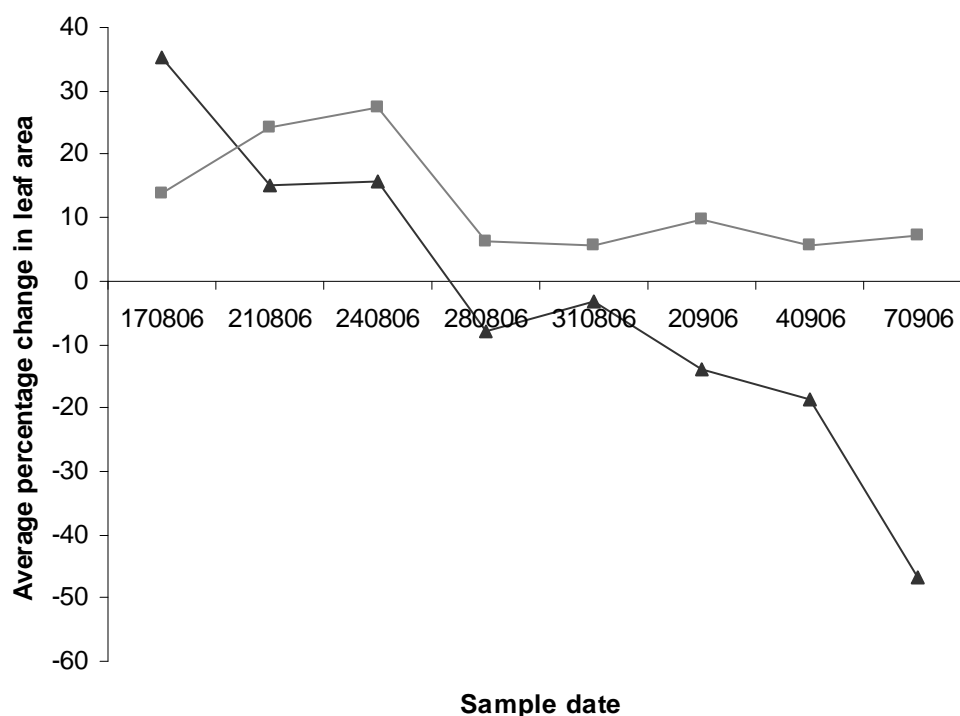


Figure 6.3.9. The average percentage change in leaf area of the tagged leaves through the progression of the experiment. The dark grey triangles represent *P. deltoides* whilst the light grey squares represent *P. trichocarpa*. The numbers on the x-axis represent the date of sampling e.g. 170806 corresponds to 17th August 2006. The average percentage change in leaf area was calculated by using the following equation;

$$\frac{\text{Average leaf area in [eCO}_2\text{]} - \text{average leaf area in [aCO}_2\text{]}}{\text{Average leaf area in [aCO}_2\text{]}} \times 100$$

Leaf area was stimulated in [eCO₂] in both *P. deltoides* and *P. trichocarpa* whilst the leaves were young. However, mid-way through the growing season (28th August 2006) the magnitude of response to [eCO₂] declined in *P. trichocarpa*. In *P. deltoides*, leaf area was reduced under [eCO₂] following this time-point. These growth patterns were mirrored in terms of changes in temporal leaf length (Figure 6.3.10) and width (Figure 6.3.11) in both species. The results of the ‘Repeated Measures’ ANOVA showed that treatment had no affect on leaf area, width or length in either species (data not shown).

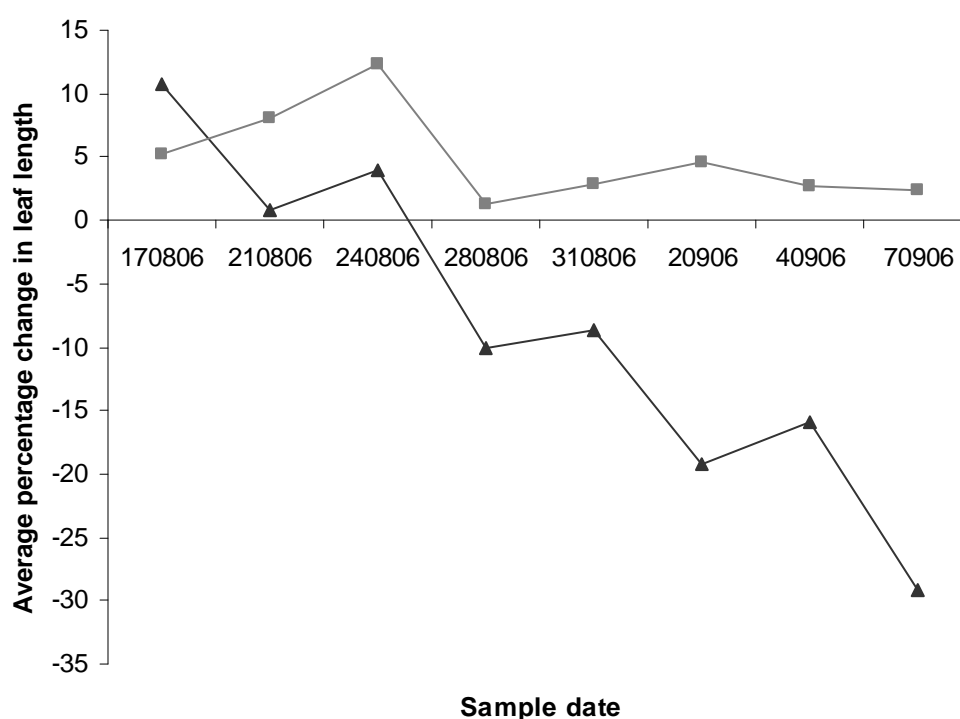


Figure 6.3.10. The average percentage change in leaf length of the tagged leaves through the progression of the experiment. Triangles (dark grey) represent *P. deltoides* whilst the squares (light grey) represent *P. trichocarpa*. The numbers on the x-axis represent the date of sampling e.g. 170806 corresponds to 17th August 2006. The average percentage change in leaf area was calculated by using the following equation;

$$\frac{\text{Average leaf length in [eCO}_2\text{]} - \text{Average leaf length in [aCO}_2\text{]}}{\text{Average leaf area in [aCO}_2\text{]}} \times 100$$

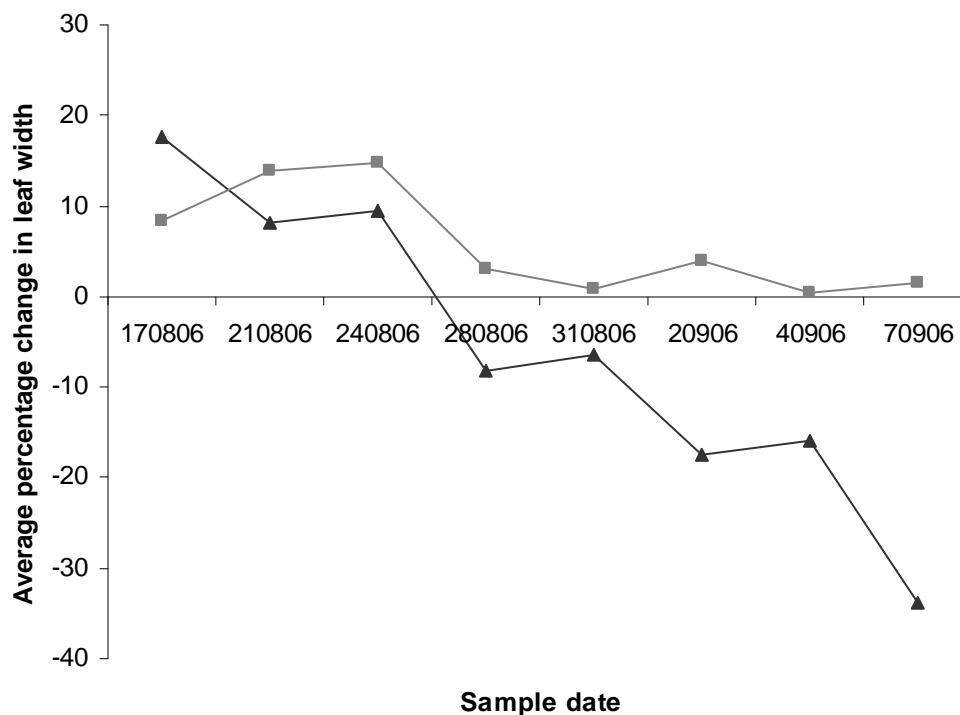
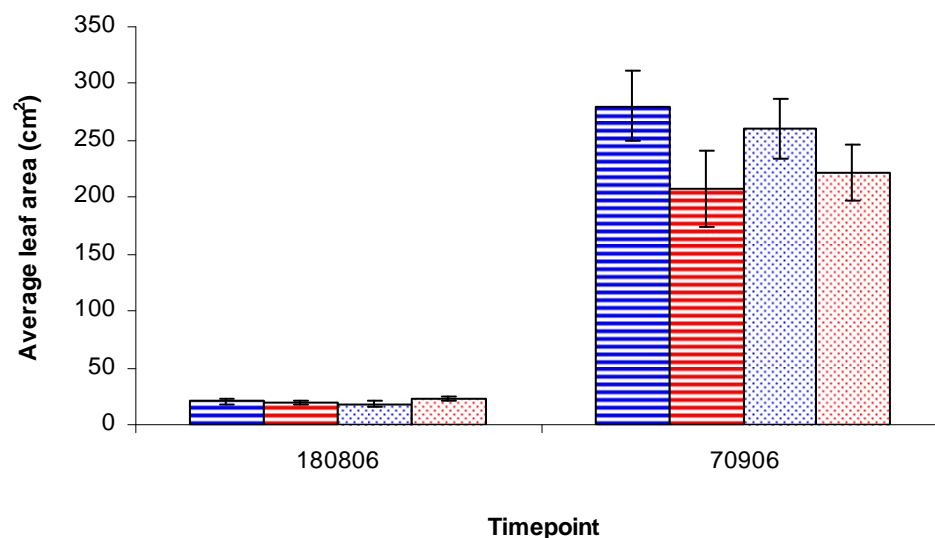


Figure 6.3.11. The average percentage change in leaf width of the tagged leaves through the progression of the experiment. Triangles (dark grey) represent *P. deltoides* whilst the squares (light grey) represent *P. trichocarpa*. The numbers on the x-axis represent the date of sampling e.g. 170806 corresponds to 17th August 2006. The average percentage change in leaf area was calculated by using the following equation;

$$\frac{\text{Average leaf width in [eCO}_2\text{]} - \text{Average leaf width in [aCO}_2\text{]}}{\text{Average leaf area in [aCO}_2\text{]}} \times 100$$

6.3.3 Temporal analyses of the F₁ and F₂ genotypes

The growth of the F₁ ('242' and '246') and F₂ (biomass extremes) genotypes were also monitored during the progression of the experiment. The results for the leaf growth analysis of the F₁ genotypes are shown in Figure 6.3.12 and Figure 6.3.13.

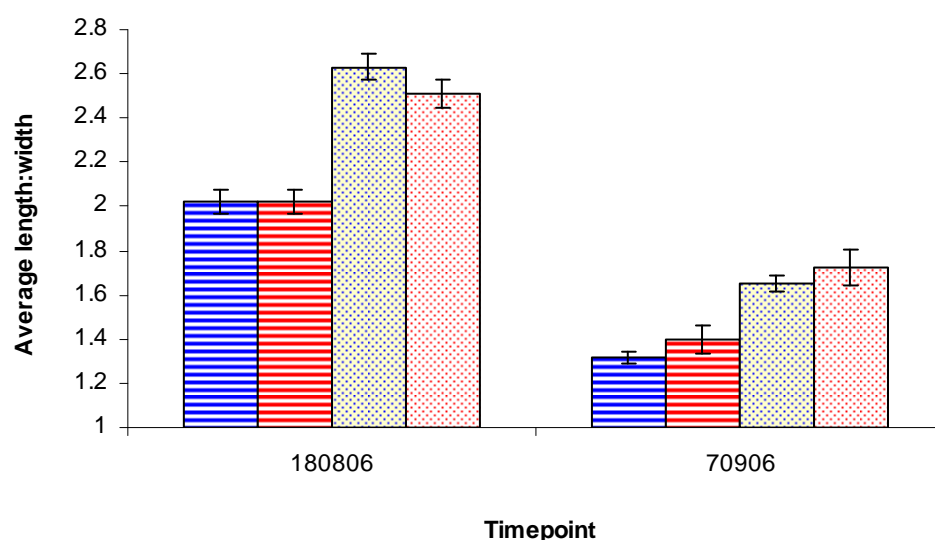


Date		
Genotype	180806	070906
242	-6.37%	-26.18%
246	25.39%	-14.63%

Treatment	0.000***
Genotype	0.733 ns
Date	0.000***
Treatment*Genotype	0.411 ns
Treatment*Date	0.000***
Genotype*Date	0.940 ns
Treatment*Genotype*Date	0.621 ns

Figure 6.3.12. The average leaf area (cm²) of the two F₁ genotypes in ambient (blue) and elevated (red) [CO₂]. Genotype 242 is represented by striped bars and 246 by dotted bars. The numbers on the x-axis represent the date of sampling e.g. 180806 corresponds to 18th August 2006. The data here shows the data collected at the first (180806) and last (070906) time-points in the experiment. Standard error bars are shown. The average percentage changes in leaf area are provided in the table beneath the graph. The results from a three-way ANOVA are provided at the bottom of the Figure (***=p<0.001; ns= not significant).

There was no significant effect of treatment on leaf area in the F₁ genotypes (Figure 6.3.12). Leaf area was stimulated by [eCO₂] in genotype 246 at the first sampling time-point only (Figure 6.3.12). This was associated with a reduction in average leaf shape index (i.e. indicating a reduction in proximo-distal/ increase in medio-lateral lamina growth compared to its counterpart grown under [aCO₂]) (Figure 6.3.13). Conversely, the reduction in leaf area in [eCO₂] in both 242 and 246 at the latter time-point corresponds with an increase in average leaf length to width ratio (i.e. increase in proximo-distal/ decrease in medio-lateral lamina growth).

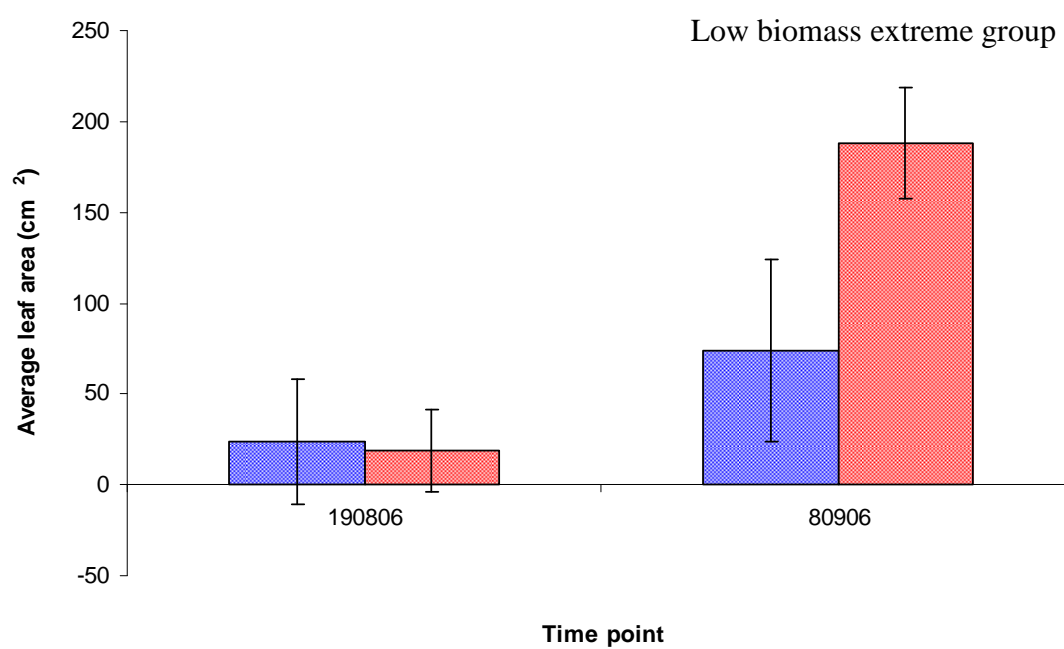
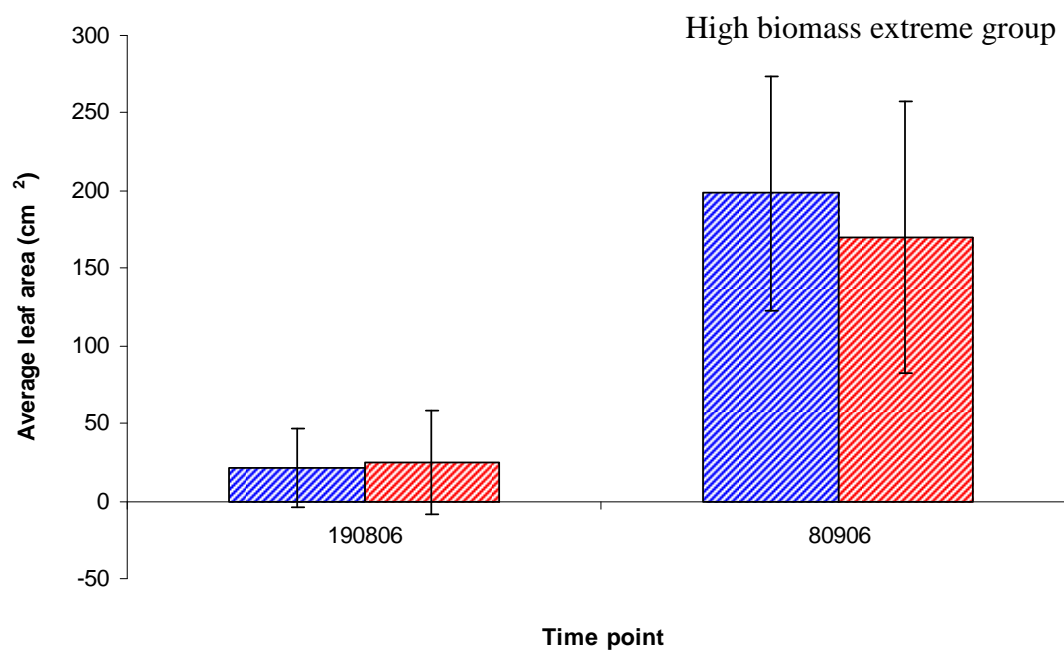


Date			
Genotype	180806	070906	
242	-0.01%	6.23%	
246	-4.61	4.34%	
Treatment	0.776 ns		
Genotype	0.000***		
Date	0.000***		
Treatment*Genotype	0.504 ns		
Treatment*Date	0.198 ns		
Genotype*Date	0.043*		
Treatment*Genotype*Date	0.528ns		

Figure 6.3.13. The average leaf shape index (length: width) of the two F₁ genotypes in ambient (blue) and elevated (red) [CO₂]. Genotype 242 is represented by striped bars and 246 by dotted bars. The numbers on the x-axis represent the date of sampling e.g. 180806 corresponds to 18th August 2006. The data here shows the data collected at the first (180806) and last (070906) time-points in the experiment. Standard error bars are shown. The averages percentage change in leaf shape index is provided in the

table beneath the graph. The results from a three-way ANOVA are provided at the bottom of the Figure (*= $p < 0.05$; ***= $p < 0.001$; ns= not significant).

The low biomass (F_2) genotypes showed a greater stimulation in leaf area in [eCO₂] than the high biomass genotypes. Whilst there was no difference between treatments at the first time-point (190806), by the final sampling point (080906) leaf area was shown to be significantly different (Figure 6.3.14). This was not the case with the high biomass genotypes, where there was no significant difference in leaf area at the beginning or end of the growth period (Figure 6.3.14), reflecting an inability to respond to an increased carbon supply.



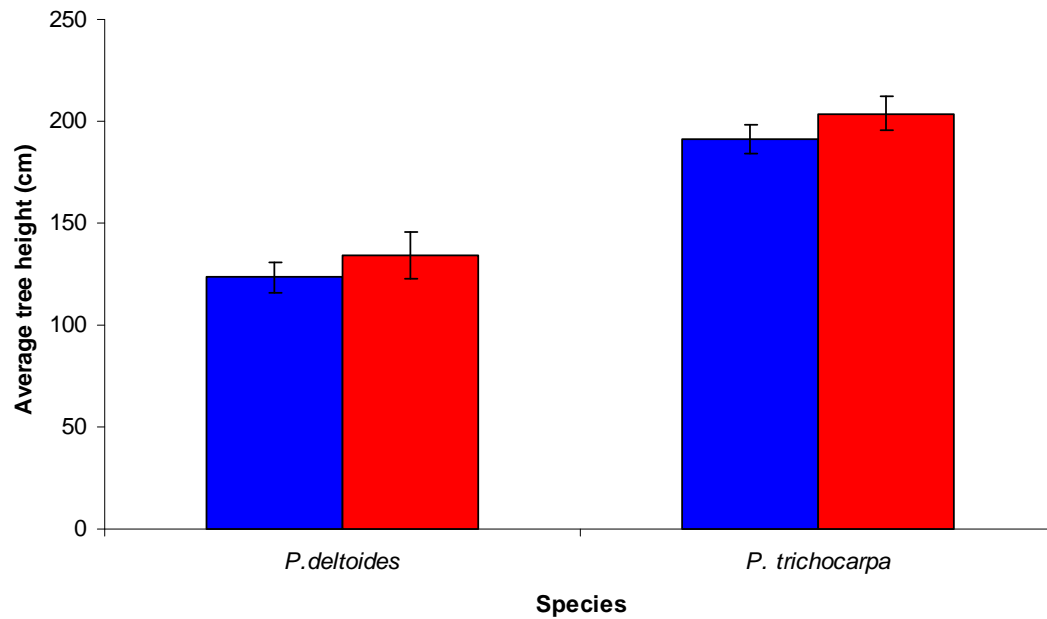
Treatment	0.132	ns
Group	0.000***	
Time-point	0.000***	
Treatment x Group	0.004**	
Treatment x Time-point	0.167	ns
Group x Time-point	0.000***	
Treatment x Group x Time-point	0.000***	

Figure 6.3.14. The average leaf area for the high-(top graph) and low-(bottom graph) biomass extreme genotypes. The red points correspond to the replicates grown in

[eCO₂] and the blue in [aCO₂]. The numbers on the x-axis represent the date of sampling e.g. 190806 corresponds to 19^h August 2006. The graph here shows the data collected at the first (190806) and last (080906) time-points in the experiment. Standard error bars are shown. The results of a three-way ANOVA are provided below the graph where group= 'high' or 'low' biomass, time-point= 190806 or 080906 and treatment= [aCO₂] or [eCO₂] (** p<0.01; ***p<0.001; ns= not significant).

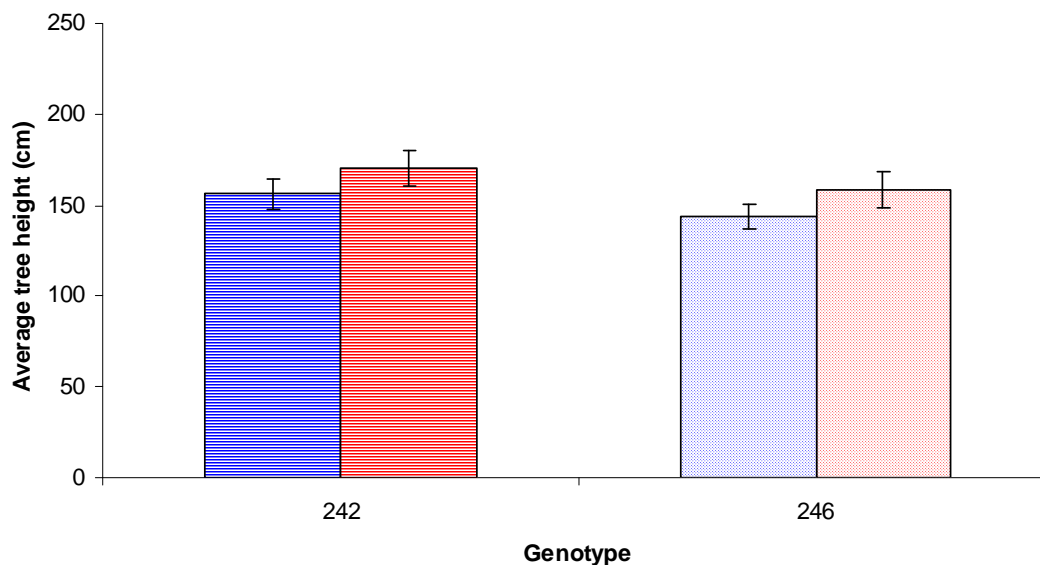
6.3.4 Temporal growth in all genotypes

Concomitant with the spatial and temporal profiles that were monitored in this experiment, a number of general growth parameters were also measured. Average tree height was measured for every individual in the experiment on 30th August 2006 (excluding the individuals that had been used in the spatial study whereby the shoot apical meristem had been removed). There was no statistical difference in tree height as a result of CO₂ exposure in *P. deltooides*, *P. trichocarpa* (Figure 6.3.15) or the F₁ genotypes (Figure 6.3.16).



Treatment	0.205	ns
Genotype	0.000	***
Treatment x Genotype	0.945	ns

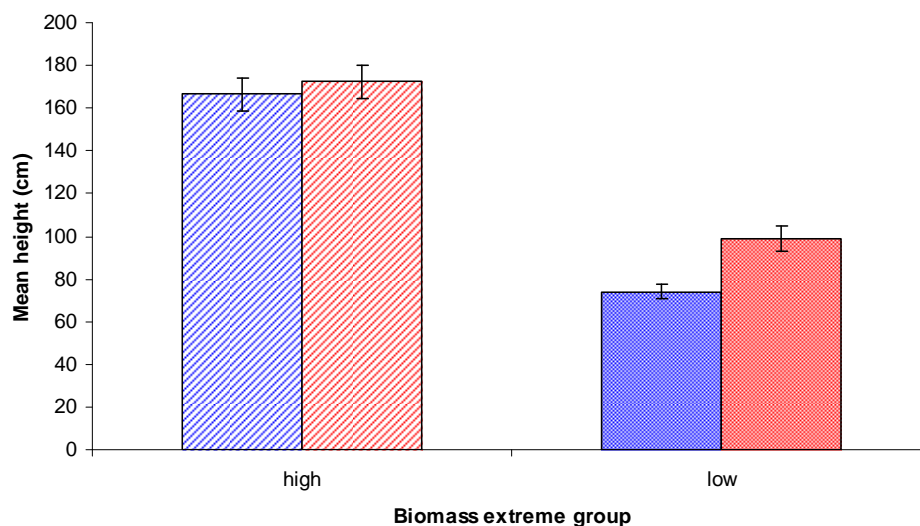
Figure 6.3.15. The average height of *P. deltooides* and *P. trichocarpa* on 30th August 2006. The blue bars represent the individuals that were exposed to [aCO₂] and the red bars represent those exposed to [eCO₂]. The standard error bars are shown. The results of a two-way ANOVA are provided beneath the graph (***p<0.001; ns= not significant).



Treatment	0.134	ns
Genotype	0.197	ns
Treatment x Genotype	0.988	ns

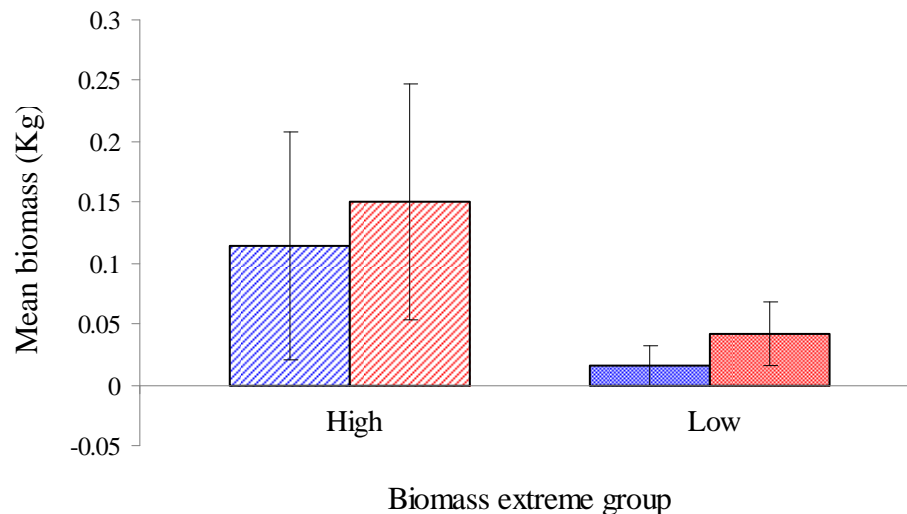
Figure 6.3.16. The average heights of the two F₁ genotypes on 30th August 2006. The blue colour represents the individuals that were grown in [aCO₂] and the red represent those grown in [eCO₂]. The striped bars indicate genotype 242 and the dotted bars represent genotype 246. The standard error bars are shown. The results of a two-way ANOVA are provided beneath the graph (ns= not significant).

Average tree height was stimulated as a result of CO₂ exposure in the F₂ biomass extremes ($F_{1,199} = 4.46$, $p < 0.05$) (Figure 6.3.17). The low biomass extremes responded to treatment to a greater degree than the high biomass genotypes in terms of height (Figure 6.3.17), final biomass (Figure 6.3.18) and stem diameter (Figure 6.3.19). Of the low biomass extreme group, genotype '1851' responded most to treatment in terms of biomass, stem diameter and height (data not shown).



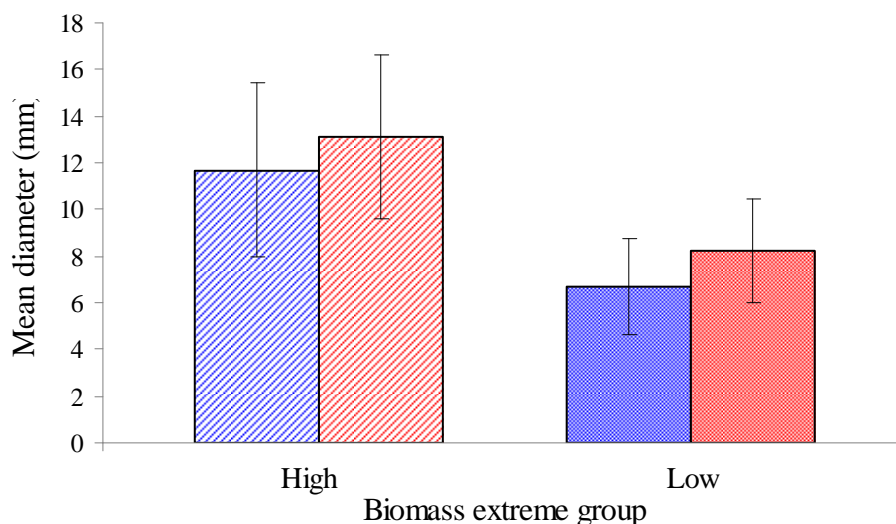
Treatment	0.036 *
Group	0.000***
Treatment x Group	0.117 ns

Figure 6.3.17. The average heights of the two groups of biomass extremes on 30th August 2006. The blue colour represent the individuals that were grown in [aCO₂] and the red represent those grown in [eCO₂]. The dotted bars indicate the low biomass genotypes and the striped bars represent the high biomass genotypes. The standard error bars are shown. The results of a two-way ANOVA are shown below the graph (*p<0.05; ***p<0.001; ns= not significant).



Treatment	0.028*
Group	0.000***
Treatment x Group	0.969 ns

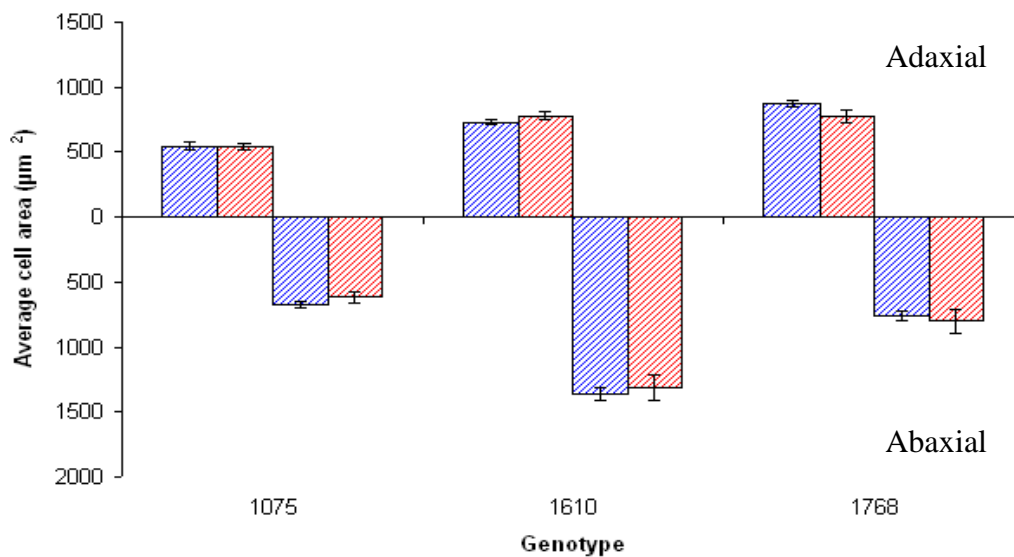
Figure 6.3.18. The average biomass of the two groups of F₂ extreme genotypes on 30th August 2006. The blue colour represent the individuals that were grown in [aCO₂] and the red represent those grown in [eCO₂]. The hatched bars indicate the low biomass genotypes and the striped bars represent the high biomass genotypes. The standard error bars are shown. The results of a two-way ANOVA are shown below the graph (*p<0.05; ***p<0.001; ns= not significant).



Treatment	0.007**
Group	0.000***
Treatment x Group	0.692 ns

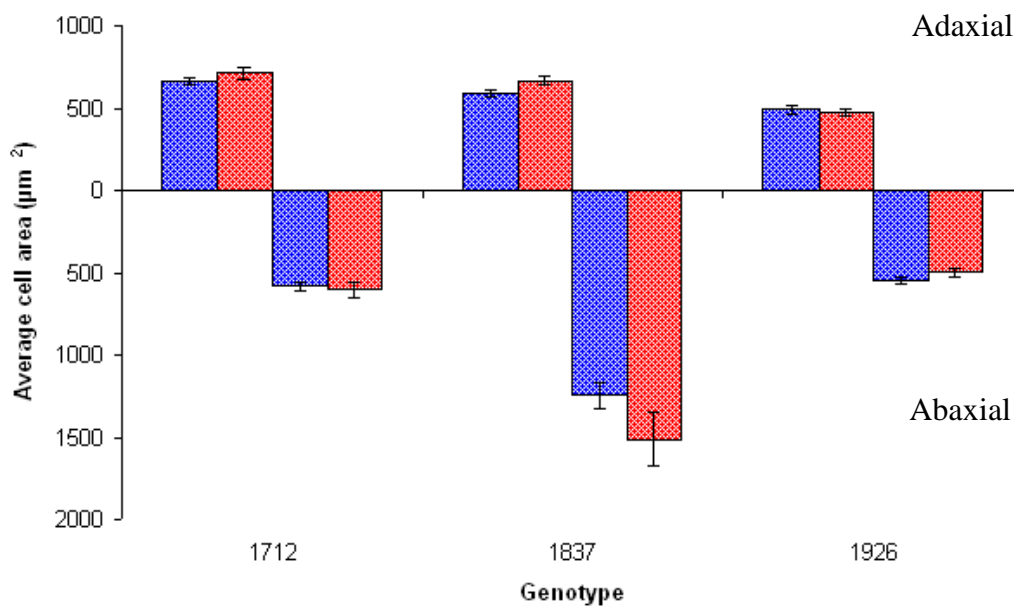
Figure 6.3.19. The average stem diameter of the two groups of biomass extremes on 30th August 2006. The blue colour represents the individuals that were grown in [aCO₂] and the red represent those grown in [eCO₂]. The hatched bars indicate the low biomass genotypes and the striped bars represent the large biomass genotypes. The standard error bars are shown. The results of a two-way ANOVA are shown below the graph (**p<0.01; ***p<0.001; ns= not significant).

CO₂ significantly affected cell area in the low biomass genotypes (Figure 6.3.21) but not the high biomass genotypes (Figure 6.3.20). This provides further evidence that the high biomass genotypes were unresponsive (in terms of overall growth) to the increased carbon availability. It is likely that the more productive high biomass genotypes were unable to assimilate any further carbon for growth, whilst the less productive low biomass genotypes did have the capacity to respond, which would explain the results observed.



Treatment	0.431 ns
Genotype	0.000***
Surface	0.000***
Treatment x Genotype	0.833 ns
Treatment x Surface	0.937 ns
Genotype x Surface	0.000***
Treatment x Genotype x Surface	0.205 ns

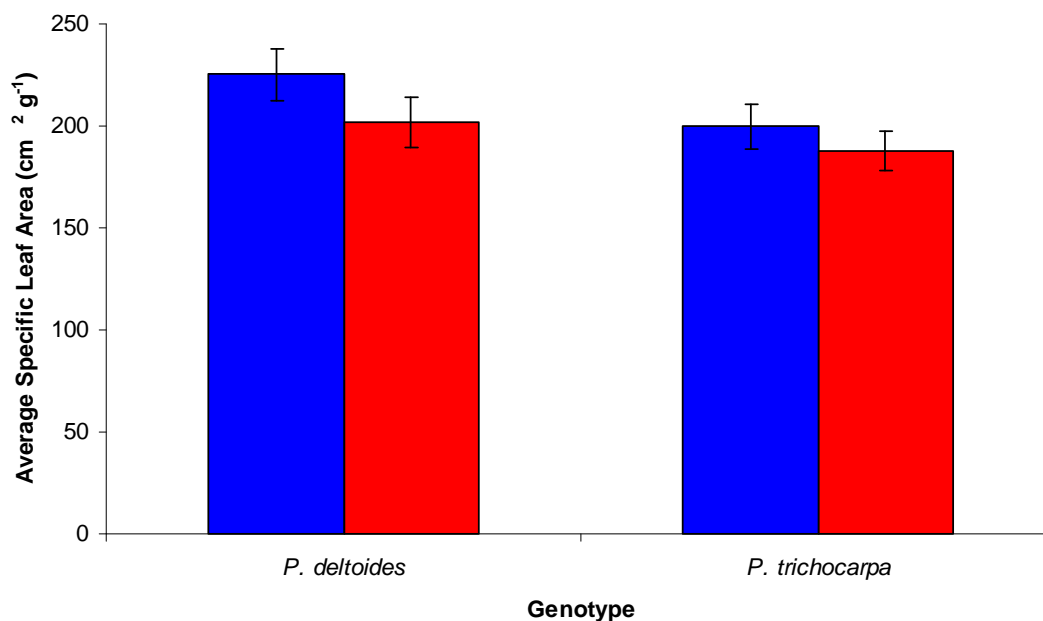
Figure 6.3.20. The average abaxial and adaxial cell areas of the high biomass genotypes exposed to either ambient (blue bars) or elevated [CO₂] (red bars). The standard error bars are shown on the graph. The results of a three-way ANOVA are shown below the graph (***p.0.001; ns= not significant).



Treatment	0.042*
Genotype	0.000***
Surface	0.000***
Treatment x Genotype	0.014*
Treatment x Surface	0.437 ns
Genotype x Surface	0.000***
Treatment x Genotype x Surface	0.194 ns

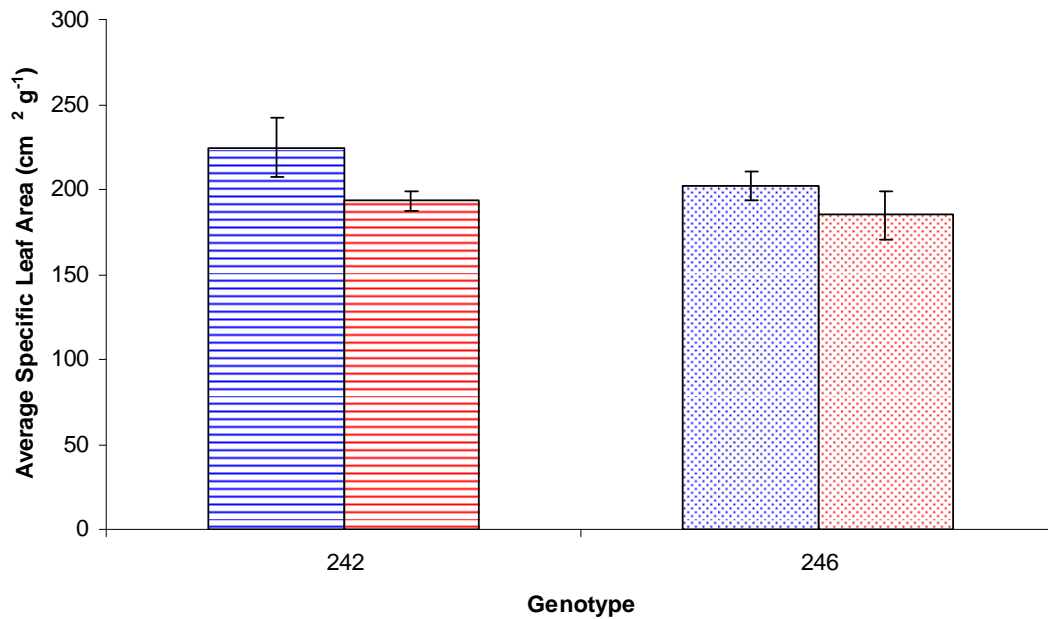
Figure 6.3.21. The average abaxial and adaxial cell areas of the low biomass genotypes exposed to either ambient (blue bars) or elevated [CO₂] (red bars). The standard error bars are shown on the graph. The results of a three-way ANOVA are shown below the graph (*p<0.05; ***p.0.001; ns= not significant).

The specific leaf area was measured in mature leaves (97 DAP/50 DFE). There was a general reduction in SLA in the mature leaves of both *P. deltoides* and *P. trichocarpa* (Figure 6.3.22), as well as the F₁ (Figure 6.3.23) and F₂ genotypes (Figure 6.3.24) although this was not statistically significant.



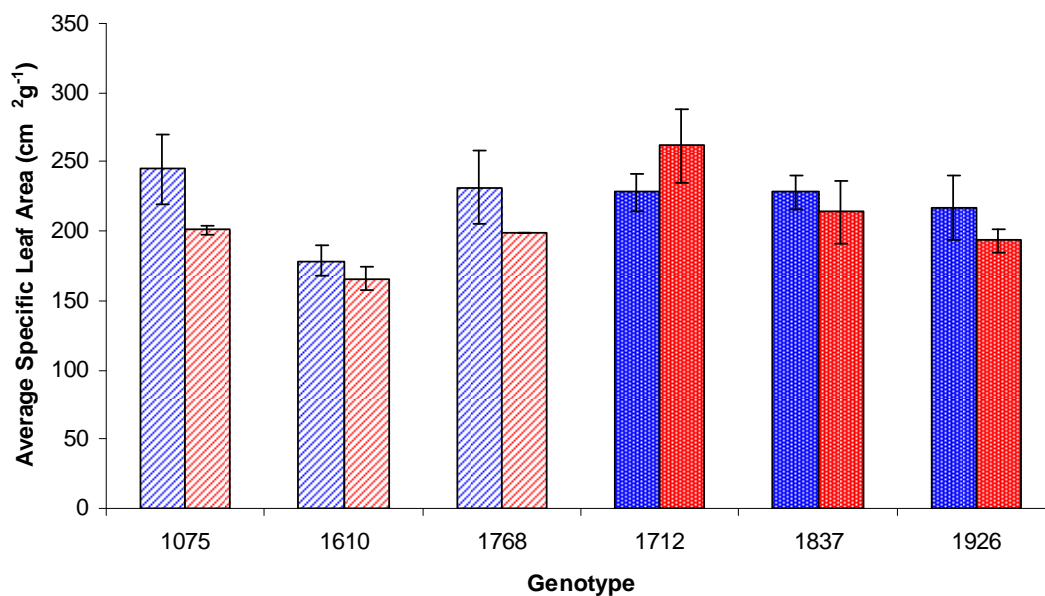
Treatment	0.129	ns
Genotype	0.094	ns
Treatment x Genotype	0.628	ns

Figure 6.3.22. The average specific leaf area for *P. deltoides* and *P. trichocarpa* exposed to ambient (blue) and elevated (red) [CO₂]. The standard errors are shown on the graphs. The results of a two-way ANOVA are shown below the graph (ns= not significant).



Treatment	0.061	ns
Genotype	0.271	ns
Treatment x Genotype	0.581	ns

Figure 6.3.23. The average specific leaf area of the two F_1 genotypes. The blue colour represents the individuals that were grown in $[aCO_2]$ and the red represent those grown in $[eCO_2]$. The striped bars represent genotype 242 and the dotted bars represent 246. The standard error bars are shown. The results of a two-way ANOVA are shown below the graph (ns= not significant).



Treatment	0.174	ns
Group	0.112	ns
Treatment x Group	0.211	ns

Figure 6.3.24. The average specific leaf area of the biomass extreme genotypes. The hatched colour represents the low biomass genotypes and the striped bars represent the high biomass genotypes. The bars coloured in blue represent the individuals grown in [aCO₂] and the red represent those grown in [eCO₂]. The standard error bars are shown. The results of a two-way ANOVA are shown below the graph (ns= not significant).

6.4 Discussion

This study has provided further insight into the response of two phenotypically distinct species to [eCO₂] predicted for the year 2050. Furthermore, ‘extreme’ genotypes were selected from a pedigree *Populus* mapping population in order to focus on characterising the growth of high- and low-yielding genotypes in response to this stimulus. The results of this second part of the investigation have widened the scope for further studies in this area.

6.4.1 Leaf growth of *P. deltoides* and *P. trichocarpa* in [eCO₂]

There have been several reviews published in the literature regarding plant growth responses to [eCO₂] exposure (e.g. see Ainsworth *et al*, 2005; Drake *et al*, 1997; Norby *et al*, 1999; Pritchard *et al*, 1999). In trees, it can generally be deduced that growth is stimulated by [eCO₂]. This does however depend upon the species under investigation, the age of the tree (Körner, 2006) as well as the particular environmental constraints and/or experimental strategies (Taylor *et al*, 2001).

Here, the results from the growth analyses (both spatial and temporal) were indicative of a subtle stimulation in some aspects of plant development as a result of exposure to [eCO₂]. In terms of leaf area, growth was stimulated in young leaves of *P. deltoides* (Table 6.3.1, Figure 6.3.1). Over time, this stimulation diminished (Figure 6.3.9). In *P. trichocarpa*, the response to [eCO₂] was less clear, but generally stimulated over time (Figure 6.3.9). This reflected a difference in the capacity of the two species to respond to [eCO₂] i.e. the leaves of *P. deltoides* were highly responsive to treatment only during the juvenile stage of development whilst all ages of *P. trichocarpa* responded positively to [eCO₂]. However, in *P. trichocarpa* the magnitude of the response was less pronounced.

6.4.2 Cellular characteristics of *P. deltoides* and *P. trichocarpa* in [eCO₂]

The leaves of *P. deltoides* consist of numerous small cells, which is achieved by frequent rounds of cell division. At an equivalent stage of development in *P. trichocarpa* however, leaves consist of fewer larger cells, due to cell expansion (see Chapter 3). Exposure to [eCO₂] caused stimulation in adaxial and abaxial epidermal cell area in *P. deltoides*, which also corresponded to an increase in leaf area in [eCO₂]

for each age category. This therefore suggests that [eCO₂] caused increased cell expansion rather than cell division (Gardner *et al*, 1995).

In *P. trichocarpa* there was no stimulatory effect of CO₂ on cell size. It is possible that under ambient conditions, the cells of *P. trichocarpa* had reached their maximal size. If indeed [eCO₂] caused an increase in cell expansion, as is suggested by the results for *P. deltoides*, then it is likely that the cells of *P. trichocarpa* were unable to expand further, even with an additional supply of carbon. However, previous studies have shown that the contribution of cell expansion to a change in leaf size as a result of growth in [eCO₂] depends on the stage of leaf development, since cell production has been shown to be more important in older leaves (Taylor *et al*, 2003).

Cell expansion is a process that may occur by vacuolation, or by increased cytoplasmic mass and endoreduplication (Sugimoto-Shirasu and Roberts, 2003). Endoreduplication is known to affect cell size and growth rates in *Poa annua* (Mowforth and Grime, 1989). However, no information is currently available regarding the ploidy levels in these two species of *Populus* but this could be an important consideration for further work.

6.4.3 Leaf anatomy of *P. deltoides* and *P. trichocarpa*

The large interspecific variation in response to [eCO₂] with regards to cell size, suggests that *P. deltoides* exhibits a greater degree of plasticity than *P. trichocarpa*, thereby allowing it to respond to the increased carbon availability. Given the large stimulation in epidermal cell size, it is rather surprising that *P. deltoides* exhibited no change in leaf anatomy. For example, in *Triticum aestivum* there was an increase in intercellular airspaces and an extra cell layer following exposure to [eCO₂] (Masle, 2000). However, there have been other reports in monocotyledonous plants whereby cell expansion (and chloroplast expansion) was affected by [eCO₂], but there was no overall change in leaf anatomy (Robertson and Leech 1995). With the increase in leaf area producing a larger surface area for gas exchange, perhaps any alterations in anatomy along the dorso-ventral axis is unnecessary.

6.4.4 Stomatal characteristics

Stomatal density is particularly sensitive to atmospheric conditions, and has been used to estimate [CO₂] from millions of years ago (Royer, 2001; McElwain and Chaloner, 1995; McElwain *et al.*, 1999). In this experiment, CO₂ enrichment had no statistically significant effect on stomatal density in the abaxial or adaxial surface of *P. trichocarpa* (Table 6.3.3) as has been reported previously in *Populus* genotypes (Radoglou and Jarvis, 1990b) and pine (Luomala *et al.*, 2005). Stomatal patterning and density are established at an early stage of leaf development (e.g. Nadeau and Sack, 2002) and it can be concluded from these results that CO₂ had no effect on stomatal initiation in this species. However, the results presented here again suggest that this response was species specific, since *P. deltoides* did respond to [eCO₂], with a general reduction in stomatal density.

Stomatal numbers (measured as density and index) vary significantly with age (Ceulemans *et al.*, 1995; Taylor *et al.*, 2003; Tricker *et al.*, 2005). *Populus deltoides* has a characteristic amphistomatous nature (i.e. stomata found on both leaf surfaces) whilst *P. trichocarpa* is hypostomatous (stomata on a single surface). There was a general reduction in stomatal density on both the abaxial and adaxial leaf surfaces of *P. deltoides*. This differs from previous reports whereby CO₂ enrichment has affected adaxial and abaxial leaf surfaces differently (Driscoll *et al.*, 2006).

The reduction in stomatal density in *P. deltoides* grown in [eCO₂] coincides with previous reports suggesting reduced stomatal density is correlated with increased atmospheric [CO₂]. For example, Woodward (1987) reported a reduction in stomatal density (40% averaged across 8 woody species) in the last 200 years but an increase in [CO₂] of 25%. A reduction in stomatal density implies that the plants are reducing the number of avenues through which they acquire CO₂, thus having the added advantage of reducing water loss. Indeed increased water use efficiency in plants grown in [eCO₂] has been reported in *Helianthus annuus* (Dafeng *et al.*, 2001) *Phaseolus vulgaris* (Radoglou *et al.*, 1992), and *Populus deltoides* (Murthy *et al.*, 2005). Furthermore, stomatal conductance has commonly been reported to decline in conditions of [eCO₂] (Medlyn *et al.*, 2001; Tricker *et al.*, 2004) and in *P. x euramericana*, stomatal aperture was responsible for determining leaf water loss under FACE conditions, rather than stomatal number (Tricker *et al.*, 2005).

The reduction in stomatal density in *P. deltoides* could simply be a consequence of increased cell expansion in [eCO₂], although stomatal index, which takes into account the ratio between the number of stomata and the number of epidermal cells, has also been reported to reduce in [eCO₂] in the first year of growth (Tricker *et al*, 2004).

The absolute stomatal number and inherent ability to respond to changes in the local environment has been recognized as the influence of an internal signal (Lake *et al*, 2002; Woodward, 2002) conveyed from mature leaves to young leaves (Lake *et al*, 2001). In Poplar, the mechanism is yet to be elucidated but in *Arabidopsis* the *HIGH IN CO₂ (HIC)* gene is involved in determining stomatal number (Gray *et al*, 2000). Unfortunately no information is currently available regarding the existence of a *HIC* gene (or a homologue) in *Populus*.

6.4.5 Nutrition

The availability of nitrogen (N) in the soil affects plant growth. Low N is associated with a decline in photosynthesis (Nie *et al*, 1995; Geiger *et al*, 2001), although this has been disputed due to the dilution of N associated with accelerated plant growth in [eCO₂] (Farage *et al*, 1998). Photosynthetic acclimation to [eCO₂] does not occur when the nitrogen supply is adequate (Stitt and Krapp, 1999; Farage *et al*, 1998).

Studies in potato (*Solanum tuberosum*) have shown that leaf area is reduced when the nitrogen (N) supply is limited, thus maintaining the [N] and photosynthetic capacity per unit leaf area (Vos and van der Putten, 1998). The reduction in leaf area associated with limited [N] is due to reduced rate of leaf expansion rather than to reduced duration of expansion, implying an effect of N supply on the cell cycle (Walter *et al*, 2003). Studies in maize (*Zea mays*) have identified an alternative strategy to coping with altered N supply (Vos *et al*, 2005). In this case, maize maintains its leaf growth strategy but this is associated with a concomitant reduction in leaf nitrogen concentration and ultimately reduced radiation use efficiency (RUE) (Vos *et al*, 2005).

Nitrogen availability affects plant responses to [eCO₂] (Geiger *et al*, 1999). Generally, above-ground plant growth in [eCO₂] is stimulated only when accompanied by a

concomitant non-deficient supply of N (e.g. Curtis and Wang, 1998). For example, Curtis *et al.*, (1995) have shown that an increase in total leaf area in [eCO₂] is dependent upon N availability. Furthermore, the stimulation in biomass in *Populus* grown in FACE was found only the high N treatment (Liberloo *et al.*, 2004). However, there are some reports whereby N fertilisation treatment has caused an increase in leaf nitrogen content, but with no effect of treatment (Calfapietra *et al.*, 2005).

Theoretically, it is possible that the commonly reported enhanced root growth in [eCO₂] (e.g. Lukac *et al.*, 2003) could result in increased N uptake from the soil. However, there is no evidence for altered N uptake in roots during [eCO₂] exposure (Stulen and den Hertog, 1993).

In this experiment, a supply of nutrients was provided when the cuttings were first planted in the chambers, but there was no subsequent addition. It is likely that the depletion of nutrients affected the growth response to [eCO₂], and if nutrients had been supplied on a regular basis, perhaps a greater stimulation in growth would have occurred.

6.4.6 CO₂ receptors

What determines the response to [eCO₂]? In plants, it is known that [eCO₂] is sensed by guard cells (reviewed in Vavasseur and Raghavendra, (2005)), and that environmental signals such as light intensity and hormone levels control stomatal aperture. For example, blue light stimulates stomatal opening (Talbot *et al.*, 2006), and ABA controls the aperture of the stomatal pore through its influence on membrane trafficking, ion channels and the cytoskeleton (Hetherington *et al.*, 2001). However, no CO₂ receptor has as yet been identified and until such a time as this occurs it is only possible to speculate as to the mechanisms involved in the response.

Despite the fact that the mechanisms involved in recognising CO₂ are yet to be elucidated, components that act to transfer the signal to the plant are beginning to be uncovered. For example, the *HIC* gene has been identified in *Arabidopsis* (Gray *et al.*, 2000). Reducing the expression of *HIC* causes an increase in stomatal density and index (a measure of the number of stomata compared to the number of epidermal cells) in young expanding leaves when mature leaves are exposed to [eCO₂]. This

suggests that during ontogeny, young leaves depend on signals derived from mature leaves to dictate their developmental strategies.

Why is there a difference in growth response between the two species? Is it possible that CO₂ receptors are absent (or minimally expressed) in young leaf tissue and that they develop during maturity? Is it possible that this is the case with *P. deltoides*, the species that responds to a higher degree to [eCO₂] in young leaves, but whose growth stimulation diminishes with time? Is there an antagonistic mechanism in plants whereby CO₂ is detected and is followed by a signal transduction cascade but can only cause an effect if permitted by a cell cycle regulator that governs plant cell size? This may go some way to explaining interspecific differences in response to [eCO₂]. Only by the identification of a CO₂ receptor in plants may this theory be addressed.

6.4.7 Yield extreme genotypes

Tree height was unaffected by treatment in both the grandparental species (*P. deltoides* and *P. trichocarpa*) (Figure 6.3.15) and the two F₁ genotypes (Figure 6.3.16). However, height, biomass and stem diameter were all stimulated in [eCO₂] in the selected F₂ genotypes (Figures 6.3.17, Figure 6.3.18, Figure 6.3.19 respectively). Above-ground biomass has previously been reported to increase in [eCO₂] (Norby *et al*, 1999). Stem diameter is known to be correlated with biomass production in poplar (Rae *et al*, 2004) and stem diameter also increases in FACE (Ainsworth and Long, 2005). Leaf area was also stimulated in the F₂ genotypes grown in [eCO₂]. The greatest stimulation in growth occurred in the low biomass extreme genotypes. It is likely that this is due to the incapacity of the high biomass genotypes to respond further to increased carbon availability.

In contrast to C₄ plants, C₃ species have the potential to respond to increased atmospheric carbon availability. C₄ plants have been shown to be less responsive to [eCO₂] in terms of photosynthesis (or the activity of the enzymes involved therein), biomass and yield (Leakey *et al*, 2006). The response of C₃ plants to carbon availability is likely to show intra-and interspecific species differences. In plants with a high sink strength (i.e. many expanding leaves) demand for photosynthate will be greater than plants with reduced sink strength (i.e. small leaves or few expanding

leaves). By this reasoning it is possible to imagine that the high biomass genotypes cannot respond to [eCO₂] simply because they lack the means and the capacity to do so. The increase in carbon availability in the high biomass genotypes will confer no advantage to growth. However, the smaller genotypes are likely to be able to respond since the increased sugar availability may be directed immediately into growth.

As mentioned previously, the proportion of expanded to expanding leaves affects carbon gain in [eCO₂] (Wait *et al.*, 1999). In [eCO₂] carbon gain is greater in expanding leaves but counteracted by reduced carbon gain in expanded leaves, which thus results in no change in biomass in [eCO₂] (Wait *et al.*, 1999). The possible differences in the ratio of expanded to expanding leaves in [eCO₂] and the differences between the two biomass genotypes may therefore explain this result.

The question still remains; which group has the greater capacity for C assimilation in future climates? In a relative comparison, low-yielding genotypes demonstrate a greater response to environmental change, whilst high-yielding genotypes consistently show greater absolute growth in both atmospheric environments. Therefore the benefit of relative versus absolute C assimilation in current and future atmospheric environments needs to be evaluated.

6.4.8 Source-sink regulation

The results presented in Chapter 3 provided the first insight into leaf growth in *P. deltoides* and *P. trichocarpa*. It was shown that leaf growth ceases at approximately age five in *P. trichocarpa* (Figure 3.3.2), but age eight in *P. deltoides* (Figure 3.3.1). This difference in maturation rate may partially explain the response of the two species to [eCO₂].

The results in Chapter 3 suggest that the leaves of *P. trichocarpa* mature faster than those of *P. deltoides*. This implies that a larger proportion of leaves are acting as sources as photosynthate in *P. trichocarpa*. If this is indeed the case, the reason that *P. trichocarpa* did not respond to [eCO₂] could be due to the fact that growth is completed at an earlier stage and further C availability is superfluous to requirements. In Figure 6.3.1 it was again clear that maximal leaf area was reached more quickly in *P. trichocarpa* than *P. deltoides*.

6.5 Conclusion

The results from this experiment have provided some ideas as to the effects of [eCO₂] on plant growth. However, the more intricate details of this story are yet to be unravelled. Of particular importance is to understand the differences in cellular dimensions in plants grown in [eCO₂], since this will ultimately affect the final size and function of the mature plant. What are the CO₂ receptors? What is responsible for the cellular differences between the two species in their response to [eCO₂]? Is the regulatory mechanism for the response linked to some endogenous factor governing cell size and hence organ and plant size? These questions still cannot be answered, although further research to identify any CO₂ receptors may begin to close the gaps in our knowledge.

The observed differences in response to [eCO₂] in the biomass extreme genotypes have also highlighted an important area of future research. Given the current interest in the potential of forest trees to mitigate the effects of increased atmospheric [CO₂], it is particularly interesting to note that genotypes categorised as low-yielding crops respond to a greater degree to increased carbon availability.

CHAPTER 7

The *Populus* transcriptome: a comparative analysis of meristematic tissues and young leaves exposed to [eCO₂] using two different microarray platforms

7.0 Overview

The experiment described in this chapter leads on from that described in Chapter 6, where the morphological responses of *Populus* to [eCO₂] (using a closed topped chamber system) were studied. From the same experimental design as described previously, gene expression studies were conducted on leaf samples collected from *P. deltoides* and *P. trichocarpa* grown under [aCO₂] and [eCO₂]. Both cDNA (POP2) and oligonucleotide microarrays (Affymetrix) were used in order to assess gene expression differences between these two divergent species. The results mirror those reported in Chapter 5, where there were few changes in gene expression as a result of [eCO₂].

This was the first time the phenotypic response to [eCO₂] (presented in Chapter 6) had been linked to its underlying genetic mechanisms through the use of microarrays in these two species.

7.1 Introduction

Microarrays are a useful genetic tool for studying global gene expression during plant development (Brinker *et al*, 2004). The application of microarray technology allows the relative expression levels of many genes to be determined simultaneously, with a high degree of sensitivity (Aharoni and Vorst, 2001).

Previous studies have attempted to identify differentially expressed transcripts as a result of plant growth in [eCO₂] using a range of species (e.g. Taylor *et al*, 2005; Gupta *et al*, 2005; Ainsworth *et al*, 2006; Miyazaki *et al*, 2004). In one particular study in *Populus*, transcripts involved in cell expansion were identified in leaf tissue (as has been shown previously, see Chapter 5), whilst in stem tissue, transcripts involved in lignin biosynthesis were up-regulated, but those involved in cell expansion were down-regulated (Druart *et al*, 2006).

In general, few transcripts with statistically significant differences in expression due to [eCO₂] have been identified in leaf tissue using microarrays. In the study by Druart *et al*, (2006) there were 95 CO₂-responsive transcripts in leaves, but almost three times as many were identified in stem tissue. In Taylor *et al*, (2005) the CO₂ effect was shown to be dependent upon developmental age, with only eight differentially expressed transcripts in young leaves and 31 in semi-mature tissue (Chapter 5 and appendix 1). In the case of FACE experiments, a small number of statistically significant differentially expressed transcripts has been attributed to possible post-translational modifications being responsible for the observed phenotypic differences associated with growth in [eCO₂] (Taylor *et al*, 2005), or due to the nature of the FACE system itself (Ainsworth *et al*, 2006).

Microarrays can be considered to be a 'closed system' (Primrose and Twyman, 2006) where only the probes that are deposited onto the arrays can be measured. The most appropriate microarray platform depends entirely upon the hypothesis in question. It may be that a global scan of the genome would be most appropriate to address the question. However, a more targeted selection of probes with a high degree of replication may be more appropriate for more focussed studies. Here, two different microarray platforms (cDNA and oligonucleotide) were used as a global screen to identify transcripts that may be responsive to [eCO₂].

The overall aim of the experiment was to link changes in growth and development following growth in [eCO₂] (presented in Chapter 6) with underlying gene expression data, using microarrays. In the first part of the experiment, cDNA microarrays (POP2 (Sterky *et al*, 2004)) were used to assess gene expression, as has been conducted previously for *P.x euramericana* (Chapter 5). However, in this case meristematic tissue and young leaves were used for the hybridisations. The meristematic tissue represented the youngest growing leaf material, still undergoing differentiation processes. This material was sampled for hybridisation in order to assess how CO₂ may affect growth at the initial stage of development, with the aim of identifying important candidate genes involved in these processes. In the second part of the experiment, young leaf samples were hybridised on the poplar Affymetrix (oligonucleotide) microarray platform. It was therefore possible to compare any differentially expressed transcripts in order to identify robust candidate genes involved in the CO₂ response.

This experiment was conducted in a single growing season in a closed topped chamber (CTC) experiment. The use of CTCs is particularly advantageous since they provide a controlled and homogeneous environment for plants to grow. However, they do have the disadvantage that they are deemed to be less representative of a ‘true’ biological system than, for example, FACE experiments. FACE systems are designed to be representative of an ecosystem, but they are also more likely to be subjected to strong environmental fluctuations when compared to more controlled conditions such as CTCs. Given our previous experience with measuring gene expression in trees grown in FACE (Chapter 5), it was thought that changes in gene expression as a result of growth in [CO₂] would be easier to identify without the intervening effects of environmental heterogeneity associated with FACE. There are no previous reports of gene expression studies conducted on *P. deltoides* and *P. trichocarpa*, grown in [eCO₂] using CTCs.

7.2 Materials and methods

The experimental design for the CTC study was as described in the materials and methods section in Chapter 6.

7.2.1 POP2 cDNA microarrays

On the 17th August 2006 (43 DFE), leaves from four biological replicates (for each species, per treatment) were sampled for transcriptomic analyses. These leaves represented a spatial profile (i.e. leaves 1-10 (where '1' represents the first fully unfurled leaf from the shoot meristem and '10' represents a mature leaf) and the meristematic tissue (the unfurled bud of leaves at the shoot meristem). Upon sampling, each leaf was picked and put into a pre-labelled foil bag and subsequently flash frozen in liquid nitrogen. The samples were transported on dry ice and stored at -80°C.

RNA was extracted from the meristematic tissue and leaf age two of *P. deltoides* and *P. trichocarpa* (sampled on the 17th August 2006). The RNA quality and quantity was assessed using the Nanodrop spectrophotometer and by running a 1% agarose gel. For the microarray design, one biological replicate grown in [aCO₂] was randomly paired with another biological replicate from the [eCO₂] treatment for each species. This is illustrated in Figure 7.2.1. The samples were hybridised onto the POP2 microarray according to the protocol in the materials and methods section in Chapter 2. The data were analysed using B-statistics.

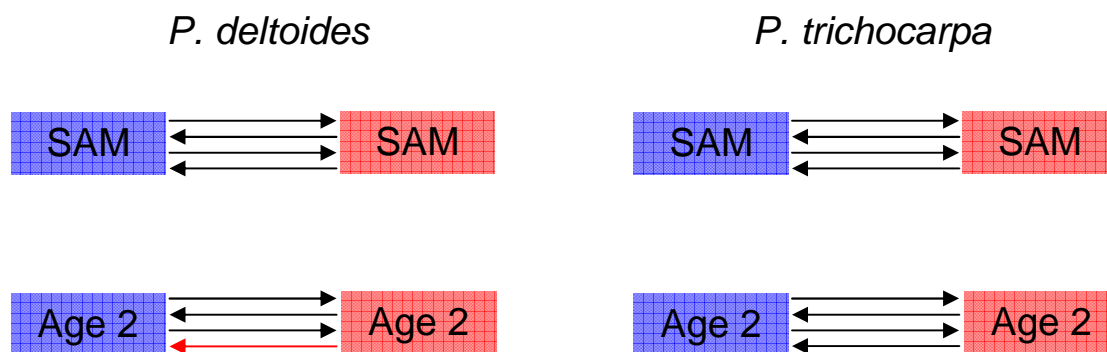


Figure 7.2.1. The design of the POP2 cDNA microarrays for the CTC experiment. The design of the arrays was the same for both *P. deltoides* and *P. trichocarpa*. Each arrow represents a single hybridisation. The blue boxes represent exposure to [aCO₂] and the red boxes represent exposure to [eCO₂]. The four individual biological replicates from each leaf age (SAM= meristematic tissue) and species were arbitrarily paired with a random biological replicate from the opposite treatment. The age groups for a single treatment group for a single species represent the same biological replicates since the RNA was extracted from the leaves that were part of the spatial growth profiles (see Chapter 6). The red arrow represents the single failed hybridisation which was subsequently removed from the analysis.

7.2.2 Affymetrix microarrays

A second set of leaves (the tagged leaves) were sampled on the 17th, 24th, 31st August and 7th September 2006 (43, 50, 57 and 64 DFE, respectively). These represented the leaves used to construct the temporal growth profile described in Chapter 6.

The samples collected on the 17th August 2006 (43 DFE) were used to assess gene expression using the Affymetrix oligonucleotide microarrays. These samples represented the youngest unfurled leaves. Total RNA was extracted (described in Chapter 2) from eight samples (two biological replicates from each of *P. deltoides* and *P. trichocarpa* exposed to either [aCO₂] or [eCO₂]). The RNA quantity and quality was assessed using the Nanodrop spectrophotometer, a 1% agarose gel and the Agilent Bioanalyser.

The samples were sent to the Nottingham Arabidopsis Stock Centre (NASC) Affymetrix service to be run on the Poplar Affymetrix chip (<http://affymetrix.Arabidopsis.info/>). The Poplar gene chip (25-mer) consists of

56,055 transcripts, including all UniGene clusters, ESTs and mRNAs, predicted gene transcripts, poplar controls and rRNAs.

Each biological replicate was hybridised on a single chip. Prior to hybridisation, the quality of RNA was again checked using an Agilent Bioanalyser to ensure the RNA had not degraded during transit. All hybridisations, scanning and analysis were completed by NASC. The results were provided in CD format in the form of .CEL files. The data on the .CEL files were normalised (RMA normalisation). The data was analysed with B-statistics using the affyGUI (Wettenhall *et al*, 2006) package in R (www.r-project.org). In Genespring, each slide from a single species and treatment was randomly paired with a second slide from the same species but different treatment in order to create an *in silico* dual channel analysis.

7.3 Results

7.3.1 cDNA microarrays

In total, 15 POP2 microarray hybridisations were successful. The single failed hybridisation represented a comparison of *P. deltoides* (age two, [aCO₂]: [eCO₂]). The results of the successful hybridisations are illustrated in Figure 7.3.1.

The results from the B-statistics are given in appendix 2. The cut-off value for this statistical analysis was a 'B-value' of 0 (thus representing a 50:50 chance of differential expression). In *P. trichocarpa*, there were just two ESTs in the meristematic tissue and only a single EST in the age two leaf tissues that met this criterion. However, in *P. deltoides*, there were 23 and 39 in the meristematic and age two leaf tissues, respectively. The ESTs representing *XYLOGLUCAN ENDOTRANSGLYCOSYLASE* were again (see Chapter 5) shown to be up-regulated in response to [eCO₂] (PU03171, PU20530 were both up-regulated in age two leaves of *P. deltoides*). The ESTs representing trypsin and protease inhibitors (PU30100, PU08678, PU08378, PU12876, PU29344, PU12387) were down-regulated in age two of *P. deltoides* (with the exception of PU12876 which was up-regulated). This represented a substantial proportion of the differentially expressed transcripts and suggests that protein turnover may have been affected in the young leaf tissue of *P. deltoides* as a result of increased carbon supply.

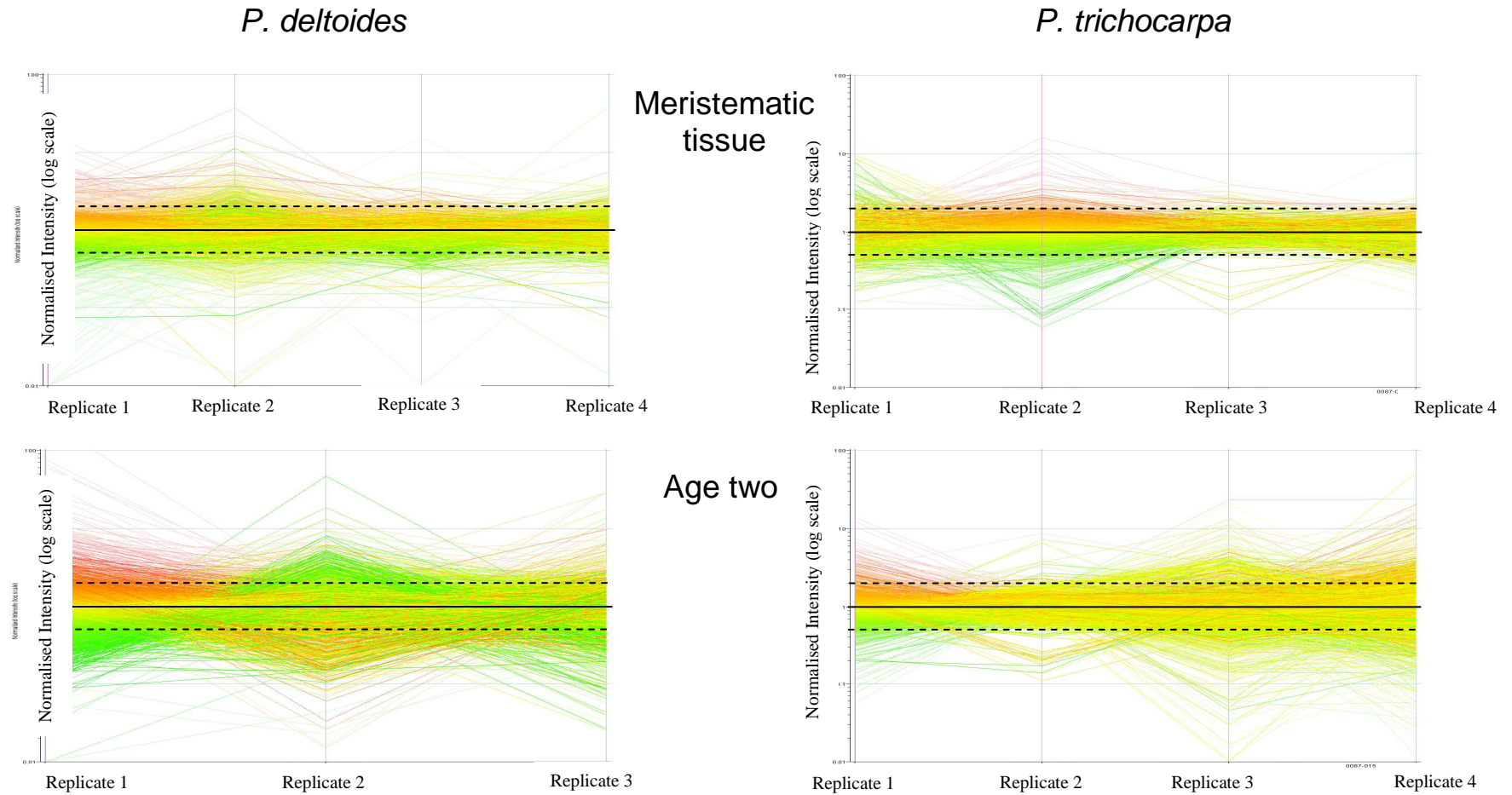


Figure 7.3.1. The results from Genespring analysis of the 15 successful hybridisations conducted on the meristematic tissue and leaf age two of *P. deltoides* and *P. trichocarpa* grown in [aCO₂] or [eCO₂]. Each line represents a single EST (expressed in at least 3/4 arrays, or in the case of *P. deltoides* age two, 3/3). Each vertical line represents a single array within the group. The solid horizontal line represents a 0 change in expression, whilst the dashed lines represent two-fold up-or down-regulation.

Further analysis was based on the fold-change of all ESTs that were present following microarray hybridisation, rather than filtered according to their statistical significance. The lack of statistical support for differential expression does limit the conclusions that may be drawn from the results, but this approach was simply used to investigate any expressional differences in [eCO₂].

7.3.1.1 Venn diagrams

In order to conduct some species and age comparisons in the microarray data, sets of Venn diagrams were constructed in Genespring (Figures 7.3.2 and 7.3.3 respectively). The Venn diagrams were constructed with the requirement that the EST must have been present in at least 3/4 of the arrays from that particular group (3/3 in the case of *P. deltoides*, age two). Reducing the stringency of the requirements (e.g. expression in 2/4 microarrays) would have generated a larger number of transcripts but also increased the risk of generating false positives by producing type I errors. Therefore using data that was consistent across three out of four microarrays was chosen as the appropriate level of stringency since the transcripts were present in 75% of the available data. Lists of the transcripts represented in each category are available in appendix 3.

Interestingly, there were very few CO₂-responsive genes. This is true of both *P. deltoides* and *P. trichocarpa*, in both the meristematic and the young leaf tissue. Furthermore there were few, if any, transcripts that were differentially regulated between the two comparative factors (represented in the middle light grey section of each Venn diagram), suggesting that any differences that could be attributed to [eCO₂] were not consistent across species (Figure 7.3.2) or age groups (Figure 7.3.3).

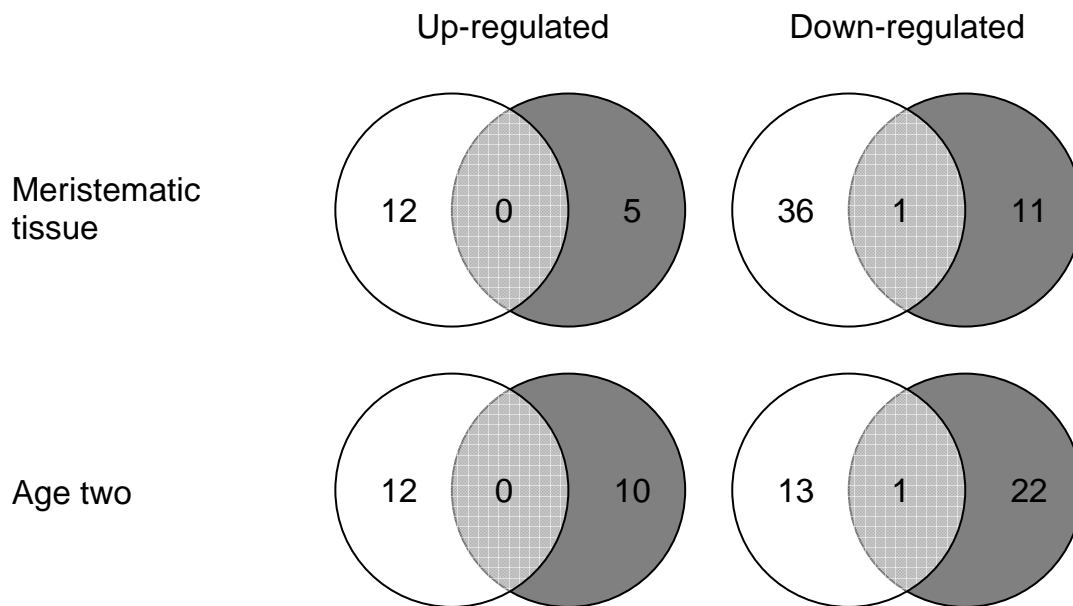


Figure 7.3.2. Venn diagrams illustrating the species comparisons made from the microarray data. The numbers in the white section represent ESTs in *P. deltoides* that were two-fold (or more) up-or down-regulated in three out of four microarrays. The numbers in the dark grey section illustrate the ESTs in *P. trichocarpa* that were two-fold (or more) up-or down-regulated in three out of four arrays. The numbers in light grey represent the ESTs that were commonly up-or down-regulated in *P. deltoides* and *P. trichocarpa*.

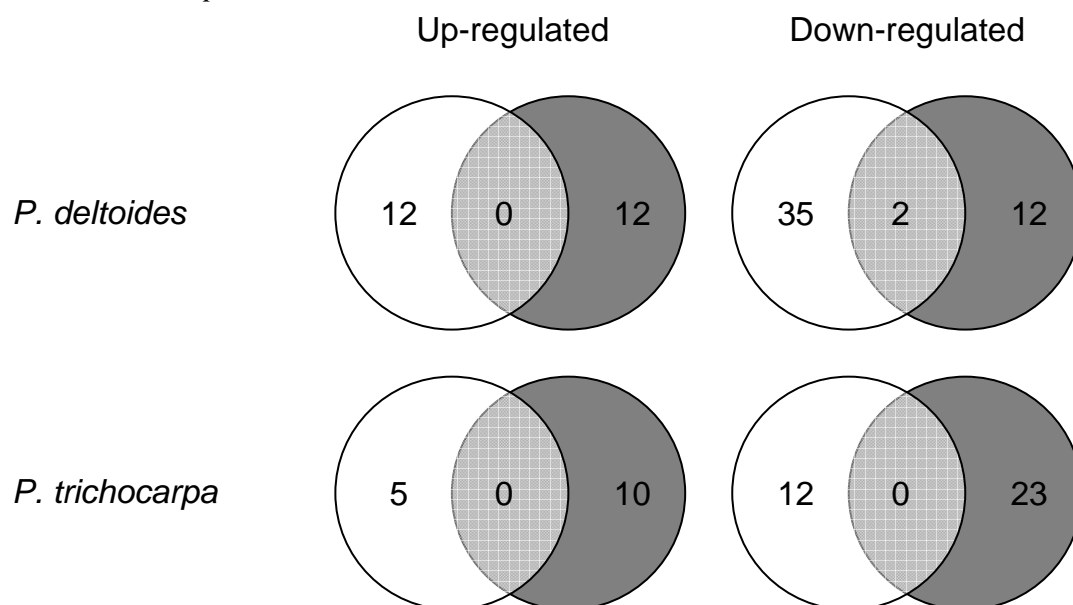
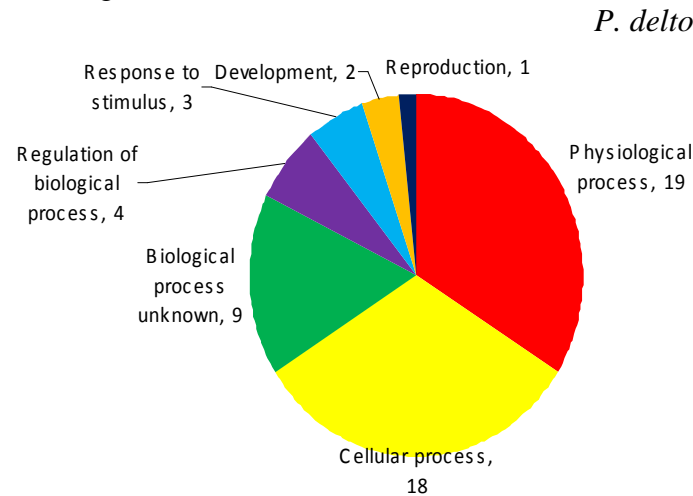


Figure 7.3.3. Venn diagrams illustrating the age comparisons made from the microarray data. The numbers in the white section represent ESTs in the meristematic tissue that were two-fold (or more) up-or down-regulated in three out of four microarrays. The numbers in the dark grey section illustrate the ESTs in leaf age two that were two-fold (or more) up-or down-regulated in three out of four microarrays. The numbers in light grey represent the ESTs that were commonly up-or down-regulated in both the meristematic tissue and age two leaves.

7.3.1.2 Gene Ontologies

The GO information was used to elucidate the functions of the differentially expressed transcripts identified in from the microarrays. The data from the two-fold (up-and down-regulated) list was used to construct the GO classification pie charts in Genespring (Figures 7.3.4 and 7.3.5). The results suggest some small differences in the functions of the genes that were differentially regulated in response to [eCO₂] in both species and age groups. For example, in age two, *P. trichocarpa* transcribed more genes involved in growth and development than either the meristematic tissue of that species or indeed of *P. deltoides*, where developmental transcripts are down-regulated in the young (age two) leaves.

Down-regulated



Up-regulated

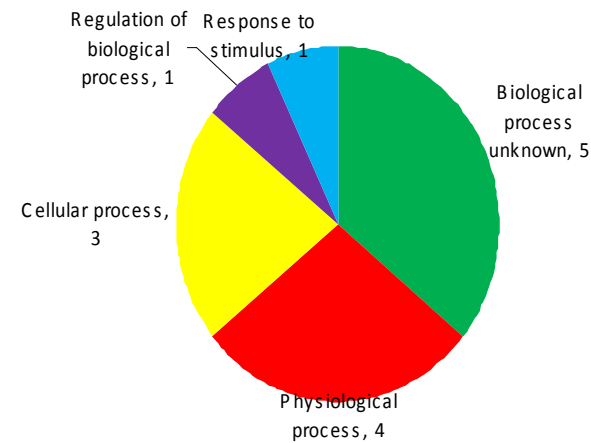
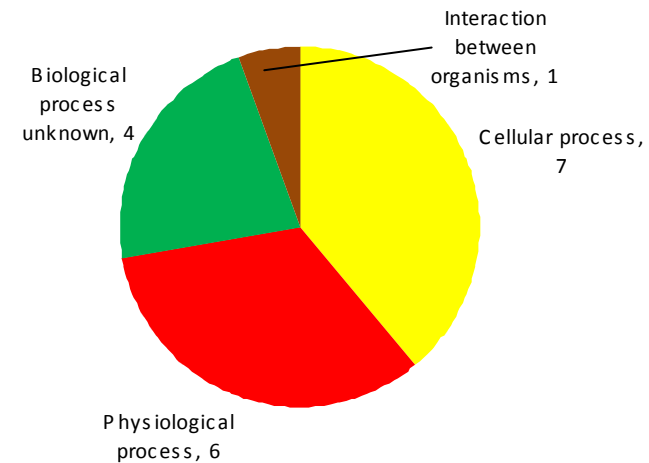
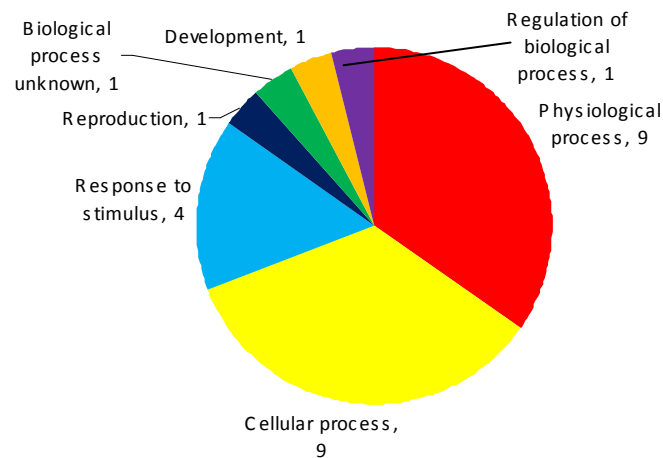
*P. deltoides*, age two leaves

Figure 7.3.4. The Gene Ontology information was constructed using Genespring for *P. deltoides* in both age groups. The requirements for inclusion in the pie chart was that the EST was two-fold up-or down-regulated in at least three of the available four microarrays that were conducted for each species/ age comparison (3/3 in the case of *P. deltoides*, age two). Each segment shows the GO category, along with the number of ESTs that represent that segment.

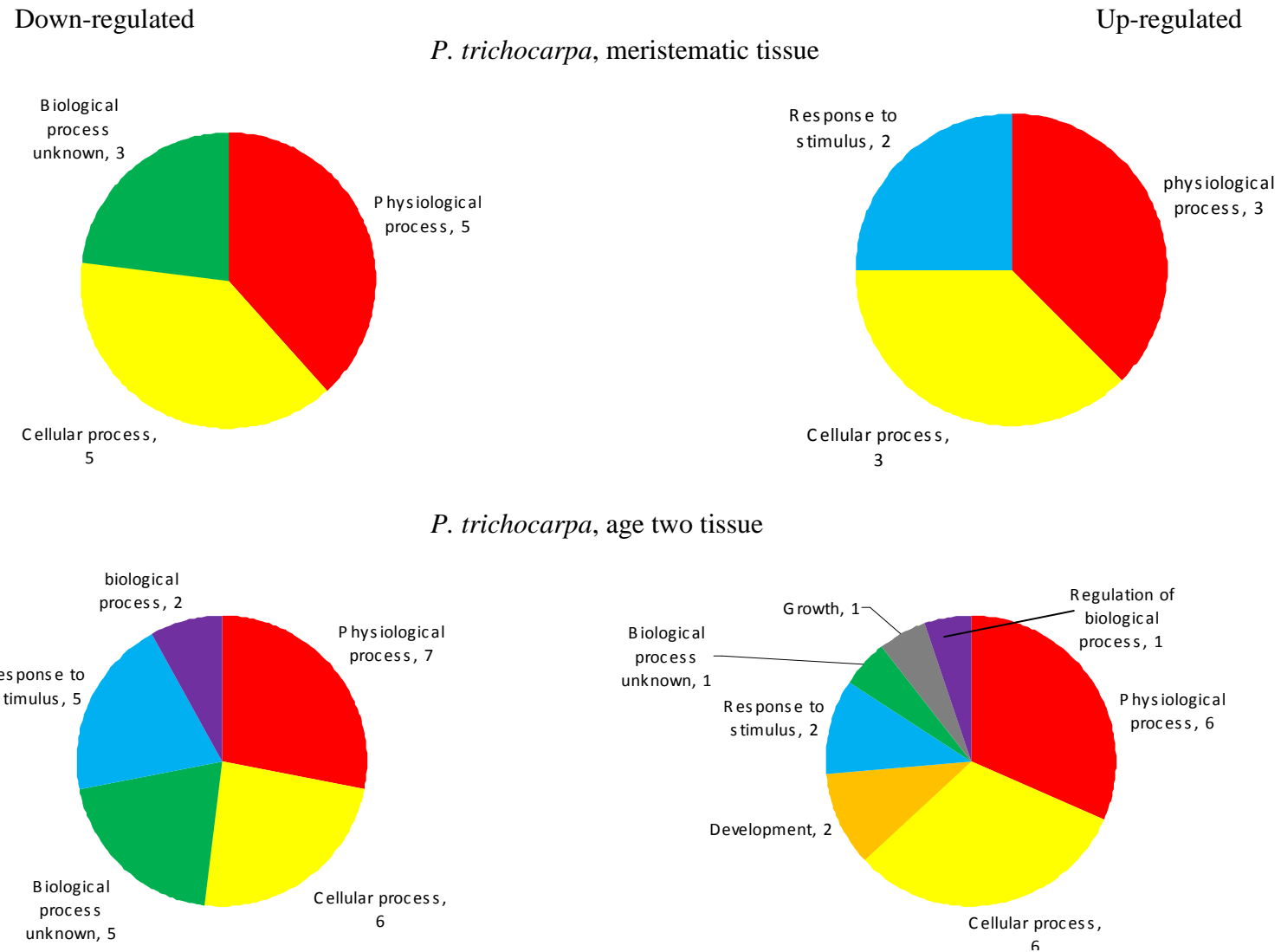


Figure 7.3.5. The Gene Ontology information was constructed using Genespring for *P. trichocarpa* in both age groups. The requirements for inclusion in the pie chart were that the EST was two-fold up-or down-regulated in at least three of the available four microarrays that were conducted for each species/ age comparison. Each segment shows the GO category, along with the number of ESTs that represent that segment.

7.3.1.3 Pathway analysis

The results from the GO analysis proved useful in providing a general overview of the classifications of the transcripts that were two-fold (or more) differentially expressed in the microarray experiment. To provide further information into the specific pathways that may have been affected by treatment, the AraCyc pathway tool (Mueller *et al*, 2003) was used (<http://www.arabidopsis.org>). Here, the average results for the entire data set for each species-age category comparison (e.g. *P. deltoides*, meristematic tissue) was imported into the software, which painted the results onto a metabolic pathway map. This proved to be valuable in providing a global view of pathways that may be affected by [eCO₂] exposure, allowing further exploration into the responses of the individual transcripts involved in the pathway in the particular species and age group being investigated.

One such investigation highlighted a portion of the Calvin Cycle as being up-regulated in the meristematic tissue of *P. deltoides* (Figure 7.3.6). Hence, all of the transcripts present on the cDNA microarray involved in the Calvin Cycle were identified and cross-referenced against the results of the microarray data (Figure 7.3.7). However, upon closer inspection of the ESTs involved in the Calvin Cycle, the results suggested that there was a general down-regulation in expression levels, thus highlighting the variable nature of the results.

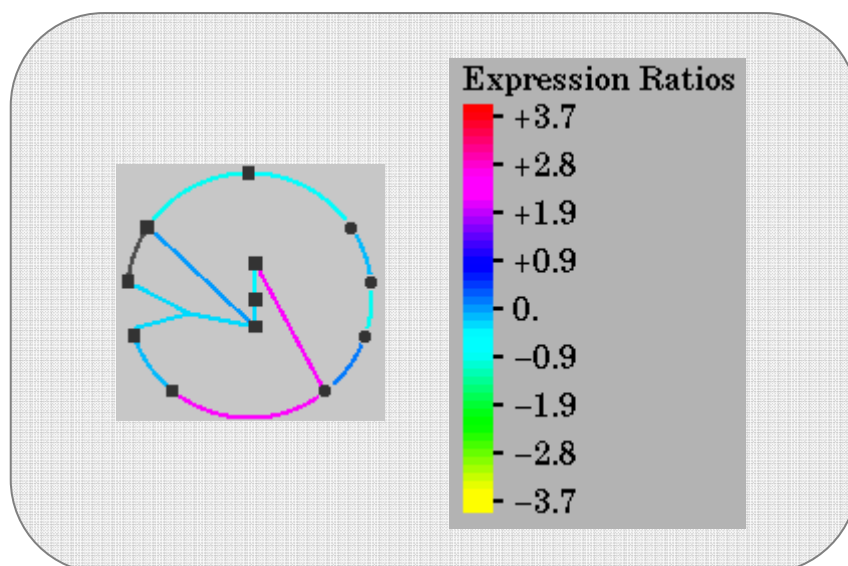


Figure 7.3.6. The metabolic pathway tool ‘Aracyc’ was used to identify any pathways that may have been affected by [eCO₂] in the microarray analysis. The diagram illustrates a portion of the results from *P. deltoides* (meristematic tissue), which was directly cut from the Aracyc software output. The segment on the left of the diagram represents the Aracyc display for the Calvin Cycle, with the results from the meristematic tissue of *P. deltoides* painted directly onto the map, according to the expression levels on the right of the diagram. Each black spot on the diagram represents a product, whilst each line represents the enzyme required for the conversion.

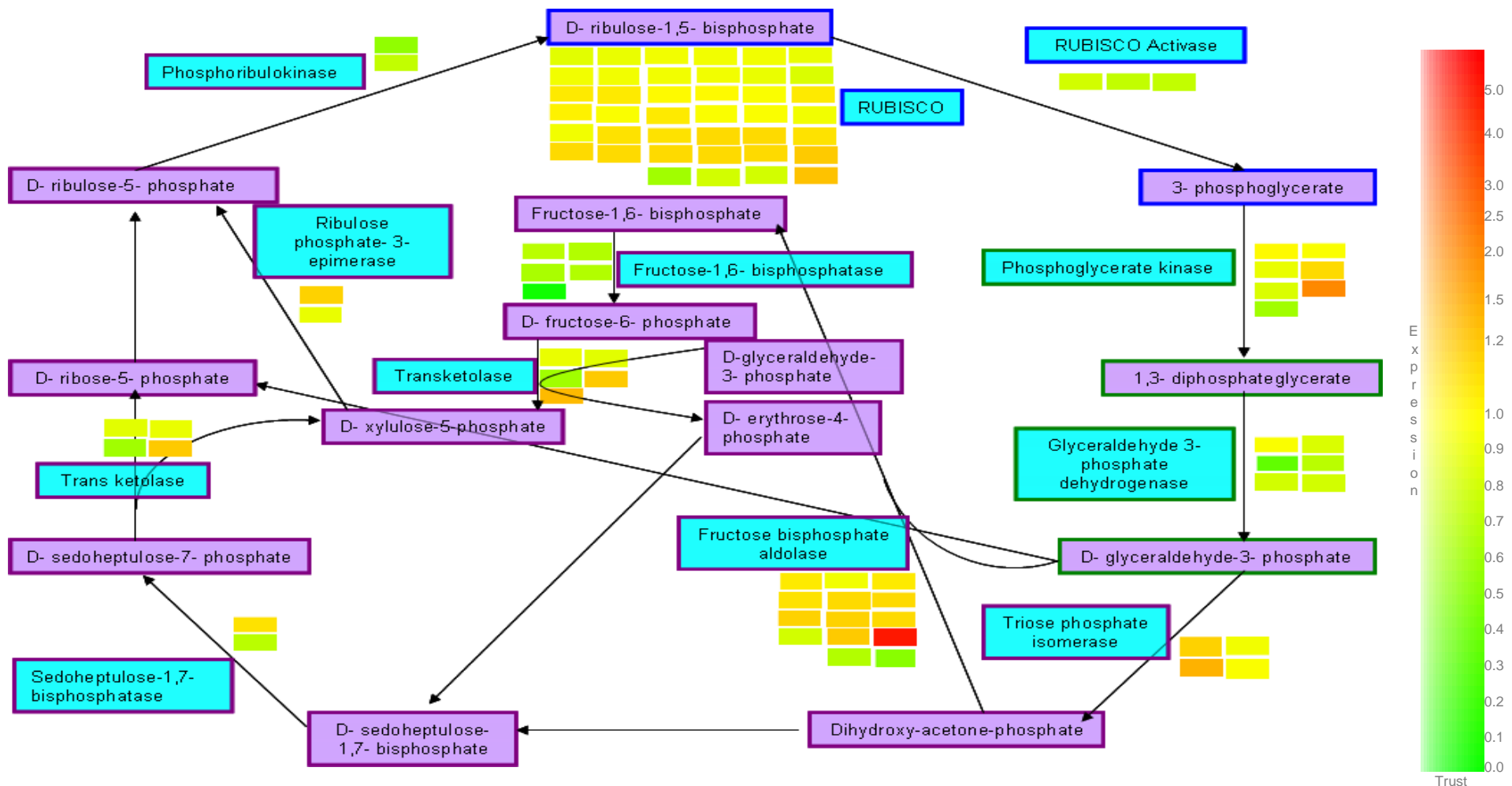


Figure 7.3.7. The Calvin cycle of *P. deltoides* (meristematic tissue). Each coloured box signifies a single EST and is positioned adjacent to the enzyme (in the blue box) that it represents. The purple boxes represent the products of the reaction. The colour of each EST box represents its expression level (red= up-regulated in [eCO₂], green = down-regulated, yellow= no change). The borders around each enzyme and product box represents the portion of the Calvin Cycle they are associated with (blue=carboxylation, green=, reduction, purple=regeneration).

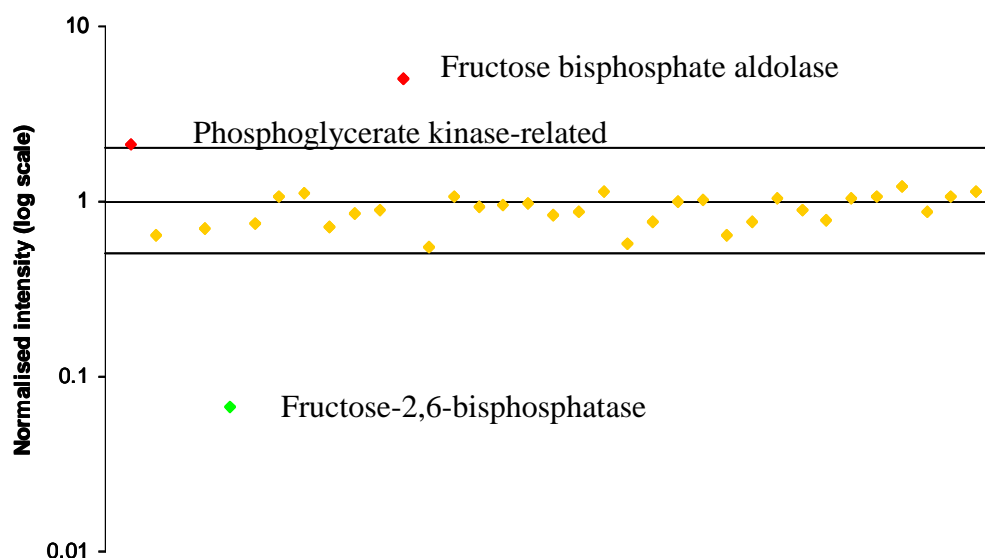


Figure 7.3.8. Each spot represents the average expression value per gene model. The data was obtained from the microarrays conducted on the meristematic tissue of *P. deltoides* exposed to [aCO₂] and [eCO₂]. The point marked in green illustrates the gene models that were more than two-fold down-regulated in [eCO₂]. The red points show the gene models that were two-fold or more up-regulated in [eCO₂]. The yellow points illustrate gene models that demonstrated less than a two-fold difference in expression levels between [aCO₂] and [eCO₂]. The horizontal lines on the graph represent two-fold differences in expression. The horizontal line at ‘1’ represents no change in expression level.

The 94 ESTs in the Calvin Cycle pathway analysis (Figure 7.3.7) represented a total of 35 gene models (results displayed in Figure 7.3.8). By inspection of the average intensity values per gene model (Figure 7.3.8) associated with the Calvin cycle (Figure 7.3.7), it is clear that there were a very small number of transcripts that were differentially expressed and the majority of results for the gene models showed a less than two-fold change in [eCO₂] in the meristematic tissue of *P. deltoides*. There were only three exceptions; fructose-bisphosphate aldolase (estExt_Genewise1_v1.C_LG_I6144), which was up-regulated (4.98-fold difference), and the EST representing a phosphoglycerate kinase-related transcript (gw1.III.2058.1) (2.10-fold difference). The EST representing fructose-2,6-bisphosphatase (estExt_fgenes4_pg.C_LG_I2027) was highly down-regulated (0.07-fold difference).

GA is known to influence plant growth. There are many genes involved in the biosynthesis of GA. One of the key enzymes in the process is GA20 oxidase (see Figure 7.4.1). Overexpression of GA20 oxidase in poplar has been shown to cause an increase in plant height (Eriksson *et al*, 2000). The Aracyc pathway analysis highlighted GA as being differentially expressed as a result of growth in [eCO₂] in *P. trichocarpa*, age two. However, further exploration into this showed that only a single transcript involved in the biosynthesis of GA was up-regulated. This transcript represented GA20 oxidase, which was up-regulated by five-fold in this species.

7.3.1.4 Leaf growth candidate genes

Potential leaf growth candidate genes were identified from the literature and cross-referenced with the cDNA microarray data in order to determine whether or not they were responsive to CO₂ treatment. In particular, the focus turned to the transcripts thought to be involved in adaxial-abaxial cell patterning.

The results for each individual EST representing *YABBY* and *KANADI* (both involved in abaxial cell patterning (Siegfried *et al*, 1999; Kerstetter *et al*, 2001)) and *ARGONAUTE1* (involved in adaxial cell patterning (Kidner and Martienssen, 2004)) on the cDNA microarrays are shown in Figure 7.3.9. The average results for each gene model representing the candidate genes are shown in Table 7.3.1.

YABBY was up-regulated in response to CO₂ in the age two leaves of both species (Table 7.3.1). This is quite clear in *P. deltoides* as shown in Figure 7.3.9, where the individual EST results are shown. By averaging across gene models, *YABBY* was up-regulated by 6.70-fold in age two of *P. trichocarpa*. However, this result was complicated by the fact that there was some considerable variation in EST expression levels in *P. trichocarpa* ($\sigma=14.9$ in age two, data not shown). The expression of *ARGONAUTE1*, was only slightly up-regulated in age two leaves of both *P. deltoides* (1.61 fold-difference) and *P. trichocarpa* (1.25 fold-difference).

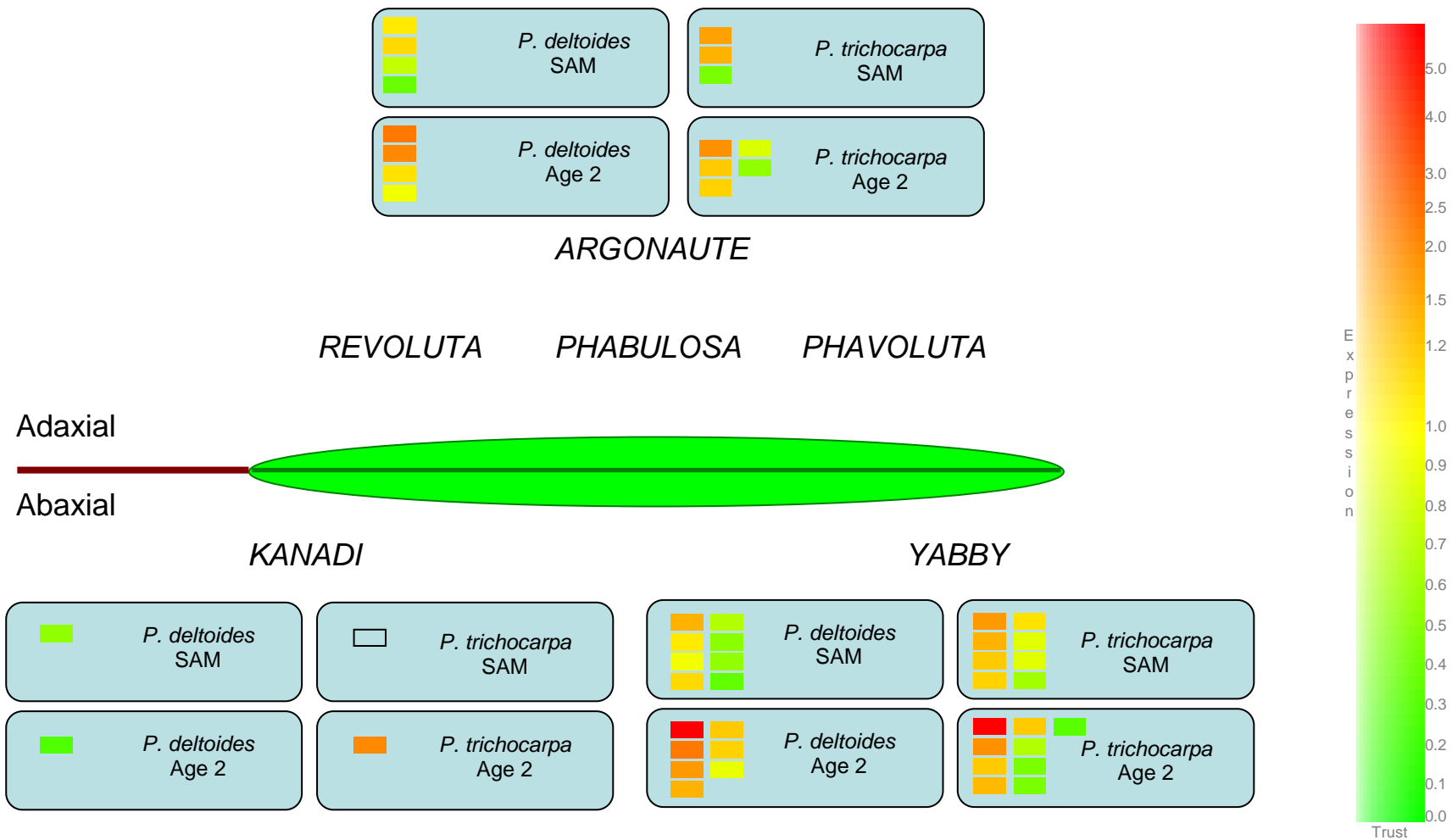


Figure 7.3.9. The expression levels of ESTs representing abaxial (*YABBY* and *KANADI*) and adaxial (*ARGONAUTE*) patterning genes. Each coloured box signifies a single EST and the colour represents its expression (red= up-regulated in [eCO₂], green= down-regulated in [eCO₂], yellow= no change). All data for the ESTs that were available on the POP2 microarray are provided on the graph. The expression data from all four groups of microarrays (*P. deltooides*, age 2; *P. deltooides*, meristematic tissue ('SAM'); *P. trichocarpa*, age 2; *P. trichocarpa*, meristematic tissue ('SAM')) are represented in the figure.

YABBY

Gene Model	<i>P. deltoides</i> SAM	<i>P. deltoides</i> Age 2	<i>P. trichocarpa</i> SAM	<i>P. trichocarpa</i> Age 2	Annotation
estExt_fgenes4_pg.C_LG_XVI0541 protein	1.42	7.02	-	1.95	Plant-specific transcription factor, YABBY family
estExt_Genewise1_v1.C_1270153	0.68	-	0.64	0.47	Axial regulator YABBY1 (YABBY1)
eugene3.00011153	0.99	1.17	1.08	1.20	Axial regulator YABBY3 (YABBY3)
grail3.0018017701	0.58	-	0.90	-	Axial regulator YABBY1 (YABBY1)
grail3.0023002901 protein	0.39	2.36	1.78	1.37	Plant-specific transcription factor, YABBY family
grail3.0035001101	0.79	1.19	1.17	0.85	Axial regulator YABBY1 (YABBY1)
grail3.6958000101	-	-	-	-	Axial regulator YABBY1 (YABBY1)
gw1.I.9758.1 protein	1.04	1.48	1.17	0.52	Plant-specific transcription factor, YABBY family
gw1.XVI.2137.1 protein	-	-	-	40.57	Plant-specific transcription factor, YABBY family
Average	0.84	2.63	1.12	6.70	-

ARGONAUTE 1

Gene Model	<i>P. deltoides</i> SAM	<i>P. deltoides</i> Age 2	<i>P. trichocarpa</i> SAM	<i>P. trichocarpa</i> Age 2	Annotation
grail3.0031006602	1.06	1.54	0.87	1.44	Argonaute protein (AGO1)
grail3.0122002801	0.58	1.68	1.34	1.06	Argonaute protein (AGO1)
Average	0.82	1.61	1.10	1.25	-

Table 7.3.1. The average expression values for each gene model representing either *YABBY* or *ARGONAUTE* for *P. deltoides* and *P. trichocarpa* (both age two leaves and the SAM (meristematic tissue)). A global expression value is provided at the bottom of each table.

7.3.1.5 Cell cycle candidate genes

The results from the cellular analysis of the growth profile trees showed that cell area (adaxial and abaxial) was affected by CO₂ exposure (Figures 6.3.3 to 6.3.6). It is highly conceivable that any phenotypic differences in cellular growth as a result of exposure to [eCO₂] involve a change in the transcript abundance of genes that affect the progression of the cell cycle. Therefore the data obtained from the microarrays was closely examined for transcripts such as cyclins, cyclin dependent kinases (CDK's) and CDK activating kinases (CAK's) in order to ascertain their expression differences in the two species, leaf ages and CO₂ treatments. The results are presented in Table 7.3.2.

In the meristematic tissue of *P. deltoides*, transcripts encoding the cyclin required for progression from G1 to S phase (CycD3) were up-regulated in [eCO₂], along with other transcripts involved in the progression of the cell cycle, such as CAK assembly factors. *KRP4*, a gene which acts to inhibit the cell cycle, was down-regulated in this species in response to treatment. The A-type cyclins were generally up-regulated in *P. trichocarpa* in both the young meristematic tissue, and the age two leaves.

Gene Model	<i>P. delt</i> 2	<i>P. delt</i> SAM	<i>P. trich</i> 2	<i>P. trich</i> SAM	Annotation
fgenes4_pm.C_LG_VIII000144	0.83	0.96	2.52	0.85	Ania-6a type cyclin (RCY1)
grail3.0017029801	1.28	1.24	1.39	0.51	Cyclin delta-2 (CYCD2)
estExt_fgenes4_pg.C_LG_V1250	1.62	2.84	0.71	0.87	Cyclin delta-3 (CYCD3)
estExt_Genewise1_v1.C_LG_IX2293	0.74	1.30	0.58	0.69	Cyclin delta-3 (CYCD3)
grail3.0040026601	0.67	2.81	0.65	1.18	Cyclin delta-3 (CYCD3)
grail3.0016020101	1.45	0.97	0.89	0.67	Cyclin family low similarity to microtubule-binding protein <i>TANGLED1</i>
estExt_fgenes4_pg.C_LG_XV0856	-	-	1.89	-	Cyclin family protein
eugene3.00400102	1.08	-	0.47	0.31	Cyclin family
eugene3.00050513	-	-	-	1.85	Cyclin family protein similar to cyclin D3.1 protein
grail3.0011035801	0.82	1.43	1.44	0.30	Cyclin family protein
eugene3.00440167	0.88	0.77	0.68	0.87	Cyclin family protein
estExt_Genewise1_v1.C_1330021	1.25	1.03	0.94	0.98	Cyclin family protein
estExt_fgenes4_pm.C_LG_III1144	-	-	0.55	-	Cyclin family protein
estExt_fgenes4_pm.C_LG_V0169	-	0.65	0.40	0.52	Cyclin, putative
fgenes4_pg.C_scaffold_70000176	1.19	-	1.54	4.58	Cyclin, putative similar to A-type cyclin
estExt_fgenes4_pg.C_LG_IX0044	-	1.17	0.34	-	Cyclin, putative similar to B-like cyclin
estExt_fgenes4_pm.C_LG_V0693	3.48	0.82	4.03	0.52	Cyclin, putative similar to B-like cyclin
eugene3.03180006	1.28	0.16	0.87	-	Cyclin, putative similar to B-like cyclin
gw1.III.684.1	-	-	0.71	2.67	Cyclin, putative similar to cyclin A2

Table 7.3.2. The expression data for transcripts related to cell cycle progression. Each value represents the average expression change for each gene model in each hybridisation category (e.g. *P. deltoides*, age two). The figures in blue represent those that were two-fold or more down-regulated upon growth in [eCO₂]. The figures in red represent the transcripts that were two-fold or more up-regulated when grown in [eCO₂]. The annotation for each gene model was derived from *Populus* DB. *P. delt*= *P. deltoides*, *P. trich*= *P. trichocarpa*, 2= age two, SAM= meristematic tissue.

Gene Model	<i>P. delt</i> 2	<i>P. delt</i> SAM	<i>P. trich</i> 2	<i>P. trich</i> SAM	Annotation
estExt_Genewise1_v1.C_LG_V0004	0.27	0.82	0.29	0.67	cyclin, putative similar to mitotic cyclin a2-type
fgeneshd4_pm.C_scaffold_40000107	-	1.12	0.81	-	cyclin, putative similar to mitotic cyclin a2-type
estExt_fgenesh4_pm.C_1630014	1.23	1.10	0.86	0.96	cyclin-dependent kinase / CDK
estExt_fgenesh4_pm.C_LG_IX0727	1.16	1.06	0.85	1.09	cyclin-dependent kinase / CDK
eugene3.00060233	-	0.42	-	-	cyclin-dependent kinase, putative / CDK,
estExt_fgenesh4_pg.C_LG_XVIII0897	0.97	0.84	0.66	0.77	cyclin-dependent kinase-activating kinase assembly factor-related
eugene3.00061321	-	6.47	-	-	cyclin-dependent kinase-activating kinase assembly factor-related
estExt_fgenesh4_pg.C_LG_XVI0424	-	-	1.02	-	cyclin-related
fgenesh4_pg.C_LG_IX000743	0.83	1.29	0.93	0.96	cyclin-related
grail3.0056004201	1.39	1.30	-	-	expressed protein contains low similarity to cyclin G-associated kinase from [Rattus norvegicus]
gw1.II.2495.1	-	1.10	0.33	0.87	kip-related protein 3 (KRP3) / cyclin-dependent kinase inhibitor 3 (ICK3)
gw1.XVII.448.1	0.26	0.46	0.88	1.31	kip-related protein 4 (KRP4) / cyclin-dependent kinase inhibitor 4 (ICK4)
estExt_fgenesh4_pg.C_LG_V0508	1.19	1.11	0.73	1.07	kip-related protein 6 (KRP6) / cyclin-dependent kinase inhibitor 6
grail3.0008033601	1.13	1.46	1.05	1.86	protein kinase, putative similar to cyclin-dependent kinase cdc2MsE

Table 7.3.2 continued. The expression data for transcripts related to cell cycle progression. Each value represents the average expression change for each gene model in each hybridisation category (e.g. *P. deltoides*, age two). The figures in blue represent those that were two-fold or more down-regulated upon growth in [eCO₂]. The figures in red represent the transcripts that were two-fold or more up-regulated when grown in [eCO₂]. The annotation for each gene model was derived from *Populus* DB. *P. delt*= *P. deltoides*, *P. trich*= *P. trichocarpa*, 2= age two, SAM= meristematic tissue.

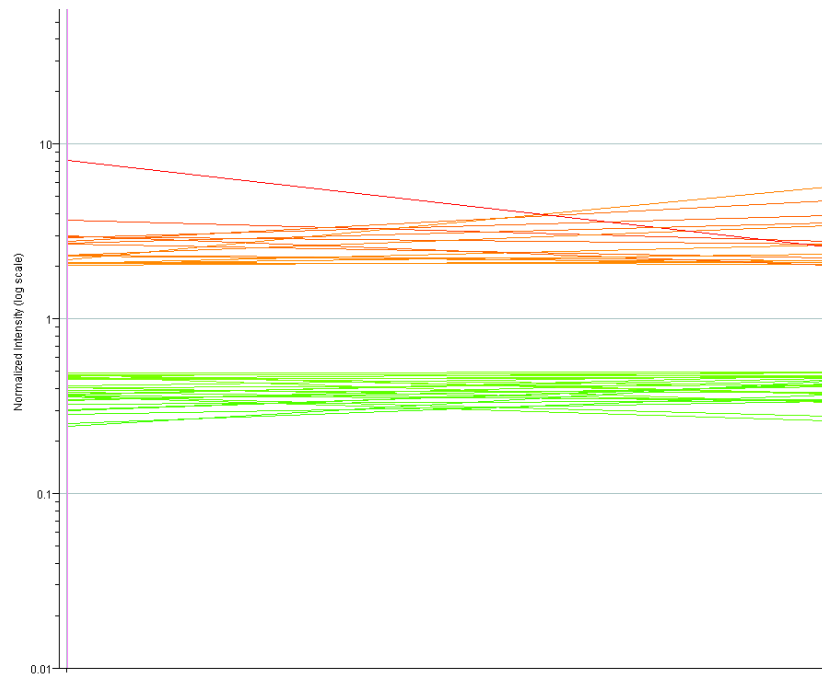
7.3.2 Affymetrix microarrays

Four samples from each species (two grown in [aCO₂] and two in [eCO₂]) were sent to NASC (<http://affymetrix.arabidopsis.info>) to be hybridised on the Poplar Affymetrix gene chip. For each species, the gene chips from leaf samples grown in [aCO₂] conditions were randomly paired with those from [eCO₂] conditions in order to create a dual channel experiment in order to assess differential gene expression (per species) as a result of CO₂ exposure.

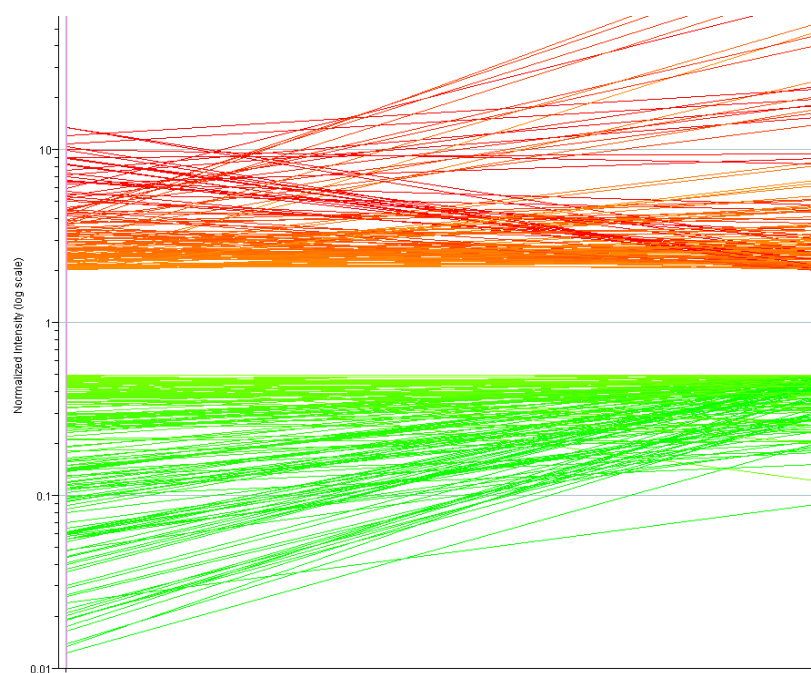
The gene expression assessment by the use of the Affymetrix microarray platform showed that *P. trichocarpa* exhibited greater changes in expression in young leaves than *P. deltoides* (Figure 7.3.10, appendix 4). In *P. deltoides* there were 45 transcripts that were two-fold or more up-(17) or down-(28) regulated in [eCO₂]. In *P. trichocarpa*, there were 292 transcripts that were up-(134) or down-(158) regulated in [eCO₂].

The Affymetrix data from both species were analysed using B-statistics. There were no transcripts that had a B-value greater than 0 (50% chance of differential expression) in either species. When filtered according to fold-change only, there were two transcripts that were consistently regulated by at least two-fold between the two species. These two transcripts were L-asparaginase (PtpAffx.47668.1.A1_at) and a WRKY family transcription factor (PtpAffx.10586.2.S1_at). The WRKY transcription factor was, on average, down-regulated in *P. trichocarpa* (0.11-fold difference) but up-regulated in *P. deltoides* (2.09 fold difference). Conversely, L-asparaginase was up-regulated in *P. trichocarpa* (3.32 fold difference) but down-regulated in *P. deltoides* (0.38-fold difference).

The results from the Affymetrix microarrays were compared with the cDNA microarrays on the basis of gene model. The results showed that the expression data across the two platforms were inconsistent since there were no genes that were found to be consistently up-or down-regulated in either species.



P. deltoides



P. trichocarpa

Figure 7.3.10. The youngest unfurled leaves of *P. deltoides* and *P. trichocarpa* were sampled 43 DFE and hybridised onto the Poplar Affymetrix gene chip available at NASC (<http://affymetrix.arabidopsis.info>). The data from each gene chip from one condition was arbitrarily paired with the data from a second chip exposed to the second condition (for a single species). The results of these pairings are shown for each species. Each line represents a single oligonucleotide. The red colour indicates up-regulation in [eCO₂] and the green represents down-regulation.

7.4 Discussion

There are many reports in the literature regarding the use of microarrays as a global screen for gene identification, particularly in relation to studying the effect of a treatment (e.g. Street *et al*, 2006). The advantage of the use of microarrays is that they can be used as a complete global screen, where one is likely to reveal novel genes previously not connected to the variable in question. Alternatively, the technology allows more targeted screening to be performed through the selection of particular probe sets. Here, it was been used in the former context.

Microarrays have been used in previous experiments to investigate the response to [eCO₂] in leaf tissue (e.g. Chapter 5) but only a few CO₂-responsive transcripts were identified. The aim of this experiment was to link changes in growth and development following growth in [eCO₂] (results presented in Chapter 6) with gene expression data, collected from two different microarray platforms in order to identify any robust CO₂-responsive genes. Further to previous reports, here it was shown that there were again rather few changes in gene expression as a result of CO₂ treatment in either species.

7.4.1 Leaf development and patterning in [eCO₂]

There are a plethora of genes that affect leaf growth and development. The majority of these genes have been discovered in mutational analyses using model organisms, particularly *Arabidopsis*. The expression of those genes is important in governing leaf dimensionality particularly under the local conditions dictated by the surrounding environment.

Leaves are asymmetrical structures which are adapted for different functional roles; light capture on the adaxial surface, and gas exchange on the abaxial surface. The formation of cell layers is thought to be, at least in part, due to the actions of the *PHANTASTICA*-like transcription factors which act to repress the expression of *KNOX* genes in the meristematic region (Fleming, 2005). An emerging model suggests that *KNOX* genes act to maintain cells in an undifferentiated state and that *PHAN* promotes adaxial tissue differentiation by repressing *KNOX* gene expression. The establishment of adaxial-abaxial polarity is defined early in primordium formation and is known to involve a subset of developmental genes including *Class*

III HD ZIP (PHABULOSA and PHAVOLUTA), YABBY and KANADI transcription factor families (Bowman *et al*, 2002).

Members of the *YABBY* family are transcription factors which are known to affect abaxial cell patterning (Kim and Cho 2006; Kerstetter *et al*, 2001; Sawa *et al*, 1999; Siegfried *et al* 1999). The results from the cDNA microarrays suggested that the *YABBY* genes and the ESTs representing *YABBY* family proteins were generally up-regulated in [eCO₂] in *P. deltoides* (age two). On average, across gene models, expression was highly up-regulated in *P. trichocarpa* (age two). However, the expression values for each gene model representing *YABBY* were extremely variable. It is possible that this result represents a degree of redundancy in *YABBY* family members (Bowman *et al*, 2002), a trait that is also true of the *KANADI* transcription factor family (Eshed *et al*, 2001). Despite the response differences between the two species, [eCO₂] did cause a general increase in the expression of *YABBY*. Hence it might be inferred that leaf development is promoted in [eCO₂] in young leaves via increased expression of such transcripts.

KANADI is a second gene family that also determines abaxial cell patterning in the leaf. *KAN* encodes Golden2/*Arabidopsis* response-regulator/ Psr1 (GARP) transcription factors (Kerstetter *et al*, 2001). Expression of *KANADI* is restricted to young leaves (Kerstetter *et al*, 2001). *KAN2* was down-regulated in [eCO₂] in *P. deltoides* by more than two-fold in age two leaves and the meristematic tissue. However, it was two-fold up-regulated in age two of *P. trichocarpa* (no data was available for the meristematic tissue of this species). The fact that a second set of genes involved in abaxial cell patterning were up-regulated in *P. trichocarpa* in response to [eCO₂] is particularly interesting. Again, a clear species difference has been highlighted.

There are also a distinct set of genes that affect adaxial cell patterning. These include *PHB*, *PHV* and *REV* (Emery *et al*, 2003). These genes all encode Class III homeodomain/leucine zipper (HD-ZIP III) transcription factors (McConnell *et al*, 2001; Otsuga *et al*, 2001). These transcripts are controlled by microRNAs (including miRNA165 and miRNA166). There was no expressional data available from the cDNA microarrays for *PHB*, *PHV* or *REV* (in either species or at either age).

However, *ARGONAUTE1* (*AGO1*) was differentially regulated in response to CO₂. This gene is known to regulate miRNA165 and miRNA166 and therefore has a role in adaxialation (Kidner and Martienssen, 2004). By averaging the values for each EST it was shown that *AGO1* was fractionally down-regulated in the meristematic tissue in [eCO₂] (0.82) but slightly up-regulated in response to treatment in age two leaves (1.61). The *AGO1* transcript was slightly up-regulated in age two and meristematic tissue of *P. trichocarpa* (1.25 and 1.10 respectively). It is possible that this ‘switching’ from down-to up-regulation represents a developmental transition in *P. deltoides*, which was absent in *P. trichocarpa*.

No information was available from the cDNA microarray data regarding the expression of other leaf patterning genes such as *ASYMMETRIC LEAVES1*, *ASYMMETRIC LEAVES2* and *ERECTA* (Iwakawa *et al*, 2002), which are thought to be involved in adaxial-abaxial polarity in leaves (Xu *et al*, 2003). Given the effects of [eCO₂] on the other cell patterning genes, it is possible a similar effect is possible in these transcripts as well, although this is merely speculative.

In a typical angiosperm, following the establishment of adaxial-abaxial identity comes further development of the leaf tissues i.e. the formation of the cell layers. The results from the leaf anatomy study suggested that abaxial cell patterning was affected by [eCO₂] in young leaves of *P. trichocarpa*. Interestingly this also corresponds to the results in Chapter 4, although in this case it was clear that cell production was increased. These leaves exhibited differences in the structure of the spongy mesophyll layer of the leaf. Intracellular air spaces were increased in the young leaves of *P. trichocarpa* grown in [eCO₂]. This pattern coincides with increased expression of transcripts involved in abaxial cell patterning, therefore suggests a possible link between phenotypic leaf anatomy, abaxial cell patterning genes and CO₂ enrichment.

The differential expression of leaf patterning genes between the two cell layers could account for the differences observed between the unfurled meristematic tissue and the young leaves in this experiment. In both species, expression levels were lower in the meristematic tissue than the age two leaves, and thus reflecting a developmental expression pattern. However, there was also a difference in expression between the two species. *KANADI* gene expression was down-regulated in both age categories of

P. deltoides and *YABBY* was up-regulated in age two only, whilst both genes were up-regulated in [eCO₂] in all the available data for *P. trichocarpa*. Interestingly, there was little visible difference in leaf anatomy for the young leaves of *P. deltoides*, suggesting that the expression of these genes may be particularly important in governing leaf structure upon carbon enrichment. *P. trichocarpa* demonstrated increased expression of both genes in both age categories in response to [eCO₂] and also demonstrated altered leaf anatomy.

7.4.2 The Cell Cycle

Previous studies have shown that increased carbon availability leads to increased leaf size (e.g. Taylor *et al*, 2003). By definition, there are two ways in which this can occur; cell production or cell expansion. The results presented in Chapter 6 demonstrated that cells responded to [eCO₂] with increased cell size, hence suggesting that cell expansion is affected. Taking this into consideration, it might be imagined that the increased carbon may be affecting an important cell cycle checkpoint.

The D-type cyclins have been proposed as an important component in the response to [eCO₂] (Taylor *et al*, 2003) since their expression is affected by sucrose availability (Rhio-Khamlichi *et al*, 2000; Lorenz *et al*, 2003; Healy *et al*, 2001). Upon closer inspection of the microarray results, it was found that cyclin D3 was up-regulated in *P. deltoides* (age two). The expression of D-type cyclins is generally associated with regulating cell number (Dewitte *et al*, 2003). Abaxial cell number increased in [eCO₂] in young leaves (age two) of *P. deltoides* (Figure 6.3.6) and this may be attributed to increased expression of cyclin D3 at this age category.

CycD3 is required for the G1/S phase transition of the cell cycle (Rhio-Khamlichi *et al*, 2000). It controls cell number in developing leaves by regulating the duration of the mitotic phase and timing of transition to endocycles (Dewitte *et al*, 2007). The fact that CycD3 has been shown to promote mitotic activity rather than endocycles could be due to either a role as a mitotic cyclin, hence affecting G2/M kinase activity and entry into M phase, or that expression of CycD3 causes commitment to mitosis during the G1/S phase transition (Dewitte *et al*, 2007). Cytokinin expression has also been shown to be necessary at this phase of the cell cycle in order to induce the expression

of CycD3 (Rhio-Khamlichi *et al*, 1999). However, there was no transcriptional data available regarding cytokinin expression levels in this experiment.

An increase in cell area as a result of growth in [eCO₂] has been shown in a number of different species, including chalk grassland herbs (Ferris and Taylor, 1994) and bean (Ranasinghe and Taylor, 1996). The stimulation in cell area due to [eCO₂] has been attributed to increased cell wall extensibility (Taylor *et al*, 1994; Ranasinghe and Taylor, 1996) and supports the findings of increased XET activity (one of the key enzymes involved in cell wall loosening and growth) in *P. deltoides* grown in FACE conditions in Chapter 4. Here XET activity was assessed by expression on the POP2 cDNA microarrays and was again generally up-regulated in response to treatment, particularly in *P. deltoides* (data not shown). This again provides evidence of the enzymes' role in morphological response to [eCO₂].

7.4.3 Hormone signalling

The results from the Aracyc pathway analysis suggested the expression of transcripts involved in the biosynthesis of GA was up-regulated in [eCO₂] in *P. trichocarpa* leaves (age two). Specifically, GA20 oxidase, a key enzyme in the GA conversion pathway, was up-regulated by five-fold in [eCO₂]. GA is a hormone involved in a variety of plant responses. It is mostly renowned for its effects on plant height (Busov *et al*, 2003) although germination, flowering and leaf growth are also affected by its activity.

The knowledge of the effects of the GA on plant phenotypes have mainly been drawn from numerous mutant studies that have been conducted to date. GA mutants have been produced in a variety of species including pea (Ingram, 1984), rice (Suge and Murakami, 1968), *Arabidopsis* (Koorneef and Van der Veen, 1980) and Poplar (Busov *et al*, 2003). Such studies have shown that a reduction in GA levels causes delayed flowering (Olszewski *et al*, 2002), defective floral development (Tyler *et al*, 2004; Cheng *et al*, 2004) and altered leaf morphology (Hay *et al*, 2002; Sakamoto *et al*, 2001; Hay *et al*, 2004). In *Populus*, increased GA biosynthesis by overexpression of GA20 oxidase caused increased tree height and stem diameter (Eriksson *et al*, 2000).

The fact that GA20 oxidase, a major enzyme in the GA biosynthetic pathway, was up-regulated in [eCO₂] may go some way to explain the increased plant height observed in [eCO₂] (particularly in *P. trichocarpa*, Figure 6.3.15). However, GA is also known to elicit other responses in plants such as increased cell elongation in rice (Matsukura, 1998) due to increased cell wall extensibility. Furthermore, GA has been shown to affect XET activity (Smith *et al*, 1996). It is possible that GA controls the direction of cell growth in monocots by controlling the orientation of cellulose microfibrils (Matsukura, 1998) which may be controlled by cortical microtubules and are known to be affected by GA and auxin (Shibaoka, 1994). However, the relationship between GA and cell expansion/ elongation is not clear, since GA had also been shown to promote cell division in rice due to the action of histone H1 kinase and cyclin genes (Sauter *et al*, 1995).

The biosynthesis of GA is a complex process involving a large number of intermediate molecules (Figure 7.4.1).

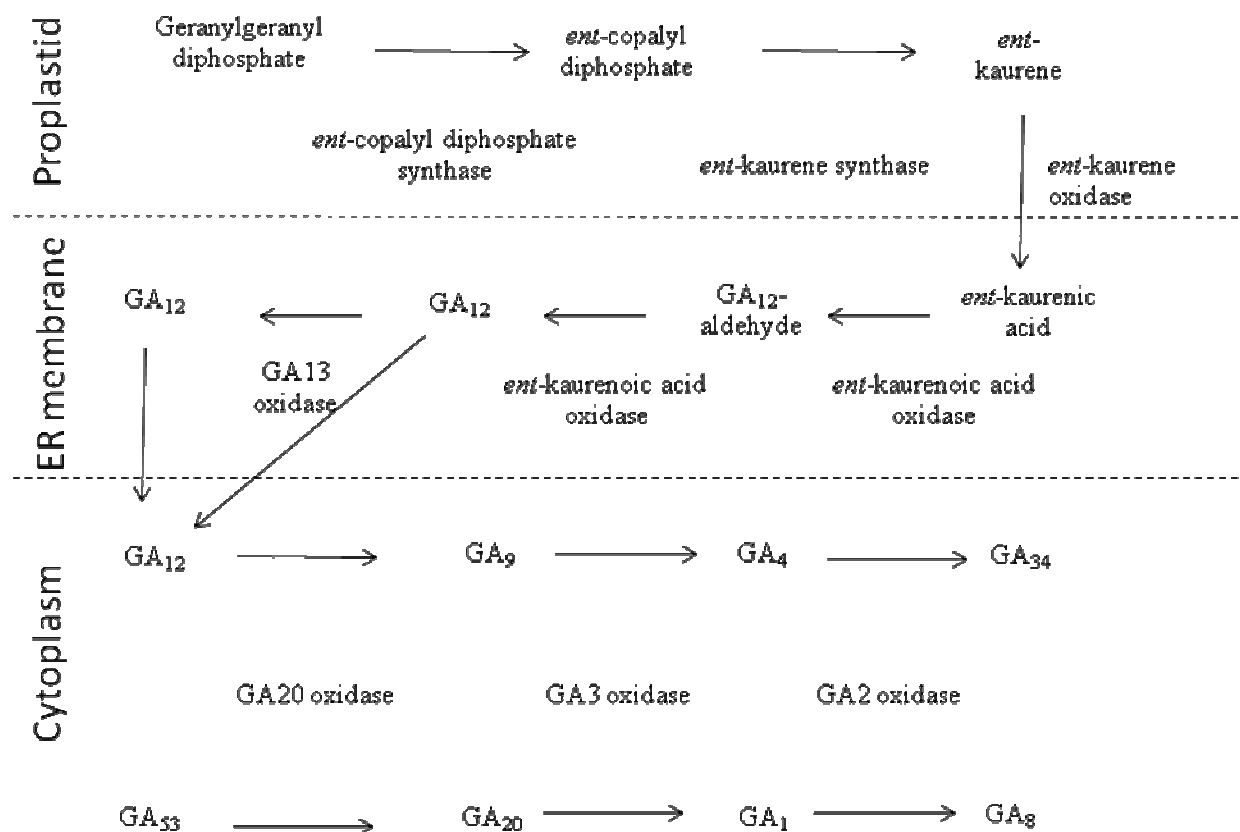


Figure 7.4.1. The major GA biosynthetic pathways in higher plants. GA₄ and GA₁ represent the bioactive GAs whilst GA₃₄ and GA₈ are their inactive catabolites. Diagram adapted from Olszewski *et al*, (2002).

If the activity of GA was truly affected by [eCO₂], one would imagine a number of other transcripts involved in the biosynthesis of GA to also be up-regulated. This was not the case and so limits the conclusions that can be drawn from this result. However, some other transcripts associated with the GA response (e.g. *GASA*) were differentially regulated in [eCO₂]. The *GASA4* transcript has been shown to be up-regulated in meristematic tissues, but has been associated with cell division rather than cell expansion (Aubert *et al*, 1998). *GASA4* was not differentially regulated in either the meristematic tissue (1.04-fold change) or leaf age two (1.34-fold change) in *P. trichocarpa*. However, *GASA2* was up-regulated in the meristematic tissue of *P. trichocarpa* (5.07-fold change), as was *GASA3* (3.69-fold change).

7.4.4 Photosynthesis

It is generally well documented that prolonged growth in [eCO₂] leads to a down-regulation in photosynthesis. Previous reports have indicated a reduction in the abundance of transcripts encoding Rubisco upon exposure to [eCO₂] (e.g. Cheng *et al*, 1998). Here, microarrays were used as a global screen to identify any transcripts that were changing in response to CO₂ treatment. By the use of pathway analysis software it was possible to focus on putative mechanisms involved in the response to the stimulus and which underlie the phenotypic differences that were observed.

The results from AraCyc highlighted *FRUCTOSE BIPHOSPHATE ALDOLASE* (At4g26530) as highly up-regulated in response to [eCO₂] in *P. deltoides* (age two). This enzyme is involved in the conversion of dihydroxyacetone phosphate to fructose-1, 6-bisphosphate in the ‘regeneration’ section of the Calvin Cycle. This initial result warranted further investigation since photosynthesis has generally been reported to be down-regulated upon exposure to [eCO₂]. Hence this led to a closer inspection of the Calvin Cycle and its associated components in order to determine whether the transcript abundance was affected by increased carbon availability. Despite the up-regulation of the transcript encoding fructose bisphosphate aldolase, it was clear that there was a general down-regulation of the expression of the other transcripts involved in the Calvin cycle in the young (age two) leaves of *P. deltoides* grown in [eCO₂]. Similar results have been reported previously for associates of the Calvin Cycle exposed to [eCO₂] (Li *et al*, 2006), such as sedoheptulose-1,7-bisphosphatase, phosphoribulokinase, phosphoglycerokinase, and the large and small subunits of Rubisco (Nie *et al*, 1995).

The down-regulation of photosynthesis in plants grown in [eCO₂] has been attributed to an inadequate sink capacity of the plant (Ainsworth *et al*, 2004). It is probable that the increased sugar supply generated by an initial increase in photosynthesis by exposure to [eCO₂] is involved in a feedback system in order to regulate further photosynthetic activities (Paul and Foyer, 2001). In this experiment however, the transcript studies were conducted on young expanding leaves of *Populus*, and it has been reported in the literature that whilst leaves are expanding, sugar associated repression of photosynthesis and its associated proteins does not occur (Moore *et al*, 1999; Van Oosten and Besford, 1996). It is therefore likely that an alternative

mechanism is involved in the down-regulation of the Calvin cycle related transcripts. For example, Wait and co-workers have shown that the ratio of expanding to expanded leaves affects the response to [eCO₂] (Wait *et al*, 1999). Furthermore, the lack of photosynthetic acclimation to [eCO₂] in young leaves has been attributed to a high degree of sucrose metabolism hence resulting in an already repressed state of photosynthetic gene expression (Jang and Sheen, 1994). The effect of [eCO₂] acclimation in young leaves has also been attributed to altered hormonal levels (Moore *et al*, 1999) since there is cross talk between sugar and hormone signalling pathways (e.g. see Jang and Sheen, 1997; Moore *et al*, 1999) although the mechanism in these two species of *Populus* is yet to be deciphered.

7.4.5 Affymetrix microarrays and platform comparisons

Two different microarray platforms were utilised in this experiment in order to assess gene expression. These two platforms were the POP2 cDNA microarray (Sterky *et al*, 2004) and the Affymetrix oligonucleotide microarray (www.nasc.nottingham.ac.uk). It is rather surprising that the results from the two platforms were inconsistent with regards to the most responsive species to CO₂ enrichment in terms of gene expression. In the case of the cDNA microarrays *P. deltoides* was most responsive, whilst *P. trichocarpa* was most responsive in the case of the oligonucleotide microarrays. Previous comparative analyses of microarray technologies have also shown inconsistencies across platforms, with oligonucleotide microarrays often displaying a greater number of differentially expressed transcripts compared to cDNA platforms (Yauk *et al*, 2004). A reduced sensitivity of cDNA compared to oligonucleotide platforms leading to a decreased responsiveness has been reported previously (Hughes *et al*, 2001; Li *et al*, 2002).

Inconsistencies can be introduced at many different stages during cDNA microarray experiments (Yang *et al*, 2002). Given the results of transcriptomic analyses of poplar to [eCO₂] have previously shown subtle changes in gene expression, it was deemed appropriate to further mine the data following the initial analysis.

The results from the two experiments were compared based upon differentially expressed (defined as two-fold regulated) transcripts. This was completed using gene model as the common reference point. It was rather surprising that there were no

transcripts that were consistently differentially regulated between the two platforms. This is surprising, given the fact that the leaves in the sample study were all young tissues. Despite the fact that the RNA used for the hybridisations were sampled from different leaf ages (meristematic tissue and age two in the cDNA microarrays, and age one in the oligonucleotide Affymetrix microarrays), these results are still surprising.

As part of the microarray analysis, transcripts that were consistently differentially regulated as a result of growth in [eCO₂] were identified by means of a cross-species comparison. Only two transcripts were identified as consistently differentially expressed across species; a WRKY family transcription factor (PtpAffx.10586.2.S1_at) and L-asparaginase (PtpAffx.47668.1.A1_at). However, rather than being consistently differentially expressed, both transcripts demonstrated opposite expression patterns in the species comparison. The WRKY transcription factor was more than two-fold up-regulated in *P. deltoides*, but more than twofold down-regulated in *P. trichocarpa*. Conversely, L-asparaginase was more than two-fold up-regulated in *P. trichocarpa* but more than two-fold down-regulated in *P. deltoides*. WRKY transcription factors have a number of roles in plants, including regulating the pathogen-induced defence program, leaf senescence and trichome development (reviewed in Elgem *et al*, 2000; Ülker and Somssich, 2004). The differences in expression of the WRKY transcription factors and the L-asparaginase, suggests that the importance of the transcripts is dependent upon the species in question.

7.4.6 Statistical analysis of microarray data

Given the amount of data produced in each microarray experiment, an appropriate strategy for analysis is required. Here, Bayesian ('B') statistics were used as a way of testing the significance of the data from both the cDNA and Affymetrix microarrays. B-statistics are the log-odds that a gene is differentially expressed. For example, if the B-value is 1.5, the likelihood of differential expression is $\exp(1.5) = 4.48$, and $(4.48 / (1+4.48)) = 0.82$ or 82% chance of differential expression. In both the cDNA and Affymetrix microarray experiments, there were few, if any, transcripts with a B-value of 0 (representing a 50% chance of differential expression). However, B-statistics have been used successfully in previous microarray experiments used to investigate the transcriptional profiles of different members of a natural population of *Populus*

nigra. In this particular experiment, the B-value was 5 (representing a 99% chance of differential expression), and more than 300 ESTs met this criterion (L. Graham, unpublished data). This stark contrast clearly demonstrates that either [eCO₂] has little effect on gene expression, or that microarrays are not an appropriate technique for assessing such transcript profiles.

In order to further explore the microarray data available, the expression data for candidate genes were extracted based on fold-change rather than statistical significance. The variability in the expression of ESTs representing the same gene model was illustrated in Figure 7.3.7 and 7.3.9. This approach was useful for gaining greater insight into the effects of [eCO₂] on particular genes of interest, but the variability of the data uncovered this way demonstrated why this approach is not appropriate for analysing microarray data.

7.4.7 The CO₂ response

The results presented in this chapter have provided further evidence that [eCO₂] induces rather few significant changes in the leaf transcript profile. This has been the general conclusion from previous results in trees (Taylor *et al*, 2005; Gupta *et al*, 2005; Druart *et al*, 2006). A similar result has also been shown in *Arabidopsis* ecotypes (Miyazaki *et al*, 2004). In this particular experiment, there were 152 and 186 transcripts that were up-, and down-regulated, respectively. The functional categories of the up-regulated transcripts included; metabolism (17%), defense (10%), redox control (6%) and unknown function (50%). The results from the experiment suggested that fluctuations in the local environmental conditions at the FACE site contributed to the results for the transcript profiles (also hypothesized to be a contributory factor to the results of the transcriptomic study at the EUROFACE site, described in Chapter 5). In the experiment described in this chapter, CTCs were used in order to reduce the impact of environmental heterogeneity associated with field grown crops. However, the resounding message remains the same; [eCO₂] induced few changes in the transcript profile of *Populus* leaves.

7.5 Conclusion

The use of microarrays is an important genetic tool for identifying patterns of gene expression. Whilst their ability to detect subtle expressional differences may be limited (due in part to the multiple stages where errors may be introduced), it is still an excellent technique to be used as a screen, allowing for more in-depth investigation to follow up any initial findings from phenotypic analyses.

The results have also shown that the type of microarray platform used greatly determines the data outcome. The assessment of young leaves by cDNA microarrays suggested that *P. deltoides* showed the greatest expressional differences, whereas *P. trichocarpa* was the most responsive according to the Affymetrix data. This further shows that adequate experimental design and data interpretation are extremely important in such studies.

CHAPTER 8

The proteome of *Populus* grown in [eCO₂]

8.0 Overview

The general consensus in the literature suggests that elevated atmospheric [CO₂] promotes plant growth. However, previous results in this thesis have illustrated that there are rather few changes in gene expression as a result of this environmental perturbation. This therefore leads to the question of where is this growth control regulated? Is it truly regulated at the transcriptional level and microarrays are simply not sensitive enough to detect the changes? Is it due to post-translational modifications? The answers to such questions are not known. In this chapter, a proteomics experiment was conducted in order to study differences in protein expression between *P. deltoides* and *P. trichocarpa* grown in [aCO₂] and [eCO₂].

The leaf material was collected from semi-mature leaves of *P. deltoides* and *P. trichocarpa* grown in the CTC experiment described in Chapter 6. Two-dimensional gel electrophoresis experiments (2-DE) were used to assess the protein profiles of these samples. The results of the analysis showed that [eCO₂] had no effect on protein expression in either species. Therefore the answer to the underlying mechanics guiding the response to increased carbon availability remains to be elucidated.

Despite this result, the experiment in this chapter presented a unique opportunity to study differential protein expression between the two, highly divergent, *Populus* species. A total of 140 proteins were statistically significantly differently expressed between *P. deltoides* and *P. trichocarpa*. The proteins were identified using tandem mass spectrometry. Differentially expressed proteins included antioxidants and those involved in photosynthesis.

8.1 Introduction

Proteomics is an analytical tool used for determining the protein complement of the genome. It is an increasingly important technology, particularly in the field of ecological genomics, where important questions and concepts that are central to our understanding of biological systems remain to be answered. The use of transcriptomics alone is not sufficient to address such issues given the large number of transitions associated with the progression from transcript to functional protein (e.g. post-translational modifications). Furthermore, transcript abundance does not correlate with translated protein levels (Gygi *et al*, 1999). However, proteomics and transcriptomics are not mutually exclusive technologies. Integrated with metabolomics, these technologies constitute a ‘systems biology’ approach to understanding biological variability.

Biological systems are hierarchical, beginning at the level of DNA and progressing through mRNA, proteins, protein interactions, informational pathways, informational networks, cells, networks of cells (tissues), organisms, populations of organisms and finally, ecologies (Ideker *et al*, 2001). ‘Systems biology’ is an all-encompassing term used to describe the integration of information from these different levels (termed the ‘system elements’) in order to build a picture of the biological system.

The immense progress in molecular biology in recent years has led to the generation of a vast amount of data from a plethora of experiments examining the effects of various biotic and abiotic stresses. The use of technologies such as DNA sequencing, transcriptomics and proteomics have permitted a global (or near global) assessment of individual system elements (Ideker *et al*, 2001). However, in the ‘post-genomics’ era there is also now a need to understand functionality within the context of a living organism (Minorsky, 2003). Associated with the increase in information gained from experiments on various system elements, there is a concomitant necessity to improve bioinformatics for modelling the system. It is the modelling of the system (i.e. creation of an ‘*in silico* plant’) that will result in a greater understanding of plant growth and development, rather than examining the system elements in isolation (Minorsky, 2003; Kitano 2002).

Proteomics is a particularly important platform since it removes some of the assumptions and ambiguity surrounding transcriptomic studies (Thomas and Klaper, 2004). The technology provides the link between the protein complement and the underlying genetics. There are a

number of different strategies that may be adopted in proteomic assessments, which fall into two general categories; gel-based and non gel-based. The non gel-based techniques include ICAT (Gygi *et al*, 1999) and ITRAQ (Ross *et al*, 2004; Zieske, 2006). The most commonly reported proteomic platform for studies in plants is the gel-based 2-DE (two-dimensional gel-electrophoresis) method (O'Farrell, 1975; Scheele *et al*, 1975; Klose, 1975). In such experiments, proteins are separated in the first dimension by differences in pH, and further separated in the second dimension according to individual molecular weight.

The majority of plant proteomic studies conducted to date have focussed on crop plants particularly in relation to water stress, e.g. grape (Vincent *et al*, 2007), rice (Salekdeh *et al*, 2002; Ali and Komatsu, 2006), and maize (Riccardi *et al*, 2004). Proteomic studies in forest trees are becoming more frequent, with reports of 2-DE analyses in pine (Gion *et al*, 2005) and in *Populus* following drought stress (Plomion *et al*, 2006). Given the promise for this technology and the clear merits of its application, there are surprisingly few studies of the proteome upon plant growth in [eCO₂]. To the best of my knowledge, such an analysis has only been conducted in *Arabidopsis* (Bae and Sicher, 2004) but not in forest trees. This experiment therefore represents the first experiment of its kind to try and reveal the effects of increased carbon availability by examining the protein complement of the genome.

Previous studies into individual protein changes in relation to growth in [eCO₂] have particularly focussed on differences in photosynthetic proteins such as Rubisco (e.g. Sicher *et al*, 1994). A general down-regulation of photosynthesis and lowered leaf nitrogen content is associated with growth in an enriched CO₂ atmosphere. It has been estimated that Rubisco constitutes 25% of total leaf nitrogen (Webber *et al*, 1994) and it has been shown that Rubisco protein content is reduced in [eCO₂] (Chen *et al*, 2005; Cheng *et al*, 1998). Furthermore, the transcripts that encode Rubisco (e.g. *rbcS* and *rbcL*) are also reduced in [eCO₂] (Cheng *et al*, 1998). Given the fact that Rubisco is the most abundant protein on Earth (Drake *et al*, 1997) and ultimately determines the photosynthetic capabilities and hence overall productivity of the plant, such detailed research into its behaviour under future atmospheric conditions is warranted. However, this is only one story within the protein elements of the system. It is likely that other important proteins are also differentially expressed when exposed to an enriched CO₂ environment, although their identities remain to be elucidated. It is known that the content of photosynthetic proteins (other than Rubisco) within the system are altered in response to growth in an enriched CO₂ atmosphere. For example, the regeneration of RuBP,

(as well as the carboxylation of RuBP) is known to limit photosynthetic capabilities (Chen *et al.*, 2005). It may therefore be predicted that the Calvin Cycle proteins involved in the regeneration of RuBP would also differ in [eCO₂].

From the results reported previously in this thesis and those available in the literature, the general consensus is that [eCO₂] stimulates plant growth. However, this cannot be explained by large changes in the transcript levels as assessed by transcriptomic studies (Chapters 5 and 7). Perhaps the sensitivity of such a technique is not adequate for such studies, or perhaps it is not at the level of the gene where the control is regulated.

Here, a 2-DE proteomic analysis of semi-mature leaves of *P. deltoides* and *P. trichocarpa* exposed to [eCO₂] in the CTC experiment (described in Chapter 6) is described. To the best of our knowledge this is the first time such an approach has been tested in forest trees exposed to [CO₂] predicted for 2050.

8.2 Materials and Methods

The leaf material was obtained from the CTC experiment described in Chapter 6. Leaf age four (where age one was defined as the first fully unfurled leaf on day one of the experiment) was sampled from four biological replicates of *P. deltoides* and *P. trichocarpa* from each experimental treatment (thus representing 16 leaf samples). The material was obtained from the same biological replicates used for the microarray analysis (and to construct the spatial leaf profile) described in Chapter 7. The leaves were sampled on the 17th August 2006 (43 DFE).

8.2.1 Protein extraction

Protein extraction was performed on the 16 leaf samples. Frozen leaf material was finely ground in liquid nitrogen using a pestle and mortar. Approximately 500mg of tissue was transferred to a 10ml Oakridge tube (pre-weighed), to which 8ml of cold precipitation buffer (10%TCA and 0.07% β mercaptoethanol in acetone) was added. The sample was homogenised by inversion and the proteins were precipitated by storing the vial at -20°C overnight (with inversion whenever possible).

Following precipitation, the samples were centrifuged at 12,000x g (-4°C) for 30 minutes. The supernatant was removed and the resultant pellets were washed twice with 10ml of cold rinsing buffer (0.07% β -mercaptoethanol in acetone). The tubes were inverted to facilitate mixing and to ensure thorough washing of the pellet. The samples were stored at -20°C for two hours for the washing steps and then centrifuged at 12,000x g (-4°C) for 30 minutes. The ensuing supernatant was removed and the pellets were dried under vacuum (200mbar). When the pellets were dry (after approximately three hours) the samples were reduced to a powder using a glass stick. The tubes were re-weighed in order to calculate the weight of the pellet from the original weight of the tube.

The solubilisation buffer (8M Urea, 2M thiourea, 2% CHAPS, 1% DTT, 0.5% proteinase inhibitor cocktail, 1% ampholytes 4-7 and 3-11 in dH₂O) was added to the powdered sample (from 5 to 15 μ l solubilization buffer per mg tissue in order to obtain approximately 1.5ml of solubilised pellet). The samples were centrifuged (12,000 x g for 10 minutes) and the supernatant was transferred into a fresh 2ml microfuge tube. The protein extract (supernatant) was stored at -20°C until use.

8.2.2 Protein quantification

The concentration of protein was quantified by spectrophotometry using the RC DC protein assay (Bio-Rad, California, USA) according to the manufacturer's recommendation. Briefly, the dye reagent was prepared by diluting one part of the dye solution to four parts of distilled de-ionized water. The solution was filtered through Whatman #1 filter paper to remove any particulates. Ovalbumin was used to create the protein standards and to calculate the protein concentration of each sample. In total, seven ovalbumin standards were prepared, representing 1 to 50µg protein. 10µl of each protein sample were transferred into a clean cuvette. 3.5ml of the diluted dye reagent was added to the cuvette and the solution was allowed to incubate at room temperature for 15 minutes. The absorbance was measured at 595nm on a Genesys 10 Bio UV-Vis spectrophotometer (Thermo Electron Corporation, Massachusetts, USA). Each protein sample was assayed twice. Its protein content was estimated using the mean of both measures.

8.2.3 1-DE gels

The quality of the protein extraction was assessed using SDS-PAGE (2 mini gels with 10 wells each, and a loading capacity of 20µl). The 10% acrylamide resolving gel (40% acrylamide/bis-acrylamide (37.5:1) (25%), 1.5M tris (pH8.8) (25%), SDS (0.1%), MQ water (47.5%), TEMED (0.1%), and APS (0.05%)) was cast into a gel rig. A small volume of isobutanol was added to the gel after it had been cast to ensure a smooth, flat surface layer. Once set, the isobutanol was removed and the 4% acrylamide stacking gel (40% acrylamide/bis-acrylamide (37.5:1) (10%), 0.5M Tris (pH6.8) (25%), SDS (0.1%), MQ water (65%), TEMED (0.1%), and APS (0.05%)) was cast directly on top of the running gel. For loading, 1µl sample was added to 99µl Laemmli mix (0.5M Tris-HCl (pH 6.8), 10% SDS, 10% glycine, 5% 2-β mercaptoethanol, trace of blue bromophenol). From this mix, 20µl was loaded onto the gel. Molecular markers were loaded in the spare wells. Both gels were run at the same time in Laemmli running buffer (25mM Tris, 0.2M glycine, 0.1M SDS in dH₂O) for 85 min at 25mA, until the blue bromophenol reached the bottom of the gel.

1-DE gels were silver-stained according to the following protocol. They were fixed using a solution containing 50% ethanol and 5% acetic acid in dH₂O. After 30 minutes, the gels were washed using a 50% ethanol solution. After 10 minutes, the gels were washed with distilled water and left for a further 10 minutes. The gels were transferred into a sensitising solution (0.02% sodium thiosulphate in dH₂O) for one minute. This was followed by two washes (each

of one minute) with distilled water. The gels were incubated in a 0.1% solution of silver nitrate (chilled to 4°C prior to use) for 20 minutes. The gels were washed twice with distilled water (one minute for each stage). The gel was transferred into a developing solution (0.04% formalin, 2% sodium carbonate in dH₂O) for approximately ten minutes when the desired level of band staining had been achieved. A 5% acetic acid solution was used to stop the reaction (10 minutes). The gels were scanned following a final wash in dH₂O for five minutes on a M141 Image Scanner using the LabScan software (Amersham Biosciences, Buckinghamshire, UK).

8.2.4 2-DE gels

IEF was conducted using 24cm IPG strips with a linear pH range of 4-7 (Bio-Rad) using an IEF Protean cell (Bio-Rad). The strips were in-gel rehydrated with the protein extract as follows. They were left for 2 hours to allow for passive rehydration before adding paper wicks at each electrode and actively completing the rehydration for 12 hours at 50V. The focusing programme was ; 30 minutes at 200V with linear ramping, 30 minutes at 500V with linear ramping, 1h at 1000V with linear ramping and 9000V for 90000Vh with rapid ramping.

Each protein extract was run in duplicate. Prior to running the SDS-PAGE, the strips were equilibrated for 15 minutes in 30% glycerol, 6M urea, 50mM Tris-HCl pH 8.8, 2% SDS, 1% DTT followed by 15 minutes in the same buffer in which DTT had been replaced with 2.5% iodoacetamide. SDS-PAGE was run in an 11% acrylamide (40% acrylamide/bis-acrylamide (37.5:1) (27.5%), piperazine diacrylamide (0.3%), 2M Tris (pH8.8) (0.5M), SDS (0.15M), MQ water (46%), TEMED (0.5%), and APS (0.03%)) home cast gel (24x20cm) using an Ettan system in which up to 20 gels can be run in parallel. Once equilibrated, the strips were transferred on top of the 2-D gels and sealed with a 1% hot agarose solution (diluted in Laemmli running buffer with a trace of blue bromophenol). The gels were run overnight according to the following programme ; 20V for one hour followed by 150V for 12 hours. At the end of the run, the blue bromophenol line had reached the bottom of the gel.

The gels were stained using the Prot1Sil stain kit (Sigma-Aldrich, Suffolk, UK) according to the manufacturer's instructions, outlined here. The gels were fixed in a solution containing 50% ethanol, 10% acetic acid in dH₂O for at least one hour. The fixing solution was removed and replaced with a 30% ethanol solution and washed for 30 minutes. The gel was washed for a further 30 minutes in dH₂O. The ethanol was decanted and replaced with a sensitisation

solution (1ml 'Proteosilver Sensitizer' solution in 99ml dH₂O per gel). After 10 minutes the gel was washed twice with dH₂O (10 minutes per wash). The gels were stained (1ml 'Proteosilver Silver' solution in 99ml dH₂O per gel) for 10 minutes and immediately washed for one minute with dH₂O. The gels were developed (5ml 'ProteoSilver Developer 1', 0.1ml 'Proteosilver Developer 2' in 95ml dH₂O per gel) for up to 10 minutes, until the appropriate level of staining had been achieved. The developing was stopped with 5ml 'ProteoSilver Stop Solution' (per gel) and incubated for five minutes. Finally the gel was washed with dH₂O and scanned immediately.

8.2.5 Image analysis

Each scanned image was saved as a .TIFF file. A total of six replicates per species per treatment (thus representing a total of 24 gels) were used for further analysis. The image analysis was conducted using the Progenesis SameSpot software, PG240 (Nonlinear Dynamics, Newcastle Upon Tyne, UK). A common reference was selected from the gel portfolio (representing *P. deltooides*, [eCO₂]). For alignment purposes, each gel was 'warped' onto this single reference gel in Progenesis. Once aligned, spots were detected using the automatic function within the software. This was followed by a manual check, to ensure the perimeter boundaries encompassed a single protein spot only. Where necessary, spots were manually divided using the cutting tools available in the software.

The background was corrected using the 'Lowest on Boundary' option in Progenesis. Here the background per spot was calculated by tracing a line outside its boundary. The lowest pixel intensity within this area was deemed the background intensity for that spot. The data was normalised using the 'Total Spot Normalisation' option in Progenesis. Here, the volume of each spot was divided by the total volume of spots in the image and a scaling factor was applied to this value. The scaling factor was calculated by multiplying the spot value by the total area of all spots across the images. This method compensated for differences in spot densities.

8.2.6 Statistical analyses

A full factorial ANOVA was performed on the normalised value for each protein in order to determine whether treatment effects in the two species were of significance. The ANOVA analysis was conducted using the statistical programming language R (www.r-project.org) according to the following linear model:

$$y_{ij}=G_i + T_j + (GT)_{ij} + \varepsilon_{ij}, \quad (1)$$

where y_{ij} denotes protein level measured for species i , and treatment j , with $1 \leq i \leq 2$, and $1 \leq j \leq 2$. The terms G_i , and T_j measure the effect of the species and treatment, respectively. The interaction term $(GT)_{ij}$ accounts for the interaction between species and treatment and ε_{ij} accounts for residual variance. An adjustment for the false discovery rate (Benjamini and Yekutieli, 2005) was made on the p -values of the individual effects. Any protein spot with an adjusted p -value of $p < 0.001$ associated to a specific effect was deemed to have a significant change attributed to the specified effect.

The results of this analysis showed that there were 140 proteins that were differentially expressed between the species. There were no proteins that were differentially expressed as a result of treatment in either species.

Following the statistical analysis of the results, each of the 140 proteins was manually checked in Progenesis in order to validate the results. A total of 96 spots were selected for identification. The selections were based upon statistical significance and by a manual inspection of the spots in the computer software.

Each selected spot was manually excised and transferred into a 96 well plate. The spots were sampled in duplicate and the sample plate was stored at -20°C until required.

8.2.7 In-gel digestion

To destain each spot, 75 μl of potassium ferricyanide (2% w/v) and 75 μl sodium thiosulphate (3.2% w/v) were pipetted into each sample well. After approximately ten minutes (when all spot stain had disappeared), the solution was removed and the spots were washed three times with dH_2O (150 μl for each wash), until the colour had disappeared. 150 μl acetonitrile (100%)

was added to each sample well in order to dehydrate the spots. After ten minutes, the solution was removed and the samples were left to dry at room temperature for 20 minutes. For the digestion, 20µg trypsin was eluted in 200µl HCl (1mM) and 450µl of ammonium bicarbonate (50mM) was added. 20µl of the solution was added to each well and left at 37°C overnight.

To extract the hydrophilic peptides, 10µl of ammonium bicarbonate (50mM) was added to each well and left at room temperature. After ten minutes the resulting solution was transferred to a new sample plate. 10µl of a solution containing acetonitrile (47.5%) formic acid (5%) and dH₂O (47.5%) was added to the original sample plate to extract hydrophobic peptides. After ten minutes the resulting solution was transferred to the second sample plate along with the hydrophilic peptide extract. The wash with the acetonitrile/ formic acid/ dH₂O solution was repeated thrice more. After the final wash the plate was placed in a speedvac to reduce the volume to 25µl per well. Finally, 1.20µl of formic acid was added to each sample in the plate.

8.2.8 Protein identification

The peptide mixtures were analysed by on-line capillary HPLC (LC Packings, Amsterdam) coupled to a nanospray LCQ ion trap mass spectrometer (ThermoFinnigan, San Jose, California). 10µl of peptide digest was loaded onto a 300µm x 5mm C18 PepMap trap column (Dionex). The peptides were eluted from the trap column onto a 75µm inner diameter x 15cm C18 PepMapTM column (LC Packings) in solvent A. Peptides were eluted using a 0–40% linear gradient of solvent B (solvent A was 0.1 % formic acid in 5% acetonitrile and solvent B was 0.1% formic acid in 80% acetonitrile) in 35 minutes. The separation flow rate was set at 200nl min⁻¹. The mass spectrometer was operated in positive ion mode at a 2kV needle voltage and a 3V capillary voltage.

Data acquisition was performed in a data-dependent mode, alternating a full scan MS over the *m/z* range 300-1700, a zoom scan on most intense ion, and a full scan MS/MS on that ion. MS/MS data were acquired using a 2 *m/z* unit ion isolation window at 35% relative collision energy.

The resulting data were examined with SEQUEST using the BioWorks 3.3.1 software (ThermoFinnigan). The protein database was composed of data from all available tissues from The Institute for Genomic Research (TIGR) (<http://compbio.dfci.harvard.edu/tgi/cgi->

bin/tgi/gimain.pl?gudb=poplar) and information on the sequenced genome available from JGI (http://genome.jgi-psf.org/Poptr1_1/Poptr1_1.home.html). This produced a total of 314,640 sequences. The search parameters within the software were set to allow for two missed trypsin cleavages. Only the proteins containing two or more matched peptide sequences were retained for further analysis. Any redundant sequences were removed from the analysis. Finally, the data was BLASTed against the Swiss Prot sequence database. The data may be accessed at the following web address; <http://cbi.labri.fr/outils2/MassAnalysis/PopulusCO2/>.

8.3 Results

The results from the 2-DE experiment showed that there were no proteins that were significantly different between plants grown in [eCO₂] and those in controlled conditions (Figure 8.3.1 and 8.3.2). However, further analysis revealed 140 proteins that were significantly different between the two species in the investigation; *P. deltoides* and *P. trichocarpa*. A total of 96 spots were selected for peptide identification purposes (Figure 8.3.3).

8.3.1. Identifying CO₂ responsive proteins

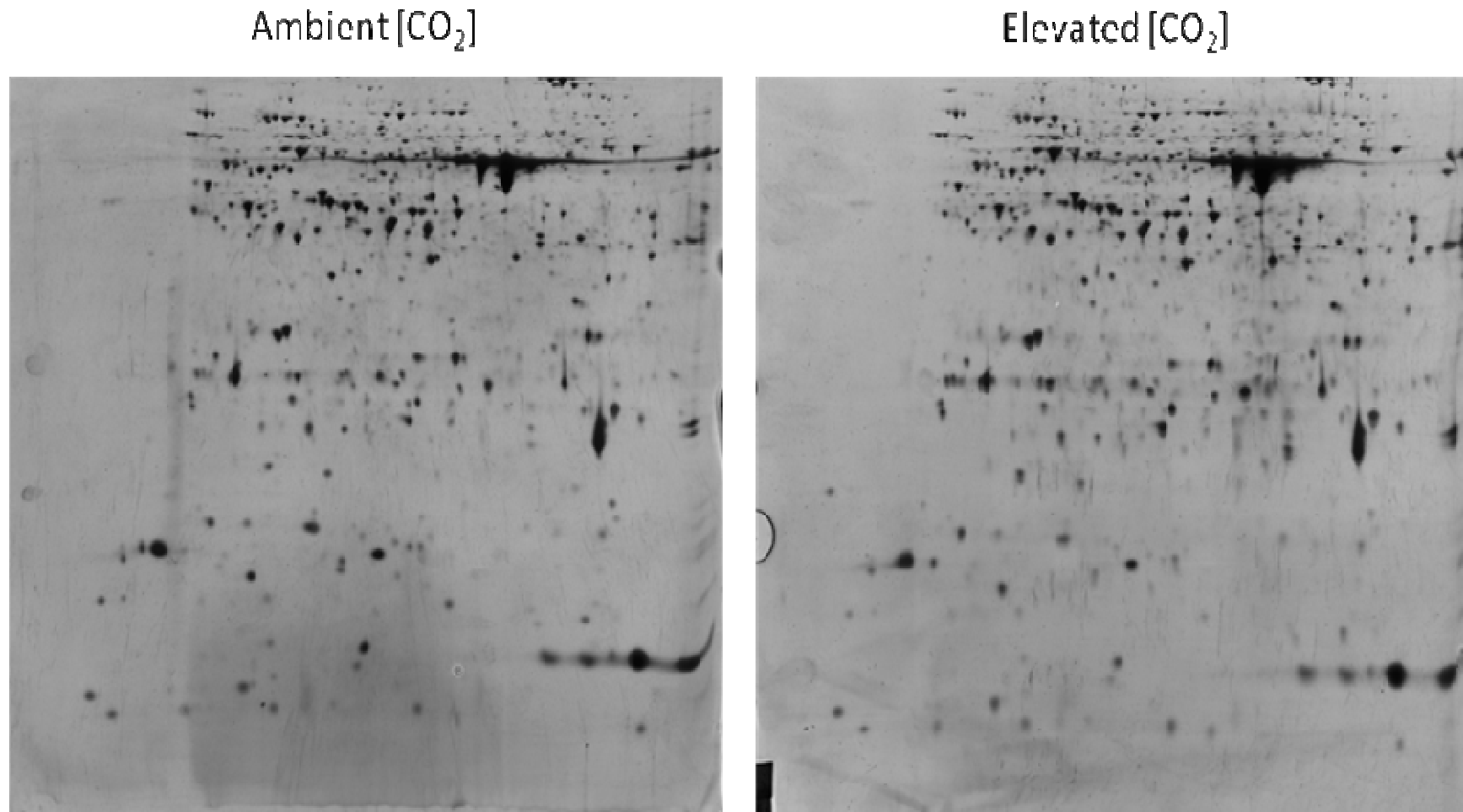


Figure 8.3.1. Representative 2-DE gels from leaf tissue of *P. deltoides* grown in [aCO₂] (left panel) and [eCO₂] (right panel). The results from the statistical analysis showed that there were no CO₂-responsive proteins in *P. deltoides*.

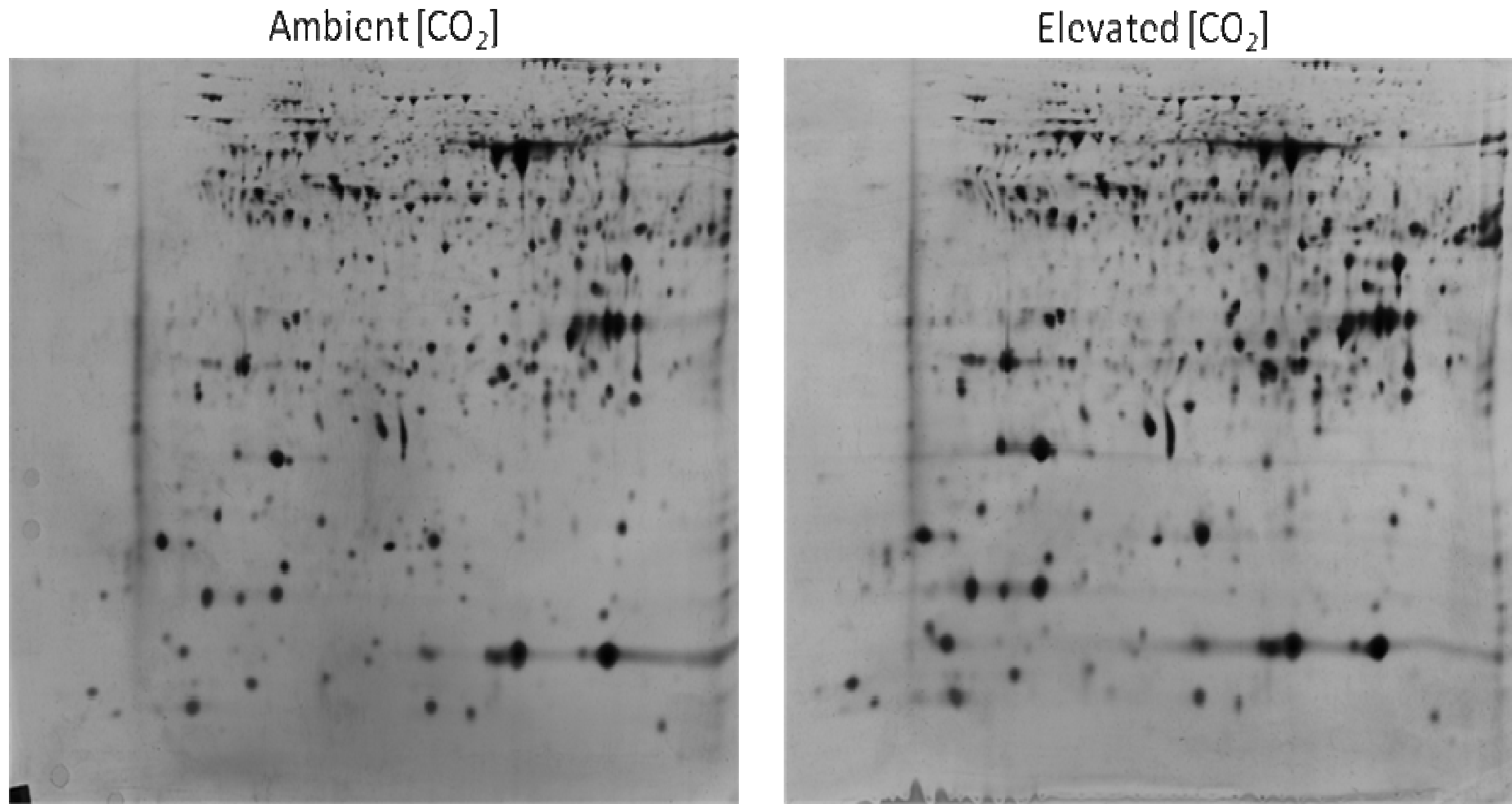


Figure 8.3.2. Representative 2-DE gels from leaf tissue of *P. trichocarpa* grown in [aCO₂] (left panel) and [eCO₂] (right panel). The results from the statistical analysis showed that there were no CO₂-responsive proteins in *P. trichocarpa*.

8.3.2. Species-specific protein expression

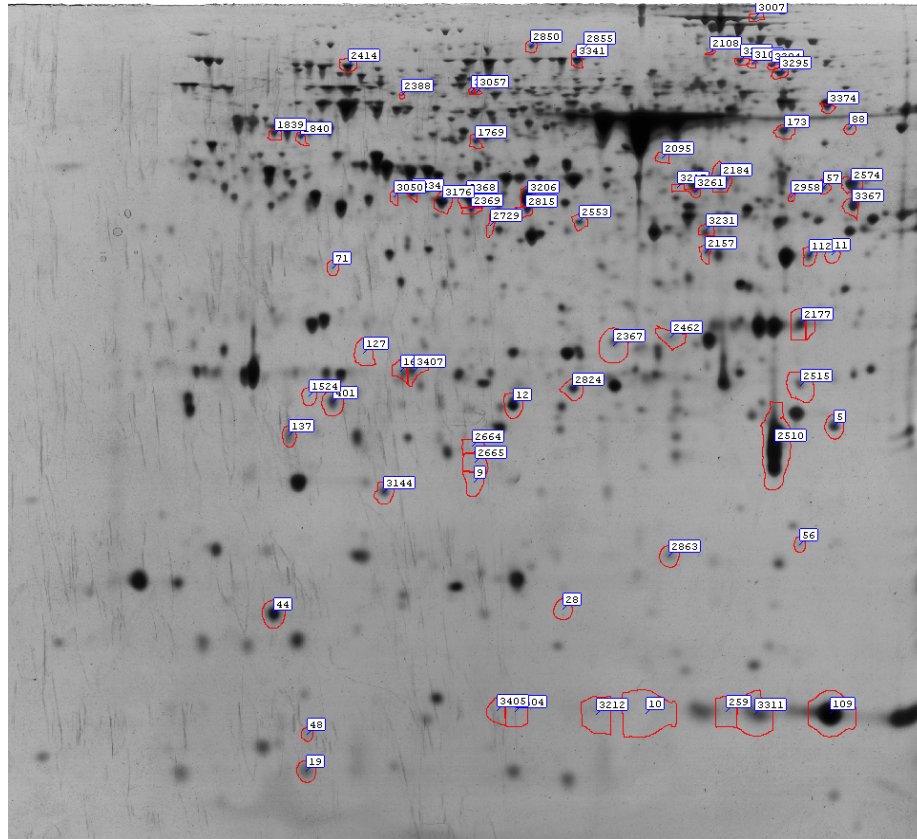
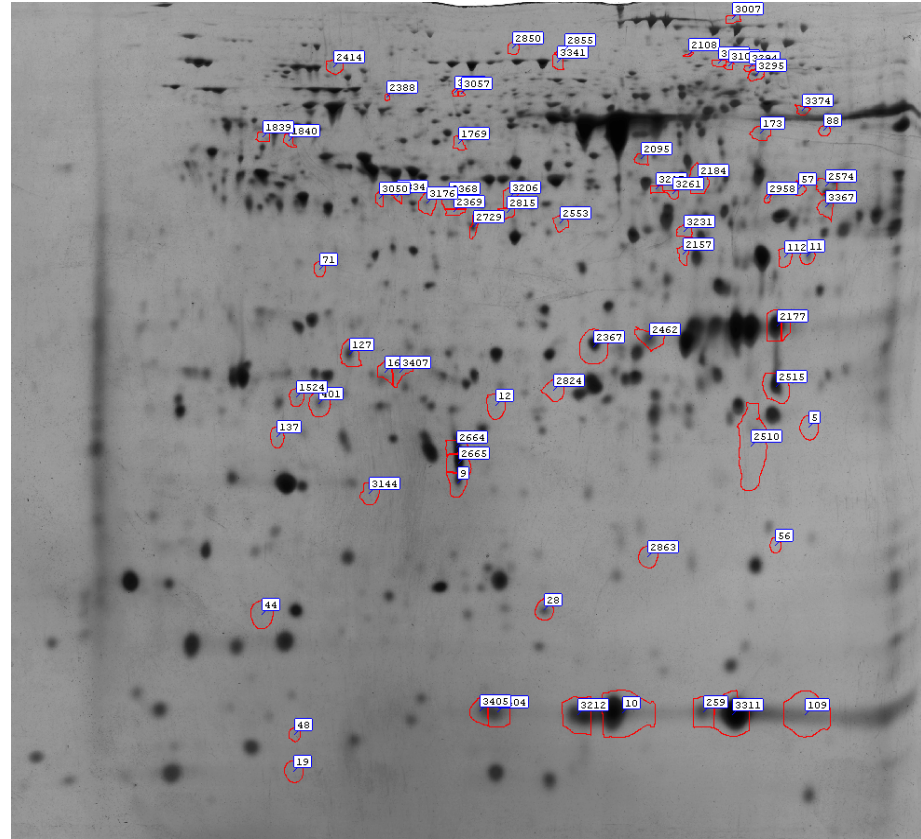
Populus deltoides*Populus trichocarpa*

Figure 8.3.3. Representative 2-DE gels from leaf samples collected from *P. deltoides* (left panel) and *P. trichocarpa* (right panel). The position of each spot that was identified for excision is indicated by a red perimeter, along with its identification number. In particular cases multiple excisions were made per spot.

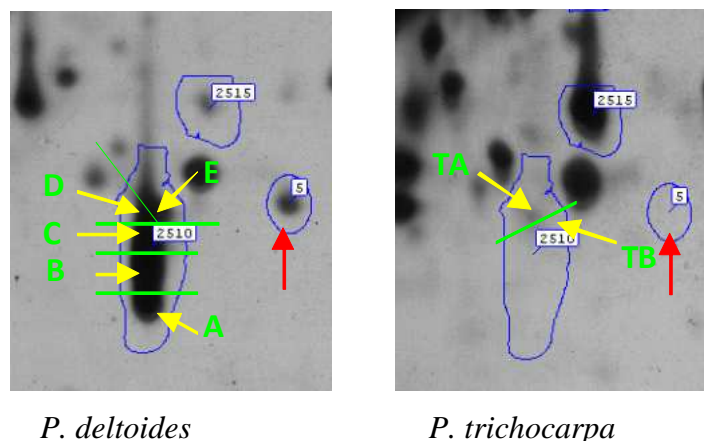














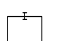

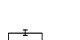


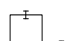



Figure 8.3.4. In some instances, the software was unable to differentiate spot boundaries, clearly visible to the human eye. The spot detection was therefore subsequently completed manually following a visual inspection of the gels. The example here (spot ‘2510’) shows one such example. In *P. deltooides* (left frame) the spot was detected by the software (blue perimeter line) but manually cut (green lines). This therefore led to the excision of five spots (A-E, yellow arrows) from the initial spot. Two spots were also detected in *P. trichocarpa* (right frame) which were also excised and identified using tandem mass spectrometry. This diagram also shows an example of the presence/absence of certain spots (red arrows) depicting species specific expression. Here spot ‘5’ was present in *P. deltooides*, but absent in *P. trichocarpa*.

The full annotations for the spots that were identified by MS/MS are provided in Table 8.3.1. In total there were 22 proteins that were identified as more highly regulated in *P. trichocarpa* and 52 in *P. deltooides*. However, in 15 cases, multiple excisions were made per spot and in two cases (spots 2177 and 2510), excisions in both species were necessary. This was in order to clarify whether the same protein was represented, or whether the presence of one protein was masking the identification of a second (Figure 8.3.4).







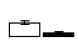

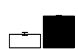


Chapter 8

Spot id	Rel. Abundance	Replicate	Accession number	Annotation	pI	No. Peptides	Score	%Coverage	MW
5			P12858	Glyceraldehyde-3-phosphate dehydrogenase A, chloroplast	6.63	2	20.24	6.42	50278.3
9			P40602	Anter-specific proline-rich protein APG	5.54	1	10.23	3.55	54010.9
10		10A	P24007	Ribulose biphosphate carboxylase small chain, chloroplast	6.07	15	40.28	17.75	31062.8
		10B	P24007	Ribulose biphosphate carboxylase small chain, chloroplast		2	20.20	7.43	36591.7
11			P51103	Dihydroflavonol-4-reductase	6.63	8	60.21	20.94	35587.4
12			P40602	Anter-specific proline-rich protein APG	5.66	9	40.26	8.77	54010.9
19			Q9LUV2	Putative protein Pop3	5.04	6	40.25	18.01	24884.7
25			P40602	Anter-specific proline-rich protein APG	5.05	4	20.26	6.26	54010.9
28			Q07796	Superoxide dismutase [Cu-Zn]	5.81	2	20.20	9.29	30135.5
44		44A	Q93VR4	MLP-like protein 423	4.94	3	30.21	14.75	27445.6
		44B	Q93VR4	MLP-like protein 423		5	40.24	18.85	27445.6
48			P48384	Thioredoxin M-type, chloroplast	5.04	4	40.25	12.58	33488.0


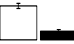




Chapter 8

56			Q64152	Transcription factor BTF3	6.53	4	40.29	25.44	25025.5
57			Q8S4Y1	Acetyl-CoA acetyltransferase, cytosolic 1	6.60	6	60.28	19.42	47136.2
71			P83941	Transcription elongation factor B polypeptide 1	5.12	7	70.28	12.40	74398.8
88			Q53196	Uncharacterized aminotransferase y4uB	6.68	8	70.25	17.51	56516.4
109		109A	P24007	Ribulose biphosphate carboxylase small chain, chloroplast	6.62	21	80.28	22.46	31062.8
		109B	P24007	Ribulose biphosphate carboxylase small chain, chloroplast		19	70.25	22.10	31062.8
112		112A	P51103	Dihydroflavonol-4-reductase	6.56	4	40.21	13.86	37850.3
		112B	P51103	Dihydroflavonol-4-reductase		4	40.21	16.73	30556.8
127		127 A	Q811Q2	Chloride intracellular channel 6	5.21	2	20.21	8.23	46282.7
		127B	Q0DYB1	Soluble inorganic pyrophosphatase		3	30.22	11.00	34681.6
137		137A	P12360	Chlorophyll a-b binding protein 6A, chloroplast	4.99	2	20.20	4.26	36191.8
		137B	P12360	Chlorophyll a-b binding protein 6A, chloroplast		4	40.24	10.03	36191.8
173			P34106	Alanine aminotransferase 2	6.48	15	120.24	24.53	53475.2
259			A4GYR8	Ribulose biphosphate carboxylase large chain	6.31	1	10.21	2.30	53052.9
401			P22302	Superoxide dismutase [Fe], chloroplast	5.12	4	40.22	10.48	48439.6

Chapter 8

1524		Q1PER6	L-ascorbate peroxidase 2, cytosolic	5.05	3	30.23	13.62	43462.9		
1612		Q9ZT66	Endo-1,3;1,4-beta-D-glucanase	5.32	2	20.22	11.58	28007.2		
1769		Q96520	Peroxidase 12	5.55	9	70.29	17.18	54098.3		
1839		P52914	Nucleoside-triphosphatase	4.94	3	30.24	9.74	41200.7		
1840		P52914	Nucleoside-triphosphatase	5.02	3	30.27	9.74	41200.7		
2095		O95340	Bifunctional synthetase 2	3'-phosphoadenosine	5'-phosphosulfate	6.12	4	40.22	13.85	47287.8
2108		P45730	Phenylalanine ammonia-lyase	6.26	5	50.21	8.66	86974.9		
2157		P28475	NADP-dependent D-sorbitol-6-phosphate dehydrogenase	6.24	3	30.21	8.33	43873.6		
2177		2177T	A4GYR8	Ribulose biphosphate carboxylase large chain	6.54	16	100.25	19.21	53052.9	
		2177DA	A4GYR8	Ribulose biphosphate carboxylase large chain		4	40.21	10.23	53052.9	
		2177DB	A4GYR8	Ribulose biphosphate carboxylase large chain		3	30.23	7.10	53052.9	
2184		2184A	P12859	Glyceraldehyde-3-phosphate dehydrogenase B, chloroplast	6.29	9	80.28	21.02	48168.8	
		2184B	P12859	Glyceraldehyde-3-phosphate dehydrogenase B, chloroplast		14	130.29	36.73	48168.8	
2334		P40602	Anter-specific proline-rich protein APG	5.36	4	40.24	11.90	54010.9		

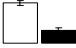

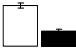


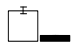

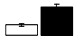
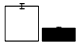


Chapter 8

2367		2367A	A4GYR8	Ribulose biphosphate carboxylase large chain	5.97	6	50.23	12.73	53052.9
		2367B	A4GYR8	Ribulose biphosphate carboxylase large chain		4	40.22	11.06	53052.9
2368			P40602	Anter-specific proline-rich protein APG	5.52	28	50.27	11.90	54010.9
2369			P40602	Anter-specific proline-rich protein APG	5.54	4	40.27	11.90	54010.9
2388			P53285	Vacuolar protein sorting-associated protein	5.33	8	80.20	20.88	59725.1
2414			P26413	Heat shock 70 kDa protein	5.16	5	50.24	12.75	72179.9
2462			A4GYR8	Ribulose biphosphate carboxylase large chain	6.14	12	120.26	22.96	53052.9
2510		2510A	O04011	Auxin-binding protein ABP20	6.46	6	50.20	15.85	27909.5
		2510B	O04011	Auxin-binding protein ABP20		9	50.16	15.85	27909.5
		2510C	O04011	Auxin-binding protein ABP20		8	50.17	15.80	27909.5
		2510D	O04011	Auxin-binding protein ABP20		6	50.19	15.47	27909.5
		2510E	P35017	Superoxide dismutase [Mn], mitochondrial		3	30.25	16.10	25660.9
		2510TA	Q96266	Glutathione S-transferase 6, chloroplast		4	40.20	13.56	52825.0
		2510TB	P35017	Superoxide dismutase [Mn], mitochondrial		6	50.30	27.95	25660.9
2515		2515A	P27140	Carbonic anhydrase, chloroplast	6.53	7	50.25	28.57	30959.8
		2515B	P27140	Carbonic anhydrase, chloroplast		8	70.25	36.07	30959.8
2553			Q9ZUC1	Quinone oxidoreductase-like protein At1g23740, chloroplast	5.87	8	80.25	24.08	46699.3

Chapter 8

2574		2574A	P12859	Glyceraldehyde-3-phosphate dehydrogenase B, chloroplast	6.68	17	130.29	33.41	48168.8
		2574B	P12859	Glyceraldehyde-3-phosphate dehydrogenase B, chloroplast		9	90.28	25.88	48168.8
2664			O81304	Probable plastid-lipid-associated protein 11, chloroplast	5.54	2	20.25	19.88	19480.1
2665			O04011	Auxin-binding protein ABP20	5.55	3	20.16	11.06	21543.8
2729			P12858	Glyceraldehyde-3-phosphate dehydrogenase A, chloroplast	5.60	4	40.25	14.52	53926.5
2815			P40602	Anter-specific proline-rich protein APG	5.70	4	40.26	11.90	54010.9
2824			Q811Q2	Chloride intracellular channel 6	5.84	13	100.27	26.88	46282.7
2850			Q8R146	Acylamino-acid-releasing enzyme	5.72	2	20.26	9.87	43120.9
2855			Q6MD85	4-hydroxy-3-methylbut-2-en-1-yl diphosphate synthase	5.88	10	100.25	15.38	82329.4
2863			Q9ASS6	Peptidyl-prolyl cis-trans isomerase CYP20-2, chloroplast	6.13	8	60.24	13.39	47644.9
2958			P52901	Pyruvate dehydrogenase E1 component subunit alpha-1, mitochondrial precursor	6.50	11	110.24	27.23	43419.3
3007			P20967	2-oxoglutarate dehydrogenase E1 component, mitochondrial	6.40	3	30.24	3.62	115876.7
3050			P51118	Glutamine synthetase cytosolic isozyme 1	5.31	3	30.25	7.43	52043.9

Chapter 8

3056		P43309	Polyphenol oxidase, chloroplast	5.54	5	50.21	14.33	67200.2
3057		Q9LQI7	Probable complex I intermediate-associated protein 30	5.56	10	90.26	19.06	65986.1
3109		O65351	Subtilisin-like protease	6.38	4	40.17	7.06	70843.8
3144		Q02758	ATP synthase delta chain, chloroplast	5.27	3	20.22	10.30	35804.9
3176		P14656	Glutamine synthetase cytosolic isozyme 1-1	5.45	7	70.25	15.63	51728.9
3206		3206A P40602	Anter-specific proline-rich protein APG	5.71	9	70.25	27.20	42294.6
		3206B P40602	Anter-specific proline-rich protein APG		15	80.30	21.33	42294.6
3212		3212A P17067	Carbonic anhydrase, chloroplast	5.92	1	10.20	4.77	49181.9
		3212B P17067	Carbonic anhydrase, chloroplast		1	10.20	4.77	49181.9
3217		P12859	Glyceraldehyde-3-phosphate dehydrogenase B, chloroplast	6.16	13	130.30	35.18	48168.8
3231		Q00874	DNA-damage-repair/toleration protein DRT100	6.25	3	30.18	8.28	47729.8
3261		Q93ZN9	LL-diaminopimelate aminotransferase, chloroplast	6.21	6	50.28	17.73	44519.0
3286		O23627	Glycyl-tRNA synthetase 1, mitochondrial	6.35	17	160.25	24.49	76958.0

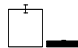
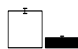




3294		Q43468	Heat shock protein STI	6.45	17	140.26	28.06	65503.4	
3295		P34105	NADP-dependent malic enzyme	6.47	15	120.25	20.05	81916.6	
3311		3311A 3311B	P24007 P24007	Ribulose biphosphate carboxylase small chain, chloroplast Ribulose biphosphate carboxylase small chain, chloroplast	6.39	2 4	20.35 40.37	9.39 9.46	30721.4 36008.4
3341		Q43848	Transketolase, chloroplast	5.86	12	110.25	20.98	68851.5	
3367		P12858	Glyceraldehyde-3-phosphate dehydrogenase A, chloroplast	6.69	18	100.26	23.98	50278.3	
3374		Q9M5K2	Dihydrolipoyl dehydrogenase 2, mitochondrial	6.61	17	170.33	38.29	69809.2	
3404		P24007	Ribulose biphosphate carboxylase small chain, chloroplast	5.67	1	10.24	7.07	31199.9	
3405		P24007	Ribulose biphosphate carboxylase small chain, chloroplast	5.62	1	10.19	3.25	30721.4	
3407		Q9ZT66	Endo-1,3;1,4-beta-D-glucanase	5.37	2	20.21	10.42	25851.4	

Table 8.3.1. The full annotation from the MS/MS data analysis. The relative abundance of the spot was calculated from the normalised data output from Progenesis (see section 8.2.5). The white bars represent *P. deltoides* and the black bars represent *P. trichocarpa* (± 1 standard error). The percentage coverage, number of peptides, score and molecular weight were all obtained from the SEQUEST data output. The percentage coverage represents the amino acid coverage of the predicted protein. The score represents a value based upon the probability that the peptide was a random match to the data in the SEQUEST database. The pI was estimated from the position of the spot on the gel. The numbers of peptides identified for each protein are also indicated in the table.

In order to consolidate the annotation information, the data for each species were grouped according to GO annotation available using the Blast2GO software (Conesa *et al*, 2005). The GO annotations for the significantly differentially expressed proteins are shown in Figure 8.3.5 and Figure 8.3.6. The results clearly indicate a large difference in functional roles of the proteins that were found to be differentially expressed between the two species. In *P. trichocarpa*, the selected proteins were found to fall into five main categories; protein binding, transferase activity, hydrolase activity, nucleotide binding and signal transducer activity. In *P. deltoides* however, the proteins represented 17 functional categories. In this case the highest proportion of proteins were categorised as having oxidoreductase activity. However, in *P. trichocarpa*, the highest proportion of proteins were categorised as ‘protein binding’.

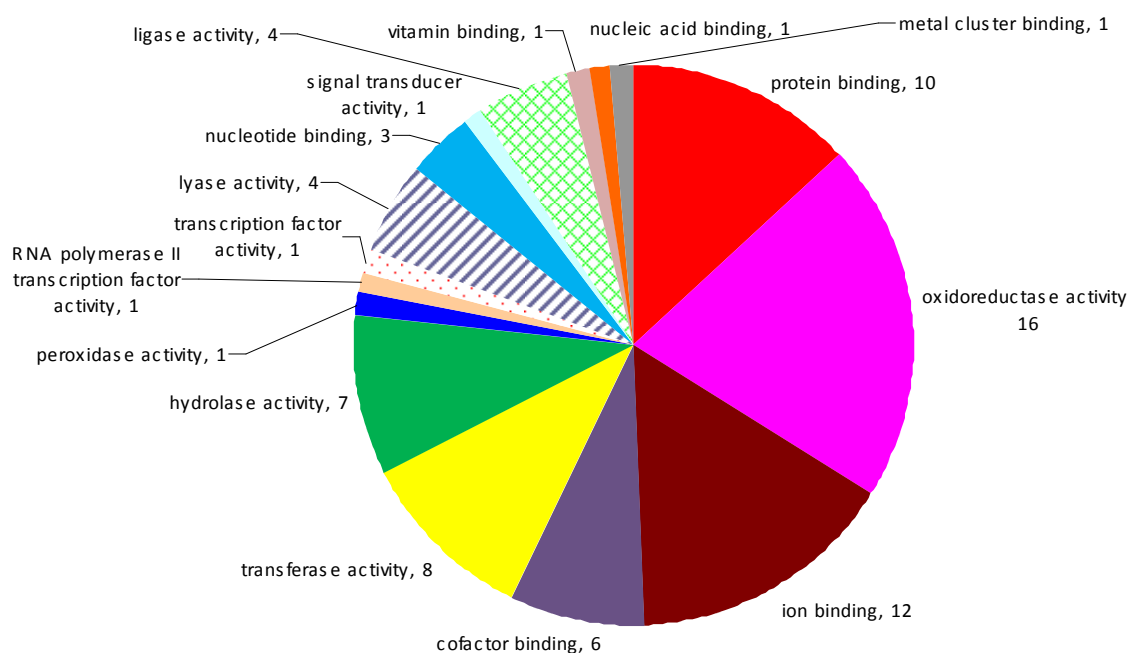


Figure 8.3.5. The GO results for protein spots with a higher abundance in *P. deltoides*. Each segment of the chart is labelled with a molecular function category, along with the number of proteins that fall into that category. All GO annotations were retrieved using the Blast2GO software.

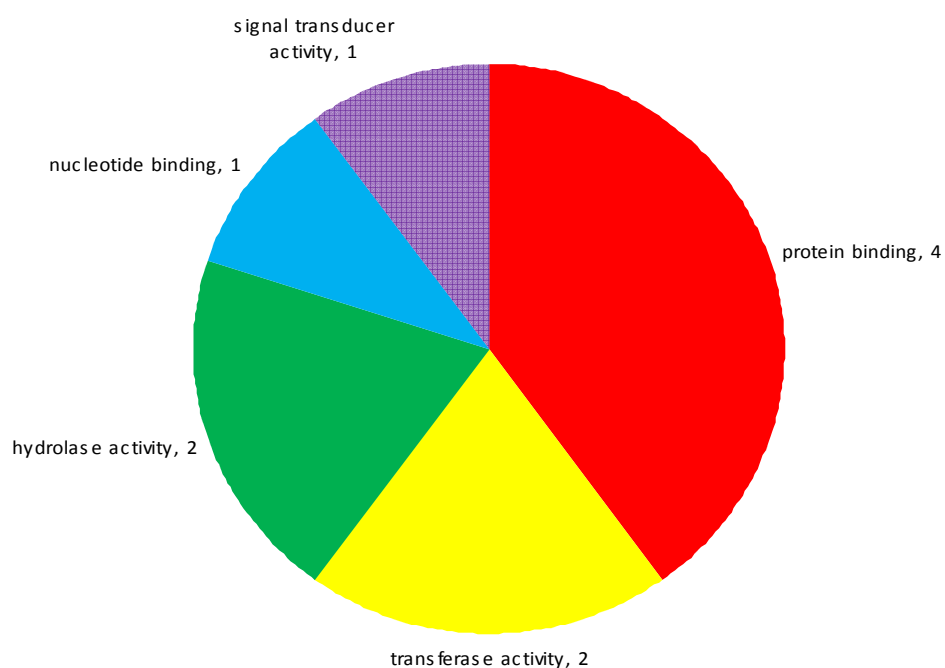


Figure 8.3.6. The GO results for protein spots with a higher abundance in *P. trichocarpa*. Each segment of the chart is labelled with a molecular function category, along with the number of proteins that fall into that category. All GO annotations were retrieved using the Blast2GO software.

8.4 Discussion

The aim of this experiment was primarily to use proteomics to identify any differentially expressed proteins in *P. deltoides* and *P. trichocarpa* grown in an enriched CO₂ environment. This represented the first study of its kind and was a natural progression from a number of previous attempts to identify differentially expressed transcripts in plants grown in [eCO₂] (for example, see Chapter 7; Taylor *et al*, 2005; Gupta *et al*, 2005; Druart *et al*, 2006).

8.4.1. Proteomics and [eCO₂]

The general consensus from various transcriptomic studies in plants grown in an enriched CO₂ environment is that there are few changes in gene expression levels. It has been predicted that this may be due to post-translational modifications (Taylor *et al*, 2005). A proteomics experiment was constructed in order to determine whether [eCO₂] elicited changes in protein profiles.

This study represented the first of its kind by investigating protein profiles of *Populus* grown in [eCO₂]. Historically, 2-DE gels have been widely used as a means of identifying differences in protein profiles. There are a number of non-gel based alternatives available, such as ICAT (Isotope Coded Affinity Tags) (Tao and Aebersold, 2003; Gygi *et al*, 1999) and iTRAQ (Isobaric Tags for Relative and Absolute Quantification) (Applied Biosystems, www.appliedbiosystems.com; Ross *et al*, 2004; Zieske *et al*, 2006). However, despite the fact that there are some limitations associated with the use of 2-DE gels, the advantages of its use in primary studies such as this are unquestionable.

Previous applications of 2-DE gels in proteomics have included drought (Salekdeh *et al*, 2002), high temperature (Ferreira *et al*, 2006), low temperature (Amme *et al*, 2006) and salt stress (Kav *et al*, 2004). There has only been a single report of using 2-DE gels to identify CO₂-responsive proteins in plants (Bae and Sicher, 2004). In this study of the *Arabidopsis* proteome, there were no spots that were consistently present in one treatment and not the other. The six proteins that they identified by analysis of the 2-DE gels and characterized by MS/MS were a myrosine precursor, luminal binding protein II, 3-β hydroxysteroid dehydrogenase/isomerase protein, nucleoside diphosphate kinase II, major latex related-protein and photosystem II oxygen evolving complex 23. However, since the proteins that were identified in the study were present in both treatments, it was concluded that [eCO₂] did not have a

major affect on protein expression in *Arabidopsis* (Bae and Sicher, 2004). Similarly, the results from this experiment in *Populus* have also shown that [eCO₂] has no affect on the protein profile of either species.

The identification of proteins whose abundance differed as a result of [eCO₂] was conducted using a statistical significance of $p > 0.001$. Whilst this is a particularly stringent analysis, this level of significance has been used in other studies on *Populus* (e.g. Plomion *et al*, 2006). Reducing the stringency of the statistics would increase the risk of type II error. The results do reinforce those of the two transcriptomic studies presented in this thesis (Chapters 5 and 7), where it was shown that there were no major changes in gene expression due to exposure to [eCO₂]. Therefore the cause of the changes in plant morphology as a result of growth in [eCO₂] is still to be answered. As suggested previously, it is possible that trees demonstrate a plastic response to [eCO₂] or that a number of small changes in gene/protein expression act additively to affect growth responses. However, both suggestions are merely speculative.

8.4.2. Interspecific differences in protein profiles

Despite the fact that the main aim of this study was to identify CO₂-responsive proteins, a secondary set of results illustrated the interspecific differences in protein profiles of *P. deltoides* and *P. trichocarpa*. Of the spots that were selected for identification by MS/MS, 52 demonstrated higher abundance in *P. deltoides* and 22 in *P. trichocarpa* (Table 8.3.1). It is particularly interesting that the proteins that were identified were categorized into different functional groups. It is possible that the different functional roles of the proteins in *P. deltoides* and *P. trichocarpa* represent their different geographical origins. *P. deltoides* originates from the warm, dry climates of the South-East of the United States of America, whilst *P. trichocarpa* originates from the North-West, where it is subjected to milder, wetter conditions (Figure 3.1.1).

A number of previous studies have used proteomics as a means of unraveling the complex nature of population biology. For example, 2-DE gels have been used to study natural variation in eight *Arabidopsis* ecotypes (Chevalier *et al*, 2004). This study permitted the identification of the major proteins in each ecotype. This allowed each ecotype to be distinguished from others by their characteristic protein profiles. Different isoforms of the same protein were also identified in this study. This was also the case with some of the

proteins identified in *P. deltoides* and *P. trichocarpa*, where the same protein (characterized by its accession number) was excised from different spots in different locations on the gel, thus having different molecular weight/ pI (e.g. see dihydroflavanol reductase (P51103), Glyceraldehyde-3-phosphate dehydrogenase B (P12859) and endo-1,3; 1,4-beta-D-glucanase (Q9ZT66) in Table 8.3.1).

In *P. trichocarpa*, a number of photosynthetic proteins were identified, such as the small (P24007) and large (A4GYR8) chain subunits of Ribulose biphosphate carboxylase. This links in with previous data that has shown high photosynthetic rates in this species (as compared to *P. deltoides*) (Rodriguez-Acosta, 2006). The proteins of particular abundance in *P. deltoides* included those involved in glycolysis (e.g. Glyceraldehyde-3-phosphate dehydrogenase), hormone signaling (auxin-binding protein), photosynthesis (Ribulose biphosphate, transketolase, chlorophyll a-b binding protein), and cell wall growth (endo-1,3; 1,4-beta-D-glucanase).

8.4.3. Leaf ontogeny

This experiment was conducted on developing leaves (age 4) in both species because it was hypothesized that the effect of [eCO₂] would have maximal difference at that stage during ontogeny. However, one of the limitations associated with this experiment, and on work with these species in general, is the assumption that the leaves of the two different species were of the same developmental age. The two species do have different growth strategies and it is possible that the leaves were of slightly different stages of development. This therefore means that the proteins that were identified may not have been species specific, but due to differences in leaf ontogeny.

8.4.4. Proteomics and population biology

The use of proteomics in studies of population variance has also encompassed the mapping of Protein Quantitative Loci (PQL) onto the genome (Thiellement *et al*, 1999). Protein quantity may be regarded as a quantitative trait, and with the availability of segregating populations and genetic maps, it is possible to locate genomic regions of interest (Thiellement *et al*, 1986; Costa and Plomion, 1999).

Given the fact that there is an F₂ mapping population available from the *P. deltoides* x *P. trichocarpa* (Family 331 (Bradshaw and Stettler, 1993)) it is certainly possible that a similar

approach may be taken in order to investigate the genetic determination of protein products in *Populus*.

8.5 Conclusion

Whilst there are some limitations associated with the use of 2-DE gels, in this particular case they were an invaluable tool for the first experiment to investigate changes in protein expression in *Populus* leaves as a result of exposure to [eCO₂]. It was clear that there were no differences in protein profiles due to growth in [eCO₂] in either *P. deltoides* or *P. trichocarpa*. This result was not entirely unexpected given the lack of support for changes in gene expression due to [eCO₂] that have been presented both in previous chapters of this thesis and also in the literature. However, it is particularly interesting that this experiment has permitted the identification of proteins whose abundance differed between the two species. This is the first time this has been done in these two species. The wide genetic resources (e.g. pedigree mapping population and a genetic map) that are available mean that further experiments may be conducted in the future in order to investigate the genetic determination of protein quantity in *Populus*.

CHAPTER 9

General discussion

9.1 Thesis overview

This thesis has examined the response of *Populus* to [eCO₂] by utilising a combination of analytical techniques. *Populus* is a model tree genus and hence a perfect candidate for assessing the effects of [eCO₂] on plant growth and development. There are thousands of reports in the literature regarding the effects of [eCO₂] on plant morphology and physiology. There are also reports of using cDNA microarrays to assess transcriptional changes (e.g. Druart *et al*, 2006; Gupta *et al*, 2005). However, the work detailed here has integrated methods to examine plant growth and development, gene expression (including both cDNA microarrays and Affymetrix oligonucleotide chips) and, for the first time, protein profiles. This thesis is unique in the fact that it represents the first attempt to begin to develop a 'systems biology' approach to understanding the growth and habit of *Populus* in [eCO₂].

The studies were conducted on three different species of the *Populus* genus; *P. x euramericana*, *P. deltoides* and *P. trichocarpa*. Two different experimental design systems were used to expose the trees to [eCO₂]; FACE rings and CTCs. *Populus euramericana* has been used in a long-term FACE study (EUROFACE) aimed at elucidating differences in carbon sequestration as a result of growth in a high CO₂ environment (www.unitus.it/euroface). Previous studies have shown that this species was responsive to [eCO₂] (e.g. Ferris *et al*, 2001; Taylor *et al*, 2003) and hence it was a suitable candidate for one of the first experiments of its kind, which aimed at identifying genes (through the use of cDNA microarrays) involved in the response. *Populus deltoides* and *P. trichocarpa* have also been shown to positively respond to increased carbon availability (Rae *et al*, 2007), and, due to their contrasting growth mechanisms, were also used to further identify mechanisms governing the response to [eCO₂].

The results showed that leaf growth was slightly stimulated by [eCO₂], particularly in young leaves. Interestingly, the cellular analysis indicated that cell expansion, rather than cell division, increased due to [eCO₂]. The results from the transcriptomic studies consistently showed that there were few transcripts whose expression differed significantly between [aCO₂] and [eCO₂]. This was confirmed by a proteomic study where it was found that there were no proteins whose abundance differed significantly between *P. deltoides* and *P. trichocarpa*.

9.2 Morphological changes in [eCO₂]

Leaf growth was slightly stimulated by [eCO₂] but this was dependent upon leaf age (Figure 6.3.1). The majority of studies that have been reported to date have generally demonstrated growth stimulation due to [eCO₂]. For example, there are reports of almost a 300% increase in leaf area as a result of CO₂ exposure in *P. trichocarpa* (Rae *et al*, 2006). The maximal percentage increase was in the youngest leaves of *P. deltoides* (80%, table 6.3.1) but the stimulation diminished with time.

Perhaps the most interesting result from the morphological data was that of the cellular analyses. The results in Chapter 3 highlighted the different leaf cellular strategies employed by *P. deltoides* and *P. trichocarpa*. The leaves of *P. deltoides* contain a large number of small cells compared to *P. trichocarpa*, which has a smaller number of large cells (Figure 3.3.7, Figure 3.3.8). However, the increased cell size in Figure 6.3.5 showed that cell expansion was stimulated in [eCO₂]. Conversely, the cells of *P. trichocarpa* did not increase in size. It is possible that under ambient atmospheric conditions, these cells were as large as they could possibly be and application of further CO₂ had no affect due to a physical constraint on cell size.

It has long been suggested that XETs play a key role in the growth response to [eCO₂] (e.g. Ferris *et al*, 2001). Using the *P. deltoides* and *P. trichocarpa* samples from the BangorFACE experiment it was finally possible to test this theory. The quantification of XET activity was shown to be increased in [eCO₂] in *P. deltoides*, the species that attains final leaf size by cell production. This therefore suggested that cell expansion was affected by increased carbon availability (a result that was clearly seen in the cell growth analyses in Chapter 7). Furthermore, transcripts encoding cell wall loosening factors (e.g. *ENDOXYLOGLUCAN TRANSGLYCOSYLASE*) were up-regulated in [eCO₂] (Chapter 5). The XET/XTHs represent a large gene family (reviewed in Rose *et al*, 2002). It is likely that there is a degree of redundancy between family members therefore an accurate measure of expression is difficult. Given the evidence presented here, perhaps a further targeted investigation into XET/XTH expression and/or cell wall biosynthesis pathways as a result of CO₂ exposure is now warranted.

9.3 Microarrays and [eCO₂]

Two microarray experiments were presented in this thesis, one of which involved *P. x euramericana*, and the other involved *P. deltoides* and *P. trichocarpa*. The general trend in the results suggested that any phenotypic differences were not reflected by substantial changes in gene expression. This was observed interspecifically suggesting that it represented a consistent trend in *Populus* species. The first transcriptome study in *P. x euramericana* (Chapter 5) showed that any changes in gene expression were more dependent upon leaf age rather CO₂ treatment (Taylor *et al.*, 2005). The lack of CO₂-responsive genes was mirrored in *P. deltoides* and *P. trichocarpa* (Chapter 7), although in this case the magnitude of the CO₂ response observed was dependent upon the microarray platform chosen.

9.3.1 An additive effect?

A possible explanation for the observed responses to [eCO₂] is that there are a large number of transcripts involved in the CO₂ response, all of which have a small additive effect upon growth. This prediction would indeed support the theory that plants maintain their usual function when grown in an enriched carbon environment and it may simply be a case that they increase the ‘machinery’ necessary to photosynthesize at a faster rate. If this is the case, microarrays may not be sensitive enough or provide enough information to assess gene expression on samples exposed to [eCO₂].

9.3.2 Magnitude of the response and experimental design

Experiments have shown that increasing the [CO₂] from 400 ([aCO₂]) to 1200 μmol mol⁻¹ caused greater differences in gene expression than at a concentration of 800 μmol mol⁻¹ (Druart *et al.*, 2006). This highlights the importance of designing the experiment to address the hypothesis in question. For example, the aim of the paper by Druart (2006) was to find CO₂ responsive genes by exaggerating the [CO₂] to concentrations that are unlikely to be experienced. In this thesis however, the aim was to model responses to future atmospheric conditions and so a [CO₂] of 550 ppm was used as a target. The differences in leaf growth reported in this thesis may have been too small to detect any transcriptional differences. Perhaps expression studies with samples demonstrating extreme differences in leaf area (such as a 300% difference in the case of *P. trichocarpa* reported in Rae *et al.*, (2007)) may have highlighted more CO₂-responsive transcripts.

9.3.3 Phenotypic plasticity

As defined by Helmuth *et al.* (2005), the effects of climate change on species response can broadly be categorised into three mechanisms;

- 1) Genetic adaptation via natural selection (a slow irreversible change in allele frequency in a population)
- 2) A rapid physiological response (a reversible 'short-term' solution)
- 3) Phenotypic plasticity

Phenotypic plasticity may be defined as the ability of a genotype to produce diverse phenotypes in response to an environmental change. The differences between phenotypes may be due to behavioural, morphological or physiological changes. Such responses confer increased tolerance to differing environments and hence enhanced fitness under such conditions. Therefore if high fitness can be achieved by a plastic response, there is no requirement for directional selection and no adaptive differentiation from the source (Price *et al.* 2003).

In plants, phenotypic plasticity is an important mechanism by which they have the ability to withstand environmental heterogeneity. This therefore presents a problem for scientists, since the mechanisms controlling organ size are complicated by the fact that plant morphogenesis includes plasticity in order to allow adaptation to changing environmental conditions (Horiguchi *et al.* 2005). In one particular example the D-type cyclins, which were shown to be differentially regulated in [eCO₂] (Chapter 7), have been proposed as key proteins that enable flexibility as environmental conditions fluctuate (Francis, 2007) hence lending support to the notion that plant plasticity governs the response to [eCO₂].

Phenotypic plasticity may improve organismal performance, but it may not necessarily improve fitness (Helmuth *et al.* 2005). For example, plasticity may involve a trade-off in a particular aspect of growth or development, such as a reallocation of resources. Alternatively, it may affect complex biological interactions, thus altering community dynamics (Helmuth *et al.* 2005). By this reasoning, building a better picture of the transcriptional response to [eCO₂] would require the integration of other aspects of plant morphology, such as stems and roots. For example, it is likely that [eCO₂] causes a change in the root to shoot ratio (Curtis and Wang, 1998). Therefore future studies should involve investigating changes from the perspective of the whole plant, rather than appendages in isolation.

9.3.4 Technical limitations associated with microarrays and [eCO₂] studies.

Microarrays are an extremely useful technique for assessing gene expression. However, the results obtained will only ever be as representative of the probes that are attached to the platform for hybridisation. The results in Chapters 5 and 7 clearly showed that the type of microarray platform chosen greatly influences the results of the analysis. In Chapter 5, the comparison of two different microarray platforms showed that there were 6322 consistent gene models represented on both the POP2 and PICME cDNA microarray platforms. Only five gene models demonstrated a consistent two-fold regulation between the two platforms is astonishing, especially given the fact that the samples represented the same biological replicates at the EUROFACE site. In Chapter 7 the data was filtered according to gene model in order to identify those that were consistently regulated between cDNA and oligonucleotide microarray platforms. In the case of the cDNA microarrays, *P. deltoides* appeared to be the species that was most responsive to [eCO₂] since it demonstrated a greater number of transcripts with two-fold differences in expression between the controlled and treated samples. However, when young leaves of both species were hybridised onto Affymetrix microarrays it was *P. trichocarpa* that demonstrated the greater response, with no overlapping transcripts between the cDNA and Affymetrix microarrays. Although the samples hybridised onto the Affymetrix microarray constituted different biological replicates and different leaf ages (Affymetrix, age one; cDNA, meristematic tissue or age two), this difference between the two is remarkable.

CO₂ is required for photosynthesis in order to provide the energy needed for survival. By increasing the concentration of this gas, photosynthesis will still occur and the plant will still undertake all of the processes required to maintain productivity. Therefore the question arises; ‘Are microarrays sensitive enough to detect relative changes in gene expression as a result of CO₂ exposure?’ Given the number of standardisation stages required in a microarray experiment, would an absolute measure of gene expression be more appropriate in such studies? During the process of a microarray experiment, and in the subsequent statistical analysis, the material in question is measured and standardised. For example, for the hybridisation one begins with x mg of tissue to extract RNA, and then y μ g RNA is used to synthesize cDNA and the samples are subsequently combined. Following hybridisation, the data is normalised (Quackenbush, 2002) in order to reduce variability. Perhaps it is the nature of the numerous standardisation stages during the progress of the experiment that influences the final result. Perhaps a more sensitive technique such as qPCR is more appropriate. Indeed,

there were similarities as well as discrepancies between qPCR and microarray data (Chapter 5). However, qPCR is only possible with a prior set of identified candidate genes, a process which usually involves the use of microarray data, although a literature-based filter for candidate genes is also appropriate.

9.4 Proteomics and [eCO₂]

The proteomics experiment in Chapter 8 was the first of its kind to assess protein abundance in *Populus* samples grown in [eCO₂]. The only other study in the literature used 2-DE gels to assess the protein profile of *Arabidopsis* grown in [eCO₂] (Bae and Sicher, 2004). The results presented here showed that there were no proteins that differed in abundance between [aCO₂] and [eCO₂], thus confirming the results from the microarray experiments. Further experiments could be conducted on the protein samples in order to confirm this initial finding. For example experiments could be conducted on mature leaf samples rather than young, expanding leaves.

9.5 Future directions

9.5.1 Leaves, stems and roots

Carbon allocation will depend on a number of different factors, including the availability of other resources such as light, water, soil nutrients (Körner *et al*, 2006). The availability of resources may drive allocation to other parts of the plant such as roots, stems and reproductive organs, as well as leaves. Furthermore, it is likely that the longevity of carbon being retained in these organs is likely to be highly variable. Therefore decoupling leaves from other possible organs as avenues for carbon assimilation may be too restrictive and a more integrated approach is more appropriate. Conducting further studies on leaves, stems and roots could provide further information as to the effects of [eCO₂] on overall plant growth and development.

9.5.2 Yield extreme genotypes

The results of the phenotypic behaviour of the plants in [eCO₂] showed that there were rather small changes in growth. The greatest differences between the controlled and the treated plants were seen in the yield extreme genotypes from Family 331, in Chapter 6. This has highlighted an important area of future research. Given the current interest in the potential of forest trees to mitigate the effects of increased atmospheric [CO₂], it is particularly interesting to note that genotypes categorised as low-yielding responded to a greater degree to [eCO₂].

Perhaps it will be possible to identify the mechanisms regulating the response to [eCO₂] in these extreme genotypes, since they exhibit the most marked changes in growth.

9.6 Closing statement

The results presented in this thesis have capitalised on the availability of a wide range of genetic and genomic resources. It represents the first experiment of its kind by using a combination of morphological, transcriptomic and proteomic analyses to assess the response of *Populus* to [eCO₂]. It has unearthed some interesting and rather unexpected results and paved the way for further focussed studies to be conducted.

PUBLICATIONS

Publications arising from the work in this thesis

The transcriptome of *Populus* in elevated CO₂. 2005. Taylor G, Street NR, Tricker PJ, Sjödin A, **Graham LE**, Skogström O, Calfapietra C, Scarascia-Mugnozza G, Jansson S. *New Phytologist*. **167**; 143- 154.

The potential of genomics and genetics to understand plant responses to elevated atmospheric [CO₂]. 2006. Taylor G, Tricker PJ, **Graham LE**, Tallis MJ, Rae AM, Trewin H, Street NR. *In*; Managed Ecosystems and CO₂. Case Studies, Processes and Perspectives. Edited by; Nösberger J, Long SP, Norby RJ, Stitt M, Hendrey GR, Blum H. Springer-Verlag Berlin Heidelberg. pp351-371.

Presentations given on work from this thesis

Plant growth and development in a high CO₂ world. 2007. *Oral presentation*. Postgraduate symposium, University of Southampton, UK.

Leaf development and senescence in elevated CO₂: linking transcriptomics and QTL analysis. 2006. *Oral presentation*. IUFRO-COST Action meeting, Madrid, Spain.

Ecological genomics- finding the genes that are sensitive to rising CO₂. 2006. *Poster presentation*. Postgraduate symposium, University of Southampton, UK.

Plant growth and the cell cycle in a high CO₂ world. 2006. *Poster presentation*. SEB Cell Cycle meeting, University of Southampton. UK.

Other publications arising during the writing of this thesis

Limited response of the *Populus* transcriptome and proteome to elevated CO₂. **Graham LE**, Vincent D, Street NR, Plomion C, Claverol S, Barre A, Jansson S, Taylor G. *In preparation*.

Why are some leaves big? Linking transcript, QTL and LD approaches to understand the genetic control of leaf size in *Populus*. Trewin H, Zaina G, Street NR, **Graham LE**, Rae AM, Stenacker M, Viger M, Bastien C, Morgante M, Taylor G. *In preparation*.

QTL for growth and development in elevated carbon dioxide in two model plant genera: a novel approach for understanding plant adaptation to climate change? Rae AM, **Graham LE**, Street NR, Hughes J, Hanley ME, Tucker J, Taylor G. *In preparation*.

REFERENCES

- Agrawal GK, Rakwal R, Yonekura M, Kubo A, Saji H.** 2002. Proteome analysis of differentially displayed proteins as a tool for investigating ozone stress in rice (*Oryza sativa* L.) seedlings. *Proteomics*. **2**; 947-959.
- Aharoni A, Vorst O.** 2001. DNA microarrays for functional plant genomics. *Plant Molecular Biology*. **48**; 99-118.
- Ainsworth EA, Long SP.** 2005. What have we learned from 15 years of free-air CO₂ enrichment (FACE)? A meta-analytic review of the responses of photosynthesis, canopy properties and plant production to rising CO₂? *New Phytologist*. **165**; 351-372.
- Ainsworth EA, Rogers A, Nelson R, Long SP.** 2004. Testing the “Source-Sink” hypothesis of down-regulation of photosynthesis in elevated [CO₂] in the field with single gene substitutions in *Glycine max*. *Agricultural and Forest Meteorology*. **122**; 85-94.
- Ainsworth EA, Rogers A, Vodkin LO, Walter A, Schurr U.** 2006. The effects of elevated CO₂ on soybean gene expression. An analysis of growing and mature leaves. *Plant Physiology*. **142**; 135-147.
- Ali GM, Komatsu S.** 2006. Proteomic analysis of rice leaf sheath during drought stress. *Journal of Proteome Research*. **5**; 396-403.
- Amme S, Matros A, Schlesier B, Mock HP.** 2006. Proteome analysis of cold stress response in *Arabidopsis thaliana* using DIGE-technology. **57**; 1537-1546.
- Appenzeller L, Doblin M, Bareiro R, Wang HY, Niu XM, Kollipara K, Carrigan L, Tomes D, Chapman M, Dhugga KS.** 2004. Cellulose synthesis in maize: isolation and expression analysis of the cellulose synthase (CesA) gene family. *Cellulose*. **11**; 287-299.
- Arabidopsis Genome Initiative.** 2000. Analysis of the genome sequence of the flowering plant of *Arabidopsis thaliana*. *Nature*. **408**; 796-815.
- Arnott D.** 2001. Basics of triple stage quadrupole/ion trap mass spectrometry: precursor, product and neutral-loss scanning. Electrospray ionisation and nanospray ionisation. In *Proteome Research: Mass Spectrometry*. Edited by James P. Springer-Verlag Berlin Heidelberg. pp 14-31.
- Asshoff R, Zotz G, Körner C.** 2006. Growth and phenology of mature temperate forest trees in elevated CO₂. *Global Change Biology*. **12**; 848-861.
- Aubert D, Chevillard M, Dorne AM, Arlaud G, Herzog M.** 1998. Expression patterns of GASA genes in *Arabidopsis thaliana*: the GASA4 gene is up-regulated by gibberellins in meristematic regions. *Plant Molecular Biology*. **36**; 871-883.
- Bae H, Sicher R.** 2004. Changes in soluble protein expression and leaf metabolite levels in *Arabidopsis thaliana* grown in elevated carbon dioxide. *Field Crops Research*. **90**; 61-73.
- Barron-Gafford G, Martens D, Grieve K, Biel K, Kudryavov V, McLain JET, Lipson D, Murthy R.** 2005. Growth of Eastern Cottonwoods (*Populus deltoides*) in elevated [CO₂] stimulates stand-level respiration and rhizodeposition of carbohydrates, accelerates soil nutrient depletion, yet stimulates above- and below-ground biomass production. *Global Change Biology*. **11**; 1220-1233.
- Baunsgaard L, Fuglsang AT, Jahn T, Korthout HAAJ, de Boer AH, Palmgren MG.** 1998. The 14-3-3 proteins associate with the plant plasma membrane H⁺ATPase to generate a fusicoccin binding complex and a fusicoccin responsive system. *The Plant Journal*. **13**; 661-671.

Beemster GTS, Fiorani F, Inze D. 2003. Cell cycle: the key to plant growth control? *Trends in Plant Science*. **8**; 154-158.

Beemster GTS, Vercruyssen S, De Veylder L, Kuiper M, Inze D. 2006. The *Arabidopsis* leaf as a model system for investigating the role of the cell cycle regulation in organ growth. *Journal of Plant Research*. **119**; 43-50.

Benjamini Y, Yekutieli D. 2005. Quantitative Trait Loci Analysis using the false discovery rate. *Genetics*. **171**; 783-790.

Berger D, Altmann T. 2000. A subtilisin-like serine protease involved in the regulation of stomatal density and distribution in *Arabidopsis thaliana*. *Genes and Development*. **14**; 1119-1131.

Bergmann D. 2005. Stomatal patterning: how do cells choose their fate? *Biologist*. **52**; 139-143.

Bergmann DC, Lukowitz W, Somerville CR. 2004. Stomatal development and pattern controlled by a MAPKK kinase. *Science*. **304**; 1494-1497.

Bernacchi CJ, Calzavara C, Davey PA, Wittig VE, Scarascia-Mugnozza GE, Raines CA, Long SP. 2003. Photosynthesis and stomatal conductance responses of poplars to free-air CO₂ enrichment (POPFACE) during the first growth cycle immediately following coppice. *New Phytologist*. **159**; 609-621.

Bhattacharya B. 2004. Greenhouse gas level hits record high. <http://www.newscientist.com/article/dn4802-greenhouse-gas-level-hits-record-high.html>. Last accessed 24th May 2008.

Bolwell GP, Slabas AR, Whitelegge JP. 2004. Proteomics; Empowering systems biology in plants. *Phytochemistry*. **65**; 1665-1669.

Borevitz JO, Chory J. 2004. Genomics tools for QTL analysis and gene discovery. *Current Opinion in Plant Biology*. **7**; 132-136.

Borevitz JO, Nordberg M. 2003. The impact of genomics on the study of natural variation in *Arabidopsis*. *Plant Physiology*. **132**; 718-725.

Boudolf V, Inzé D, De Veylder L. 2006. What if higher plants lack a CDC25 phosphatase? *Trends in Plant Science*. **11**; 474-479.

Boudolf V, Vlieghe K, Beemster GTS, Magyar Z, Torres Acosta JA, Maes S, Van Der Schueren E, Inzé D, De Veylder L. 2004. The plant-specific cyclin-dependent kinase CDKB1;1 and transcription factor E2Fa-Dpa control the balance of mitotically dividing and endoreduplicating cells in *Arabidopsis*. *The Plant Cell*. **16**; 2683-2692.

Bourquin V, Nishikubo N, Abe H, Brumer H, Denman S, Eklund M, Christiernin M, Teeri TT, Sundberg B, Mellerowicz. 2002. Xyloglucan endotransglycosylases have a function during the formation of secondary cell walls of vascular tissues. *The Plant Cell*. **14**; 3073-3088.

Bowman JL. 2000. The *YABBY* gene family and abaxial cell fate. *Current Opinion in Plant Biology*. **3**; 17-22.

Bowman JL, Eshed Y, Baum SF. 2002. Establishment of polarity in angiosperm lateral organs. *Trends in Genetics*. **18**; 134-141.

- Bowman JL, Smyth DR.** 1999. *CRABS CLAW*, a gene that regulates carpel and nectar development in *Arabidopsis*, encodes a novel protein with zinc finger and helix-loop-helix domains. *Development*. **126**; 2387-2396.
- Bradshaw HD, Ceulemans R, Davis J, Stettler R.** 2000. Emerging Model Systems in Plant biology: Poplar (*Populus*) as a model forest tree. *Journal of Plant Growth Regulation*. **19**; 306-313.
- Bradshaw HD, Stettler RF.** 1993. Molecular-genetics of growth and development in *Populus*.1. Triploidy in hybrid poplars. *Theoretical and Applied Genetics*. **86**; 301-307.
- Bradshaw HD, Villar M, Watson BD, Otto KG, Stewart S, Stettler RF.** 1994. Molecular genetics of growth and development in *Populus*.3. A genetic linkage map of a hybrid poplar composed of RFLP STS and RAPD markers. *Theoretical and Applied Genetics*. **89**; 167-178.
- Brand U, Fletcher JC, Hobe M, Meyerowitz EM, Simon R.** 2000. Dependence of stem cell fate in *Arabidopsis* on a feedback loop regulated by CLV3 activity. *Science*. **289**; 617-619.
- Brett C, Waldron K.** 1996. Physiology and Biochemistry of Plant Cell Walls. Second Edition. Chapman and Hall. University Press, Cambridge. p57.
- Breyne P, Zabeau M.** 2001. Genome-wide expression analysis of plant cell cycle modulated genes. *Current Opinion in Plant Biology*. **4**; 136-142.
- Brownlee C.** 2002. Role of the extracellular matrix in cell-cell signalling; paracrine paradigms. *Current Opinion in Plant Biology*. **5**; 396-401.
- Brinker M, van Zyl L, Liu W, Craig D, Sederoff RR, Clapham DH, von Arnold S.** 2004. Microarray analysis of gene expression analysis during adventitious root development in *Pinus contorta*. *Plant Physiology*. **135**; 1526-1539.
- Brunner AM, Busov VB, Strauss SH.** 2004. Poplar genome sequence: functional genomics in an ecologically dominant plant species. *Trends in Plant Science*. **9**; 49-56.
- Bunce JA.** 2001. Are annual plants adapted to the current atmospheric concentration of carbon dioxide? *International Journal of Plant Sciences*. **162**; 1261-1266.
- Busov VB, Meilan R, Pearce DW, Ma C, Rood SB, Strauss SH.** 2003. Activation tagging of a dominant gibberellins catabolism gene (*GA2-oxidase*) from poplar that regulates tree stature. *Plant Physiology*. **132**; 1-9.
- Burgess J.** 2001. Gene Expression Studies Using Microarrays. *Clinical and Experimental Pharmacology and Physiology*. **28**; 321-328.
- Burstin J.** 2000. Differential expression of two barley XET-related genes during coleoptile growth. *Journal of Experimental Botany*. **51**; 847-852.
- Byrne ME, Barley R, Curtis M, Arroyo JM, Dunham M, Hudson A, Martienssen RA.** 2000. *Asymmetric leaves1* mediates leaf patterning and stem cell function in *Arabidopsis*. *Nature*. **408**; 967-971.
- Byrne ME, Simorowski J, Martienssen RA.** 2001. *ASYMMETRIC LEAVES1* reveals *KNOX* gene redundancy in *Arabidopsis*. *Development*. **129**; 1957-1965.
- Byrne M, Timmermans M, Kidner C, Martienssen R.** 2001. Development of leaf shape. *Current Opinion in Plant Biology*. **4**; 38-43.

Calfapietra C, Gielen B, Galema ANJ, Lukac M, De Angelis P, Moscatelli MC, Ceulemans R, Scarascia-Mugnozza G. 2003. Free air CO₂ enrichment (FACE) enhances biomass production in a short-rotation poplar plantation. *Tree Physiology*. **23**; 805-814.

Calfapietra C, Tulva I, Eensalu E, Perez M, De Angelis P, Scarascia-Mugnozza G, Kull O. 2005. Canopy profiles of photosynthetic parameters under elevated CO₂ and N fertilization in a poplar plantation. *Environmental Pollution*. **137**; 525-535.

Campbell P, Braam J. 1999. Xyloglucan endotransglycosylases: diversity of genes, enzymes and potential wall-modifying functions. *Trends in Plant Science*. **4**; 361-366.

Canales C, Grigg S, Tsiantis M. 2005. The formation and patterning of leaves: recent advances. *Planta*. **221**; 752-756.

Catalá C, Rose JKC, York WS, Albersheim P, Darvill AG, Bennett AB. 2001. Characterisation of a tomato xyloglucan endotransglycosylases gene that is down-regulated by auxin in etiolated hypocotyls. *Plant Physiology*. **127**; 1180-1192.

Ceulemans R. 1990. Genetic variation in functional and structural productivity determinants in Poplar. Amsterdam Publishers. pp16.

Ceulemans R, Vanpraet L, Jiang XN. 1995. Effects of CO₂ enrichment, leaf position and clone on stomatal index and epidermal-cell density in poplar. *New Phytologist*. **131**; 99-107.

Chang S, Puryear J, Cairney J. 1993. A simple and efficient method for isolating RNA from pine trees. *Plant Molecular Biology Reporter*. **11**; 113-116.

Charrier B, Champion A, Henry Y, Kreis M. 2002. Expression profiling of the whole *Arabidopsis* Shaggy-like kinase multigene family by real-time reverse transcriptase-polymerase chain reaction. *Plant Physiology*. **130**, 577-590.

Chen GY, Yong ZH, Liao Y, Zhang DY, Chen Y, Zhang HB, Chen J, Zhu JG, Xu DQ. 2005. Photosynthetic acclimation in rice leaves to Free-air CO₂ Enrichment related to both Ribulose-1,5-bisphosphate carboxylation limitation and Ribulose-1,5-bisphosphate regeneration limitation. *Plant Cell Physiology*. **46**; 1036-1045.

Cheng SH, Moore BD, Seemann JR. 1998. Effects of short-and long-term elevated CO₂ on the expression of Ribulose-1,5-bisphosphate carboxylase/oxygenase genes and carbohydrate accumulation in leaves of *Arabidopsis thaliana* (L.) Heynh. *Plant Physiology*. **116**; 715-723.

Cheng H, Qin L, Lee S, Fu X, Richards DE, Cao D, Luo D, Harberd NP, Peng J. 2004. Gibberellin regulates *Arabidopsis* floral development via suppression of DELLA protein function. *Development*. **131**; 1055-1064.

Chevalier F, Martin O, Rofidal V, Devauchelle AD, Barteau S, Sommerer N, Rossignol M. 2004. Proteomic investigation of natural variation between *Arabidopsis* ecotypes. *Proteomics*. **4**; 1372-1381.

Chivasa S, Ndimba BK, Simon WJ, Robertson D, Yu X-L, Knox JP, Bolwell P, Slabas AR. 2002. Proteomic Analysis of the *Arabidopsis thaliana* cell wall. *Electrophoresis*. **23**; 1754-1765.

Cho HT, Cosgrove DJ. 2000. Altered expression of expansin modulates leaf growth and pedicel abscission in *Arabidopsis thaliana*. *Proceedings of the National Academy of Science USA*. **97**; 9783-9788.

Chuck G, Lincoln C, Hake S. 1996. *KNAT1* induces lobed leaves with ectopic meristems when over-expressed in *Arabidopsis*. *The Plant Cell*. **8**; 1277-1289.

Clauser KR, Baker P, Burlingame AL. 1999. Role of accurate mass measurement (± 10 ppm) in protein identification strategies employing MS or MS/MS and database searching. *Analytical Chemistry*. **71**; 2871-2882.

Cockcroft CE, den Boer BGW, Healy JMS, Murray JAH. 2000. Cyclin D control of growth rate in plants. *Nature*. **405**; 575-579.

Coleman HD, Ellis DD, Gilbert M, Mansfield SD. 2006. Up-regulation of sucrose synthase and UDP-glucose pyrophosphorylation impacts plant growth and metabolism. *Plant Biotechnology Journal*. **4**; 87-101.

Conesa A, Götz S, Garcia-Gomez JM, Terol J, Talón Robles M. 2005. Blast2GO : A universal tool for annotation, visualization and analysis in functional genomics research. *Bioinformatics*. **21** ; 3674-3676.

Cosgrove DJ. 1993. How do plant cell walls extend? *Plant Physiology*. **102**; 1-6.

Cosgrove DJ. 2000. Loosening of plant cell walls by expansins. *Nature*. **407**; 321-326.

Cosgrove DJ. 2004. Expansins Central. Available; <http://www.bio.psu.edu/expansins>. (January, 2005)

Costa P, Plomion C. 1999. Genetic analysis of needle proteins in maritime pine 2. Variation of protein accumulation. *Silvae Genetica*. **48**; 146-150.

Curtis PS, Vogel CS, Pregitzer KS, Zak DR, Teeri JA. 1995. Interacting effects of soil fertility and atmospheric CO₂ on leaf growth and carbon gain physiology in *Populus x euramericana*. *New Phytologist*. **129**; 253-263.

Curtis PS, Wang X. 1998. A meta-analysis of elevated CO₂ effects on woody plant mass, form and physiology. *Oecologia*. **113**; 299-313.

Curtis PS, Vogel CS, Pregitzer KS, Zak DR, Teeri JA. 1995. Interacting effects of soil fertility and atmospheric CO₂ on leaf area growth and carbon gain physiology in *Populus x euramericana* (Dode) Guinier. *New Phytologist*. **129**; 253-263.

Dafeng H, Luo Y, Cheng W, Coleman JS, Johnson DW, Sims DA. 2001. Canopy radiation- and water-use efficiencies as affected by elevated [CO₂]. *Global Change Biology*. **7**; 75-91.

De Jager SM, Maughan S, Dewitte W, Scofield S, Murray JAH. 2005. The developmental context of cell-cycle control in plants. *Seminars in Cell and Developmental Biology*. **16**; 385-396.

De Veylder , Beeckman T, Beemster GTS, de Almeida Engler J, Ormenese S, Maes S, Naudts M, Van Der Schueren E, Jacqmard A, Engler G, Inzé D. 2002. Control of the proliferation, endoreduplication and differentiation by the *Arabidopsis* E2Fa-DPa transcription factor. *The EMBO journal*. **21**; 1360-1368.

De Veylder L, Beeckman T, Beemster GTS, Krols L, terras, Landrieu I, Van der Schueren E, Maes S, Naudts M, Inzé D. 2001b. Functional Analysis of Cyclin Dependent Kinase Inhibitors of *Arabidopsis*. *The Plant Cell*. **13**; 1653-1667.

- De Veylder L, Beemster G, Beeckman T, Inzé D.** 2001. CKS1At overexpression in *Arabidopsis thaliana* inhibits growth by reducing meristem size and inhibiting cell cycle progression. *The Plant Journal*. **25**; 617-626.
- Dewitte W, Riou-Khamlichi C, Scofield S, Healy JM, Jacquemard A, Kilby NJ, Murray JA.** 2003. Altered cell cycle distribution, hyperplasia and inhibited differentiation in *Arabidopsis* caused by the D-type cyclin CYCD3. *Plant Cell*. **15**; 79-92.
- Dewitte W, Scofield S, Alcasabas AA, Maughan SC, Menges M, Braun N, Collins C, Nieuwland J, Prinsen E, Sundaresan V, Murray JAH.** 2007. *Arabidopsis* CYCD3 D-type cyclins link cell proliferation and endocycles and are rate-limiting for cytokinin responses. *Proceedings of the National Academy of Science USA*. **104**; 14537-14542.
- Djerbi S, Lindskog M, Arvestad L, Sterky F, Teeri TT.** 2005. The genome sequence of black cottonwood (*Populus trichocarpa*) reveals 18 conserved cellulose synthase (*CesA*) genes. *Planta*. **221**; 739-746.
- Donnelly PM, Bonetta D, Tsukaya H, Dengler RE, Dengler NG.** 1999. Cell Cycling and Cell Enlargement in Developing Leaves of *Arabidopsis*. *Developmental Biology*. **215**; 407-419.
- Donson J, Fang Y, Espiritu-Santo G, Xing W, Salazar A, Miyamoto S, Armendarez V, Volkmuth W.** 2002. Comprehensive gene expression analysis by transcript profiling. *Plant Molecular Biology*. **48**; 75-97.
- Doonan J.** 2000. Social Control on cell proliferation in plants. *Current Opinion in Plant Biology*. **3**; 482-487.
- Drake BG, González-Meyer MA, Long SP.** 1997. More efficient plants: A consequence of rising CO₂? *Annual Review of Plant Physiology and Plant Molecular Biology*. **48**; 609-639.
- Driscoll SP, Prins A, Olmos E, Kunert KJ, Foyer CH.** 2006. Specification of adaxial and abaxial stomata epidermal structure and photosynthesis to CO₂ enrichment in maize leaves. *Journal of Experimental Botany*. **57**; 381-390.
- Druart N, Rodriguez-Buey M, Barron-Gafford G, Sjödin A, Bhalerao R, Hurry V.** 2006. Molecular targets of elevated [CO₂] in leaves and stems of *Populus deltoides*: implications for future tree growth and carbon sequestration. *Functional Plant Biology*. **33**; 121-131.
- Dudley AM, Aach J, Steffen MA, Church GM.** 2002. Measuring absolute expression with microarrays with a calibrated reference sample and an extended signal intensity range. *Proceedings of the National Academy of Science USA*. **99**; 7554-7559.
- Duggan DJ, Bittner M, Chen Y, Meltzer P, Trent JM.** 1999. Expression profiling using cDNA microarrays. *Nature Genetics Supplement*. **21**; 10-14.
- Emery JF, Floyd SK, Alvarez J, Eshed Y, Hawker NP, Izhaki A, Baum SF, Bowman JL.** 2003. Radial patterning of *Arabidopsis* shoots by class III HD-ZIP and *KANADI* genes. *Current Biology*. **13**; 1768-1774.
- Emiliani G.** 2006. Identificazione, caratterizzazione molecolare e studio dell'espressione di geni coinvolti nella risposta alla radiazione UV in alberi forestali. *Thesis*. Università degli Studi Firenze.
- Eng JK, McCormack AL, Yates I, John R.** 1994. An approach to correlate tandem mass spectral data of peptides with amino acid sequences in a protein database. *Journal of the American Society for Mass Spectrometry*. **5**; 976-989.

Eriksson ME, Israelsson M, Olson O, Moritz T. 2000. Increased gibberellins biosynthesis in transgenic trees promotes growth, biomass production and xylem fibre length. *Nature Biotechnology*. **18**; 784-788.

Eshed Y, Izhaki A, Baum SF, Floyd SK, Bowman JL. 2004. Asymmetric leaf development and blade expansion in *Arabidopsis* are mediated by *KANADI* and *YABBY* activities. *Development*. **131**; 2997-3006.

Eulgem T, Rushton PJ, Robatzek S, Somssich IE. 2000. The WRKY superfamily of plant transcription factors. *Trends in Plant Science*. **5**; 199-206.

Falge E, Tenhunen J, Baldocchi D, Aubinet M, Bakwin P, Berbigier P, Bernhofer C, Bonnefond JM, Burba G, Clement R, Davis KJ, Falk M, Goldstein AH, Grelle A, Granier A, Grunwald T, Gudmundsson J, Hollinger D, Janssens IA, Keronen P, Kowalski AS, Katul G, Law BE, Malhi Y, Meyers T, Monson RK, Moors E, Munger JW, Oechel WUKTP, Pilegaard K, Rannik U, Rebmann C, Suyker A, Thorgiersson H, Tirone G, Turnipseed A, Wilson K, Wofsy S. 2002. Phase and amplitude of ecosystem carbon release and uptake potentials derived from FLUXNET measurements. *Agricultural and Forest Meteorology*. **113**; 75-95.

Farage PK, McKee IF, Long SP. 1998. Does a low nitrogen supply necessarily lead to acclimation of photosynthesis to elevated CO₂? *Plant Physiology*. **118**; 573-580.

Feder ME, Mitchell-Olds. 2003. Evolutionary and ecological functional genomics. *Nature Reviews in Genetics*. **4**; 651-657.

Ferreira S, Hjerne K, Larsen M, Wingsle G, Larsen P, Fey S, Roepstorff P, Pais MS. 2006. Proteome profiling of *Populus euphratica* upon heat stress. *Annals of Botany*. **98**; 361-377.

Ferreira P, Hemerly A, De Almeida Engler J, Bergounioux, Burssens S, Van Montagu M, Engler G, Inzé D. 1994. Three discrete classes of *Arabidopsis* cyclins are expressed during different intervals of the cell cycle. *Proceedings of the National Academy of Science USA*. **91**; 11313-11317.

Ferris R, Long L, Bunn SM, Robinson KM, Bradshaw HD, Rae AM, Taylor G. 2002. Leaf stomatal and epidermal cell development: identification of putative quantitative trait loci in relation to elevated carbon dioxide concentration in poplar. *Tree Physiology*. **22**; 633-640.

Ferris R, Taylor G. 1993. Contrasting effects of elevated CO₂ on the root and shoot growth of four native herbs commonly found in chalk grassland. *New Phytologist*. **125**; 855-866.

Ferris R, Taylor G. 1994. Elevated CO₂, water relations and biophysics of leaf extension in four chalk grassland herbs. *New Phytologist*. **127**; 297-307.

Ferris R, Sabatti M, Miglietta F, Mills RF, Taylor G. 2001. Leaf area is stimulated in *Populus* by free air CO₂ enrichment (POPFACE), through increased cell expansion and production. *Plant, Cell and Environment*. **24**; 305-315.

Fiorani F, Beemster GTS. 2006. Quantitative analyses of cell division in plants. *Plant Molecular Biology*. **60**; 963-979.

Fiorani F, Beemster GTS, Bultynck L, Lambers H. 2000. Can meristematic activity determine variation in leaf size and elongation rate among four *Poa* species? A kinematic study. *Plant Physiology*. **124**; 845-855.

Fleming AJ. 2002. The mechanism of leaf morphogenesis. *Planta*. **216**; 17-22.

- Fleming AJ.** 2003. The molecular regulation of leaf form. *Plant Biology*. **5**; 341-349.
- Fleming AJ.** 2005. The control of leaf development. *New Phytologist*. **167**; 9-20.
- Fleming AJ, Caderas D, Wehrli E, McQueen-Mason S, Kuhlemeier C.** 1999. Analysis of expansin-induced morphogenesis on the apical meristem of tomato. *Planta*. **208**; 166-174.
- Fleming AJ, McQueen-Mason S, Mandel T, Kuhlemeier C.** 1997. Induction of leaf primordia by the cell wall protein expansin. *Science*. **276**; 1415-1418.
- Fletcher JC, Brand U, Running MP, Simon R, Meyerowitz EM.** 1999. Signalling of cell fate decisions by CLAVATA3 in *Arabidopsis* shoot meristems. *Science*. **283**; 1911-1914.
- Francis D.** 2007. The plant cell cycle-15 years on. *New Phytologist*. **174**; 261-278.
- Francis D, Sorrell DA.** 2001. The interface between the cell cycle and plant growth regulators; a mini review. *Plant Growth Regulation*. **33**; 1-12.
- Fry SC.** 1997. Novel 'dot-blot' assays for glycosyltransferases and glycosylhydrolases: optimisation for xyloglucan endotransglycosylases (XET) activity. *The Plant Journal*. **11**; 1141-1150.
- Fry SC.** 1998. Oxidative scission of plant cell wall polysaccharides by ascorbate-induced hydroxyl radicals. *Biochemical Journal*. **332**; 507-515.
- Fry SC, Smith RC, Renwick KF, Martin DJ, Hodge SK, Matthews KJ.** 1992. Xyloglucan endotransglycosylases, a new wall-loosening enzyme activity from plants. *Biochemical Journal*. **282**; 821-828.
- Galway M, Masucci J, Lloyd A, Walbot V, Davis R, Schiefelbein J.** 1994. The *TTG* gene is required to specify epidermal cell fate and cell patterning in the *Arabidopsis* root. *Developmental Biology*. **166**; 740-754.
- Gardner SDL, Taylor G, Bosac C.** 1995. Leaf growth of hybrid poplar following exposure to eCO₂. *New Phytologist*. **131**; 81-90.
- Gaudin V, Lunness PA, Fobert PR, Towers M, Riou-Khamlichi C, Murray JAH, Coen E, Doonan JH.** 2000. The expression of D-cyclin genes defines distinct developmental zones in Snapdragon apical meristems and is locally regulated by the *Cycloidea* gene. *Plant Physiology*. **122**; 1137-1148.
- Geiger M, Haake V, Ludewig F, Sonnewald U, Stitt M.** 1999. The nitrate and ammonium nitrate supply have a major influence on the response of photosynthesis, carbon metabolism, nitrogen metabolism and growth to elevated carbon dioxide in tobacco. *Plant Cell and Environment*. **22**; 1177-1199.
- Geisler M, Nadeau J, Sack FD.** 2000. Oriented asymmetric divisions that generate the stomatal spacing pattern in *Arabidopsis* are disrupted by the *TOO MANY MOUTHS* mutation. *Plant Cell*. **12**; 2075-2086.
- Geisler M, Sack FD.** 2002. Variable timing of developmental progression in the stomatal pathway in *Arabidopsis* cotyledons. *New Phytologist*. **153**; 469-476.

Gesch RW, Boote KJ, Vu JCV, Hartwell Allen Jr L, Bowes G. 1998. Changes in growth CO₂ result in rapid adjustment of Ribulose-1,5- biphosphate carboxylase/ oxygenase small subunit gene expression in expanding and mature leaves of rice. *Plant Physiology*. **118**; 521-529.

Gibson G. 2002. Microarrays in ecology and evolution: a preview. *Molecular Ecology*. **11**; 17-24.

Gielen B, Calfapietra C, Sabatti M, Ceulemans R. 2001. Leaf area dynamics in a closed poplar plantation under free air CO₂ enrichment. *Tree Physiology*. **21**; 1245-1255.

Gielen B, Ceulemans R. 2001. The likely impact of rising atmospheric CO₂ on natural and managed *Populus*: a literature review. *Environmental Pollution*. **115**; 335-358.

Gielen B, Liberloo M, Bogaert J, Calfapietra C, de Angelis P, Miglietta F, Scarascia-Mugnozza G, Ceulemans R. 2003. Three years of Free Air CO₂ Enrichment (POPFACE) only slightly affects profiles of light and leaf characteristics in closed canopies of *Populus*. *Global Change Biology*. **9**; 1022-1037.

Gion JM, Lalanne C, Provost GL, Ferry-Dumzet H, Paiva J, Chaumeil P, Frigerio JM, Brach J, Barre A, de Daruvar A, Claverol S, Bonneau M, Sommerer Z, Negroni L, Plomion C. 2005. The proteome of maritime pine wood forming tissue. *Proteomics*. **5**; 3731-3751.

Goldschmidt EE, Huber SC. 1992. Regulation of end-product accumulation in leaves of plants storing starch, sucrose and hexose sugars. *Plant Physiology*. **99**; 1443-1448.

Golz JF, Hudson A. 1999. Plant development: YABBYs claw to the fore. *Current Biology*. **9**; R861-R863.

Grace J. 2004. Understanding and managing the global carbon cycle. *Journal of Ecology*. **92**; 189-202.

Graf J. 1921. Beitrage zur Kenntnis der Gattung *Populus*. *Beih Bot Central*. **38**; 405-434.

Grafi G, Burnett RJ, Helentjaris T, Larkins BA, DeCaprio JA, Sellers WR, Kaelin Jr WG. 1996. A maize cDNA encoding a member of the retinoblastoma protein family; Involvement in endoreduplication. *Proceedings of the National Academy of Science USA*. **93**; 8962-8967.

Granier C, Tardieu F. 1998. Spatial and temporal analyses of expansion and cell cycle in sunflower leaves. *Plant Physiology*. **116**; 991-1001.

Gray JE, Holroyd GH, van der Lee FM, Bahrami AR, Sijmons PC, Woodward FI, Schuch W, Hetherington AM. 2000. The *HIC* signalling pathway links CO₂ perception to stomatal development. *Nature*. **408**; 713-716.

Gupta P, Duplessis S, White H, Karnosky DH, Martin F, Podila GK. 2005. Gene expression patterns of trembling aspen trees following long-term exposure to interacting elevated CO₂ and tropospheric O₃. *New Phytologist*. **167**; 129-142.

Gutierrez C. 1998. The retinoblastoma protein in plant cell cycle and development. *Current Opinion in Plant Biology*. **1**; 492-497.

Gygi SP, Rist B, Gerber SA, Turecek F, Gelb MH, Aebersold R. 1999. Quantitative analysis of complex protein mixtures using isotope-coded affinity tags. *Nature Biotechnology*. **17**; 994-999.

Hager A. 2003. Role of the plasma membrane H⁺ATPase in auxin-induced elongation growth; historical and new aspects. *Journal of Plant Research*. **116**; 483-505.

- Harrison JWH.** 1924. A preliminary account of the chromosomes and chromosome behaviour in the Salicaceae. *Annals of Botany*. **38**; 361-378.
- Hay A, Barkoulas M, Tsiantis M.** 2004. PINning down the connections: transcription factors and hormones in leaf morphogenesis. *Current Opinion in Plant Biology*. **7**; 575-581.
- Hay A, Barkoulas M, Tsiantis M.** 2006. *ASYMMETRIC LEAVES1* and auxin activities converge to repress *BREVIPEDICELLUS* expression and promote leaf development in *Arabidopsis*. *Development*. **133**; 3955-3961.
- Hay A, Kaur H, Phillips A, Hedden P, Hake S, Tsiantis M.** 2002. The gibberellins pathway mediates *KNOTTED1*-type homeobox function in plants with different body parts. *Current Biology*. **12**; 1557-1565.
- Healy JMS, Menges M, Doonan JH, Murray JAH.** 2001. The *Arabidopsis* D-type cyclins CycD2 and CycD3 both interact *in vivo* with the PSTAIRE cyclin dependent kinase Cdc2a but are differentially controlled. *Journal of Biological Chemistry*. **276**; 7041-7047.
- Heath LS, Ramakrishnan N, Sederoff RR, Whetten RW, Chevone BI, Struble CA, Jouenne VY, Chen D, van Zyl L, Grene R.** 2002. Studying the functional genomics of stress responses of loblolly pine with the Expresso microarray experiment management system. *Comparative and Functional Genomics*. **3**; 226-243.
- Heller MJ.** 2002. DNA Microarray Technology: Devices, Systems and Applications. *Annual Review of Biomedical Engineering*. **4**; 129-53.
- Helmuth B, Kingsolver JG, Carrington E.** 2005. Biophysics, physiological ecology and climate change: Does mechanism matter? *Annual Review of Physiology*. **67**; 177-201.
- Hemerly AS, Ferreira P, de Almeida Engler J, Van Montagu M, Engler G, Inzé D.** 1993. Cdc2a Expression in *Arabidopsis* is linked with competence for cell division. *The Plant Cell*. **5**; 1711-1723.
- Hemerly AS, Ferreira PCG, Montagu MC, Inzé D.** 1999. Cell Cycle control and plant morphogenesis; is there an essential link? *BioEssays*. **21**; 29-37.
- Hetherington AM.** 2001. Guard cell signalling. *Cell*. **107**; 711-714.
- Hetherington AM, Woodward FI.** 2003. The role of stomata in sensing and driving environmental change. *Nature*. **424**; 901-908.
- Holland P, Abramson R, Watson R, Gelfand D.** 1991. Detection of specific polymerase chain reaction product by utilizing the 5'-3' exonuclease activity of *Thermus aquaticus* DNA polymerase. *Proceedings of the National Academy of Science USA*. **88**; 7276-7280.
- Horiguchi G, Ferjani A, Fujikura U, Tsukaya H.** 2005. Coordination of cell proliferation and cell expansion in the control of leaf size in *Arabidopsis thaliana*. *Journal of Plant Research*. **119**; 37-42.
- Horiguchi G, Kim GT, Tsukaya H.** 2005. The transcription factor AtGRF5 and the transcription coactivator AN3 regulate cell proliferation in leaf primordia of *Arabidopsis thaliana*. *The Plant Journal*. **43**; 68-78.
- Howe GT, Brunner AM.** 2005. An evolving approach to understanding plant adaptation. *New Phytologist*. **167**; 1-5.

Hughes TR, Mao M, Jones AR, Burchard J, Marton MJ, Shannon KW, Lefkowitz SM, Ziman M, Schelter JM, Meyer MR, Kobayashi S, Davis C, Dai HY, He YDD, Stephanians SB, Cavet G, Walker WL, West A, Coffey E, Shoemaker DD, Stoughton R, Blanchard AP, Friend SH, Linsley PS. 2001. Expression profiling using microarrays fabricated by an ink-jet oligonucleotide synthesizer. *Nature Biotechnology*. **19**; 342-347.

Hudson A. 1999. Axioms and axes in leaf formation? *Current Opinion in Plant Biology*. **2**; 56-60

Hudson A, Goodrich J. 1997. Plant Meristems; Cell signalling keeps the balance. *Current Biology*. **7**; R427-R429.

Hülkamp M, Misera S, Jürgens G. 1994. Genetic dissection of trichome cell development in *Arabidopsis*. *Cell*. **76**; 555-566.

Ideker T, Galitski T, Hood L. 2001. A new approach to decoding life: Systems Biology. *Annual Review of Genomics and Human Genetics*. **2**; 343-372.

IGBP Terrestrial Carbon Working Group. 1998. CLIMATE: The Terrestrial Carbon Cycle: Implications for the Kyoto Protocol. *Science*. **280**; 1393-1394.

Ingram GC. 2004. Between the sheets; inter-cell-layer communication in plant development. *Philosophical Transactions of the Royal Society of London B*. **359**; 891-906.

Ingram TJ, Reid JB, Murfet IC, Gaskin P, Willis CL, MacMillan J. 1984. Internode length in *Pisum*. The *Le* gene controls the 3 β -hydroxylation of gibberellin A₂₀ to gibberellin A₁. *Planta*. **160**; 455-463.

Inzé D, De Veylder L. 2006. Cell cycle regulation in plant development. *Annual Review of Genetics*. **40**; 77-105.

IPCC. 2007. Summary for policymakers. In; *Climate Change 2007. The physical science basis. Contribution of Working Group I to the Fourth Assessment Report of the Intergovernmental Panel on Climate Change* [Solomon S, Qin D, Manning M, Chen Z, Marquis M, Averyt KB, Tignor M, Miller HL (eds)]. Cambridge University Press, Cambridge, United Kingdom and New York, NY, USA.

Iwakawa H, Ueno Y, Semiarti E, Onouchi H, Kojima S, Tsukaya H, Hasebe M, Soma T, Ikezaki M, Machida C, Machida Y. 2002. The *ASYMMETRIC LEAVES2* gene of *Arabidopsis thaliana* required for formation of a symmetric flat lamina, encodes a member of a novel family of proteins characterised by cysteine repeats and a leucine zipper. *Plant Cell Physiology*. **43**; 467-478.

Jaccoud D, Peng K, Feinstein D, Kilian A. 2001. Diversity Arrays: a solid state technology for sequence information independent genotyping. *Nucleic Acids Research*. **29**; e25.

Jackson D, Veit B, Hake S. 1994. Expression of maize *KNOTTED1* related homeobox genes in the shoot apical meristem predicts patterns of morphogenesis in the vegetative shoot. *Development*. **120**; 405-413.

Jang JC, Sheen J. 1994. Sugar sensing in higher plants. *Plant Cell*. **6**; 1665-1679.

Jang JC, Sheen J. 1997. Sugar sensing in higher plants. *Trends in Plant Science*. **2**; 208-214.

Janssens IA, Freibauer A, Ciais P, Smith P, Nabuurs GJ, Folberth G, Schlamadinger B, Hutjes RWA, Ceulemans R, Schulze ED, Valentini R, Dolman AJ. 2003. Europe's terrestrial biosphere absorbs 7 to 12% of European anthropogenic CO₂ emissions. *Science*. **300**; 1538-1542.

- Jansson S, Douglas C.** 2007. *Populus*: A model system for plant biology. *Annual Review of Plant Biology*. **58**; 435-458.
- Jański S, Piazza P, Craft J, Hay A, Woolley L, Rieu I, Phillips A, Hedden P, Tsiantis M.** 2005. *KNOX* action in *Arabidopsis* is mediated by coordinate regulation of cytokinin and gibberellin activities. *Current Biology*. **15**; 1560-1565.
- Jenkins RE, Pennington SR.** 2001. Arrays for protein expression profiling: Towards a viable alternative to two-dimensional gel electrophoresis? *Proteomics*. **1**; 13-29.
- Jordens JZ, Lanham S, Pickett MA, Amarasekara S, Abeywickrema I, Watt PJ.** 2000. Amplification with molecular beacon primers and reverse line blotting for the detection and typing of human papillomaviruses. *Journal of Virology Methods*. **89**; 29-37.
- Joshi CP, Bhandari S, Ranjan P, Kalluri UC, Liang X, Fujino T, Samuga A.** 2004. Genomics of cellulose biosynthesis in poplars. *New Phytologist*. **164**; 53-61.
- Joubes J, Chevalier C, Dudits D, Heberle-Bors E, Inzé D, Umeda M, Renaudi JP.** 2000. CDK-related protein kinases in plants. *Plant Molecular Biology*. **43**; 607-620.
- Karnosky DF, Zak DR, Pregitzer KS, Awmack CS, Bockheim JG, Dickson RE, Hendrey GR, Host GE, King JS, Kopper BJ, Kruger EL, Kubiske ME, Lindroth RL, Mattson WJ, McDonald EP, Noormets A, Oksanen E, Parsons WFJ, Percy KE, Podila GK, Riemenschneider DE, Sharma P, Thakur R, Sôber A, Sôber J, Jones WS, Anttonen S, Vapaavuori E, Mankovska B, Heilman W, Isebrands JG.** 2003. Tropospheric O₃ moderates responses of CO₂: a synthesis of molecular to ecosystem results from Aspen FACE project. *Functional Ecology*. **17**; 289-304.
- Kav NNV, Srivastava S, Goonewardene L, Blade SF.** 2004. Proteome level changes in the root of *Pisum sativum* in response to salinity. *Annals of Applied Biology*. **145**; 130-217.
- Keeling CD, Whorf TP, Wahlen M, van der Plicht J.** 1995. Interannual extremes in the rate of rise of atmospheric carbon dioxide since 1980. *Nature*. **375**; 666-670.
- Kehr J, Hustiak F, Walz C, Willmitzer L, Fisahn J.** 1998. Transgenic plants changed in carbon allocation pattern display a shift in diurnal growth pattern. *The Plant Journal*. **16**; 497-503.
- Keller CP, Van Volkenburgh.** 1998. Evidence that auxin-induced growth of tobacco leaf tissues does not involve cell wall acidification. *Plant Physiology*. **118**; 557-564.
- Kendzierski C, Irizarry RA, Chen KS, Haag JD, Gould MN.** 2005. On the utility of pooling biological samples in microarray experiments. *Proceedings of the National Academy of Science USA*. **102**; 4252-4257.
- Kendzierski CM, Zhang Y, Lan H, Attie AD.** 2003. The efficiency of pooling mRNA in microarray experiments. *Biostatistics*. **4**; 465-477.
- Kerr MK.** 2003. Design considerations for efficient and effective microarray studies. *Biometrics*. **59**; 822-828.
- Kerr MK, Churchill GA.** 2001. Statistical design and the analysis of gene expression microarray data. *Genetical Research*. **77**; 123-128.
- Kerstetter RA, Bollman K, Taylor RA, Bomblies K, Poethig RS.** 2001. *KANADI* regulates organ polarity in *Arabidopsis*. *Nature*. **411**; 706-709.

- Kidner CA, Martienssen RA.** 2004. Spatially restricted microRNA directs leaf polarity through *ARGONAUTE1*. *Nature*. **428**; 81-84.
- Kim GT, Cho KH.** 2006. Recent advances in the genetic regulation of the shape of simple leaves. *Physiologia Plantarum*. **126**; 494–502.
- Kim GT, Shoda K, Tsuge T, Cho KH, Uchimiya H, Yokoyama R, Nishitani K, Tsukaya H.** 2002. The *ANGUSTIFOLIA* gene of *Arabidopsis*, a plant CtBP gene, regulates leaf-cell expansion, the arrangement of cortical microtubules in leaf cells and expression of a gene involved in cell-wall formation. *EMBO Journal*. **21**; 1267-1279.
- Kim GT, Tsukaya H, Saito Y, Uchimiya H.** 1999. Changes in the shapes of leaves and flowers upon overexpression of cytochrome P450 in *Arabidopsis*. *Proceedings of the National Academy of Science USA*. **96**; 9433-9437.
- Kim GT, Tsukaya H, Uchimiya H.** 1998. The *ROTUNDIFOLIA3* gene of *Arabidopsis thaliana* encodes a new member of the cytochrome P450 family that is required for the regulated polar elongation of leaf cells. *Genes and Development*. **12**; 2381-2391.
- Kim GT, Tsukaya H, Uchimiya H.** 1998. The *CURLY LEAF* gene controls both division and elongation of cells during the expansion of the leaf blade in *Arabidopsis thaliana*. *Planta*. **206**; 175-183.
- Kimura S, Laosinchai W, Itoh T, Cui X, Linder CR, Brown Jr RM.** 1999. Immunogold labelling of rosette terminal cellulose-synthesizing complexes in the vascular plant *Vigna angularis*. *The Plant Cell*. **11**; 2075-2085.
- King JS, Pregitzer KS, Zak DR, Sôber J, Isebrands JG, Dickson RE, Hendrey GR, Karnosky DF.** 2001. Fine root biomass and fluxes of soil carbon in young stands of paper birch and trembling aspen as affected by elevated atmospheric CO₂ and tropospheric O₃. *Oecologia*. **128**; 237-250.
- Kinsman EA, Lewis C, Davis MS, Young JE, Francis D, Vilhar B, Ougham HJ.** 1997. Elevated CO₂ stimulates cells to divide in grass meristems; a differential effect in two natural populations of *Dactylis glomerata*. *Plant, Cell and Environment*. **20**; 1309-1316.
- Kinter M, Sherman NE.** 2000. Protein sequencing and identification using tandem mass spectrometry. John Wiley and Sons, Canada. pp32.
- Kitano H.** 2002. Systems Biology: A Brief Overview. *Science*. **295**; 1662-1664.
- Klose J.** 1975. Protein mapping by combined isoelectric focusing and electrophoresis of mouse tissues. A novel approach to testing for induced point mutations in mammals. *Humangenetik*. **26**; 231-243.
- Kono A, Umeda-Hara C, Lee J, Ito M, Uchimiya H, Umeda M.** 2003. *Arabidopsis* D-Type Cyclin CYCD4;1 is a novel cyclin partner of B2-type cyclin-dependent kinase. *Plant Physiology*. **132**; 1315-1321.
- Koornneef M, van der Veen JH.** 1980. Induction and analysis of gibberellin sensitive mutants in *Arabidopsis thaliana*. *Theoretical and Applied Genetics*. **58**; 257-263.
- Koornneef M.** 1981. The complex syndrome of *ttg* mutants. *Arabidopsis Information Service*. **18**; 45-51.

- Koornneef M, Dellaert LWM, Vanderveen JH.** 1982. EMS-induced and radiation-induced mutation frequencies at individual loci in *Arabidopsis thaliana*. *Mutational Research*. **93**; 109-123.
- Körner C.** 2003. Carbon limitation in trees. *Journal of Ecology*. **91**; 4-17.
- Körner C.** 2006. Plant CO₂ responses: an issue of definition, time and resource supply. *New Phytologist*. **172**; 393-411.
- Kutschera U, Schopfer P.** 1985. Evidence against the acid-growth theory of auxin action. *Planta*. **163**; 483-493.
- Lake JA, Quick WP, Beerling DJ, Woodward FI.** 2001. Plant development- signals from mature to new leaves. *Nature*. **411**; 154-154.
- Lake JA, Woodward FI, Quick WP.** 2002. Long-distance CO₂ signalling in plants. *Journal of Experimental Botany*. **53**; 183-193.
- Landrieu I, Da Costa M, De Veylder L, Dewitte F, Vandepoele K, Hassan S, Wieruszeski JM, Corellou F, Faure JD, Montagu MV, Inzé D, Lippens G.** 2004. A small CDC25 dual-specificity tyrosine-phosphatase isoform in *Arabidopsis thaliana*. *Proceedings of the National Academy of Science USA*. **101**; 13380-13385.
- Larkin JC, Young N, Prigge M, Marks MD.** 1996. The control of trichome spacing and number in *Arabidopsis*. *Development*. **122**; 997-1005.
- Leakey ADB, Uribealarea M, Ainsworth EA, Naidu SL, Rogers A, Ort DR, Long SP.** 2006. Photosynthesis, productivity and yield of maize are not affected by open-air elevation of CO₂ concentration in the absence of drought. *Plant Physiology*. **140**; 779-790.
- Lekanne Deprez RH, Fijnvandraat AC, Ruijter JM, Moorman AFM.** 2002. Sensitivity and accuracy of quantitative real-time polymerase chain reaction using SYBR green I depends on cDNA synthesis conditions. *Analytical Biochemistry*. **307**; 63-69.
- Li P, Bohnert HJ, Grene R.** 2007. All about FACE-plants in a high [CO₂] world. *Trends in Plant Science*. **12**; 87-89.
- Li J, Pankratz M, Johnson JA.** 2002. Differential gene expression patterns revealed by oligonucleotide versus long cDNA arrays. *Toxicological Sciences*. **69**; 383-390.
- Li P, Sioson A, Mane SP, Ulanov A, Grothaus G, Heath LS, Murali TM, Bohnert HJ, Grene R.** 2006. Response diversity of *Arabidopsis thaliana* ecotypes in elevated [CO₂] in the field. *Plant Molecular Biology*. **62**; 593-609.
- Liberloo M, Dillen SY, Calfapietra C, Marinri S, Luo ZB, De Angelis P, Ceulemans R.** 2005. Elevated CO₂ concentration, fertilization and their interaction: growth stimulation in a short-rotation poplar coppice (EUROFACE). *Tree Physiology*. **25**; 179-189.
- Liberloo M, Gielen B, Calfapietra C, Veys C, Pigliacelli R, Scarascia-Mugnozza G, Ceulemans R.** 2004. Growth of a poplar short rotation coppice under elevated atmospheric CO₂ concentrations (EUROFACE) depends on fertilisation and species. *Annals of Forest Science*. **61**; 299-307.
- Lin W, Shuai B, Springer PS.** 2003. The *Arabidopsis* LATERAL ORGAN BOUNDARIES-domain gene *ASYMMETRIC LEAVES2* functions in the repression of *KNOX* gene expression and in adaxial-abaxial patterning. *The Plant Cell*. **15**; 2241-2252.

- Lipinski MM, Jacks T.** 1999. The retinoblastoma gene family in differentiation and development. *Oncogene*. **18**; 7873-7882.
- Lipshutz RJ, Fodor SPA, Gingeras TR, Lockhart DJ.** 1999. High density synthetic oligonucleotide arrays. *Nature Genetics Supplement*. **21**; 20-24.
- Lloyd A, Walbot V, Davis R.** 1992. *Arabidopsis* and *Nicotiana* anthocyanin production activated by maize regulator-R and regulator-C1. *Science*. **258**; 1773-1775.
- Lockhart JA.** 1965. An analysis of irreversible plant cell elongation. *Journal of Theoretical Biology*. **8**; 264-275.
- Lodish H, Berk A, Zipursky SL, Matsudaira P, Baltimore D, Darnell J.** 2000. *Molecular Cell Biology*. WH Freeman and Company. p495.
- Long SP, Ainsworth EA, Rogers A, Ort DR.** 2004. Rising Atmospheric Carbon Dioxide: Plants FACE the future. *Annual Review of Plant Biology*. **55**; 591-628.
- Lorenz S, Tinteln S, Reski R, Decker EL.** 2003. Cyclin-D knockout uncouples developmental progression from sugar availability. *Plant Molecular Biology*. **53**; 227-236.
- Lukac M, Calfapietra C, Godbold DL.** 2003. Production, turnover and mycorrhizal colonization of root systems of three *Populus* species grown under elevated CO₂ (POPFACE). *Global Change Biology*. **9**; 838-848.
- Luomala E-M, Laitinen K, Sutinen S, Kellomäki S, Vapaavuori E.** 2005. Stomatal density, anatomy and nutrient concentrations of Scots pine needles are affected by elevated CO₂ and temperature. *Plant, Cell and Environment*. **28**; 733-749.
- Magyar Z, De Veylder L, Atanassova A, Bako L, Inze D, Bogre L.** 2005. The role of the *Arabidopsis* E2FB transcription factor in regulating auxin-dependent cell division. *The Plant Cell*. **17**; 2527-2541.
- Mann M.** 1999. Quantitative proteomics? *Nature Biotechnology*. **17**; 954-955.
- Mann M, Wilm M.** 1994. Error Tolerant Identification of Peptides in Sequence Databases by Peptide Sequence Tags. *Analytical Chemistry*. **66**; 4390-4399.
- Mantripagada KK, Buckley PG, de Ståhl TD, Dumanski JP.** 2004. Genomic microarrays in the spotlight. *Trends in Genetics*. **20**; 87-94.
- Matsubara S, Hurry V, Druart N, Benedict C, Janzik I, Chavarría-Krauser A, Walter A, Schurr U.** 2006. Nocturnal changes in leaf growth of *Populus deltoides* are controlled by cytoplasmic growth. *Planta*. **223**; 1315-1328.
- Matsukura C, Itoh S, Nemoto K, Tanimoto E, Yamaguchi J.** 1998. Promotion of leaf sheath growth by gibberellic acid in a dwarf mutant of rice. *Planta*. **205**; 145-152.
- Mariconti L, Pellegrini B, Cantoni R, Stevens R, Bergounioux C, Cella R, Albani D.** 2002. The E2F family of transcription factors from *Arabidopsis thaliana*. *The Journal of Biological Chemistry*. **277**; 9911-9919.

- Masle J.** 2000. The effects of elevated CO₂ concentrations on cell division rates, growth patterns and blade anatomy in young wheat plants are modulated by factors related to leaf position, vernalization, and genotype. *Plant Physiology*. **122**; 1399-1415.
- Mayer KFX, Schoof H, Haecker A, Lenhard M, Jürgens G, Laux T.** 1998. Role of *WUSCHEL* in regulating stem cell fate in the *Arabidopsis* shoot meristem. *Cell*. **95**; 805-815.
- McConnell JR, Emery J, Eshed Y, Bao N, Bowman J Barton MK.** 2001. Role of *PHABULOSA* and *PHAVOLUTA* in determining radial patterning in shoots. *Nature*. **411**; 709-713.
- McElwain JC, Chaloner WG.** 1995. Stomatal density and index of fossil plants track atmospheric carbon dioxide in the paleozoic. *Annals of Botany*. **76**; 389-395.
- McElwain JC, Beerling DJ, Woodward FI.** 1999. Fossil plants and global warming at the Triassic-Jurassic boundary. *Science*. **285**; 1386-1390.
- McLeod AR, Long SP.** 1999. Free-air carbon dioxide enrichment (FACE) in global change research: a review. *Advances in Ecological Research*. **28**; 1-56.
- McQueen-Mason SJ, Fry SC, Durachko DM, Cosgrove DJ.** 1993. The relationship between xyloglucan endotransglycosylases and *in vitro* cell wall extension in cucumber hypocotyls. *Planta*. **190**; 327-331.
- Medlyn BE, Barton CVM, Broadmeadow MSJ, Ceulemans R, De Angelis P, Forstreuter M, Freeman M, Jackson SB, Kellomäki S, Laitat E, Rey A, Roberntz P, Sigurdsson BD, Strassemeier J, Wang K, Curtis PS, Jarvis PG.** 2001. Stomatal conductance of forest species after long-term exposure to elevated CO₂ concentration: a synthesis. *New Phytologist*. **149**; 247-264.
- Menges M de Jager SM, Gruitsem W, Murray JAH.** 2005. Global analysis of the core cell cycle regulators of *Arabidopsis* identifies novel genes, reveals multiple and highly specific profiles of expression and provides a coherent model for plant cell cycle control. *Plant Journal*. **41**; 546-566.
- Micol JL, Hake S.** 2003. The development of plant leaves. *Plant Physiology*. **131**; 389-394.
- Miglietta F, Peressotti A, Vaccari FP, Zaldei A, deAngelis P, Scarascia-Mugnozza G.** 2001. Free Air CO₂ enrichment (FACE) of a poplar plantation: the POPFACE fumigation system. *New Phytologist*. **150**; 465-476.
- Minorsky PV.** 2003. Achieving the *In Silico* plant. Systems biology and the future of plant biological research. *Plant Physiology*. **132**; 404-409.
- Mironov V, De Veylder L, Van Montagu M, Inzé D.** 1999. Cyclin-dependent kinases and cell division in plants: the nexus. *Plant Cell*. **11**; 509-521.
- Miyazaki S, Fredricksen M, Hollis KC, Poroyko V, Shepley D, Galbraith DW, Long SP, Bohnert HJ.** 2004. Transcript expression profiles of *Arabidopsis thaliana* grown under controlled conditions and open-air elevated concentrations of CO₂ and of O₃. *Field Crops Research*. **90**; 47-59.
- Moore BD, Cheng SH, Rice J, Seeman JR.** 1998. Sucrose cycling, Rubisco expression, and prediction of photosynthetic acclimation to elevated atmospheric CO₂. *Plant Cell and Environment*. **21**; 905-915.
- Moore BD, Cheng SH, Sims D, Seemann JR.** 1999. The biochemical and molecular basis for photosynthetic acclimation to elevated atmospheric CO₂. *Plant Cell and Environment*. **22**; 567-582.

- Moore BD, Palmquist DE, Seeman JR.** 1997. Influence of plant growth at high CO₂ concentrations on leaf content of Ribulose-1,5-bisphosphate carboxylase/ oxygenase and intracellular distribution of soluble carbohydrates in tobacco, snapdragon, and parsley. *Plant Physiology*. **115**; 241–246.
- Morgan DO.** 1997. CYCLIN-DEPENDENT KINASES: Engines, Clocks, and Microprocessors. *Annual Review of Cell and Developmental Biology*. **13**; 261-291.
- Mowforth MA, Grime JP.** 1989. Intra-population variation in nuclear DNA amount, cell size and growth rate in *Poa annua* L. *Functional Ecology*. **3**; 289-295.
- Mueller LA, Zhang P, Rhee SY.** 2003. AraCyc: A biochemical pathway database for *Arabidopsis*. *Plant Physiology*. **132**; 453-460.
- Murray JAH.** 1997. The retinoblastoma protein is in plants! *Trends in Plant Science*. **2**; 82-84.
- Murthy R, Barron-Gafford G, Dougherty PM, Engel VC, Grieve K, Handley L, Klimas C, Potosnak MJ, Zarnoch SJ, Zhang J.** 2005. Increased leaf area dominates carbon flux response to elevated CO₂ in stands of *Populus deltoides*. *Global Change Biology*. **11**; 716-731.
- Myneni RB, Dong J, Tucker CJ, Kaufmann RK, Kauppi PE, Liski J, Zhou L, Alexeyev V, Hughes MK.** 2001. A large carbon sink in the woody biomass of Northern Forests. *Proceedings of the National Academy of Science USA*. **98**; 14784-14789.
- Nadeau JA, Sack FD.** 2002. Control of stomatal distribution on the *Arabidopsis* leaf surface. *Science*. **296**; 1697-1700.
- Nadeau JA, Sack FD.** 2003. Stomatal development: cross talk puts mouths in place. *Trends in Plant Science*. **8**; 294-299.
- Nakaya M, Tsukaya H, Murakami N, Kato M.** 2002. Brassinosteroids control the proliferation of leaf cells in *Arabidopsis thaliana*. *Plant Cell Physiology*. **43**; 239-244.
- Narita NN, Moore S, Horiguchi G, Kubo M, Demura T, Fukuda H, Goodrich J, Tsukaya H.** 2004. Overexpression of a novel small peptide *ROTUNDIFOLIA4* decreases cell proliferation and alters leaf shape in *Arabidopsis thaliana*. *Plant Journal*. **38**; 699–713.
- Nath U, Crawford BCW, Carpenter R, Coen E.** 2003. Genetic control of surface curvature. *Science*. **299**; 1404-1407.
- Nesi N, Debeaujon I, Jond C, Pelletier G, Caboche M, Lepiniec L.** 2000. The *TT8* gene encodes a basic helix-loop-helix domain protein required for expression of *DFR* and *BAN* genes in *Arabidopsis* siliques. *Plant Cell*. **12**; 1863-1878.
- Nie G, Hendrix DL, Webber AN, Kimball BA, Long SP.** 1995. Increased accumulation of carbohydrates and decreased photosynthetic gene transcript levels in wheat grown at an elevated CO₂ concentration in the field. *Plant Physiology*. **108**; 975-983.
- Norby RJ, Sholtis JD, Gunderson CA, Jawdy SS.** 2003. Leaf dynamics of a deciduous forest canopy: no response to elevated CO₂. *Oecologia*. **136**; 574-584.
- Norby RJ, Wullschleger SD, Gunderson CA, Johnson DW, Ceulemans R.** 1999. Tree responses to rising CO₂ in field experiments: implications for the future forest. *Plant, Cell and Environment*. **22**; 683-714.

- O'Farrell PH.** 1975. High resolution two-dimensional electrophoresis of proteins. *Journal of Biological Chemistry*. **250**; 4007-4021.
- Okamoto-Nakazato A, Nakamura T, Okamoto H.** 2000. The isolation of wall bound proteins regulating yield threshold tension in glycerinated hollow cylinders of cowpea hypocotyl. *Plant Cell and Environment*. **23**;145-154.
- Okamoto-Nakazato A, Takahashi K, Katoh-Semba R, Katou K.** 2001. Distribution of Yieldin, a regulatory protein of the cell wall yield threshold, in etiolated cowpea seedlings. *Plant Cell Physiology*. **42**; 952-958.
- Oksanen E, Sober J, Karnosky DF.** 2001. Impacts of elevated CO₂ and/or O₃ on leaf ultrastructure of aspen (*Populus tremuloides*) and birch (*Betula papyrifera*) in the Aspen FACE experiment. *Environmental Pollution*. **115**; 437-446.
- Olszewski N, Sun TP, Gubler F.** 2002. Gibberellin signalling: biosynthesis, catabolism and response pathways. *Plant Cell*. S61-S80.
- Ori N, Eshed Y, Chuck G, Bowman JL, Hake S.** 2000. Mechanisms that control knox gene expression in the *Arabidopsis* shoot. *Development*. **127**; 5523-5532.
- Otsuga D, DeGuzman B, Prigge MJ, Drews GN, Clark SE.** 2001. *REVOLUTA* regulates meristem initiation at lateral positions. *The Plant Journal*. **25**; 223-236.
- Ouborg NJ, Vriezen WH.** 2006. An ecologist's guide to ecogenomics. *Journal of Ecology*. **95**; 8-16.
- Paradez AR, Somerville CR, Ehrhardt DW.** 2006. Visualisation of cellulose synthase demonstrates functional association with microtubules. *Science*. **312**; 1491-1495.
- Paul MJ, Foyer CH.** 2001. Sink regulation of photosynthesis. *Journal of Experimental Botany*. **52**; 1383-1400.
- Payne C, Zhang F, Lloyd A.** 2000. *GL3* encodes a bHLH protein that regulates trichome development in *Arabidopsis* through interaction with *GL1* and *TTG1*. *Genetics*. **156**; 1349-1362.
- Pepin S, Körner C.** 2002. Web-FACE: a new canopy free-air CO₂ enrichment system for tall trees in mature forests. *Oecologia*. **133**; 1-9.
- Pego JV, Kortstee AJ, Huijser C, Smeeckens SCM.** 2000. Photosynthesis, sugars and the regulation of gene expression. *Journal of Experimental Botany*. **51**; 407-416.
- Perkins DN, Pappin DJC, Creasy DM, Cottrell JS.** 1999. Probability-based protein identification by searching sequence databases using mass spectrometry data. *Electrophoresis*. **20**; 3551-3567.
- Petit JR, Jouzel J, Raynaud D, Barkov NI, Barnola JM, Basile I, Bender M, Chappellaz J, Davis M, Delaygue G, Delmotte M, Kotlyakov VM, Legrand M, Lipenkov VY, Lorius C, Pepin L, Ritz C, Saltzman E, Stievenard M.** 1999. Climate and atmospheric history of the past 420,000 years from the Vostok ice core, Antarctica. *Nature*. **399**; 429-436.
- Pfaffl MW.** 2001. A new mathematical model for relative quantification in real-time RT-PCR. *Nucleic Acids Research*. **29**; e45.
- Pien S, Wyrzykowska J, McQueen-Mason S, Smart C, Fleming A.** 2001. Local expression of expansin induces the entire process of leaf development and modifies leaf shape. *Proceedings of the National Academy of Science USA*. **98**; 11812-11817.

Plomion C, Lelanne C, Claverol S, Meddour H, Kohler A, Bogeat-Triboulot MB, Barre A, Provost GL, Dumazet H, Jacob D, Bastien C, Dreyer E, de Daruvar A, Guehl JM, Schmitter JM, Martin F, Bonneau M. 2006. Mapping the proteome of poplar and application to the discovery of drought-stress responsive proteins. *Proteomics*. **6**; 6509-6527.

Prentice IC, Farquhar G, Fasham M, Goulden M, Heimann M, Jaramillo V, Kheshgi H, Le Quere C, Scholes RJ. 2001. The carbon cycle and atmospheric carbon dioxide. In: *Climate change 2001: The scientific basis. Contribution of working Group I to the Third Assessment Report of the Intergovernmental panel on Climate Change* [Houghton JT, Ding Y, Griggs DJ, Noger M, van der Linden PJ, Dai X, Maskell K, Johnson CA (eds)], pp. 183-237. Cambridge University Press, Cambridge.

Price TD, Qvarnström A, Irwin DE. 2003. The role of phenotypic plasticity in driving genetic evolution. *Proceedings of the Royal Society of London Series B-Biological Sciences*. **270**; 1433-1440.

Primrose SB, Twyman RM. 2006. Principles of Gene Manipulation and Genomics. Seventh edition. Blackwell Publishing, Oxford, UK. pp418-420.

Pritchard J, Hetherington PR, Fry SC, Tomos AD. 1993. Xyloglucan endotransglycosylases activity, microfibril orientation and the profiles of cell wall properties along growing regions of maize roots. *Journal of Experimental Botany*. **44**; 1281-1289.

Pritchard SG, Rogers HH, Prior SA, Peterson CM. 1999. Elevated CO₂ and plant structure: a review. *Global Change Biology*. **5**; 807-837.

Qin J, Fenyo D, Zhao YM, Hall WW, Chao DM, Wilson CJ, Young RA, Chait BT. 1997. A strategy for rapid, high confidence protein identification. *Analytical Chemistry*. **69**; 3995-4001.

Quackenbush J. 2001. Computational analysis of microarray data. *Nature Reviews Genetics*. **2**; 418-427.

Quadroni M, James P. 1999. Proteomics and automation. *Electrophoresis*. **20**; 664-677.

Radoglou KM, Jarvis PG. 1990. Effects of CO₂ enrichment on four poplar clones. I. Growth and Anatomy. *Annals of Botany*. **65**; 617-626.

Radoglou KM, Jarvis PG. 1990b. Effects of CO₂ enrichment on four poplar clones. II. Leaf surface properties. *Annals of Botany*. **65**; 626-632.

Radoglou KM, Aphalo P, Jarvis PG. 1992. Response of photosynthesis, stomatal conductance and water-use efficiency to elevated CO₂ and nutrient supply in acclimated seedlings of *Phaseolus vulgaris*. *Annals of Botany*. **70**; 257-264.

Rae AM, Ferris R, Tallis MJ, Taylor G. 2006. Elucidating genomic regions determining enhanced leaf growth and delayed senescence in elevated CO₂. *Plant, Cell and Environment*. **29**; 1730-1741.

Rae AM, Robinson KM, Street NR, Taylor G. 2004. Morphological and physiological traits influencing biomass productivity in short term rotation coppice poplar. *Canadian Journal of Forest Research*. **34**; 1488-1498.

Rae AM, Street NR, Rodriguez-Acosta M. 2007. *Populus* trees. In; Genome Mapping and Molecular Breeding in Plants, Volume 7 Forest Trees. Ed; C. Kole. Springer-Verlag Berlin Heidelberg. pp1-28.

- Rae AM, Tricker PJ, Bunn SM, Taylor G.** 2007. Adaptation of tree growth to elevated CO₂: quantitative trait loci for biomass in *Populus*. *New Phytologist*. **175**;59-69.
- Ramakers C, Ruijter JM, Deprez RHL, Moorman AFM.** 2003. Assumption-free analysis of quantitative real-time polymerase chain reaction (PCR) data. *Neuroscience Letters*. **339**; 62-66.
- Ranasinghe S, Taylor G.** 1996. Mechanism for increased leaf growth in elevated CO₂. *Journal of Experimental Botany*. **47**;349-358.
- Rayle DL, Cleland RE.** 1992. The acid growth theory of auxin-induced cell elongation is alive and well. *Plant Physiology*. **99**; 1271-1274.
- Reidy B, Nösberger J, Fleming A.** 2001. Differential expression of XET-related genes in the leaf elongation zone of *F. pratensis*. *Journal of Experimental Botany*. **52**; 1847-1856.
- Reinhardt D, Mandel T, Kuhlemeier C.** 2000. Auxin regulates the initiation and radial position of plant lateral organs. *Plant Cell*. **12**; 507-518.
- Riccardi F, Gazeau P, Jacquemot MP, Vincent D, Zivy M.** 2004. Deciphering genetic variations of proteome responses to water deficit in maize leaves. *Plant Physiology and Biochemistry*. **42**; 1003-1011.
- Rhio-Khamlichi C, Huntley R, Jacqmard A, Murray JAH.** 1999. Cytokinin activation of *Arabidopsis* cell division through D-type Cyclin. *Science*. **283**; 1541-1544.
- Rhio-Khamlichi C, Menges M, Healy JMS, Murray JAH.** 2000. Sugar control of the plant cell cycle: differential regulation of *Arabidopsis* D-type cyclin gene expression. *Molecular and Cellular Biology*. **20**; 4513-4521.
- Richard C, Lescot M, Inzé D, De Veylder L.** 2002. Effect of auxin, cytokinin, and sucrose on cell cycle gene expression in *Arabidopsis thaliana* cell suspension cultures. *Plant Cell, Tissue and Organ Culture*. **69**; 167-176.
- Richmond T.** 2000. Higher plant cellulose synthases. *Genome Biology*. **1**; reviews 3001.1-3001.6.
- Ridge CR, Hinckley TM, Stettler RF, Van Volkenburgh E.** 1986. Leaf growth characteristics of fast-growing poplar hybrids *Populus trichocarpa* x *P. deltoides*. *Tree Physiology*. **1**; 209-216.
- Ririe KM, Rasmussen RP, Wittwer CT.** 1997. Product Differentiation by Analysis of DNA Melting Curves during the Polymerase Chain Reaction. *Analytical Biochemistry*. **245**; 154-160.
- Robertson EJ, Leech RM.** 1995. Significant changes in cell and chloroplast development in young wheat leaves (*Triticum aestivum*) grown in elevated CO₂. *Plant Physiology*. **107**; 63-71.
- Rodriguez-Acosta M.** 2006. The ecophysiology and genetics of drought tolerance in *Populus*. *Thesis*, University of Southampton.
- Rogers A, Ainsworth EA.** 2006. The response of foliar carbohydrate to elevated [CO₂]. *In: Managed ecosystems and CO₂*. Edited by J Nösberger, SP Long, RJ Norby, M Stitt, GR Hendrey, H Blum. Springer, Berlin Heidelberg New York. pp293-308
- Rogers A, Allen DJ, Davey PA, Morgan PB, Ainsworth EA, Bernacchi CJ, Cornic G, Dermody O, Dohleman FG, Heaton EA, Mahoney J, Zhu XG, Delucia EH, Ort DR, Long SP.** 2004. Leaf photosynthesis and carbohydrate dynamics of soybeans grown throughout their life-cycle under Free-Air Carbon dioxide Enrichment. *Plant, Cell and Environment*. **27**; 449-558.

Rose JKC, Braam J, Fry SC, Nishitani K. 2002. The XTH family of enzymes involved in xyloglucan endotransglycosylation and endohydrolysis: current perspectives and a new unifying nomenclature. *Plant Cell Physiology*. **43**; 1421-1435.

Ross PL, Huang YN, Marchese JN, Williamson B, Parker K, Hattan S, Khainovski N, Pillai S, Dey S, Daniel S, Purkayastha S, Juhasz P, Martin S, Bartlett-Jones M, He F, Jacobson A, Pappin DJ. 2004. Multiplexed protein quantitation in *Saccharomyces cerevisiae* using amine reactive isobaric tagging elements. *Molecular and Cellular Proteomics*. **3**; 1154-1169.

Royer DL. 2001. Stomatal density and stomatal index as indicators of paleoatmospheric CO₂ concentration. *Review of Palaeobotany and Palynology*. **114**; 1-28.

Saiki RK, Gelfand DH, Stoffel S, Scharf SJ, Higuchi R, Horn GT, Mullis KB, Erlich HA. 1988. Primer-Directed Enzymatic Amplification of DNA with a Thermostable DNA-Polymerase. *Science*. **239**; 487-491.

Sakamoto T, Kamiya N, Ueguchi-Tanaka M, Iwahori S, Matsuoka M. 2001. *KNOX* homeobox protein directly suppresses the expression of a gibberellin biosynthetic gene in the tobacco shoot apical meristem. *Genes and Development*. **15**; 581-590.

Salekdeh GH, Siopongco J, Wade LJ, Ghareyazie B, Bennett J. 2002. Proteomic analysis of rice leaves during drought stress and recovery. *Proteomics*. **2**; 1131-1145.

Salnikov VV, Grimson MJ, Delmer DP, Haigler CH. 2001. Sucrose synthase localises to cellulose synthesis sites in trachery elements. *Phytochemistry*. **57**; 823-833.

Sampedro J, Carey RE, Cosgrove DJ. 2006. Genome histories clarify evolution of the expansin superfamily: new insights from the poplar genome and pine ESTs. *Journal of Plant Research*. **119**; 11-21.

Sato S, Kato T, Kakegawa K, Ishii T, Liu YG, Awano T, Takebe K, Nishiyama Y, Kuga S, Sato S, Nakamura Y, Tabata S, Shibata D. 2001. Role of the putative membrane bound endo-1,4- β -glucanase *KORRIGAN* in cell elongation and cellulose synthesis in *Arabidopsis thaliana*. *Plant and Cell Physiology*. **42**; 251-263.

Sauter M, Mekhedov SL, Kende H. 1995. Gibberellin promotes histone H1 kinase activity and the expression of *cdc2* and cyclin genes during the induction of rapid growth in deepwater rice internodes. *Plant Journal*. **7**; 623-632.

Savaldi-Goldstein S, Peto C, Chory J. 2007. *Nature*. **446**; 199-202.

Sawa S, Watanabe K, Goto K, Kanaya E, Morita EH, Okada K. 1999. *FILAMENTOUS FLOWER*, a meristem and organ identity gene of *Arabidopsis*, encodes a protein with a zinc finger and HMG-related domains. *Genes and Development*. **13**; 1079-1088.

Saxena IM, Brown Jr RM. 2005. Cellulose biosynthesis: Current views and evolving concepts. *Annals of Botany*. **96**; 9-21.

Schena M, Heller RA, Theriault TP, Konrad K, Lachenmeier E, Davis RW. 1998. Microarrays; biotechnology's discovery platform for functional genomics. *Trends in biotechnology*. **16**; 301-306.

Schneeberger R, Tsiantis M, Freeling M, Langdale JA. 1998. The *rough sheath2* gene negatively regulates homeobox gene expression during maize leaf development. *Development*. **125**; 2857-2865.

- Schnittger A, Folkers U, Schwab B, Jürgens G, Hülskamp M.** 1999. Generation of a spacing pattern: the role of *TRIPTYCHON* in trichome patterning in *Arabidopsis*. *The Plant Cell*. **11**; 1105-1116.
- Schopfer P, Liszkay A, Bechtold M, Frahry G, Wagner A.** 2002. Evidence that hydroxyl radicals mediate auxin induced extension growth. *Planta*. **214**; 821-828.
- Scheele GA.** 1975. Two dimensional gel analysis of soluble proteins. Characterisation of guinea pig exocrine pancreatic proteins. *Journal of Biological Chemistry*. **250**; 5375-5385.
- Scheres B.** 2007. The force from without. *Nature*. **446**; 151-152.
- Schimel DS.** 1995. Terrestrial ecosystems and the carbon cycle. *Global Change Biology*. **1**; 77-91.
- Schoof H, Lenhard M, Haecker A, Mayer KFX, Jürgens G, Laux T.** 2000. The stem cell population of *Arabidopsis* shoot meristems is maintained by a regulatory loop between *CLAVATA* and *WUSCHEL* genes. *Cell*. **100**; 635-644.
- Shaul O, Mironov V, Burssens S, Van Montagu M, Inzé D.** 1996. Two *Arabidopsis* cyclin promoters mediate distinctive transcriptional oscillation in synchronized tobacco BY-2 cells. *Proceedings of the National Academy of Science USA*. **93**; 4868-4872.
- Sherlock G, Hernandez-Boussard T, Kasarskis A, Binkley G, Matese JC, Dwight SS, Kaloper M, Weng S, Jin H, Ball CA, Eisen MB, Spellman PT, Brown PO, Botstein D, Cherry JM.** 2001. The Stanford Microarray Database. *Nucleic Acids Research*. **29**; 152-155.
- Shibaoka H.** 1994. Plant hormone-induced changes in the orientation of cortical microtubule:alterations in the cross-linking between microtubules and the plasma membrane. *Annual Review of Plant Physiology and Plant Molecular Biology*. **45**; 527-544.
- Shih JH, Michalowska AM, Dobbin K, Ye Y, Qui TH, Green JE.** 2004. Effects of pooling mRNA in microarray class comparisons. *Bioinformatics*. **20**; 3318-3325.
- Shimotohno A, Umeda-Hara C, Bisova K, Uchimiya H, Umeda M.** 2004. The plant-specific kinase CDKF;1 is involved in activating phosphorylation of cyclin dependent kinase-activating kinases in *Arabidopsis*. *The Plant Cell*. **16**; 2954-2966.
- Sicher RC, Kremer DF, Rodermel SR.** 1994. Photosynthetic acclimation to elevated CO₂ occurs in transformed Tobacco with decreased Ribulose-1,5-bisphosphate carboxylase/oxygenase content. *Plant Physiology*. **104**; 409-415.
- Siegenthaler U, Stocker TF, Monnin E, Luthi D, Schwander J, Stauffer B, Raynaud D, Barnola JM, Fischer H, Masson-Delmotte V, Jouzel J.** 2005. Stable carbon cycle-climate relationship during the late Pleistocene. *Science*. **310**; 1313-1317.
- Siegfried KR, Eshed Y, Baum SF, Otsuga D, Drews GN, Bowman JL.** 1999. Members of the *YABBY* gene family specify abaxial cell fate in *Arabidopsis*. *Development*. **126**; 4117-4128.
- Sjödin A, Bylesjö M, Skogström O, Eriksson D, Nilsson P, Ryden P, Jansson S, Karlsson J.** 2006. UPSC-BASE- *Populus* transcriptomics online. *The Plant Journal*. **48**; 806-817.
- Smeeckens S.** 2000. Sugar induced signal transduction in plants. *Annual Review of Plant Physiology and Plant Molecular Biology*. **51**; 49-81.

- Smith RC, Matthews PR, Schünmann PHD, Chandler PM.** 1996. The regulation of leaf elongation and xyloglucan endotransglycosylase by gibberellin in ‘himalaya’ barley (*Hordeum vulgare* L.) *Journal of Experimental Botany*. **47**; 1395-1404.
- Somerville C.** 2006. Cellulose synthesis in higher plants. *Annual Review of Cell and Developmental Biology*. **22**; 53-78.
- Somerville C, Bauer S, Brininstool G, Facette M, Hamann T, Milne J, Osborne E, Paradez A, Persson S, Raab T, Vorwerk S, Youngs H.** 2004. Towards a systems approach to understanding plant cell walls. *Science*. **306**; 2206-2211.
- Soni R, Carmichael JP, Shah ZH, Murray JA.** 1995. A family of cyclin D homologs from plants differentially controlled by growth regulators and containing the conserved retinoblastoma protein interaction motif. *Plant Cell*. **7**; 85-103.
- Southern E, Mir K, Shchepinov M.** 1999. Molecular interactions on microarrays. *Nature Genetics Supplement*. **21**; 5-9.
- Sozzani R, Maggio C, Varotto S, Canova S, Bergounioux C, Albani D, Cella R.** 2006. Interplay between *Arabidopsis* activating factors E2Fb and E2Fa in cell cycle progression and development. *Plant Physiology*. **140**; 1355-1366.
- Sterky F, Bhalerao RR, Unneberg P, Segerman B, Nilsson P, Brunner AM, Charbonnel-Campaa L, Lindvall JJ, Tandre K, Strauss SH, Sundberg B, Gustafsson P, Uhlén M, Bhalerao RP, Nilsson O, Sandberg G, Karlsson J, Lundeberg J, Jansson S.** 2004. A *Populus* EST resource for plant functional genomics. *Proceedings of the National Academy of Science USA*. **101**; 13951-13956.
- Stitt M.** 1991. Rising CO₂ levels and their potential significance for carbon flow in photosynthetic cells. *Plant Cell and Environment*. **14**; 741-762.
- Stitt M, Krapp A.** 1999. The interaction between elevated carbon dioxide and nitrogen nutrition: the physiological and molecular background. *Plant Cell and Environment*. **22**; 583-621.
- Strauss SH, Martin FM.** 2004. Poplar genomics comes of age. *New Phytologist*. **164**; 1-4.
- Street NR.** 2005. The genetics and genomics of drought response in *Populus*. *Thesis*. University of Southampton.
- Street NR, Skogström O, Sjödin A, Tucker J, Rodríguez-Acosta M, Nilsson P, Jansson S, Taylor G.** 2006. The genetics and genomics of the drought response in *Populus*. *The Plant Journal*. **48**; 321-341.
- Stulen I, den Hertog J.** 1993. Root growth and functioning under atmospheric CO₂ enrichment. *Vegetatio*. **104**; 99-115.
- Suge H, Murakami Y.** 1968. Occurrence of a rice mutant deficient in gibberellin-like substances. *Plant Cell Physiology*. **9**; 411-414.
- Sugimoto-Shirasu K, Roberts K.** 2003. “Big it up”: endoreduplication and cell-size control in plants. *Current Opinion in Plant Biology*. **6**; 544-553.
- Süle A, Vanrobaeys F, Hajós G, Beeumen J V, Devreese B.** 2004. Proteomic analysis of small heat shock protein isoforms in barleys shoots. *Phytochemistry*. **65**; 1853-1863.

Sun Y, Dilkes BP, Zhang C, Dante RA, Carneiro NP, Lowe KS, Jung R, Gordon-Kamm WJ, Larkins BA. 1999. Characterisation of maize (*Zea mays*) Wee1 and its activity in developing endosperm. *Proceedings of the National Academy of Sciences USA*. **96**; 4180-4185.

Sussex IM. 1954. Experiments on the cause of dorsiventrality in leaves. *Nature*. **174**; 351-352.

Sussex IM. 1955. Morphogenesis in *Solanum tuberosum* L: Experimental investigation of leaf dorsoventrality and orientation in the juvenile shoot. *Phytomorphology*. **5**; 286-300.

Talbott LD, Hammad JW, Harn LC, Nguyen VH, Patel J, Zeiger E. 2006. Reversal by green light of blue light-stimulated stomatal opening in intact, attached leaves of *Arabidopsis* operates only in the potassium-dependent, morning phase of movement. *Plant Cell Physiology*. **47**; 332-339.

Taiz L, Zeiger E. 2002. *Plant Physiology*. Third Edition. Sinauer Associates.

Tanaka K, Murata K, Yamazaki M, Onosato K, Miyao A, Hirochika H. 2003. Three distinct rice cellulose synthase catalytic subunit genes required for cellulose synthesis in the secondary wall. *Plant Physiology*. **133**; 1-11.

Tanimoto E, Masuda Y. 1968. Effect of auxin on cell wall degrading enzymes. *Physiologia Plantarum*. **21**; 820-826.

Tao WA, Aebersold R. 2003. Advances in quantitative proteomics via stable isotope tagging and mass spectrometry. *Current Opinion in Biotechnology*. **14**; 110-118.

Taylor G. 2002. *Populus*; *Arabidopsis* for forestry. Do we need a model tree? *Annals of Botany*. **90**; 681-689.

Taylor G, Ceulemans R, Ferris R, Gardner SDL, Shao BY. 2001. Increased leaf area expansion of hybrid poplar in elevated CO₂. From controlled environments to open-top chambers and to FACE. *Environmental Pollution*. **115**; 463-472.

Taylor G, Ranasinghe S, Bosac C, Gardner SDL, Ferris R. 1994. Elevated CO₂ and plant growth: cellular mechanisms and responses of whole plants. *Journal of Experimental Botany*. **45**; 1761-1774.

Taylor G, Street NR, Tricker PJ, Sjodin A, Graham LE, Skogstrom O, Calfapietra C, Scarascia-Mugnozza G, Jansson S. 2005. The transcriptome of *Populus* in elevated CO₂. *New Phytologist*. **167**; 143-154.

Taylor G, Tallis MJ, Giardina CP, Percy KE, Miglietta F, Gupta PS, Gioli B, Calfapietra C, Gielen B, Kubiske ME, Scarascia-Mugnozza GE, Kets K, Long SP, Karnosky DF. 2008. Future atmospheric CO₂ leads to delayed autumnal senescence. *Global Change Biology*. **14**; 264-275.

Taylor G, Tricker PJ, Zhang FZ, Alston VJ, Miglietta F, Kuzminsky E. 2003. Spatial and temporal effects of Free-Air CO₂ Enrichment (POPFACE) on leaf growth, cell expansion, and cell production in a closed canopy of Poplar. *Plant Physiology*. **131**; 177-185.

Taylor JA, Walsh KA, Johnson RS. 1996. Sherpa: a Macintosh-based Expert System for the Interpretation of Electrospray Ionization LC/MS and MS/MS data from protein digests. *Rapid Communications in Mass Spectrometry*. **10**; 679-687.

Tharakan PJ, Abrahamson LP, Isebrands JG, Robison DJ. 1998. First year growth and development of willow and poplar bioenergy crops as related to foliar characteristics. Available from <http://bioenergy.ornl.gov/papers/bioen98/tharakan.html>.

Thiellement H, Bahrman N, Colas des Francs C. 1986. Regulatory effects of homologous chromosome arms on wheat proteins at two developmental stages. *Theoretical and Applied Genetics*. **73**; 246-251.

Thiellement H, Bahrman N, Damerval C, Plomion C, Rossignol M, Santoni V, de Vienne D, Zivy M. 1999. Proteomics for genetic and physiological studies in plants. *Electrophoresis*. **20**; 2013-2026.

Thimm O, Bläsing O, Gibon Y, Nagel A, Meyer S, Krüger P, Selbig J, Müller LA, Rhee SY, Stitt M. 2004. MAPMAN: a user-driven tool to display genomics data sets onto diagrams of metabolic pathways and other biological processes. *The Plant Journal*. **37**; 914-939.

Thomas MA, Klaper R. 2004. Genomics for the ecological toolbox. *Trends in Ecology and Evolution*. **19**; 439-445.

Thomas RB, Strain BR. 1991. Root restriction as a factor in photosynthetic acclimation of cotton seedlings grown in elevated carbon dioxide. *Plant Physiology*. **96**: 627-634.

Tian B, Rentz SS, Gorman GS, Rogers T, Page JG. 2004. Comparison of real-time PCR assay methods in detection and quantification of β -actin genes in mouse tissues. *Preclinica*. **2**; 214-220.

Timmermans MCP, Hudson A, Becraft PW, Nelson T. 1999. *ROUGH SHEATH2*: a Myb protein that represses *knox* homeobox genes in maize lateral organ primordia. *Science*. **284**; 151-153.

Tjoelker MG, Oleksyn J, Reich PB. 1998. Seedling of five boreal tree species differ in acclimation of net photosynthesis to elevated CO₂ and temperature. *Tree Physiology*. **18**; 715-726.

Tode K, Lüthen H. 2001. Fusicoccin- and IAA-induced elongation growth share the same pattern of K⁺ dependence. *Journal of Experimental Botany*. **52**; 251-255.

Torres Acosta JA, de Almeida Engler J, Raes J, Magyar Z, de Groodt R, Inzé D, De Veylder L. 2004. Molecular Characterization of *Arabidopsis* PHO80-like proteins, a novel class of CDKA; 1-interacting cyclins. *Cellular and Molecular Life Sciences*. **61**; 1485-1497.

Traas J, Vernoux T. 2002. The shoot apical meristem: the dynamics of a stable structure. *Philosophical Transactions of the Royal Society of London B*. **357**; 737-747.

Tricker PJ, Calfapietra C, Kuzminsky E, Puleggi R, Ferris R, Nathoo M, Pleasants LJ, Alston V, de Angelis P, Taylor G. 2004. Long-term acclimation of leaf production, development, longevity and quality following 3 year exposure to free-air CO₂ enrichment during canopy closure in *Populus*. *New Phytologist*. **162**; 413-426.

Tricker PJ, Trewin H, Kull O, Clarkson GJJ, Eensalu E, Tallis MJ, Colella E, Doncaster CP, Sabatti M, Taylor G. 2005. Stomatal conductance and not stomatal density determines the long-term reduction in leaf transpiration of poplar in elevated CO₂. *Oecologia*. **143**; 652-660.

Tsiantis M, Schneeberger R, Golz JF, Freeling M, Langdale JA. 1999. The maize rough sheath2 gene and leaf development programs in monocot and dicot plants. *Science*. **284**; 154-156.

Tsuge T, Tsukaya H, Uchimiya H. 1996. Two independent and polarized processes of cell elongation regulate leaf blade expansion in *Arabidopsis thaliana*. *Development*. **122**; 1589-1600.

Tsukaya H. 2002. Leaf development. In: Somerville CR, Meyerowitz EM (eds) *The Arabidopsis Book*. American Society of Plant Biologists, Rockville. Available at <http://www.aspb.org/downloads/Arabidopsis/tsukaya.pdf>.

Tsukaya H. 2002b. The Leaf Index: Heteroblasty, natural variation and the genetic control of polar processes of leaf expansion. *Plant Cell Physiology*. **43**; 372-378.

Tsukaya H. 2002c. Interpretation of mutants in leaf morphology: genetic evidence for a compensatory system in leaf morphogenesis that provides a new link between cell and organismal theories. *International Review of Cytology- A survey of Cell Biology*. **217**; 1-39.

Tsukaya H. 2003. Organ shape and size: a lesson from studies of leaf morphogenesis. *Current Opinion in Plant Biology*. **6**; 57-62.

Tsukaya H. 2005. Leaf shape: genetic controls and environmental factors. *International Journal of Developmental Biology*. **49**; 547-555.

Tsukaya H. 2006. Mechanism of leaf-shape determination. *Annual Review of Plant Biology*. **57**; 477-496.

Tucker J. 2006. The genetics, genomics and physiology of the response of *Populus* to elevated ozone. *Thesis*. University of Southampton.

Turgeon R. 1989. The sink-source transition in leaves. *Annual Review of Plant Physiology and Plant Molecular Biology*. **40**; 119-138.

Tuskan GA, DiFazio S, Jansson S, Bohlmann J, Grigoriev I, Hellsten U, Putnam N, Ralph S, Rombauts S, Salamov A, Schein J, Sterck L, Aerts A, Bhalerao RR, Bhalerao RP, Blaudez D, Boerjan W, Brun A, Brunner A, Busov V, Campbell M, Carlson J, Chalot M, Chapman J, Chen GL, Cooper D, Coutinho PM, Couturier J, Covert S, Cronk Q, Cunningham R, Davis J, Degroove S, Dejardin A, dePamphilis C, Detter J, Dirks B, Dubchak I, Duplessis S, Ehlting J, Ellis B, Gendler K, Goodstein D, Gribskov M, Grimwood J, Groover A, Gunter L, Hamberger B, Heinze B, Helariutta Y, Henrissat B, Holligan D, Holt R, Huang W, Islam-Faridi N, Jones S, Jones-Rhoades M, Jorgensen R, Joshi C, Kangasjarvi J, Karlsson, J, Kelleher C, Kirkpatrick R, Kirst M, Kohler A, Kalluri U, Larimer F, Leebens-Mack J, Leple JC, Locascio P, Lou Y, Lucas S, Martin F, Montanini B, Napoli C, Nelson DR, Nelson C, Nieminen K, Nilsson O, Pereda V, Peter G, Philippe R, Pilate G, Poliakov A, Razumovskaya J, Richardson P, Rinaldi C, Ritland K, Rouze P, Ryaboy D, Schmutz J, Schrader J, Segerman B, Shin H, Siddiqui A, Sterky F, Terry A, Tsai CJ, Uberbacher E, Unneberg P, Vahala J, Wall K, Wessler S, Yang G, Yin T, Douglas C, Marra M, Sandberg G, Van de Peer Y, Rokhsar D. 2006. The genome of Black Cottonwood, *Populus trichocarpa* (Torr. & Gray). *Science*. **313**;1596-1604.

Tyler L, Thomas SG, Hu J, Dill A, Alonso JM, Ecker JR, Sun TP. 2004. DELLA proteins and gibberellin-regulated seed germination and floral development in *Arabidopsis*. *Plant Physiology*. **135**; 1008-1019.

Ülker B, Somssich IE. 2004. WRKY transcription factors: from DNA binding towards biological function. *Current Opinion in Plant Biology*. **7**; 491-498.

Umeda M, Shimotohno A, Yamaguchi M. 2005. Control of cell division and transcription by cyclin dependent kinase activating kinases in plants. *Plant Cell Physiology*. **46**; 1437-1442.

Uozu S, Tanaka-Ueguchi M, Kitano H, Hattori K, Matsuoka M. 2000. Characterisation of XET-related genes of rice. *Plant Physiology*. **122**; 853-859.

Valentini R, Matteucci G, Dolman AJ, Schulze ED, Rebmann C, Moors EJ, Granier A, Gross P, Jensen NO, Pilegaard K, Lindroth A, Grelle A, Bernhofer C, Grunwald T, Aubinet M, Ceulemans R, Kowalski AS, Vesala T, Rannik U, Berbigier P, Loustau D, Guomundsson J, Thorgeirsson H, Ibrom A, Morgenstern K, Clement R, Moncrieff J, Montagnani L, Minerbi S, Jarvis PG. 2000. Respiration as the main determinant of carbon balance in European forests. *Nature*. **404**; 861-865.

Vandepoele K, Raes J, De Veylder L, Rouzé P, Rombauts S, Inzé D. 2002. Genome-wide analysis of core cell cycle genes in *Arabidopsis*. *The Plant Cell*. **14**; 903-916.

Van Oijen, M, Schapendonk AHCM, Jansen MJH, Pot CS, Maciorowski R. 1999. Do open-top chambers overestimate the effects of rising CO₂ on plants? An analysis using spring wheat. *Global Change Biology*. **5**; 411-421.

Van Oosten JJ, Besford RT. 1996. Acclimation of photosynthesis to elevated CO₂ through feedback regulation of gene expression: Climate of opinion. *Photosynthesis Research*. **48**; 353-365.

Van Volkenburgh E, Taylor G. 1996. Leaf growth physiology. In *Biology of Populus and its implications for management and conservation*. Part II, Chapter 12. Edited by RF Stettler, HD Bradshaw Jr, PE Heilman, TM Hinckley TM. NRC Research Press, National Research Council of Canada, Ottawa, ON. pp. 283-299.

Vavasseur A, Raghavendra AS. 2005. Guard cell metabolism and CO₂ sensing. *New Phytologist*. **165**; 665-682.

Villanueva JM, Broadhvest J, Hauser BA, Meister RJ, Schneitz K, Gasser CS. 1999. *INNER NO OUTER* regulates abaxial-adaxial patterning in *Arabidopsis* ovules. *Genes and Development*. **13**; 3160-3169.

Vincent D, Ergül A, Bohlman MC, Tattersall EAR, Tillett RL, Wheatley MD, Woolsey R, Quilici DR, Joets J, Schlauch K, Schooley DA, Cushman JC, Cramer GR. 2007. Proteomics analysis reveals differences between *Vitis vinifera* L. Cv. Chardonnay and cv. Cabernet Sauvignon and their responses to water deficit and salinity. *Journal of Experimental Botany*. **58**; 1873-1892.

Vissenberg K, Martinez-Vilchez IM, Verbelen JP, Miller JG, Fry SC. 2000. *In vivo* co-localization of Xyloglucan Endotransglycosylase activity and its donor substrate in the elongation zone of *Arabidopsis* roots. *The Plant Cell*. **12**; 1229-1237.

Volin JC, Reich PB. 1996. Interaction of elevated CO₂ and O₃ growth, photosynthesis and respiration of three perennial species grown in low and high nitrogen. *Physiologia Plantarum*. **97**; 674-684.

Vos J, van der Putten PEL. 1998. Effect of nitrogen supply on leaf growth, leaf nitrogen economy and photosynthetic capacity in potato. *Field Crops Research*. **59**; 63-72.

Vos J, van der Putten PEL, Birch CJ. 2005. Effect of nitrogen supply on leaf appearance, leaf growth, leaf nitrogen economy and photosynthetic capacity in maize (*Zea mays*). *Field Crops Research*. **93**; 64-73.

Wagstaff C, Clarkson GJJ, Zhang F, Rothwell SD, Fry SC, Taylor G, Dixon MS. 2008. Modification of cell wall properties in lettuce improves shelf life. *Journal of Experimental Botany*. *In press*.

Wait DA, Jones CG, Wynn J, Woodward FI. 1999. The fraction of expanding to expanded leaves determines the biomass response of *Populus* to elevated CO₂. *Oecologia*. **121**; 193-200.

- Waites R, Hudson A.** 1995. *phantastica*; a gene required for dorsiventrality of leaves in *Antirrhinum majus*. *Development*. **121**; 2143-2154.
- Walker JD, Oppenheimer DG, Concienne J, Larkin JC.** 2000. *SIAMESE*, a gene controlling the endoreduplication cell cycle in *Arabidopsis thaliana* trichomes. *Development*. **127**; 3931-3940.
- Walter A, Christ MM, Barron-Gafford GA, Grieve KA, Murthy R, Rascher U.** 2005. The effect of elevated CO₂ on diel leaf growth cycle, leaf carbohydrate content and canopy growth performance of *Populus deltoides*. *Global Change Biology*. **11**; 1207-1219.
- Walter A, Lambrecht SC.** 2004. Biosphere 2 Center as a unique tool for environmental studies. *Journal of Environmental Monitoring*. **6**; 267-277.
- Walter A, Roggatz U, Schurr U.** 2003. Expansion kinematics are an intrinsic property of leaf development and are scaled from cell to leaf level at different nutrient availabilities. *Plant Biology*. **5**; 642-650.
- Wang X, Curtis PS.** 2001. Gender-specific responses of *Populus tremuloides* to atmospheric CO₂ enrichment. *New Phytologist*. **150**; 675-684.
- Wang H, Fowke LC, Crosby WL.** 1997. A plant cyclin dependent kinase inhibitor gene. *Nature*. **386**; 451.
- Wang H, Zhou Y, Gilmer S, Whitwill S, Fowke LC.** 2000. Expression of the plant cyclin-dependent kinase inhibitor ICK1 affects cell division, plant growth and morphology. *Plant Journal*. **24**; 613-623.
- Watson BS, Lei Z, Dixon RA, Sumner LW.** 2004. Proteomics of *Medicago sativa* cell walls. *Phytochemistry*. **65**; 1709-1720.
- Webber AN, Nie GY, Long SP.** 1994. Acclimation of photosynthetic proteins to rising atmospheric CO₂. *Photosynthesis research*. **39**; 413-425.
- Wenzl P, Carling J, Kudrna D, Jaccoud D, Huttner E, Kleinhofs A, Kilian A.** 2004. Diversity Arrays Technology (DART) for whole-genome profiling of barley. *Proceedings of the National Academy of Science USA*. **101**; 9915-9920.
- Wettenhall JM, Simpson KM, Satterley K, Smyth GK.** 2006. affyImGUI: a graphical user interface for linear modelling of single channel microarray data. *Bioinformatics*. **22**; 897-899.
- Whetten R, Sun Y-H, Zhang Y, Sederoff R.** 2001. Functional genomics and cell wall biosynthesis in loblolly pine. *Plant Molecular Biology*. **47**; 275-291.
- Wilson ID, Barker GL, Edwards KJ.** 2003. Genotype to phenotype: a technological challenge. *Annals of Applied Biology*. **142**; 33-39.
- Wittig VE, Bernacchi CJ, Zhu XG, Calfapietra C, Ceulemans R, De Angelis P, Gielen B, Miglietta F, Morgan P, Long SP.** 2005. Gross primary production is stimulated for three *Populus* species grown under Free Air CO₂ Enrichment from planting through canopy closure. *Global Change Biology*. **11**; 644-656.
- Woodward FI.** 1987. Stomatal numbers are sensitive to increases in CO₂ from pre-industrial levels. *Nature*. **327**; 617-618.

- Woodward FI, Lake JA, Quick WP.** 2002. Stomatal development and CO₂: ecological consequences. *New Phytologist*. **153**; 477-484.
- Xu L, Dong A, Sun Y, Pi L, Xu Y, Huang H.** 2003. Novel *as1* and *as2* defects in leaf adaxial-abaxial polarity reveal the requirement for *ASYMMETRIC LEAVES1* and 2 and *ERECTA* functions in specifying leaf adaxial identity. *Development*. **130**; 4097-4107.
- Yamaguchi M, Fabian T, Sauter M, Bhalerao RP, Schrader J, Sandberg G, Umeda M, Uchimiya H.** 2000. Activation of CDK-activating kinase is dependent upon interaction with H-type cyclins in plants. *The Plant Journal*. **24**; 11-20.
- Yang YH, Dudoit S, Luu P, Lin DM, Peng V, Ngai J, Speed TP.** 2002. Normalization for cDNA microarray data: a robust composite method addressing single and multiple slide systematic variation. *Nucleic Acids Research*. **30**; e15.
- Yauk CL, Berndt ML, Williams A, Douglas GR.** 2004. Comprehensive comparison of six microarray technologies. *Nucleic Acids Research*. **32**; e124.
- Zhang SD, Gant TW.** 2005. Effect of pooling samples on the efficiency of comparative studies using microarrays. *Bioinformatics*. **21**; 4378-4383.
- Zhang F, Gonzalez A, Zhao M, Payne CT, Lloyd A.** 2003. A network of redundant bHLH proteins functions in all TTG1-dependent pathways of *Arabidopsis*. *Development*. **130**; 4859-4869.
- Zhou Y, Wang H, Gilmer S, Whitwill S, Fowke LC.** 2003. Effects of co-expressing the plant CDK inhibitor ICK1 and D-type cyclin genes on plant growth, cell size and ploidy in *Arabidopsis thaliana*. *Planta*. **216**; 604-613.
- Zieske LR.** 2006. A perspective on the use of iTRAQ reagent technology for protein complex and profiling studies. *Journal of Experimental Botany*. **57**; 1501-1508.

APPENDICES

Appendix 1

(Chapter 5)

The ESTs with positive B-statistic values and associated p-values. The M value represents the regulation of the EST (e.g. a negative number indicates down-regulated expression in elevated compared to ambient [CO₂]). A B-value of 0 represents a 50% chance of differential expression.

Young leaves

Identifier	Annotation	M	B	p
PU28532	Leucine-rich repeat family protein	1.62	2.22	0.341
PU27165	GDSL-motif lipase/hydrolase family protein	1.89	1.95	0.341
PU20530	Xyloglucan	1.64	1.05	0.467
PU20437	Calcium-dependent protein kinase isoform 2 (CPK2)	2.03	0.80	0.467
PU09556	Harpin-induced family protein	1.46	0.56	0.527
PU09305	GDSL-motif lipase/hydrolase family protein	2.57	0.41	0.552
PU08476	Proline-rich family protein	-3.6	0.36	0.467
PU05763	Polcalcin, putative / calcium-binding pollen allergen	1.78	0.05	0.564

Semi-mature leaves

Identifier	Annotation	M	B	p
PU10409	No annotation available	-2.47	3.42	0.052
PU12448	Ras-related GTP-binding protein, putative	-5.76	3.24	0.025
PU28637	Potassium transporter (KUP1)	-2.40	3.02	0.059
PU11724	Suppressor protein SRP40	-3.56	2.19	0.089
PU00177	GATA transcription factor 1 (GATA-1)	-1.54	1.67	0.135
PU08917	Chloroplastic RNA-binding protein P67	-10.20	1.38	0.026
PU22860	Chloroplast inner envelope protein-related	-1.62	1.09	0.162
PU25517	Heavy-metal-associated domain-containing protein	-5.82	0.95	0.087
PU06984	Pyruvate kinase, putative	-6.31	0.93	0.087

PU21852	Ras-related protein (ARA-3) / small GTP-binding protein	-3.84	0.73	0.162
PU21030	Expressed protein	1.87	0.72	0.162
PU12050	Heat shock protein	-1.64	0.61	0.162
PU05072	Elongation factor 2, putative / EF-2	-4.97	0.61	0.138
PU06234	Adenylate kinase family protein	5.25	0.60	0.138
PU09638	T-complex protein 1 alpha subunit	-1.94	0.59	0.162
PU08927	Eukaryotic translation initiation factor	-2.26	0.49	0.162
PU22579	Nodulin MtN3 family protein	-1.35	0.38	0.162
PU10293	Endomembrane protein 70, putative TM4 family	4.73	0.36	0.162
PU11079	COP9 signalosome complex subunit 7ii	3.24	0.34	0.162
PU04471	ATP-dependent Clp protease proteolytic subunit	-4.76	0.30	0.162
PU07311	F-box family protein	-1.24	0.29	0.162
PU10127	WWE domain-containing protein / ceo protein	2.14	0.28	0.162
PU26674	CTP synthase, putative / UTP-ammonia ligase	-5.46	0.21	0.162
PU29459	60S ribosomal protein	2.20	0.19	0.162
PU06463	60S ribosomal protein-related	-2.11	0.17	0.162
PU02302	Peptidyl-prolyl cis-trans isomerase	-1.15	0.17	0.162
PU03360	Aspartyl-tRNA synthetase	-3.62	0.13	0.162
PU06179	No annotation available	-1.10	0.13	0.162
PU08744	Expressed protein	4.00	0.08	0.162
PU08796	Expressed protein	-3.78	0.06	0.162
PU28466	ARF GTPase-activating domain-containing protein	-1.33	0.03	0.162

Appendix 2

(Chapter 7)

The ESTs with positive B-statistic values and associated p-values. The M value represents the regulation of the EST (e.g. a negative number indicates down-regulated expression in elevated compared to ambient [CO₂]). A B-value of 0 represents a 50% chance of differential expression.

P. deltoides

Meristematic tissue (23)

Identifier	Annotation	M	p	B
PU05576	Hydroxyproline-rich glycoprotein family protein	1.43	0.092	3.29
PC20402	-	1.39	0.092	2.95
PU11070	-	1.29	0.092	2.80
PU07079	Cullin family protein	3.00	0.123	2.30
PU20844	Ubiquitin extension protein 6 (UBQ6)	1.25	0.164	1.70
PU09585	Polyubiquitin	0.96	0.164	1.70
PU05891	Expressed protein	1.03	0.166	1.32
PU12148	GDSL-motif lipase/hydrolase family protein	0.93	0.180	1.00
PU22002	Expressed protein similar	1.91	0.166	0.92
PU21461	Heat shock protein 70	1.40	0.180	0.91
PU03249	Polyubiquitin (UBQ14	1.14	0.180	0.87
PU07813	RNA-dependent RNA polymerase	0.90	0.180	0.82
PU10395	Leucine-rich repeat family protein	1.15	0.180	0.79
PU20266	Expressed protein	1.17	0.180	0.68
PU11177	9-cis-epoxycarotenoid dioxygenase	1.05	0.180	0.63
PU04341	Zinc finger (C2H2 type) family protein	-1.33	0.180	0.62
PU20339	DC1 domain-containing protein	1.13	0.180	0.55

PU03968	Polyubiquitin (UBQ10) (SEN3) senescence-associated protein	1.03	0.180	0.51
PU31226	Hypothetical protein	0.82	0.180	0.51
PU11403	Expressed protein	0.85	0.185	0.35
PU01249	Expressed protein	0.93	0.185	0.29
PU21460	Heat shock protein 70	1.69	0.181	0.28
PU04238	Expressed protein	1.60	0.185	0.14

P. deltooides

Age two (39)

Identifier	Annotation	M	p	B
PU08833	Cys/Met metabolism pyridoxal-phosphate-dependent enzyme family protein	-3.13	0.075	4.04
PU31076	Expressed protein	-4.09	0.115	2.63
PU00482	L-ascorbate peroxidase 1	-2.82	0.115	2.55
PU20958	Omega-3 fatty acid desaturase	-1.95	0.115	1.54
PU24969	Threonine ammonia-lyase	-2.94	0.115	1.46
PU30100	Trypsin and protease inhibitor family protein	-2.01	0.115	1.41
PU20553	Cupin family protein	-2.26	0.115	1.37
PU08678	Trypsin and protease inhibitor family protein	-1.84	0.115	1.37
PU27331	Protease inhibitor/seed storage/lipid transfer protein (LTP) family protein	-2.12	0.115	1.11
PU30951	Oxidoreductase, 2OG-Fe(II) oxygenase family protein	-3.38	0.115	1.10
PU00912	Calmodulin-binding family protein	-2.09	0.115	1.10
PU00326	Expressed protein	-1.94	0.115	1.03
PU23451	C2 domain-containing protein	3.00	0.115	0.99
PU10779	Expressed protein	-1.75	0.115	0.96
PU12956	23.6 kDa mitochondrial small heat shock	7.49	0.115	0.89
PU00028	Zinc finger (Ran-binding) family protein	-3.95	0.115	0.82
PU10690	Pentatricopeptide (PPR) repeat-containing protein	-2.37	0.115	0.77

PU25700	UDP-glucuronosyl/UDP-glucosyl transferase family protein	-1.62	0.115	0.65
PU08378	Trypsin and protease inhibitor family protein	-2.02	0.115	0.64
PU02292	Lesion inducing protein-related similar to ORF	6.18	0.115	0.62
PU29068	Pectate lyase family protein	-1.64	0.115	0.61
PU12876	Trypsin and protease inhibitor family protein	-2.90	0.119	0.58
PU31077	Protease inhibitor/seed storage/lipid transfer protein (LTP) family protein	-2.24	0.115	0.56
PU20132	Gibberellin-regulated family protein	1.96	0.115	0.54
PU09704	Expressed protein	5.70	0.115	0.49
PU09807	Phytochrome-interacting factor 4 (PIF4)	5.66	0.115	0.48
PU04282	O-methyltransferase family 2 protein	-2.28	0.130	0.47
PU29344	Trypsin and protease inhibitor family protein	-2.06	0.119	0.47
PU23265	17.6 kDa class I small heat shock protein	5.47	0.115	0.42
PU02164	Eukaryotic translation initiation factor 6	5.37	0.115	0.39
PU09687	BAG domain-containing protein	5.36	0.115	0.38
PU03171	Xyloglucan:xyloglucosyl transferase	2.45	0.132	0.38
PU11811	Peptidyl-prolyl cis-trans isomerase	5.17	0.115	0.31
PU12387	Trypsin and protease inhibitor family protein	-1.82	0.130	0.28
PU11347	Formate dehydrogenase	-4.95	0.115	0.23
PU30059	Endo-1,4-beta-glucanase, putative / cellulase	-2.63	0.139	0.18
PU20530	Xyloglucan:xyloglucosyl transferase, putative	1.64	0.139	0.10
PU02188	Expressed protein	4.61	0.130	0.07
PU25144	Phosphorylase family protein	-1.87	0.139	0.02

P. trichocarpa

Meristematic tissue (2)

Identifier	Annotation	M	p	B
PU20450	phosphatase-related weak similarity to CTD phosphatase-like 3	1.42	0.398	0.36
PU26552	transcription factor jumonji (jnjC) domain-containing protein	1.10	0.398	0.23

P. trichocarpa

Age two (1)

Identifier	Annotation	M	p	B
PU20249	basic endochitinase	-2.54	0.358	0.39

Appendix 3

(Chapter 7)

The annotation and average expression levels of the ESTs represented in the Venn diagrams in Figures 7.3.2 and 7.3.3.

P. deltoides

Meristematic tissue

Down-regulated (36)

Identifier	Expression	Annotation
PC20402	0.38	-
PU27641	0.46	Expressed protein
PU05576	0.37	Hydroxyproline-rich glycoprotein family protein
PU12629	0.07	Auxin-responsive GH3 family protein
PU07079	0.12	Cullin family protein
PU07708	0.47	-
PU05979	0.18	Nodulin family protein
PU02435	0.15	Nascent polypeptide associated complex alpha chain protein
PU28146	0.54	Polyubiquitin (UBQ14)
PU04541	0.13	Nucleolar protein
PU08424	0.14	GYF domain-containing protein
PU22002	0.19	Expressed protein
PU10299	0.50	Peptidase M3 family protein
PU12403	0.20	-
PU20083	0.44	Scarecrow transcription factor family protein
PU02065	0.35	Endomembrane protein 70
PU01307	0.34	Expressed protein
PU21460	0.28	Heat shock protein 70, putative / HSP70
PU20845	0.27	Protein kinase
PU21923	0.32	Calcium-dependent protein kinase
PU08723	0.38	Expressed protein
PU21744	0.31	Pentatricopeptide (PPR) repeat-containing protein
PU22403	0.15	Hypothetical protein
PU11070	0.41	-
PU10616	0.51	CP12 domain-containing protein
PU08634	0.11	CCAAT-box binding transcription factor subunit B
PU08407	0.47	CBL-interacting protein kinase 10 (CIPK10)
PU03249	0.45	Polyubiquitin (UBQ14)
PU20844	0.42	Ubiquitin extension protein 6 (UBQ6)
PU04238	0.30	Expressed protein
PU03968	0.49	Polyubiquitin (UBQ10) (SEN3) senescence-associated protein
PU26290	0.30	Hypothetical protein
PU21461	0.38	Heat shock protein 70, putative / HSP70
PU20266	0.54	Expressed protein
PU20339	0.45	DC1 domain-containing protein
PU10038	0.37	-

Common to *P. deltooides* and *P. trichocarpa*

Meristematic tissue

Down-regulated (1)

Identifier	Expression <i>P. deltooides</i>	Expression <i>P. trichocarpa</i>	Annotation
PU05891	0.49	0.32	Expressed protein

P. trichocarpa

Meristematic tissue

Down-regulated (11)

Identifier	Expression	Annotation
PU03727	0.46	Expressed protein
PU30008	0.42	Seven in absentia (SINA) protein
PU20010	0.53	-
PU10242	0.51	Expressed protein
PU29120	0.51	Adenosine kinase 2 (ADK2)
PU11403	0.38	-
PU11568	0.42	Heavy-metal-associated domain-containing protein
PU26552	0.47	Transcription factor jumonji (jmiC) domain-containing protein
PU20450	0.37	Phosphatase-related weak similarity to CTD phosphatase-like 3
PU21815	0.49	-
PU07815	0.25	Expressed protein

P. trichocarpa

Meristematic tissue

Up-regulated (5)

Identifier	Expression	Annotation
PU24842	3.69	Gibberellin-regulated protein 3 (GASA3)
PU20204	2.19	Metallothionein protein, putative (MT2A)
PU08798	2.54	Phosphoesterase family protein
PU25150	3.47	Metallothionein protein, putative (MT2A)
PU29397	2.60	Hydrophobic protein (RCI2A)

P. deltooides

Meristematic tissue

Up-regulated (12)

Identifier	Expression	Annotation
PU26992	2.14	Expressed protein
PU28826	2.23	Glycine-rich RNA-binding protein (GRP7)
PU04341	2.52	Zinc finger (C2H2 type) family protein
PU12354	5.75	Expressed protein
PU00287	5.06	Expressed protein
PU04202	4.07	Expressed protein
PU07693	2.41	Phosphate-responsive 1 family protein
PU26576	3.50	-
PU10757	2.79	4-coumarate-CoA ligase
PU02965	2.31	Nuclear transport factor 2 (NTF2) family protein
PU20282	1.98	Expressed protein
PU20278	3.13	-

P. deltooides

Age two

Down-regulated (13)

Identifier	Expression	Annotation
PU06682	0.27	GDP-mannose pyrophosphorylase (GMP1)
PU28060	0.37	Ceramidase family protein
PU23814	0.06	Expressed protein
PU21460	0.33	Heat shock protein 70, putative / HSP70
PU06571	0.42	Two-component responsive regulator
PU07079	0.13	Cullin family protein similar
PU08367	0.43	Hydroxyproline-rich glycoprotein family protein
PU12158	0.31	-
PU12098	0.42	Leucoanthocyanidin dioxygenase
PU12477	0.30	-
PU09203	0.25	Vacuolar processing enzyme
PU27456	0.12	Hypothetical protein
PU11811	0.09	Peptidyl-prolyl cis-trans isomerase

Common to *P. deltooides* and *P. trichocarpa*

Age two (1)

Identifier	Expression <i>P. deltooides</i>	Expression <i>P. trichocarpa</i>	Annotation
PU05792	0.33	0.35	Luminal binding protein 1 (BiP-1)

P. trichocarpa

Age two

Down-regulated (22)

Identifier	Expression	Annotation
PU03416	0.38	Xyloglucan:xyloglucosyl transferase
PU02394	0.17	Cysteine proteinase
PU28733	0.39	5-methyltetrahydropteroyltriglutamate-homocysteine
PU20378	0.25	-
PU25527	0.49	Trypsin and protease inhibitor family protein
PU20554	0.31	Cysteine proteinase
PU00208	0.31	Minichromosome maintenance family protein
PU08456	0.41	Haloacid dehalogenase-like hydrolase family protein
PU06916	0.39	Cucumisin-like serine protease
PU29375	0.43	Hydrophobic protein
PU26544	0.44	Protein kinase
PU10962	0.51	-
PU08234	0.17	Expressed protein
PU10725	0.24	-
PU10690	0.51	Pentatricopeptide (PPR) repeat-containing protein
PU10814	0.39	-
PU13048	0.40	Expressed protein
PU26321	0.50	beta-ketoacyl-CoA synthase
PU22118	0.39	Expressed protein
PU23402	0.31	Trypsin and protease inhibitor family protein
PU12876	0.46	Trypsin and protease inhibitor family protein

P. deltoides

Age two

Up-regulated (12)

Identifier	Expression	Annotation
PU09645	4.11	Protein kinase family protein
PU09587	3.87	Expressed protein
PU08964	2.78	Cytochrome P450
PU25164	3.28	C2 domain-containing protein
PU21210	3.04	Expressed protein
PU12349	5.30	TIP120 protein
PU04285	3.74	Expressed protein
PU04191	9.81	Expressed protein
PU00019	3.33	Galactosyl transferase
PU07208	8.58	Zinc finger (C3HC4-type RING finger) family protein
PU07185	2.94	Leucine-rich repeat transmembrane protein kinase, putative
PU04356	2.78	Pyruvate decarboxylase family

P. trichocarpa

Age two

Up-regulated (10)

Identifier	Expression	Annotation
PU00226	2.99	Expressed protein
PU00968	4.72	40S ribosomal protein
PU09889	2.45	2-oxoacid-dependent oxidase
PU00259	2.29	Exonuclease
PU01007	2.51	Eukaryotic translation initiation factor
PU24805	2.80	High mobility group
PU23618	4.69	SOUL heme-binding family protein
PU29854	2.65	Dehydrin
PU13279	2.00	Dehydrin family protein
PU09319	2.64	Expansin, putative

Meristematic tissue

Age 2

P. deltoides (35)

Identifier	Expression	Annotation
PC20402	0.38	-
PU27641	0.46	Expressed protein
PU05576	0.37	Hydroxyproline-rich glycoprotein family protein
PU12629	0.07	Auxin-responsive GH3 family
PU07708	0.47	-
PU05979	0.18	Nodulin family protein
PU02435	0.15	Nascent polypeptide associated complex alpha chain protein
PU28146	0.54	Polyubiquitin (UBQ14)
PU04541	0.13	Nucleolar protein
PU08424	0.14	GYF domain-containing protein
PU22002	0.19	Expressed protein
PU10299	0.50	Peptidase M3 family protein
PU12403	0.20	-
PU20083	0.44	Scarecrow transcription factor family protein
PU02065	0.35	Endomembrane protein 70
PU01307	0.34	Expressed protein
PU20845	0.27	Protein kinase
PU05891	0.49	Expressed protein
PU21923	0.32	Calcium-dependent protein kinase
PU08723	0.38	Expressed protein
PU21744	0.31	Pentatricopeptide
PU22403	0.15	Hypothetical protein
PU11070	0.41	-
PU10616	0.51	CP12 domain-containing protein
PU08634	0.11	CCAAT-box binding transcription factor subunit B
PU08407	0.47	CBL-interacting protein kinase 10 (CIPK10)
PU03249	0.45	Ppolyubiquitin (UBQ14
PU20844	0.42	Ubiquitin extension protein 6 (UBQ6)

PU04238	0.30	Expressed protein
PU03968	0.49	Polyubiquitin (UBQ10) (SEN3) senescence-associated protein
PU26290	0.30	Hypothetical protein
PU21461	0.38	Heat shock protein 70
PU20266	0.54	Expressed protein
PU20339	0.45	DC1 domain-containing protein
PU10038	0.37	-

Age two

Down-regulated

P. deltooides (12)

Identifier	Expression	Annotation
PU06682	0.27	GDP-mannose pyrophosphorylase (GMP1)
PU28060	0.37	Ceramidase family protein
PU05792	0.33	Luminal binding protein 1 (BiP-1)
PU23814	0.06	Expressed protein
PU06571	0.42	Two-component responsive regulator
PU08367	0.43	Hydroxyproline-rich glycoprotein family protein
PU12158	0.31	-
PU12098	0.42	Leucoanthocyanidin dioxygenase, putative
PU12477	0.30	-
PU09203	0.25	Vacuolar processing enzyme
PU27456	0.12	Hypothetical protein
PU11811	0.09	Peptidyl-prolyl cis-trans isomerase

Common to age two and meristematic tissue

Down-regulated

P. deltooides (2)

Identifier	Expression <i>P. deltooides</i>	Expression <i>P. trichocarpa</i>	Annotation
PU07079	0.13	0.12	Cullin family
PU21460	0.33	0.28	Heat shock protein 70

Meristematic tissue

Up-regulated

P. deltooides (12)

Identifier	Expression	Annotation
PU26992	2.14	Expressed protein
PU28826	2.23	Glycine-rich RNA-binding protein (GRP7)
PU04341	2.52	Zinc finger (C2H2 type) family protein
PU12354	5.75	Expressed protein
PU00287	5.06	Expressed protein
PU04202	4.07	Expressed protein
PU07693	2.41	Phosphate-responsive 1 family protein
PU26576	3.50	-
PU10757	2.79	4-coumarate-CoA ligase
PU02965	2.31	Nuclear transport factor 2 (NTF2) family protein
PU20282	1.98	Expressed protein
PU20278	3.13	-

Age two
Up-regulated
P. deltoides (12)

Identifier	Expression	Annotation
PU09645	4.11	Protein kinase family protein
PU09587	3.87	Expressed protein
PU08964	2.78	Cytochrome P450
PU25164	3.28	C2 domain-containing protein
PU21210	3.04	Expressed protein
PU12349	5.30	TIP120 protein
PU04285	3.74	Expressed protein
PU04191	9.81	Expressed protein
PU00019	3.33	Galactosyl transferase
PU07208	8.58	Zinc finger (C3HC4-type RING finger) family protein
PU07185	2.94	Leucine-rich repeat transmembrane protein kinase
PU04356	2.78	Pyruvate decarboxylase family protein

Meristematic tissue
Up-regulated
P. trichocarpa (5)

Identifier	Expression	Annotation
PU24842	3.69	Gibberellin-regulated protein 3 (GASA3)
PU20204	2.19	Metallothionein protein, putative (MT2A)
PU08798	2.54	Phosphoesterase family protein
PU25150	3.47	Metallothionein protein, putative (MT2A)
PU29397	2.60	Hydrophobic protein (RCI2A)

Age two
Up-regulated
P. trichocarpa (10)

Identifier	Expression	Annotation
PU00226	2.99	Expressed protein
PU00968	4.72	40S ribosomal protein
PU09889	2.45	2-oxoacid-dependent oxidase
PU00259	2.29	Exonuclease RRP41
PU01007	2.51	Eukaryotic translation initiation factor
PU24805	2.80	High mobility group
PU23618	4.69	SOUL heme-binding family protein
PU29854	2.65	Dehydrin (RAB18)
PU13279	2.00	Dehydrin family protein
PU09319	2.64	Expansin

Meristematic tissue

Down-regulated

P. trichocarpa (12)

Identifier	Expression	Annotation
PU03727	0.46	Expressed protein
PU30008	0.42	Seven in absentia (SINA) protein
PU20010	0.53	-
PU10242	0.51	Expressed protein
PU05891	0.32	Expressed protein
PU29120	0.51	Adenosine kinase 2 (ADK2)
PU11403	0.38	-
PU11568	0.42	Heavy-metal-associated domain-containing protein
PU26552	0.47	Transcription factor jumonji (jmiC) domain-containing protein
PU20450	0.37	Phosphatase-related
PU21815	0.49	-
PU07815	0.25	Expressed protein

Age two

Down-regulated

P. trichocarpa (23)

Identifier	Expression	Annotation
PU03416	0.38	Xyloglucan:xyloglucosyl transferase
PU02394	0.17	Cysteine proteinase (RD21A)
PU28733	0.39	5-methyltetrahydropteroyltriglutamate-homocysteine methyltransferase
PU20378	0.25	-
PU25527	0.49	Trypsin and protease inhibitor family protein
PU20554	0.31	Cysteine proteinase (RD21A)
PU05792	0.35	Luminal binding protein 1 (BiP-1)
PU00208	0.31	Minichromosome maintenance family protein
PU08456	0.41	haloacid dehalogenase-like hydrolase family protein
PU06916	0.39	Cucumisin-like serine protease
PU29375	0.43	Hydrophobic protein
PU26544	0.44	Protein kinase
PU10962	0.51	-
PU08234	0.17	Expressed protein
PU10725	0.24	-
PU10690	0.51	Pentatricopeptide (PPR) repeat-containing protein
PU10814	0.39	-
PU13048	0.40	Expressed protein
PU26321	0.50	beta-ketoacyl-CoA synthase
PU29211	0.34	Phosphoinositide-specific phospholipase C (PLC2)
PU22118	0.39	Expressed protein
PU23402	0.31	Trypsin and protease inhibitor family protein
PU12876	0.46	Trypsin and protease inhibitor family protein

Appendix 4

(Chapter 7)

Gene lists from the Affymetrix microarrays conducted for *P. deltoides* and *P. trichocarpa*.

P. trichocarpa

Down-regulated (158)

Affymetrix identifier	Expression	Gene model	Annotation
PtpAffx.146922.2.A1_at	0.06	eugene3.00090672	similar to glucosyltransferase -like protein
PtpAffx.10586.2.S1_at	0.11	estExt_fgenes4_pm.C_LG_III0624	WRKY family transcription factor
Ptp.6958.1.S1_s_at	0.12	eugene3.00140929	glucosyltransferase like
PtpAffx.2311.2.A1_at	0.12	estExt_fgenes4_pm.C_LG_I0800	glutamine-dependent asparagine synthetase
Ptp.2399.1.S1_s_at	0.13	estExt_fgenes4_pg.C_LG_IV1432	putative DnaJ
PtpAffx.153051.1.A1_at	0.13	estExt_Genewise1_v1.C_LG_VIII2439	ATP sulfurylase
PtpAffx.10803.1.S1_at	0.14	estExt_fgenes4_pg.C_LG_IV1432	putative DnaJ protein
PtpAffx.14721.1.S1_at	0.15	estExt_fgenes4_pg.C_LG_VI1840	-
Ptp.5332.1.S1_x_at	0.15	estExt_Genewise1_v1.C_LG_XIV0633	salt-tolerance zinc finger protein
PtpAffx.158492.1.S1_at	0.15	estExt_Genewise1_v1.C_LG_IX3026	glutamine-dependent asparagine synthetase
Ptp.2164.1.S1_s_at	0.15	grail3.0007034202	WRKY family transcription factor
PtpAffx.987.4.S1_a_at	0.16	estExt_Genewise1_v1.C_LG_XVI0181	Expressed protein
PtpAffx.135026.1.S1_at	0.16	-	-
PtpAffx.2179.1.S1_at	0.16	grail3.0011008901	NAC domain protein
PtpAffx.10911.1.S1_at	0.16	eugene3.00110945	Putative protein : stem-specific protein
PtpAffx.152367.1.S1_at	0.16	grail3.0007034202	WRKY family transcription factor
PtpAffx.14116.1.S1_at	0.17	estExt_Genewise1_v1.C_LG_III1841	-
PtpAffx.675.9.S1_s_at	0.17	grail3.0046016501	Dormancy-associated protein
PtpAffx.119343.2.A1_a_at	0.17	gw1.207.4.1 gw1.V.1857.1	Putative protein
PtpAffx.31211.1.A1_at	0.17	eugene3.00140929	glucosyltransferase like protein
PtpAffx.203877.1.S1_at	0.17	grail3.0046016501	dormancy-associated protein

PtpAffx.203877.1.S1_x_at	0.18	grail3.0046016501	dormancy-associated protein
PtpAffx.36367.1.S1_at	0.19	gw1.I.6556.1	DEAD:DEAH box RNA helicase
PtpAffx.38305.1.S1_at	0.19	grail3.0020002201	TPA: DVL10 [Arabidopsis thaliana]
Ptp.5265.1.S1_x_at	0.19	eugene3.00140672	putative protein
PtpAffx.730.2.S1_at	0.19	grail3.0013010301	similar to putative hydrolase
PtpAffx.74101.1.A1_at	0.20	gw1.III.2417.1	WRKY family transcription factor
Ptp.5332.1.S1_at	0.20	estExt_Genewise1_v1.C_LG_XIV0633	salt-tolerance zinc finger protein
Ptp.3396.1.S1_s_at	0.20	eugene3.00050488	protein kinase-like protein
PtpAffx.49881.1.A1_at	0.20	estExt_fgenes4_pg.C_LG_XI0435	Expressed protein
PtpAffx.94207.1.S1_at	0.20	estExt_Genewise1_v1.C_LG_III1818	tat-binding protein
Ptp.7317.1.S1_at	0.21	-	-
PtpAffx.2179.2.S1_at	0.22	eugene3.00050086	NAC domain protein
Ptp.3337.1.S1_s_at	0.22	eugene3.00191070	-
Ptp.4832.2.A1_s_at	0.22	eugene3.00060795	putative protein
PtpAffx.61554.1.S1_s_at	0.22	gw1.III.2417.1	WRKY family transcription factor
Ptp.987.1.S1_at	0.22	estExt_Genewise1_v1.C_LG_II0603	hypothetical protein
PtpAffx.139063.1.S1_at	0.22	grail3.0021016501 grail3.0021016401	glucosyltransferase like protein
Ptp.5265.1.S1_s_at	0.23	eugene3.00140672	putative protein
Ptp.7711.2.A1_a_at	0.23	eugene3.00091201	UDP-glucose glucosyltransferase
PtpAffx.2311.1.S1_s_at	0.23	estExt_Genewise1_v1.C_LG_IX3026	glutamine-dependent asparagine synthetase
PtpAffx.84734.2.S1_at	0.23	estExt_Genewise1_v1.C_LG_XIII2678	SCARECROW gene regulator-like
PtpAffx.93656.1.S1_s_at	0.23	estExt_Genewise1_v1.C_LG_I8988	4-coumarate-CoA ligase -like protein
Ptp.3380.1.S1_at	0.24	-	-
Ptp.3327.1.S1_s_at	0.24	estExt_Genewise1_v1.C_LG_XV2908	ripening-related protein - like
PtpAffx.43573.2.A1_at	0.24	estExt_Genewise1_v1.C_LG_VIII2439	ATP sulfurylase
PtpAffx.224322.1.S1_s_at	0.25	eugene3.00031524	-
PtpAffx.4795.1.A1_s_at	0.25	-	-
Ptp.6281.1.S1_at	0.25	estExt_Genewise1_v1.C_LG_I8988	4-coumarate-CoA ligase -like protein
Ptp.2629.1.S1_s_at	0.25	estExt_fgenes4_pg.C_LG_V1271	unknown protein
PtpAffx.4795.1.A1_a_at	0.25	-	-

Ptp.2176.1.S1_at	0.25	estExt_Genewise1_v1.C_LG_III524	putative DnaJ protein
Ptp.4035.1.S1_at	0.25	grail3.0020002201	-
Ptp.4945.1.A1_at	0.25	estExt_Genewise1_v1.C_LG_I8988	4-coumarate-CoA ligase -like protein
PtpAffx.4462.1.S1_at	0.25	fgenes4_pg.C_LG_X001297	glycosyl hydrolase family 17
PtpAffx.101182.1.A1_at	0.25	estExt_fgenes4_pm.C_LG_XVIII0207	putative zinc finger protein
Ptp.6986.1.S1_at	0.25	fgenes4_pg.C_LG_I001468	putative protein
PtpAffx.20626.1.S1_at	0.25	eugene3.00020187	putative DnaJ protein
Ptp.8041.2.A1_s_at	0.26	eugene3.00170087	mitochondrial carrier protein family
PtpAffx.10075.1.S1_at	0.26	-	-
PtpAffx.209941.1.S1_x_at	0.26	eugene3.00110845	9-cis-epoxycarotenoid dioxygenase
PtpAffx.84734.1.S1_a_at	0.26	estExt_Genewise1_v1.C_LG_XIII2678	SCARECROW gene regulator-like
PtpAffx.10586.1.S1_at	0.27	estExt_fgenes4_pm.C_LG_III0624	WRKY family transcription factor
Ptp.3327.1.S1_at	0.28	estExt_Genewise1_v1.C_LG_XV2908	ripening-related protein - like
PtpAffx.4010.2.A1_a_at	0.28	fgenes4_pg.C_LG_IX000110	expressed protein
PtpAffx.6322.3.A1_a_at	0.28	estExt_Genewise1_v1.C_LG_XIV0616	calcium-transporting ATPase 1
Ptp.7530.1.S1_x_at	0.28	estExt_Genewise1_v1.C_2020055	photosystem II polypeptide
PtpAffx.202465.1.S1_at	0.28	fgenes4_pg.C_LG_II002007	putative RHO GDP-dissociation inhibitor 1
PtpAffx.158231.1.A1_at	0.28	grail3.0021016501 grail3.0021016401	glucosyltransferase like protein
PtpAffx.2759.3.A1_a_at	0.28	fgenes4_pg.C_LG_XIV000009	-
PtpAffx.209941.1.S1_at	0.29	eugene3.00110845	9-cis-epoxycarotenoid dioxygenase
PtpAffx.249.639.S1_a_at	0.29	eugene3.00130614	cold stress protein
Ptp.662.1.S1_s_at	0.29	estExt_fgenes4_pg.C_LG_IV0455	Csf-2-related
PtpAffx.998.1.A1_at	0.29	eugene3.00160232	putative protein
PtpAffx.608.3.S1_at	0.29	eugene3.00060844	anthranilate N-benzoyltransferase - like protein
PtpAffx.120153.1.S1_s_at	0.30	estExt_Genewise1_v1.C_LG_VII0038	xyloglucan endotransglycosylase
PtpAffx.136423.1.S1_s_at	0.30	gw1.IV.2436.1	lemir (miraculin)
PtpAffx.608.2.A1_at	0.30	eugene3.00060844	anthranilate N-benzoyltransferase - like protein
PtpAffx.222339.1.S1_at	0.31	grail3.0064018101	type 1 ribosome-inactivating protein musarmin 1

PtpAffx.129974.1.S1_s_at	0.31	eugene3.00110845	9-cis-epoxycarotenoid dioxygenase
Ptp.5112.2.S1_a_at	0.32	grail3.0092008201	WRKY family transcription factor
PtpAffx.57533.1.S1_a_at	0.32	estExt_fgenes4_pg.C_LG_XIV0981	putative lysosomal acid lipase :
PtpAffx.33735.1.S1_s_at	0.32	estExt_Genewise1_v1.C_LG_VI2708	serine:threonine protein kinase-like protein
PtpAffx.84025.1.S1_at	0.33	grail3.0030001201	-
Ptp.1510.1.S1_s_at	0.33	estExt_Genewise1_v1.C_LG_XIV3201	putative protein
PtpAffx.205722.1.S1_at	0.33	gw1.V.1006.1	potential calcium-transporting ATPase
PtpAffx.4337.2.S1_at	0.33	fgenes4_pm.C_scaffold_164000007	putative transporter
PtpAffx.4337.1.A1_s_at	0.33	fgenes4_pm.C_LG_IV000203	putative protein
PtpAffx.163109.1.S1_s_at	0.33	gw1.66.741.1	putative protein
PtpAffx.63624.1.A1_at	0.34	gw1.XII.1041.1	calcium-binding protein
PtpAffx.105555.2.S1_s_at	0.34	grail3.0033005901	expressed protein
PtpAffx.4337.1.A1_a_at	0.34	fgenes4_pm.C_LG_IV000203	putative protein
Ptp.6961.1.S1_at	0.34	-	-
Ptp.3855.1.S1_a_at	0.35	grail3.0001112401	putative protein
PtpAffx.127511.1.A1_at	0.35	fgenes4_pg.C_LG_XIX000854	O-methyltransferase
PtpAffx.211473.1.S1_at	0.35	gw1.XIV.821.1	CALMODULIN-RELATED PROTEIN 2
PtpAffx.4733.7.S1_s_at	0.35	estExt_fgenes4_pm.C_LG_IV0266	glutamine synthetase
PtpAffx.30585.1.A1_at	0.35	-	-
PtpAffx.27878.2.S1_a_at	0.36	grail3.0058009901	
		estExt_fgenes4_pg.C_640197	glutaredoxin
Ptp.2274.1.S1_s_at	0.36	estExt_fgenes4_pg.C_LG_II1800	putative protein
Ptp.7126.1.S1_at	0.36	eugene3.00061405	short chain alcohol dehydrogenase
Ptp.5922.1.S1_s_at	0.36	estExt_fgenes4_pm.C_LG_I0202	light regulated protein
Ptp.7015.1.S1_s_at	0.37	eugene3.01070081	putative protein
PtpAffx.133294.1.A1_at	0.37	fgenes4_pg.C_LG_VII000476	-
PtpAffx.201861.1.S1_at	0.37	fgenes4_pg.C_LG_II000742	aldehyde dehydrogenase
PtpAffx.10446.2.S1_at	0.37	gw1.III.1493.1	glycosyl hydrolase family 9
Ptp.866.1.S1_s_at	0.37	estExt_Genewise1_v1.C_LG_VII0556	ethylene responsive element binding factor 8
Ptp.1448.2.S1_x_at	0.37	eugene3.00060718	metallothionein-like

PtpAffx.202000.1.S1_at	0.37	fgenes4_pg.C_LG_II001043	unknown protein
PtpAffx.31347.1.A1_at	0.37	estExt_Genewise1_v1.C_LG_VII0556	ethylene responsive element binding factor
PtpAffx.59002.1.S1_s_at	0.38	estExt_fgenes4_pg.C_LG_XIX0409	glutamate dehydrogenase
PtpAffx.13918.1.S1_at	0.38	estExt_fgenes4_pm.C_LG_IV0578	nodulin - like
PtpAffx.27878.3.A1_a_at	0.38	grail3.0058009901	glutaredoxin
Ptp.536.2.A1_at	0.38	grail3.0045025401	putative zinc finger protein
PtpAffx.216927.1.S1_at	0.38	grail3.1564000301	expressed protein
Ptp.7045.2.S1_at	0.38	gw1.IV.2436.1	lemir (miraculin)
Ptp.2230.1.S1_at	0.38	grail3.0033005901	expressed protein
PtpAffx.206414.1.S1_at	0.38	fgenes4_pg.C_LG_VI001035	-
PtpAffx.152340.1.S1_s_at	0.39	eugene3.00150904	glutamate dehydrogenase 2
PtpAffx.88104.1.A1_at	0.39	-	-
PtpAffx.203845.1.S1_s_at	0.39	eugene3.00040414	
		fgenes4_pg.C_LG_IV000428	
		fgenes4_pg.C_scaffold_16707000001	hypothetical protein
PtpAffx.224739.1.S1_at	0.39	fgenes4_pg.C_LG_XI000523	subtilisin-like protease
PtpAffx.205086.1.S1_at	0.39	eugene3.00091601	-
PtpAffx.200551.1.S1_at	0.39	gw1.I.9744.1	glycosyl hydrolase family 1
PtpAffx.10911.2.A1_at	0.40	eugene3.01070081	putative protein
Ptp.2777.1.S1_s_at	0.40	gw1.125.52.1	hypothetical protein
PtpAffx.2768.1.S1_at	0.40	-	-
PtpAffx.294.3.S1_s_at	0.40	eugene3.00061170	putative reverse transcriptase
PtpAffx.9739.1.S1_at	0.41	estExt_Genewise1_v1.C_1470180	unknown protein
PtpAffx.212222.1.S1_at	0.41	estExt_fgenes4_pg.C_LG_XIX0409	glutamate dehydrogenase
Ptp.7361.1.S1_s_at	0.42	grail3.0001031201	putative DnaJ protein
PtpAffx.249.48.S1_x_at	0.42	estExt_fgenes4_pg.C_LG_X0149	drought-induced protein like
PtpAffx.10446.1.S1_a_at	0.42	fgenes4_pm.C_LG_I000271	glycosyl hydrolase family 9
PtpAffx.211014.1.S1_x_at	0.42	fgenes4_pg.C_LG_XIII000226	phosphoenolpyruvate carboxylase kinase
PtpAffx.12076.1.A1_at	0.43	estExt_fgenes4_pg.C_LG_II0599	expressed protein

PtpAffx.86916.1.A1_at	0.44	grail3.0042013901	floral homeotic gene APETALA1
PtpAffx.162370.1.S1_at	0.44	estExt_fgenes4_pg.C_LG_VIII0748	ribonuclease
PtpAffx.22704.2.S1_at	0.44	estExt_fgenes4_pg.C_LG_XIII0172	putative cytidine deaminase - like
PtpAffx.20317.2.S1_at	0.44	grail3.0130000201	-
PtpAffx.4559.1.A2_s_at	0.44	eugene3.01650006	proline-rich protein
PtpAffx.202769.1.S1_at	0.44	gw1.III.2328.1	aluminium tolerance associated - like protein
PtpAffx.92352.1.S1_a_at	0.44	eugene3.00060298	peptide transporter
PtpAffx.4733.3.S1_at	0.44	eugene3.00090586	expressed protein
PtpAffx.95760.1.A1_a_at	0.44	fgenes4_pm.C_LG_I000717	putative fatty acid elongase
PtpAffx.207984.1.S1_at	0.45	eugene3.00081064	putative phosphoenolpyruvate carboxylase
Ptp.2165.1.S1_at	0.45	estExt_Genewise1_v1.C_LG_II0002	photosystem II type I chlorophyll a :b binding protein
PtpAffx.203864.1.S1_at	0.45	fgenes4_pg.C_LG_IV000468	O-methyltransferase
Ptp.4476.1.S1_a_at	0.45	eugene3.00150904	
		estExt_fgenes4_pg.C_2320019	glutamate dehydrogenase 2
PtpAffx.156265.1.S1_at	0.46	gw1.VI.693.1	glutamate hydroxypeptidase
PtpAffx.34437.2.S1_at	0.46	eugene3.00010573	unknown protein
PtpAffx.78536.1.S1_at	0.46	estExt_Genewise1_v1.C_1290051	ABC transporter family protein
PtpAffx.11491.1.S1_at	0.46	gw1.IV.2596.1	major intrinsic protein (MIP)- like
PtpAffx.219700.1.S1_at	0.46	eugene3.00280038	ABC transporter permease protein-like
PtpAffx.1601.3.S1_x_at	0.47	eugene3.00060718	metallothionein-like protein
PtpAffx.210813.1.S1_at	0.47	grail3.0079017801	hypothetical protein
PtpAffx.148817.1.S1_at	0.48	estExt_Genewise1_v1.C_LG_XIII0762	MtN3-like protein
PtpAffx.207697.1.S1_at	0.48	eugene3.00080465	-
PtpAffx.7589.1.S1_s_at	0.50	eugene3.00081063	putative phosphoenolpyruvate carboxylase

P. trichocarpa

Up-regulated (134)

Affymetrix identifier	Expression	Gene model	Annotation
PtpAffx.39736.3.A1_a_at	2.18	eugene3.00081724	cytochrome p450 family
PtpAffx.5103.1.S1_a_at	4.34	eugene3.00870003	putative protein
Ptp.4151.1.A1_s_at	4.24	estExt_fgenesh4_pm.C_LG_XVII0021	lipoxygenase AtLOX2
Ptp.5131.1.S1_at	2.17	gw1.XVII.379.1	UDP-glucose glucosyltransferase
PtpAffx.209959.1.S1_at	2.28	eugene3.00110893	unknown protein
Ptp.5186.1.S1_at	2.49	gw1.I.700.1	Expressed protein
Ptp.3951.1.S1_at	2.52	gw1.X.5933.1	copper amine oxidase
PtpAffx.91812.1.S1_s_at	2.35	estExt_Genewise1_v1.C_LG_II2639	pectinesterase (pectin methylesterase)
PtpAffx.135376.1.S1_at	2.89	estExt_fgenesh4_pg.C_LG_I0284	putative annexin
PtpAffx.249.558.A1_a_at	25.08	-	-
PtpAffx.138763.1.A1_at	2.27	grail3.1757000202	cytosolic O-acetylserine(thiol)lyase
PtpAffx.202059.1.S1_at	2.16	eugene3.00021169	cytochrome P450
PtpAffx.115895.1.S1_s_at	2.39	eugene3.00820009	putative glycerophosphodiester phosphodiesterase
PtpAffx.4290.2.A1_at	2.16	grail3.0049006403	chorismate synthase
PtpAffx.210205.1.S1_at	2.10	grail3.0031007801	-
PtpAffx.153960.1.A1_at	2.11	-	-
PtpAffx.8690.1.A1_at	2.20	eugene3.00121203	subtilisin-like serine protease
PtpAffx.3955.2.S1_at	2.20	estExt_fgenesh4_pg.C_LG_VIII0179	expressed protein
PtpAffx.33897.1.S1_at	2.80	estExt_fgenesh4_pg.C_LG_III0833	expressed protein
PtpAffx.158042.2.A1_a_at	2.11	fgenesh4_pg.C_LG_XII000270	putative protein
PtpAffx.213445.1.S1_s_at	2.24	eugene3.00160714	expressed protein
Ptp.5046.1.S1_at	2.68	eugene3.00820009	putative glycerophosphodiester phosphodiesterase
Ptp.2985.1.S1_at	2.56	gw1.XII.1732.1	unknown protein
PtpAffx.30330.1.A1_at	2.51	eugene3.00090512	myb family transcription factor
PtpAffx.208576.1.S1_at	2.66	fgenesh4_pg.C_LG_X000365	expressed protein
PtpAffx.2752.1.S1_at	3.51	estExt_fgenesh4_pg.C_LG_I0283	putative annexin

PtpAffx.60092.1.S1_at	2.53	-	-
PtpAffx.87600.2.S1_at	2.40	gw1.XVIII.2818.1	putative 4-coumarate:CoA ligase 2
Ptp.4185.1.S1_at	2.65	-	-
PtpAffx.153960.1.A1_s_at	2.47	eugene3.00820009	putative glycerophosphodiester phosphodiesterase
PtpAffx.5103.1.S1_s_at	4.23	eugene3.00870003	putative protein : storage protein
PtpAffx.200143.1.S1_at	3.38	estExt_fgenes4_pg.C_LG_I0284	putative annexin
PtpAffx.77835.1.S1_at	2.96	gw1.182.19.1	polyphenol oxidase
Ptp.1442.1.S1_x_at	2.79	-	-
PtpAffx.23537.2.A1_at	2.27	-	-
Ptp.7985.1.S1_at	2.33	gw1.XIX.1560.1	putative PTR2 family peptide transporter
PtpAffx.225371.1.S1_s_at	2.54	fgenes4_pg.C_scaffold_193000016	3-hydroxyisobutyryl-coenzyme A hydrolase
PtpAffx.1235.1.A1_at	2.34	eugene3.00141311	-
PtpAffx.25946.1.S1_at	2.28	-	-
PtpAffx.220774.1.S1_s_at	3.47	gw1.X.5935.1	copper amine oxidase
PtpAffx.1741.1.S1_a_at	2.61	eugene3.00190336	putative protein : storage protein
PtpAffx.2522.4.S1_at	13.63	-	-
PtpAffx.58533.1.S1_at	2.58	grail3.0022032101	fatty acid elongase - like protein
PtpAffx.8550.3.S1_a_at	3.92	eugene3.00190357	apyrase
Ptp.5373.1.S1_s_at	2.44	estExt_Genewise1_v1.C_LG_XV0224	cytochrome b5
PtpAffx.202059.1.S1_x_at	2.32	eugene3.00021169	cytochrome P450
PtpAffx.219280.1.S1_x_at	2.32	gw1.2535.2.1	GDSL-motif lipase:hydrolase protein
Ptp.4364.1.S1_at	2.67	grail3.0074012402	steroid sulfotransferase-like protein
Ptp.4107.2.S1_a_at	2.54	estExt_fgenes4_pg.C_10830002	unknown protein
PtpAffx.5103.2.A1_x_at	5.29	eugene3.00870003	putative protein
PtpAffx.7936.2.A1_a_at	2.43	estExt_Genewise1_v1.C_700420	dehydroquinase dehydratase:shikimate dehydrogenase
PtpAffx.209732.1.S1_at	2.28	eugene3.00110333	Cyclin D6:1
PtpAffx.159543.2.A1_a_at	5.48	eugene3.00060878	leucoanthocyanidin dioxygenase-like protein
PtpAffx.8143.1.S1_s_at	2.58	eugene3.01210023	NADPH-ferrihemoprotein reductase (ATR2)
PtpAffx.101117.1.A1_at	3.61	estExt_Genewise1_v1.C_LG_VI0902	myb family transcription factor
PtpAffx.70015.1.A1_at	2.51	grail3.0047009702	-

PtpAffx.3989.1.S1_at	2.43	grail3.0049017002	putative water channel protein
PtpAffx.211991.1.S1_at	2.34	fgenes4_pg.C_LG_XIV001231	hypothetical protein
PtpAffx.152696.1.S1_at	2.40	gw1.57.332.1	expressed protein
PtpAffx.28382.1.S1_at	2.49	estExt_Genewise1_v1.C_LG_XV0224	cytochrome b5
PtpAffx.32431.1.S1_at	2.43	gw1.X.1458.1	glycosyl hydrolase family 1
PtpAffx.224650.1.S1_s_at	2.62	eugene3.00101070	-
PtpAffx.7936.1.A1_at	2.61	estExt_Genewise1_v1.C_700420	dehydroquate dehydratase:shikimate dehydrogenase
PtpAffx.214488.1.S1_at	2.44	eugene3.00181018	hypothetical protein
PtpAffx.249.577.A1_at	3.60	-	-
PtpAffx.112753.1.A1_s_at	3.75	estExt_Genewise1_v1.C_LG_I8330	hypothetical protein
PtpAffx.105086.1.S1_s_at	3.24	estExt_Genewise1_v1.C_LG_I8330	hypothetical protein
Ptp.4107.1.S1_at	2.77	estExt_fgenes4_pg.C_10830002	unknown protein
PtpAffx.249.14.A1_x_at	28.36	-	-
Ptp.3508.1.S1_at	3.51	estExt_Genewise1_v1.C_LG_XV1100	unknown protein
PtpAffx.201927.1.S1_at	2.71	eugene3.00020896	hypothetical protein
PtpAffx.2286.3.S1_a_at	2.52	gw1.11561.1.1	glutathione transferase
PtpAffx.122427.1.S1_at	3.30	-	-
Ptp.871.1.S1_at	2.59	estExt_fgenes4_pg.C_LG_XII0286	cytochrome b5
PtpAffx.7214.1.S1_s_at	2.56	grail3.0010009501	hypothetical protein
PtpAffx.207006.1.S1_s_at	2.87	fgenes4_pg.C_LG_VII000272	myrcene:ocimene synthase
PtpAffx.147010.1.A1_at	2.68	-	-
PtpAffx.212290.1.S1_at	2.66	gw1.XIX.1560.1	putative PTR2 family peptide transporter
PtpAffx.249.9.A1_at	10.18	estExt_Genewise1_v1.C_LG_X3770	-
PtpAffx.47668.1.A1_at	3.32	estExt_Genewise1_v1.C_400931	putative L-asparaginase
PtpAffx.218021.1.S1_at	2.84	fgenes4_pm.C_scaffold_187000008	flavonol 3-O-glucosyltransferase-like protein
PtpAffx.34799.1.S1_at	2.66	gw1.IX.1617.1	putative CDC21 protein
PtpAffx.67540.1.A1_s_at	2.92	fgenes4_pm.C_scaffold_187000008	flavonol 3-O-glucosyltransferase-like protein:
PtpAffx.215217.1.S1_at	2.71	fgenes4_pg.C_scaffold_120000012	ankyrin-repeat-containing protein-like
PtpAffx.33787.1.A1_at	3.33	estExt_Genewise1_v1.C_LG_IV4161	cytochrome p450 family
Ptp.4458.1.S1_s_at	2.85	estExt_fgenes4_pm.C_LG_XIV0571	glutathione transferase

Ptp.5023.1.S1_s_at	4.29	gw1.I.4122.1	putative adenosine phosphosulfate kinase
Ptp.6689.1.S1_at	2.85	fgenes4_pg.C_LG_VI000243	unnamed protein product
PtpAffx.159543.1.A1_at	11.99	eugene3.00060878	leucoanthocyanidin dioxygenase-like protein
PtpAffx.249.12.A1_x_at	46.05	estExt_Genewise1_v1.C_LG_X3770	-
PtpAffx.3541.1.S1_at	4.05	gw1.40.791.1	unknown protein
PtpAffx.221813.1.S1_at	4.45	fgenes4_pg.C_LG_XIX000232	S-adenosyl-L-methionine:jasmonic acid carboxyl methyltransferase (JMT)
PtpAffx.2522.1.A1_a_at	74.75	estExt_fgenes4_pg.C_LG_IV1532	glycosyl hydrolase family 19
PtpAffx.203697.1.S1_at	3.37	gw1.IV.1792.1	glucose-6-phosphate:phosphate-translocator precursor
PtpAffx.4.3.A1_x_at	8.93	-	-
Ptp.5347.1.S1_s_at	3.08	estExt_Genewise1_v1.C_LG_XIV0250	glutathione transferase
PtpAffx.249.13.A1_x_at	65.60	-	-
PtpAffx.120725.1.A1_at	3.17	fgenes4_pg.C_LG_II001874	-
Ptp.4364.1.S1_s_at	4.12	grail3.0074012402	steroid sulfotransferase-like protein
PtpAffx.249.20.S1_x_at	52.79	estExt_fgenes4_pg.C_LG_X0093	trypsin inhibitor homolog
PtpAffx.160390.2.A1_at	3.37	estExt_Genewise1_v1.C_LG_XV0083	flavanone 3-hydroxylase-like protein
PtpAffx.17014.1.A1_at	4.10	eugene3.00410022	-
PtpAffx.249.23.A1_a_at	25.05	estExt_fgenes4_pg.C_LG_X0093	trypsin inhibitor homolog
PtpAffx.249.23.A1_x_at	22.26	eugene3.00100092	-
PtpAffx.222340.1.S1_at	10.47	estExt_Genewise1_v1.C_640646	DYW7 protein
PtpAffx.3539.1.S1_a_at	4.22	eugene3.00130815	terpene synthase:cyclase family
PtpAffx.201911.1.S1_s_at	3.93	gw1.II.1557.1	expressed protein
PtpAffx.4.1.A1_a_at	11.67	grail3.0001024001	glycosyl hydrolase family 19
PtpAffx.201911.1.S1_at	3.94	gw1.II.1557.1	expressed protein
PtpAffx.4.4.A1_a_at	14.35	grail3.0001024001	glycosyl hydrolase family 19
PtpAffx.224821.1.S1_at	5.02	eugene3.00121141	GDSL-motif lipase:hydrolase-like protein
PtpAffx.162311.1.S1_at	4.04	estExt_Genewise1_v1.C_1450155	expressed protein
PtpAffx.218513.1.S1_s_at	39.89	gw1.I.9788.1	prolylcarboxypeptidase-like protein
PtpAffx.25980.1.S1_at	7.63	eugene3.00120122	putative flavonol sulfotransferase
PtpAffx.202805.1.S1_at	5.64	gw1.III.1280.1	unknown protein

Ptp.6874.1.S1_s_at	4.82	fgenes4_pg.C_LG_IV000603	Anthocyanin 5-aromatic acyltransferase
PtpAffx.225728.1.S1_at	4.93	eugene3.65260001	acyltransferase -like protein
Ptp.2908.1.A1_at	4.65	gw1.XIII.2464.1	DNA helicase-like
PtpAffx.215154.1.S1_at	11.21	gw1.XIX.631.1	S-adenosyl-L-methionine:jasmonic acid carboxyl
			methyltransferase (JMT_
Ptp.6057.1.S1_at	4.80	gw1.I.9239.1	putative leucoanthocyanidin dioxygenase
PtpAffx.200558.1.S1_s_at	12.79	gw1.I.9788.1	prolylcarboxypeptidase-like protein
PtpAffx.22414.1.S1_at	5.14	grail3.0191001701	expressed protein
PtpAffx.75508.1.A1_at	5.17	estExt_fgenes4_pg.C_LG_XVI0273	-
PtpAffx.1169.13.S1_a_at	5.70	estExt_fgenes4_pg.C_LG_VII1167	CONSTANS B-box zinc finger family protein
PtpAffx.24335.1.A1_at	5.55	eugene3.00121209	putative protein
Ptp.6755.1.S1_at	9.26	gw1.XIX.2223.1	similar to Dr4(protease inhibitor)
Ptp.8030.1.S1_s_at	5.60	estExt_Genewise1_v1.C_401069	cytochrome b5
PtpAffx.42186.1.A1_at	5.95	-	-
Ptp.6755.1.S1_x_at	9.16	gw1.XIX.2223.1	similar to Dr4(protease inhibitor)
PtpAffx.159832.1.A1_a_at	6.21	fgenes4_pg.C_scaffold_193000002	signal peptidase subunit
PtpAffx.149991.1.A1_s_at	15.21	grail3.0040008002	glycine-tRNA ligase precursor
PtpAffx.121276.1.A1_at	17.25	fgenes4_pg.C_LG_XIX000232	S-adenosyl-L-methionine:jasmonic acid carboxyl
			methyltransferase (JMT)
PtpAffx.204221.1.S1_at	7.95	fgenes4_pm.C_LG_IV000458	myb family transcription factor
PtpAffx.9044.2.S1_at	8.15	gw1.I.9239.1	putative leucoanthocyanidin dioxygenase

P. deltooides

Down-regulated (28)

Affymetrix identifier	Expression	Gene model	Annotation
Ptp.6735.1.S1_a_at	0.31	-	-
PtpAffx.216821.1.S1_s_at	0.31	gw1.IV.4286.1	glycosyl hydrolase family 1
PtpAffx.16371.3.A1_at	0.31	-	-
PtpAffx.215082.1.S1_at	0.32	eugene3.01170079	legumin-like protein
PtpAffx.215992.1.S1_at	0.33	fgenes4_pg.C_scaffold_133000007	anthranilate N-benzoyltransferase
Ptp.6679.1.A1_at	0.34	eugene3.00090950	-
PtpAffx.218009.1.S1_s_at	0.35	eugene3.18780001	anthranilate N-benzoyltransferase
PtpAffx.215081.1.S1_s_at	0.36	gw1.117.213.1	legumin-like protein
PtpAffx.2057.1.S1_s_at	0.36	fgenes4_pg.C_scaffold_1330000	anthranilate N-benzoyltransferase
PtpAffx.204075.1.S1_s_at	0.36	gw1.IV.4286.1	glycosyl hydrolase family 1
PtpAffx.69877.1.A1_a_at	0.37	eugene3.00081409	expressed protein
PtpAffx.47668.1.A1_at	0.38	estExt_Genewise1_v1.C_400931	putative L-asparaginase
PtpAffx.11916.1.S1_a_at	0.38	fgenes4_pg.C_LG_XVII00006	MADS-box protein
PtpAffx.212818.1.S1_s_at	0.39	eugene3.00150645	terpene synthase:cyclase family
PtpAffx.5430.5.S1_at	0.40	-	-
Ptp.5150.1.S1_s_at	0.41	fgenes4_pg.C_LG_VII000323	putative trypsin inhibitor
PtpAffx.200430.1.S1_s_at	0.41	gw1.I.8997.1	anthranilate phosphoribosyltransferase
PtpAffx.224440.1.S1_at	0.42	eugene3.00090964	-
Ptp.5249.1.S1_at	0.43	gw1.XII.1231.1	putative protein
PtpAffx.203271.1.S1_at	0.43	grail3.0018035401	hypothetical protein
Ptp.5150.1.S1_at	0.44	fgenes4_pg.C_LG_VII000320	putative trypsin inhibitor
Ptp.6580.1.S1_a_at	0.44	estExt_Genewise1_v1.C_LG_VII054	glycosyl hydrolase family 18
PtpAffx.204078.1.S1_s_at	0.46	gw1.IV.4286.1	glycosyl hydrolase family 1
PtpAffx.88399.1.A1_at	0.46	gw1.II.3380.1	peptide transport - like protein
PtpAffx.3155.1.A1_at	0.47	fgenes4_pg.C_scaffold_107000083	putative protein
Ptp.5321.1.S1_at	0.47	fgenes4_pg.C_LG_I001601	glycosyl hydrolase family 17
PtpAffx.47213.1.S1_at	0.48	gw1.III.2017.1	unnamed protein product

Ptp.5321.1.S1_s_at	0.49	gw1.5405.1.1	glycosyl hydrolase family 17
--------------------	------	--------------	------------------------------

P. deltoides

Up-regulated (17)

Affymetrix identifier	Expression	Gene model	Annotation
PtpAffx.9932.3.S1_a_at	2.08	eugene3.00030462	putative pectin methylesterase
Ptp.4947.1.S1_s_at	2.09	eugene3.00660215	putative protein
PtpAffx.10586.2.S1_at	2.09	estExt_fgenesh4_pm.C_LG_III0624	WRKY family transcription factor
PtpAffx.222499.1.S1_s_at	2.19	eugene3.00660215	putative protein
Ptp.1280.1.S1_at	2.21	eugene3.00051523	pectinesterase (pectin methylesterase)
PtpAffx.47285.1.S1_s_at	2.24	eugene3.00660215	putative protein
PtpAffx.7336.1.A1_at	2.36	gw1.XI.2669.1	GDSL-motif lipase:hydrolase-like protein
PtpAffx.3575.3.S1_at	2.45	grail3.0001065201	similar to gibberellin-regulated proteins
PtpAffx.69503.1.A1_at	2.51	estExt_Genewise1_v1.C_290296	putative pectin methylesterase
Ptp.2326.1.S1_s_at	2.81	eugene3.00011774	-
PtpAffx.14646.1.A1_a_at	2.88	grail3.0041013401	MADS-box protein
PtpAffx.250002.1.S1_s_at	3.13	gw1.9190.1.1	-
PtpAffx.102427.1.A1_s_at	3.23	eugene3.00130049	xyloglucan endotransglycosylase
PtpAffx.43661.1.A1_at	3.40	-	-
Ptp.7376.1.S1_a_at	3.76	gw1.XVIII.2856.1	xyloglucan endotransglycosylase
PtpAffx.12353.1.A1_at	3.94	-	-
PtpAffx.54408.1.S1_at	5.34	eugene3.00080459	-